Multiplex Screening Using Enzyme Inhibition, Fluorescence Detection and Chemometrics

By

Supaporn Kownarumit

A Doctoral Thesis submitted in partial fulfilment of

the requirements for the award of

DOCTOR OF PHILOSOPHY

of Loughborough University

Supervisor: *Professor James N. Miller*

Department of Chemistry

Loughborough University

ACKNOWLEDGEMENTS

I would initially like to thank Professor James N. Miller for his guidance, and support throughout this project. He gave me the opportunity to start the work and made sure that I had the opportunity to finish.

The second group of people I would like to show appreciation to are my colleagues in Bioanalysis group at Loughborough University; Marie, Rob, Dave, Lorna, Louise and especially Dongfang. They welcomed me into their group and helped at every opportunity. I would like to include Mohammad, an academic visitor from Iran; I learned some chemometrics from him.

The third group of people I would like to thank are my housemates and Thai friends at Loughborough University, especially Nak and Paew. They were always there with me to listen and encourage.

The fourth group I would like to thank is my colleagues in water analysis group in Thailand for their support. I would also like to thank Thai Government for the financial support.

Finally, I wish to thank are my family. They have always been there when I needed them. They gave me the grounding I needed to succeed and I hope I can return some of the support they have given me.

ABSTRACT

Fluorescence enzyme inhibition assays have been established for a number of years as valuable methods of analysis in clinical chemistry and other fields. Those in common use are normally single analyte assays. However, in many cases (e.g. drug screening) dual or multiplex assays would be much more valuable, with the advantages of increased information content, saving in time and costs, and the elimination of some sources of sampling variance.

This project has investigated single and dual screening assays of enzyme inhibitors, namely 3-nitrophenylboronic acid (3-NPBA), phenylethyl β-D-thiogalactopyranoside (PETG) and sodium vanadate (VI), using flow injection fluorescence spectroscopy and chemometric methods to resolve strongly overlapping fluorescence spectra. The single and dual screening assays have been based on flow injection analysis methodology, with immobilised enzymes on solid phase reactors to investigate the enzyme inhibitors. The assays were rapid, allowing around 15-25 measurements to be made per hour. The inhibitions of alkaline protease, alkaline phosphatase and β-galactosidase with their inhibitors at μg/ml levels were achieved. An alternative approach to these dual assays has been investigated by the use of multivariate techniques. Such techniques allow accurate and reliable results to be obtained even from spectra that contain extremely overlapping signals. Moreover, preliminary investigation of three fluorophores which gave strongly overlapping spectra, using flow injection fluorescence spectroscopy and partial least squares (PLS-1) model has been successful.

By combination of this flow injection fluorescence spectroscopy with the use of chemometrics, many applications can be envisaged in biochemical, clinical, and pharmaceutical industries. With the findings of this research the system described here can be developed for use in high throughput screening of candidate drug molecules and many screening processes throughout the different industries.

RESEARCH AIMS

The object of this investigation was to develop new fluorescence methods for the multiplex determination of enzyme inhibitors, in a format suitable for the rapid screening of candidate drug molecules. The methods used immobilised enzyme reactors in flow injection analysis systems. Multiplexing was achieved by incorporating time-dependent manifolds in the flow systems, and by using chemometric methods for the resolution of overlapping fluorescence spectra.

SCOPE AND OUTLINE OF THE THESIS

The thesis reports in seven chapters the work carried out to achieve the above aims.

Chapter 1 gives a brief overview of the subjects pertinent to the investigation, while Chapter 2 covers the area of chemometrics, emphasising the important methods of multivariate calibration.

Chapter 3 summarises the materials, instruments, and general procedures used during the research. Lists of suppliers are given in the appendices.

Chapters 4 and 5 describe the use of fluorescence spectroscopy with labelled proteins as enzyme substrates. The use of these substrates with immobilised enzyme reactors and a time-dependent flow injection analysis system for the dual determination of inhibitors is demonstrated.

Chapter 6 shows that these methods can be extended by the application of chemometric techniques such as partial least squares to the determination of fluorophores with strongly overlapping emission spectra.

Finally Chapter 7 summarises and comments on the work carried out and offer ideas for its further development. References and appendices complete the thesis.

TABLE OF CONTENTS

ACKNOWLEDGEMENTS I

ABSTRACT II

RESEARCH AIMS III

SCOPE AND OUTLINE OF THE THESIS III

TABLE OF CONTENTS IV

LIST OF FIGURES XII

LIST OF TABLES XVIII

LIST OF ABBREVIATIONS XX

CHAPTER 1 1

1.1 MULTIPLEX SCREENING IN DRUG DISCOVERY 2

1.1.1 The drug discovery process 2

1.1.2 Concept of high-throughput screening 4

1.1.3 Multiplex assays 5

1.1.3.1 Multiplex immunoassays 6

1.1.3.2 Multiplex determination in flow injection analysis 7

1.1.3.3. Multiplex determination with fluorescence spectroscopy 7

1.1.3.4 Multiplex determination with chemometrics 8

1.2 FLUORESCENCE 9

1.2.1 Theory of fluorescence 9

1.2.2 Fluorescence intensity 12

1.2.3 Advantages of fluorescence 13

1.2.4 Limitations of fluorescence 13

1.2.4.1 Photochemical decomposition 13

1.2.4.2 Quenching 14

1.2.5 Fluorophores 15

1.2.5.1 Fluorescein isothiocyanate 16

1.2.5.2 BODIPY Dyes 17

1.2.6 Fluorigenic substrates 18

1.2.6.1 Fluorescein digalactoside 18

1.2.6.2 Fluorescein diphosphate 19

1.3 FLOW INJECTION ANALYSIS 20

1.4 ENZYMES 23

1.4.1 Introduction to enzymes 23

1.4.2 Factors affecting enzyme activity 24

1.4.3 Free enzymes 24

1.4.3.1 Alkaline proteases 24

1.4.3.2 Alkaline phosphatase 25

1.4.3.3 β-Galactosidases 25

1.4.4 Enzyme kinetics 26

1.4.5 Quenched over-labelled fluorigenic assays for proteolytic enzymes 28

1.5 IMMOBILISED ENZYMES 29

1.5.1 Why immobilise enzymes? 30

1.5.2 Methods of immobilisation 31

1.5.3 Immobilised enzyme support 31

1.5.3.1 UltraLink® biosupport medium 32

1.5.4 Changes in enzyme properties after immobilisation 33

1.5.5 Analytical applications of immobilised enzymes 34

1.5.5.1 Immobilised enzyme electrodes 34
1.5.5.2 Immobilised enzyme reactors 35
a) Packed-bed reactors 35
b) Open-tubular reactors 36
1.5.6 Immobilised enzymes in FIA 37
1.6 ENZYME INHIBITION 38
1.6.1 Reversible inhibition 39
1.6.1.1 Competitive inhibition 39
1.6.1.2 Uncompetitive inhibition 39
1.6.1.3 Noncompetitive inhibition 40
1.6.2 Irreversible inhibition 41
1.7 ENZYME INHIBITORS 42
1.7.1 3-Nitrophenylboronic acid 42
1.7.2 Vanadate 42
1.7.3 Phenylethyl β-D-thiogalactopyranoside 43
CHAPTER 2 44
2.1 WHAT IS CHEMOMETRICS? 45
2.2 MULTIVARIATE CALIBRATION 46
2.2.1 Multivariate calibration decision tree 47
2.2.2 Principal component regression 52
2.2.3 Partial least squares 52
2.2.4 Orthogonal PLS-1 algorithm 54
2.3 UNSCRAMBLER SOFTWARE 59
2.4 VALIDATION 59
2.4.1 Cross validation 60

2.4.2 Leverage correction 61

2.4.3 Residual variance 62

CHAPTER 3 64

3.1 MATERIALS AND INSTRUMENTATION 65

3.1.1 Reagents 65

3.1.2 Balances 66

3.1.3 Cells 67

3.1.4 Chromatographic columns and frits 67

3.1.5 Flow system equipment 67

3.1.6 Pipettes 67

3.1.7 pH Meter 67

3.1.8 Spectrometers 67

3.1.9 Temperature control 68

3.1.10 Other equipments 68

3.2 GENERAL PROCEDURES 68

3.2.1 Water purification 68

3.2.2 Buffer preparation 68

3.2.3 pH measurement 68

3.2.4 Mass determination 68

3.2.5 Pipetting 68

3.2.6 Fluorescence measurement 69

3.2.7 Absorbance measurement 69

3.2.8 Flow system measurement 69

3.2.9 General dye: protein conjugation procedure 69

3.2.9.1 FITC- α-casein and BODIPY® 493/503- α-casein conjugates .. 70

3.2.9.2 BODIPY® FL- α-casein conjugates 70

3.2.9.3 Final dye: protein ratio or degree of labelling calculations..... 71

3.2.10 Immobilisation of enzyme onto Pierce UltraLink biosupport medium .. 72

3.2.11 Bicinchoninic acid (BCA) assay for determination of protein concentration 73

3.2.12 Preparation of Fluorescein di-galactoside (FDG) solution..... 73

3.2.13 Preparation of Fluorescein di-phosphate (FDP) solution..... 73

CHAPTER 4 74

4.1 INTRODUCTION 75

4.2 SINGLE ENZYME SCREENING ASSAYS IN STATIC SYSTEM 75

4.2.1 Determination of dye to protein ratios of conjugate substrates..... 75

4.2.2 Effect of excitation wavelength on the emission spectra of Bodipy FL-α-casein-AlkP, FDG-β-Gal and FDP-AP 76

4.2.3 Enzyme assays in a static system..... 79

4.2.3.1 Optimisation of Enzyme assay conditions..... 79

4.3 ENZYME IMMOBILISATION ON ULTRALINK BIOSUPPORT MEDIUM..... 85

4.3.1 Effect of enzyme concentration..... 86

4.3.2 Effect of salt concentration in the coupling buffer..... 86

4.4 ENZYME ASSAYS IN A FLOWING SYSTEM 87

4.4.1 Effect of pH 88

4.4.2 Effect of buffer concentration 89

4.4.3 Effect of temperature..... 90

4.4.4 Effect of enzyme concentration on the reaction rate 91

4.4.5 Influence of the enzyme reactor volume 92

4.4.6 Effect of flow rate 93

4.4.7 Effect of substrate volume 93

4.4.8 Calibration graphs for Bodipy FL-α-casein-AlkP, FDG-β-Gal and FDP-AP 94

4.5 ENZYME INHIBITION ASSAYS 96

4.5.1 Enzyme reactivation 96

4.5.2 Inhibition of β-Gal by PETG 97

4.5.3 Inhibition of AlkP by 3-NPBA 98

4.5.4 Inhibition of AP by VI 99

4.6 CONCLUSIONS AND DISCUSSION 100

CHAPTER 5 102

5.1 INTRODUCTION 103

5.2 FLUORESCENCE SPECTRA OF BODIPY FL-α-CASEIN, FDP AND FDG. 103

5.3 INVESTIGATION OF SIMULTANEOUS ASSAYS BY A FLOW-INJECTION METHOD BASED ON THE USE OF IMMOBILISED ENZYME REACTORS 104

5.3.1 Investigation of interference between the substrates and enzymes 106

5.3.2 Determination of length of flow tubing required for separation of peaks 107

5.3.3 Effect of flow rate 109

5.3.4 Simultaneous FDG and Bodipy FL-α-casein using immobilized β-Gal and AlkP reactors 110

5.3.5 Simultaneous FDG and FDP using immobilized β-Gal and AP reactors 112

5.3.6 Simultaneous Bodipy FL-α-casein and FDP using AlkP and AP 113

5.4 INVESTIGATION OF SIMULTANEOUS SCREENING FOR DUAL ENZYME INHIBITORS BY USING IMMOBILISED ENZYME REACTORS 115

5.4.1 Effects of Dimethyl sulphoxide on components in the system..... 116

5.4.2 Investigation of simultaneous screening for PETG and 3-NPBA by using immobilised β-Gal and AlkP enzyme reactors 117

5.4.3 Investigation of simultaneous screening for PETG and VI inhibitors by using immobilised β-Gal and AP enzyme reactors 118

5.4.4 Investigation of simultaneous screening for 3-NPBA and VI by using immobilised AlkP and AP enzyme reactors 122

5.5 CONCLUSIONS AND DISCUSSION..... 124

CHAPTER 6 127

6.1 INTRODUCTION 128

6.2 THE INVESTIGATION OF DUAL SCREENING ENZYME INHIBITIONS USING A FLOW-INJECTION METHOD AND CHEMOMETRIC METHODS129

6.2.1 Procedure 129

6.2.2 Results and discussion 130

6.2.2.1 PLS treatment of spectrofluorimetric data..... 130

6.2.2.2 Prediction and deviations..... 137

6.2.2.3 Variable (data point) selection..... 140

6.2.2.4 Noise addition 140

6.3 THE INVESTIGATION OF TERNARY ANALYTE MIXTURES WITH STRONGLY OVERLAPPING SPECTRA FOR MULTIPLEX SCREENING . 148

6.3.1 Procedure 149

6.3.2 Results and discussion 151

6.3.2.1 PLS-1 treatment of fluorescence data..... 151

6.3.2.2 Prediction and deviations..... 154

6.4 CONCLUSIONS..... 156

CHAPTER 7 ..... **157**

7.1 CONCLUSIONS 158

7.2 FUTURE WORK 161

REFERENCES **166**

APPENDICES **188**

APPENDIX A 189

APPENDIX B 192

APPENDIX C 193

APPENDIX D 194

APPENDIX E 195

LIST OF FIGURES

Figure 1.1 Average periods for steps in the drug discovery and development procedure 2

Figure 1.2 Applied fields of modern pharmaceutical analysis in drug discovery 3

Figure 1.3 Biochemical classes of drug targets of current therapies 4

Figure 1.4 Classification of multi-analyte immunoassays 7

Figure 1.5 Jablonski diagram showing absorption and emission processes of fluorescence and phosphorescence. S_0 = ground singlet state, S_1 and S_2 = first and second singlet levels respectively, T_1 and T_2 = first and second triplet levels respectively 11

Figure 1.6 Excitation and emission spectra of Fluorescein isothiocyanate 11

Figure 1.7 Structure of FITC, Isomer I 16

Figure 1.8 Structure of BODIPY ® FL-X, SE 17

Figure 1.9 Structure of BODIPY ® 493/503, SE 18

Figure 1.10 Sequential hydrolysis of FDG to FMG and fluorescein by β-gal 19

Figure 1.11 Structure of fluorescein diphosphate (FDP) 20

Figure 1.12 Schematic diagram of a single line FIA manifold 20

Figure 1.13 A typical FIA peak 21

Figure 1.14 Dependence of initial velocity on substrate concentration for a single-substrate enzyme-catalysed reaction 26

Figure 1.15 The Lineweaver-Burk plot 28

Figure 1.16 Schematic principle of an intramolecularly quenched protein substrate 29

Figure 1.17 Classification of methods employed for enzyme immobilisation 31

Figure1.18 Reaction of azlactone ring on UltraLink® Biosupport medium with amine-containing ligand. 33

Figure 1.19 Principle of an immobilised enzyme electrode 34

Figure 1.20 Immobilised enzyme reactors (a) packed-bed (b) open-tubular 36

Figure 1.21 Lineweaver-Burk plot for different modes of reversible inhibition 41

Figure 1.22 Molecular structure of phenylethyl β-D-thiogalactopyranoside 43

Figure 2.1 How chemometrics relates to other disciplines 45

Figure 2.2 Multivariate calibration decision tree 48

Figure 2.3 Graphical representation of matrices of calibrations used in analytical chemistry 51

Figure 4.1 Effect of excitation wavelength on the emission spectrum of Bodipy FL-α-casein-AlkP (a), FDG-β-Gal (b) and FDP-AP (c) 78

Figure 4.2 Influence of incubation time on FDG-β-Gal 80

Figure 4.3 Influence of FDG concentration on FDG-β-Gal 81

Figure 4.4 Influence of β-Gal concentration on FDG-β-Gal 81

Figure 4.5 Influence of temperature on FDG-β-Gal 82

Figure 4.6 Influence of pH on FDG-β-Gal 82

Figure 4.7 Fluorescence emission spectra showing enhancement seen upon incubation of Bodipy FL-α-casein with AlkP 83

Figure 4.8 Fluorescence emission spectra showing enhancement seen upon incubation of FDG with β-Gal 84

Figure 4.9 Fluorescence emission spectra showing enhancement seen upon incubation of FDP with AP 84

Figure 4.10 Manifold for flow injection enzyme and enzyme inhibition assays 85

Figure 4.11 Influence of β-Gal concentration on immobilisation on UltraLink biosupport medium 86

Figure 4.12 Effect of sodium citrate concentration on coupling for β-Gal..... 87

Figure 4.13 Effect of pH on the activity of FDG-β-Gal..... 89

Figure 4.14 Effect of buffer concentration on the activity of β-Gal 89

Figure 4.15 Effect of temperature on the activity of β-Gal..... 90

Figure 4.16 Influence of β-Gal concentrations on the formation of product..... 91

Figure 4.17 Effect of the enzyme reactor volume..... 92

Figure 4.18 Effect of flow rate on the response of FDG-β-Gal..... 93

Figure 4.19 Effect of substrate volume on the response of FDG-β-Gal 94

Figure 4.20 Influence of substrate concentration on the production of Bodipy FL-α-casein-AlkP (a), FDG-β-Gal (b) and FDP-AP (c) in a flow system..... 96

Figure 4.21 Inhibition of β-Gal by PETG determined with FDG at 37 °C..... 98

Figure 4.22 Inhibition of AlkP by 3-NPBA determined with Bodipy FL-α-casein at 37 °C 99

Figure 4.23 Inhibition of AP by VI determined with FDP at 37 °C..... 100

Figure 5.1 Emission spectra of Bodipy FL-α-casein-AlkP, FDP-AP and FDG-β-Gal 103

Figure 5.2 Schematic of flow injection analysis system for dual assay..... 105

Figure 5.3 Appearance of the enzyme reactors..... 105

Figure 5.4 Interference of Bodipy FL-α-casein-AlkP and FDG-β-Gal..... 106

Figure 5.5 (a) and (b) – Actual layout and equipment used for flow analysis enzyme and enzyme inhibition assays..... 108

Figure 5.6 Effect of flow rate on dual Bodipy FL-AlkP and FDP-AP assay 109

Figure 5.7 Typical flow injection analyses obtained by Bodipy FL-α-casein and FDG using a dual enzyme system, (a) AlkP and (b) β-Gal..... 110

Figure 5.8 Calibration graph for (a) FDG and (b) Bodipy FL-α-casein using a dual enzyme system 111

Figure 5.9 Typical flow injection analyses obtained by FDG and FDP using a dual enzyme system, (a) β-Gal and (b) AP 112

Figure 5.10 Calibration graph for (a) FDG and (b) FDP using a dual enzyme system 113

Figure 5.11 Typical flow injection analyses obtained by Bodipy FL-α-casein and FDP using a dual enzyme system, (a) AlkP and (b) AP 114

Figure 5.12 Calibration graph for (a) Bodipy FL-α-casein and (b) FDP using a dual enzyme system 115

Figure 5.13 Effect of DMSO on FDP-AP with/ without VI 117

Figure 5.14 FIA peaks for Bodipy FL-α-casein and FDG with 3-NPBA and PETG, using AlkP (a) and β-Gal (b) reactors 118

Figure 5.15 Interaction between phenyl boronic acid and sugar at near neutral pH 118

Figure 5.16 Calibration graph for PETG and VI using a dual enzyme system ... 121

Figure 5.17 Calibration graph for 3-NPBA and VI using a dual enzyme system 124

Figure 6.1 AlkP and AP enzyme reactors in series 130

Figure 6.2 Mixture design for the binary mixtures used in the data set for the PLS-1 method. 131

Figure 6.3 The analysis plots of calibration set for VI using PLS-1 and FCV 133

Figure 6.4 The analysis plots of calibration set for 3-NPBA using PLS-1 and FCV 134

Figure 6.5 The residual sample variance plot for outlier checking of 3-NPBA calibration set using PLS-1 and FCV 135

Figure 6.6 The analysis plots of calibration set without the outlying sample for 3-NPBA using PLS-1 and FCV 136

Figure 6.7 A comparison of the predicted results using PLS-1 and FCV with the actual results for the new data set: (a) 3-NPBA and (b) VI..... 139

Figure 6.8 The calibration set spectra with 3% noise adding..... 141

Figure 6.9 The analysis plots of calibration set with 3% noise for VI using PLS-1 and FCV..... 142

Figure 6.10 The analysis plots of calibration set with 3% noise for 3-NPBA using PLS-1 and FCV..... 143

Figure 6.11 The residual sample variance plot for outlier checking of 3-NPBA calibration set with 3% noise adding using PLS-1 and FCV..... 144

Figure 6.12 The analysis plots of calibration set (without outlying samples) with 3% noise adding for 3-NPBA using PLS-1 and FCV..... 145

Figure 6.13 A comparison of the predicted results using the 3% noise adding, PLS-1 and FCV with the actual results for the validation set: (a) 3-NPBA and (b) VI..... 147

Figure 6.14 Fluorescence emission spectra of Bodipy FL conjugate, Bodipy 493 conjugate, FITC conjugate and a mixture of the three conjugates... 148

Figure 6.15 The residual sample variance plot for outlier checking of 3 conjugates calibration set using PLS-1 and FCV: (a) FITC conjugate, (b) BFL conjugate, and (c) B493 conjugate..... 153

Figure 6.16 A comparison of the predicted results using PLS-1 and FCV with actual results for the new data set: (a) FITC conjugate, (b) BFL conjugate, and (c) B493 conjugate..... 155

Figure 7.1 Possible set-ups for multi-determination assays..... 161

Figure 7.2 Schematic diagram showing the set-up of the microchip..... 163

Figure 7.3 The chip design, showing the channel configuration..... 164

Figure B-1 Appearance of the F-4500 in our laboratory..... 192

Figure C-1 Internal block diagram of the F-4500..... 193

Figure E-1 The analysis plots of calibration set for FITC conjugate using PLS-1 and FCV 195

Figure E-2 The analysis plots of calibration set for BFL conjugate using PLS-1 and FCV 196

Figure E-3 The analysis plots of calibration set for B493 conjugate using PLS-1 and FCV 197

Figure E-4 The analysis plots of calibration set for FITC conjugate using PLS-1 and FCV without outlier 198

Figure E-5 The analysis plots of calibration set for BFL conjugate using PLS-1 and FCV without outlier 199

Figure E-6 The analysis plots of calibration set for B493 conjugate using PLS-1 and FCV without outlier 200

LIST OF TABLES

Table 1.1 Diagnostically related groups of test suitable for the multi-analyte immunoassays format 6

Table 1.2 Simultaneous fluorescence spectrophotometric determinations using chemometrics 9

Table 1.3 Spectral characteristics of the dyes 18

Table 3.1 Reagents and Suppliers 65

Table 4.1 Initial reaction mixture and calculated final dye: protein ratios for Bodipy FL- α-casein conjugates 75

Table 4.2 Assay parameters studied and optimum conditions for various enzyme and substrates in a static system 79

Table 4.3 Assay parameters studied and optimum conditions for various enzymes and substrates in a flow system 88

Table 4.4 Effect of the volume and concentration of PETG on % inhibition of β-Gal 97

Table 6.1 Concentration data used in the calibration set for determination of 3-NPBA and VI 131

Table 6.2 Concentration data used in the new data set for determination of 3-NPBA and VI 137

Table 6.3 A full analysis for 3-NPBA and VI with FCV for the PLS-1 model 138

Table 6.4 A full analysis for 3-NPBA and VI with FCV for the PLS-1 model with 3% Noise adding 146

Table 6.5 The composition of the calibration set for ternary mixtures 150

Table 6.6 The composition of the new data set for ternary mixtures..... 151

Table 6.7 Summarisation of statistical parameters of 3 analytes with PLS-1 and FCV..... 152

Table 6.8 Summarisation of statistical parameters of 3 analytes with PLS-1 and FCV without outliers..... 152

Table 6.9 A full analysis for 3 conjugates prediction set with FCV for the PLS-1 model..... 154

Table D-1 Instrument parameters of the F-4500..... 194

LIST OF ABBREVIATIONS

AP	Alkaline phosphatases
AlkP	Alkaline proteases
β-gal	Beta-galactosidases
BCA	Bicinchoninic acid
Bodipy FL-α-casein	Bodipy FL dye conjugated with α-casein
Bodipy FL-α-casein-AlkP	Bodipy FL conjugate reacted with alkaline proteases
CAC	Chemometrics in analytical chemistry
CLS	Classical least squares
COMPANA	Computer applications in analytics
COBAC	Computer-based analytical chemistry
CPG	Controlled pore glass
CF	Correction factor
r	Correlation coefficient
DOL	Degree of labelling
DMSO	Dimethyl sulphoxide
DCLS	Direct classical least squares
D: P	Dye: protein
EC	Enzyme code
ELISA	Enzyme linked immunosorbent assay
Eq	Equation
ε	Extinction coefficient

FITC	Fluorescein isothiocyanate
FDG	Fluorescein di-β-D-galactopyranoside
FMG	Fluorescein mono-β-D-galactopyranoside
FDP	Fluorescein diphosphate
FCV	Full cross validation
FDG-β-Gal	Fluorescein di-β-D-galactopyranoside reacted with beta-galactosidases
FDP-AP	Fluorescein diphosphate reacted with alkaline phosphatases
FIA	Flow injection analysis
I_F	Fluorescence intensity
HTS	High-throughput screening
HIV	Human immunodeficiency virus
ILS	Inverse least squares
ICLS	Indirect classical least squares
K_m	The Michaelis-Menten constant
DL	Limit of detection
LC	Leverage correction
MLR	Multiple linear regression
NIPALS	Non-linear iterative partial least squares algorithm
NC	Nitrocellulose
PBS	Phosphate buffer saline
PETG	Phenylethyl β-D-thiogalactopyranoside
PCR	Principal components regression

PLS	Partial least squares
PCs	Principal components
PCA	Principle component analysis
φ	Quantum efficiency
3-NPBA	3-Nitrophenylboronic acid
RMSEP	Root mean squared error of prediction
RMSEC	Root mean squared error of calibration
TRV	Total residual variance
VI	Sodium vanadate inhibitor
S.D.	Standard deviation

CHAPTER 1

INTRODUCTION

1.1 MULTIPLEX SCREENING IN DRUG DISCOVERY

1.1.1 The drug discovery process

The discovery of a new drug is a long and expensive process. From the synthesis of a compound to its approval can take 10-20 years, with an estimated average of about 12-15 years of development, including the cost and time to discover potential biological targets.[1] Out of the around 15 years in development time of a successful compound about 6 years are devoted to the drug discovery and the preclinical phase [2] (figure 1.1). There are numerous references on drug discovery and development.[3-7]

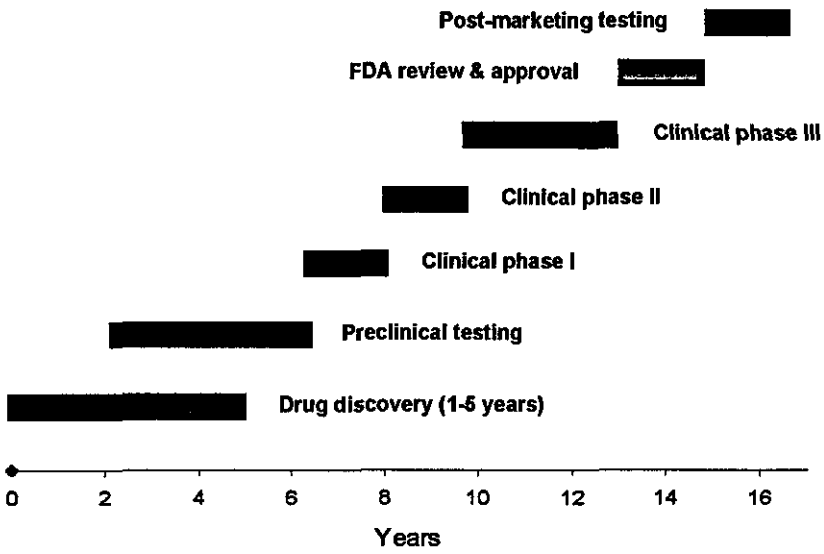

Figure 1.1 Average periods for steps in the drug discovery and development procedure

A recent survey of 68 randomly selected new drugs yielded a total pre-approval cost estimate of 802 million US dollars for the research and development costs when unsuccessful projects were also included.[8]

Traditionally, pharmaceutical analysis referred to the chemical analysis of drug molecules. However, over the years, modern pharmaceutical analysis has evolved beyond this to encompass combination techniques, high-throughput screening,

chemometrics, miniaturization and nanotechnology. Figure 1.2 shows the applied fields of modern pharmaceutical analysis in drug discovery.[9]

The progress made in biochemistry, genomic sciences, combinatorial chemistry, etc. gave rise to the establishment of high-throughput screening (HTS) technologies. The demand for higher productivity has increased the need to screen more targets with higher throughput and lower costs.

A comprehensive analysis of the drug targets underlying current drug therapy showed that present-day therapy address only 500 molecular targets and as shown in figure 1.3, cell membrane receptors, largely heterotrimeric GTP-binding protein - coupled receptors, constitute the largest subgroup with 45% of all targets, and enzymes and inhibitors account for 28% of all current drug targets.[6]

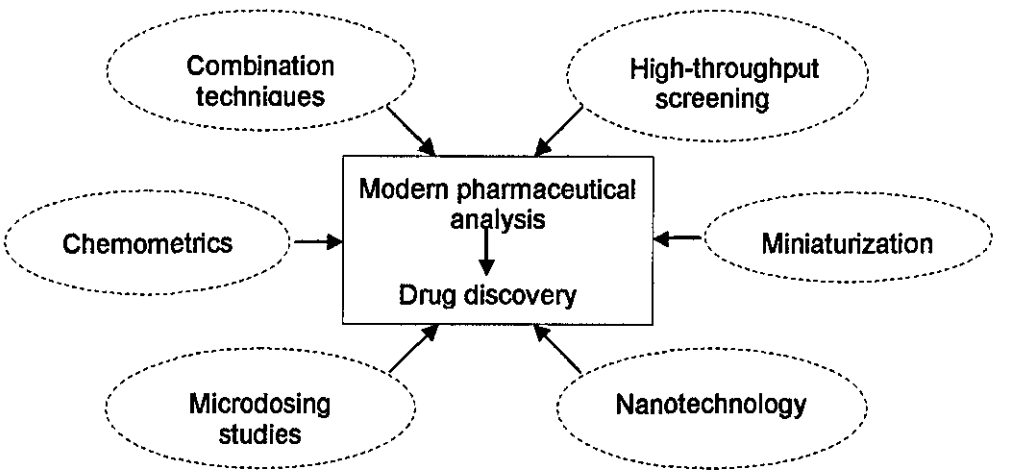

Figure 1.2 Applied fields of modern pharmaceutical analysis in drug discovery

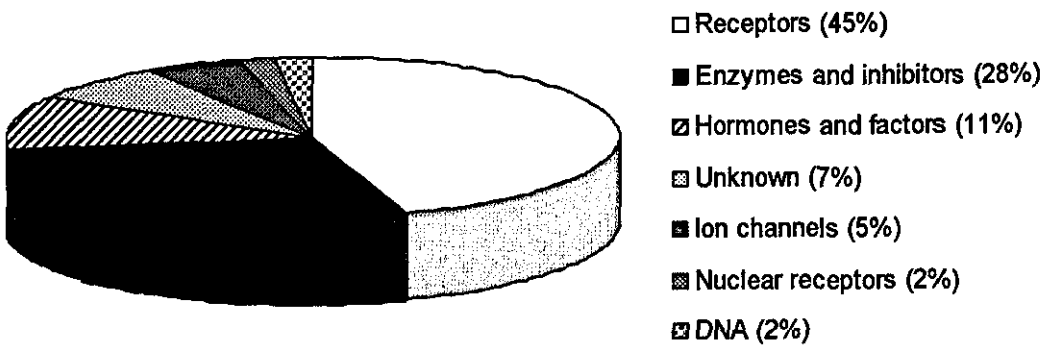

Figure 1.3 Biochemical classes of drug targets of current therapies

1.1.2 Concept of high-throughput screening

In the past decade the world of high-throughput screening (HTS), which targets lead discovery for pharmaceutical applications, is in a highly rapid developmental stage. For an effective HTS infrastructure the fundamental working fields of target discovery and validation, screen design, assay technology, detection method, sample generation and handling, laboratory automation and robotics, as well as of data management have to be integrated, coordinated and optimized. At present, latest technology and laboratory automation in all parts of the early stages of drug discovery play crucial roles in the success of HTS strategies.[10] Nearly all drug discovery research projects in the pharmaceutical industry employ HTS assays as initial steps to discover the chemical leads. The primary role of the technology is to detect lead compounds and supply directions for their optimisation using other techniques.

Enabling technologies that characterize HTS [11] are:

- Increase in compound library diversity and size
- Exponential increase in targets from genomics/ proteomics
- Miniaturization
- Integrated systems
- Automation

- More sensitive and efficient assay and detection systems
- Cellular assay system improvements
- Sensitive alternatives to radioactive assays
- Computational methods for assay simulation
- Data management improvements and innovations
- Outsourcing and customization
- Lead optimization tools

However, drug discovery is extremely complex and the goals, company resources, products portfolio, as well as future expectations of the different players vary widely.

A number of assay formats have been developed or modified over the past few years to conform to the constraints imposed by HTS. Several of the more developed or exploited assay protocols for HTS have been the focus of several papers.[12-15]

1.1.3 Multiplex assays

The development of multiplex assays has been gaining in importance over the years due to the increasing demands being placed upon the speed and complexity of analysis. Such assays are widely used by many of the different industries including pharmaceutical industries and medical sciences. This is mainly due to the many advantages that these assays bring over single analyte assays such as a reduction in cost, time and reagent as well as sample consumption.

Multiplex determinations usually require an extra step, which normally involves the separation of the analytes prior to their detection. The most classical separation techniques include chromatography or some form of extraction. However, due to the ever-increasing need for more rapid screening assay throughput, separation methods such as chromatography are very time consuming and give relatively low sample turnovers. Many authors have looked at combining the technique of flow injection analysis with multiplex assays.

1.1.3.1 Multiplex immunoassays

Immunoassays traditionally are performed as discrete tests, i.e., each assay is only able to analyse one analyte. An alternative option is multi-analyte immunoassays, in which two or more analytes are measured simultaneously in a single assay. Generally, the multi-analyte immunoassays can be classified into two main formats:

- Assays based on more than one label
- The assay based on spatially separated test zones

These are shown in table 1.1 and figure 1.4

There are numerous sources of dual and multiplex immunoassays.[16-23]

Table 1.1 Diagnostically related groups of test suitable for the multi-analyte immunoassays format [16]

Type of testing	Example
Allergen testing	IgE and IgG antibodies
Blood banking	Antibodies to HIV and hepatitis B
Cardiac markers	Troponin and myoglobin
Dried blood spot analysis	Thyrotropin and immunoreactive trypsin
Drugs of abuse testing	Cocaine and amphetamines
Dual and triple testing	Alpha fetoprotein
Fertility testing	Lutropin, follitropin and prolactin

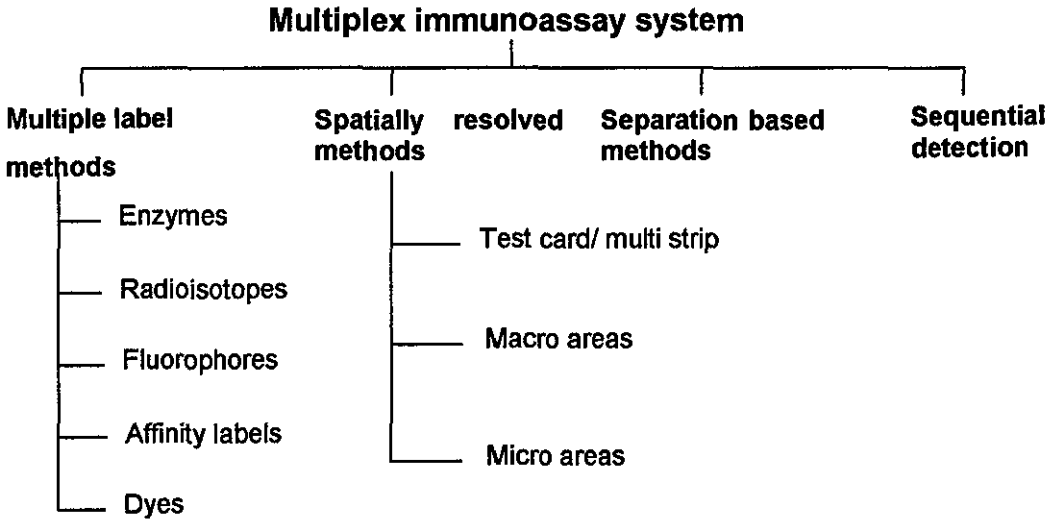

Figure 1.4 Classification of multi-analyte immunoassays [17]

1.1.3.2 Multiplex determination in flow injection analysis

A typical sample sometimes needs to be analysed for more than one species, which is important, for example, in food processing, in clinical and industrial analysis and in process control. In order to eliminate the limitation of flow injection analysis (FIA) for the determination of only one species at a time many attempts to achieve multiplex analysis have been made with a variety of procedures and manifolds, for example by using a single injection with several detectors in series or parallel[24] or by using a 16-way switching valve.[25] Enzymatic assays have particular importance in clinical analysis. A number of enzyme reactors have been reported to be used for simultaneous determination of more than one component in a mixture.[26] Moreover, an automated flow injection method was developed for the determination of six different analytes simultaneously, by using six enzyme reactors in parallel, with a single detector and a single injection valve.[27]

1.1.3.3. Multiplex determination with fluorescence spectroscopy

Fluorescence spectroscopy has been extensively used as a detection method in a wide range from clinical chemistry to environmental monitoring on account of its

high sensitivity and selectivity, and relatively low cost. However, spectra for complex mixtures often cannot be successfully resolved, mainly because the individual components of the mixture exhibit spectra with broad bands that tend to overlap; this necessitates combining spectrofluorimetry and a separation technique or using a highly specific method. This usually increases analysis costs; hence there is interest in improving the selectivity of the spectrofluorimetric technique in order to accomplish simultaneous multiplex analyses without the need for expensive or time-consuming procedures.

There are various approaches to increasing the selectivity of spectrofluorimetry, including derivative spectroscopy[28], synchronous spectroscopy[29] and synchronous derivative spectroscopy[30], in which the fluorescence intensity is a function of a single parameter (the excitation or emission wavelength or a constant difference between the two).

1.1.3.4 Multiplex determination with chemometrics

Due to the recent advances in computer technology and the development of statistical software packages, multiplex assays do not necessarily require multiple methods of detection. It is now possible to use only one method of detection for the quantification of various analytes simultaneously from just one sample. The highly sensitivity spectrofluorimetry and flexible multivariate calibration methods make a novel, effective combination for the simultaneous determination of several analytes in mixtures that cannot be resolved by conventional spectrofluorimetry. In studies by Lindberg et al.[31] and Sjostrom et al.[32] concentrations of two and three component synthetic mixtures are successfully predicted from fluorescence emission spectra by the method of partial least-squares regression. There have been many publications that use fluorometric method for the simultaneous determination of analytes (table 1.2).

Table 1.2 Simultaneous fluorescence spectrophotometric determinations using chemometrics

Application	References
Inorganic substances, i.e. ultratrace Niobium (V), Tantalum (V) and Zirconium (IV)	33
Ternary micellar ion-association complexes; Zirconium (IV), Hafnium (IV) ions and quercetin	34
Canrenone and spironolactone in Urine	35
Naproxen and Salicylate in human serum	36
Pesticides, i.e. carbaryl (CBL), fuberidazole (FBZ), thiabendazole (TBZ) and warfarin (W)	37
Juvenile and mature eucalyptus wood samples	38
Refined sugar samples	39
Furosemide and Triamterene in pharmaceutical and urine samples	40
(Acetyl) Salicylic acid, Codeine and Pyridoxine in pharmaceutical preparations	41
Albumin and Immunoglobulin G	42

1.2 FLUORESCENCE

Fluorescence spectroscopy is an extremely powerful analytical tool that has seen a remarkable growth in its use over the past 20 years, in a wide range of areas from clinical chemistry to environmental monitoring. There are numerous sources of information on the theory of fluorescence and its applications.[43-49]

1.2.1 Theory of fluorescence

The sequence of events that occurs in fluorescence from a single molecule is shown in figure 1.5 and is as follows:

- A quantum of light is absorbed by a dipole (a)
- Rapid radiationless relaxation (internal conversation) takes the dipole to the thermally relaxed S_1 level (b)

- The dipole retains this energy for a certain period of time, generally designated as the lifetime (τ)
- The excess energy is dissipated through radiationless de-excitation (c, d, and e) caused predominantly through vibrational and rotational modes and collisions with solvent molecules, or by photon emission (f, g). When this photon emission is from a singlet electronic state, it is referred to as fluorescence (f). Conversely, when the emission is from a triplet state, phosphorescence is the result (g).

Fluorescence differs from phosphorescence in that the electronic energy transitions responsible for the fluorescence do not involve a change in electron spin. As a consequence, fluorescence is short-lived, with luminescence ceasing almost immediately ($<10^{-5}$ s).[44]

In nearly all cases, fluorescence arises from the lowest vibrational level of the ground state of a molecule to a higher vibrational level of the first excited singlet state. Upper vibrational levels quickly relax to the lowest vibrational level of the particular electronic level, since vibrational relaxation occurs in about 10^{-12} sec, much faster than other energy dissipation processes. On reversion to the ground electronic level fluorescence may result, with the molecule usually ending up in an excited vibrational level. Because the vibrational levels of both ground and excited states are similar, the fluorescence spectrum often is a sort of mirror image of the exciting absorption spectrum (figure 1.6). The lifetime of an excited singlet state is usually $10^{-9} - 10^{-6}$ sec and fluorescence lifetimes fall in this range.

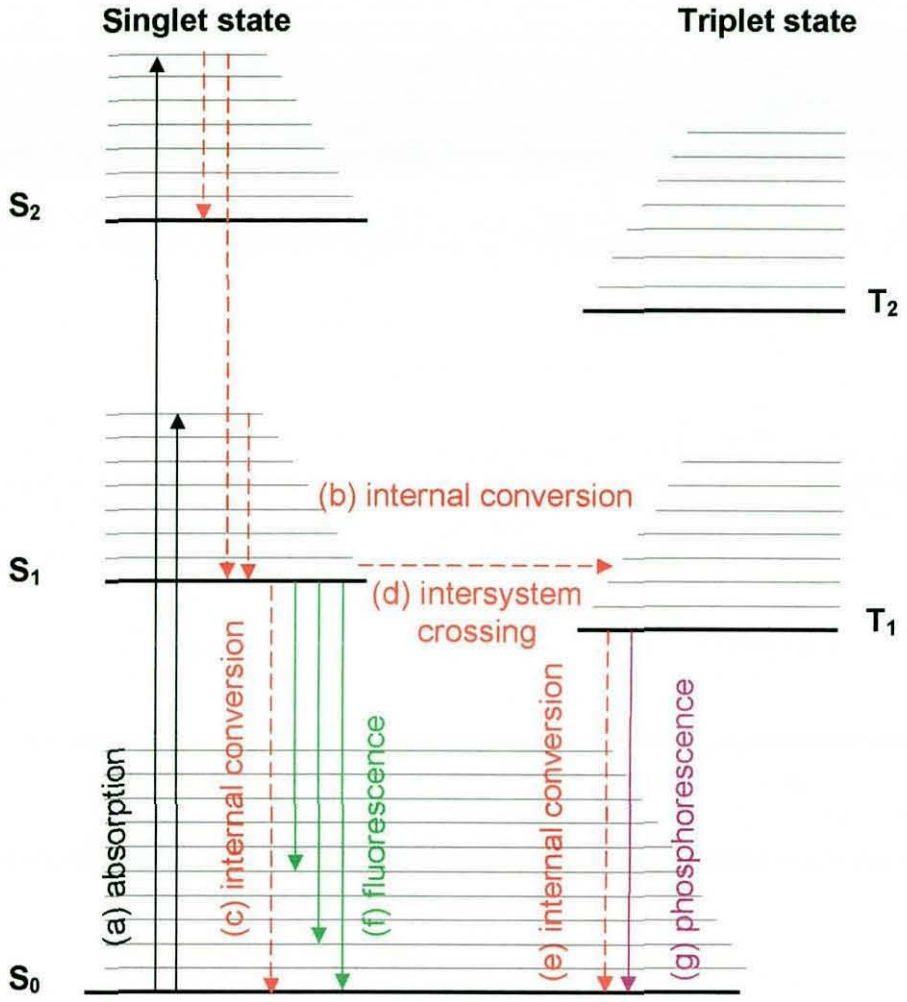

Figure 1.5 Jablonski diagram showing absorption and emission processes of fluorescence and phosphorescence. S_0 = ground singlet state, S_1 and S_2 = first and second singlet levels respectively, T_1 and T_2 = first and second triplet levels respectively

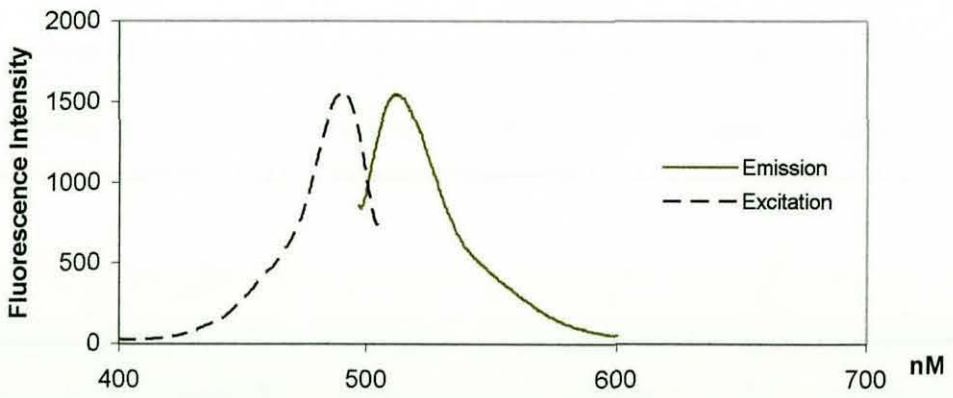

Figure 1.6 Excitation and emission spectra of Fluorescein Isothiocyanate

To ascertain the excitation and emission spectra (figure 1.6) the following procedure is commonly followed. The excitation monochromator is varied until fluorescence occurs; often this can simply be viewed visually. The excitation monochromator is then set at this wavelength (or at any point within the excitation wavelength band) and the emission monochromator is allowed to scan, recording the emission spectrum. The emission monochromator is then set at the wavelength at which maximum fluorescence occurred, the excitation monochromator is allowed to scan, and the excitation spectrum is recorded. In turn, setting the excitation wavelength and again scanning the emission monochromator gives the final emission spectrum.[50] For analytical applications the emission spectrum is used. Often an excitation spectrum is first made to confirm the identity of the substance and to select the optimum excitation wavelength.

1.2.2 Fluorescence intensity

Fluorescence intensity (I_F) in dilute solutions is directly proportional to the intensity of the excitation light source and solution concentration and is given by equation 1.1.

$$I_F = \varphi I_0(1-10^{-\varepsilon bc}) \qquad \text{(Eq.1.1)}$$

φ is the quantum efficiency, I_0 is the incident radiant power at the wavelength of interest, ε is the molar absorptivity at that wavelength, b is the cell path length and c is the molar concentration.[51]

For a very dilute solution where $A < 0.05$ absorbance units, equation 1.1 approximates to equation 1.2:

$$\text{Observed } I_F' = k\varphi I_0 \varepsilon bc \qquad \text{(Eq.1.2)}$$

k is an instrumental factor, it is a proportionality constant due to the fact that although fluorescence is emitted in all directions, only that of a limited aperture is measured.

In order to emit radiation as fluorescence, a molecule must first absorb radiation. The higher the molar absorptivity (ε), the more intensely fluorescent a compound will be. Because fluorescent emission in organic compounds comes predominately

from the higher singlet state, it is often found that the quantum efficiency (φ) is independent of the excitation wavelength.[51] For highly fluorescent molecules, such as fluorescein, under some conditions φ approach one.

In theory, the observed fluorescence intensity, which is only a fraction of I_F because of instrumental factors, is proportional to both the solute concentration and to the intensity of the exciting light source at the absorption wavelength, suggesting the more intense the light source the greater the fluorescence. However, in practice a highly intensive radiation source can cause photodecomposition of the sample, therefore a moderate intensity is used.

1.2.3 Advantages of fluorescence

One of the most attractive features of fluorescence methods is their inherent sensitivity, with detection limits often being one to three orders of magnitude smaller than those encountered in absorption spectroscopy. Typical detection limits are in the parts-per-billion range. As fluorescence is measured at right angles to the incident beam, it is considered a zero background technique.

Another advantage of fluorescence methods is their large linear concentration ranges, which are often significantly greater than those encountered in absorption methods.

Finally, the selectivity of fluorescence procedures is often better than that of absorption methods. Fluorescence methods, however, are much less widely applicable than absorption methods because of the relatively limited number of chemical systems that can be made to produce luminescence. [44]

1.2.4 Limitations of fluorescence [51]

The principle disadvantage of fluorescence as an analytical tool is its serious dependence on the environment (temperature, pH, ionic strength, etc.).

1.2.4.1 Photochemical decomposition

The ultraviolet bright light used for excitation may cause photochemical changes in, or destruction of, the fluorescent compound, giving a gradual decrease in the intensity reading. In a practical sense one can take three measures to avoid

photochemical decomposition: (a) always use the longest wavelength radiation for excitation; (b) measure the fluorescence of the sample immediately after excitation, not allowing the exciting radiation to strike the sample for long periods; (c) protect photochemically unstable standard solutions, such as quinine sulphate, from sunlight and ultraviolet laboratory light by storing in a black bottle.

1.2.4.2 Quenching

Quenching, the reduction of fluorescence by a competing deactivating process resulting from the specific interaction between a fluorophore and another substance present in the system, is also frequently a problem.

The general mechanism for the quenching process can be denoted as follows:

$$M + h\nu \rightarrow M^* \qquad \text{(light absorption)}$$

$$M^* \rightarrow M + h\nu \qquad \text{(fluorescence emission)}$$

$$M^* + Q \rightarrow Q^* + M \qquad \text{(quenching)}$$

$$Q^* \rightarrow Q + \text{energy}$$

Sometimes also, $M + Q \rightarrow [MQ]$

or $M^* + M \rightarrow [MM^*]$

etc.

Four common types of quenching are observed in luminescence processes: temperature, oxygen, concentration, and impurity quenching. One of the most notorious quenchers in organic solvents is dissolved oxygen, which causes a reduction in fluorescence intensity and a complete destruction of phosphorescent intensity; however, oxygen quenching is not usually serious in aqueous solutions. Small amounts of iodide and nitrogen oxides are very effective quenchers and interfere.

Small amounts of highly absorbing substances like dichromate interfere by robbing the fluorescent species of the light available for excitation. For this reason most workers prefer not to wash their cuvettes with dichromate cleaning solution.

Temperature quenching. As the temperature is increased, fluorescence decreases. The degree of temperature dependence varies from compound to compound. Tryptophan, quinine, and indoleacetic acid are compounds whose fluorescence varies greatly with temperature. The change in fluorescence is normally 1% per 1°C; however, in some compounds, such as Tryptophan or Rhodamine B, it can be as high as 5%. Temperature effects on luminescence are a type of excited-state quenching by encounter. The fluorescence changes are mainly those of molecular activity with temperature, which suggests that increasing temperature increases molecular motion and collisions, and hence robs the molecule of energy.

Concentration quenching. Absorption causes many problems during a fluorometric assay, just as fluorescence causes a problem when the absorbance of a solution is measured.

In order for fluorescence to be observed absorption must occur. The fluorescence intensity is proportional to the molar absorptivity: the more highly absorbing the substance, the greater its fluorescence. However, when the absorption is too large, no light can pass through to cause excitation. Thus, at low concentrations, when the absorbance is less than about 0.05, there is a linear relationship between fluorescence and concentration. At intermediate concentrations the light is not evenly distributed along the path of light. The portion of the solution nearest the light source absorbs so much radiation that less and less is available for the rest of the solution. As a result, considerable excitation occurs at the front of the solution, but less and less occurs throughout the rest of the cell. This type of concentration quenching causes a fluorescence loss that is called the inner-filter effect.

1.2.5 Fluorophores

Fluorophores can be broadly divided into two main classes: intrinsic and extrinsic. Intrinsic fluorophores are those which occur naturally. They include the aromatic amino acids — tryptophan, tyrosine and phenylalanine in proteins, vitamin A and B2, NADH derivatives of pyridoxal and chlorophyll. Extrinsic fluorophores are added to the sample to provide fluorescence when none exists or to change the

spectral properties of the sample. Indeed, there are many instances when the molecule of interest is non-fluorescent or when the intrinsic fluorescence is not adequate for the desired experiment. For example, in the case of proteins, it is frequently desirable to label them with chromophores that have longer excitation and emission wavelengths than the aromatic amino acids.[52]

A variety of fluorophores have been used in this study, and the structure, and brief descriptions of each fluorophore are given below and in table 1.3. The energy capture efficiency of a fluorescent dye is expressed as the extinction coefficient (ε) and usually ranges from 10000 – 250000 $cm^{-1}M^{-1}$. The emission efficiency is expressed as the quantum yield or quantum efficiency (φ), and usually ranges from 0.05 – 1.0. Quantum yield is strongly influenced by the local environment and so is not usually reported as a 'constant' like the extinction coefficient. The best fluorophores will have both a high extinction coefficient and high quantum yield.

1.2.5.1 Fluorescein isothiocyanate

A more detailed description of fluorescein isothiocyanate (FITC) can be found elsewhere.[53] The structure and spectral characteristics of FITC are shown in figure 1.7 and table 1.3.

Advantages: high extinction coefficient, excellent fluorescence quantum yield (~0.9) and good water solubility.

Disadvantages: relative high rate of photobleaching and pH-sensitive fluorescence that is significantly reduced below pH 7.0 (pK_a ~6.4).

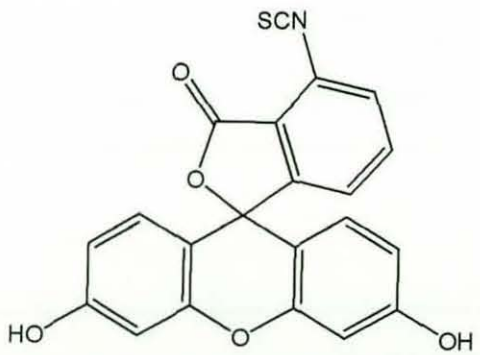

λ_{ex} = 494 nm, λ_{em} = 520 nm, MW = 389.4

Figure 1.7 Structure of FITC, Isomer I

1.2.5.2 BODIPY Dyes

The BODIPY dyes are dibenzopyrrometheneboron difluoride compounds. All the BODIPY dyes have a difluoro-bora-diaza-indacene structure. Different substituents are then added onto this basic structure to produce different BODIPY dyes with different excitation and emission wavelengths. Numerous sources of information can be found on these fluorophores.[54-56] The particular BODIPY dyes that have been used in this study are shown in figure 1.8 and 1.9, and their spectral characteristics can be seen in table 1.3.

Advantages: high extinction coefficients, high fluorescence quantum yields (often approaching 1.0, even in water), greater photostability than fluorescein – they remain intensely fluorescent even when constantly illuminated.

Disadvantages: expensive (~ £188 per 5 mg) and small Stokes shift (~10 nm).

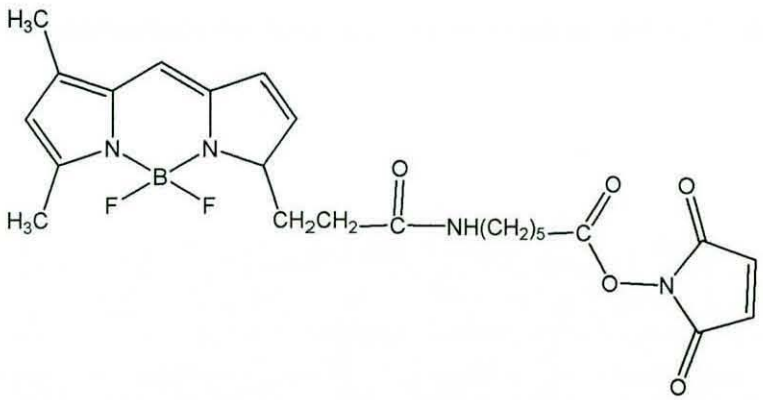

λ_{ex} = 504 nm, λ_{em} = 513 nm, MW = 502.32

Figure 1.8 Structure of BODIPY ® FL-X, SE

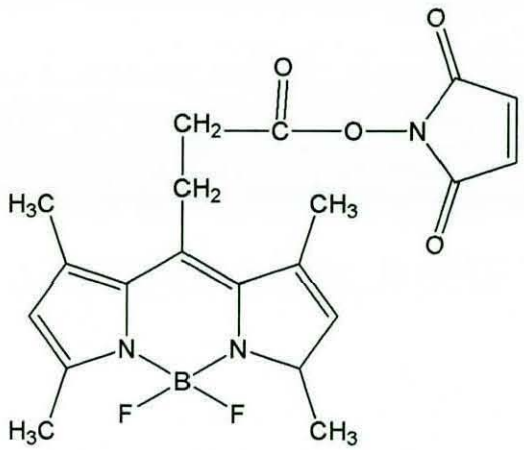

λ_{ex} = 500 nm, λ_{em} = 509 nm, MW = 417.22

Figure 1.9 Structure of BODIPY ® 493/503, SE

Table 1.3 Spectral characteristics of the dyes [57]

Dyes	λ_{abs}*	λ_{em}*	ε #	CF_{280}♦
BODIPY ® FL-X, SE	504	513	68 000	0.04
BODIPY ® 493/503, SE	501	508	87 000	0.14
FITC	494	518	73 000	0.20

* Absorbance and fluorescence emission maxima in nm
# Extinction coefficient at λ_{Max} in $cm^{-1}M^{-1}$
♦ Correction factor (A_{280} free dye / A_{max} free dye)
ε and CF_{280} employed for calculating the final dye: protein ratio

1.2.6 Fluorigenic substrates

In this work two of fluorigenic substrates or fluorophores conjugates have been investigated and thus a brief description of each is given.

1.2.6.1 Fluorescein digalactoside [58]

Fluorescein di-β-D-galactopyranoside (FDG) is a fluorigenic substrate for β-galactosidases (β-gal). Nonfluorescent FDG is sequentially hydrolyzed by the enzyme, first to fluorescein monogalactoside (FMG) and then to highly fluorescent fluorescein (figure 1.10)

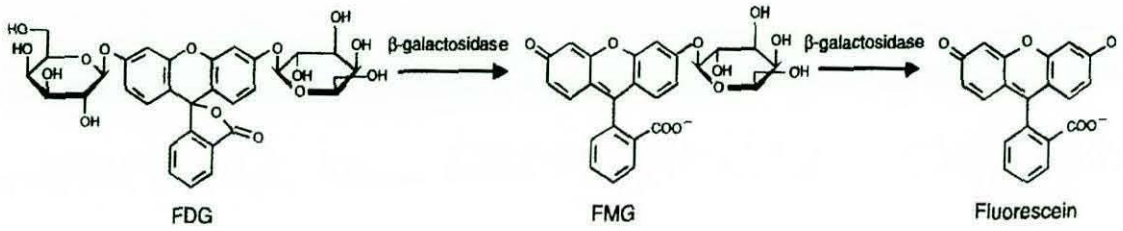

Figure 1.10 Sequential hydrolysis of FDG to FMG and fluorescein by β-gal

The K_m for FDG conversion to FMG has been determined to be approximately 18 μM, although much higher values (>600 μM) have also been reported. The turnover rate for hydrolysis of FDG to FMG (1.9 μmol min^{-1} mg^{-1}) is much slower than for conversion of FMG to fluorescein (22.7 μmol min^{-1} mg^{-1}). Low levels of β-gal activity are readily detectable with FDG due to the superior spectral characteristics of fluorescein.

1.2.6.2 Fluorescein diphosphate [59]

Fluorescein diphosphate (FDP) is a fluorigenic alkaline phosphatase substrate that was first described in 1963 and has been isolated in pure form and made commercially available by Molecular Probes. Molecular Probes' researchers have used the substrate in an alkaline phosphatase-based enzyme-linked immunosorbent assay (ELISA), finding that it provided a detection limit 50 times lower than that obtained with the chromogenic substrate, p-nitrophenyl phosphate. The high pH used to monitor alkaline phosphatase activity is advantageous as it also produces optimal absorptivity and fluorescence of fluorescein. FDP is colourless and nonfluorescent. Sequential alkaline phosphatase mediated hydrolysis of the two phosphate substituents (figure 1.11) yields weakly fluorescent fluorescein monophosphate followed by strongly fluorescent fluorescein (excitation/emission ~490/518 nm).[60]

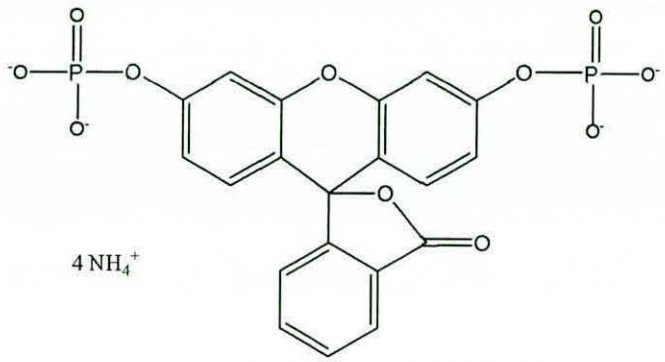

Figure 1.11 Structure of fluorescein diphosphate (FDP)

1.3 FLOW INJECTION ANALYSIS

The theory, application and developments of flow injection analysis (FIA) are covered by many papers and books.[61-66] The term 'flow injection analysis' was first used by Ruzica and Hansen in 1975,[67] who described the use of sample injection directly into an unsegmented flowing stream for rapid continuous – flow analysis. FIA is now widely used and well characterized; its simple basis, relatively inexpensive equipment and ease of result generation are excellent in view of the rapidity, accuracy and precision with which results are obtained. The critical features of FIA can be described as: unsegmented flow, direct injection, controlled partial dispersion and reproducible operational timing.

The fundamental scheme of an FIA system is shown in figure 1.12.

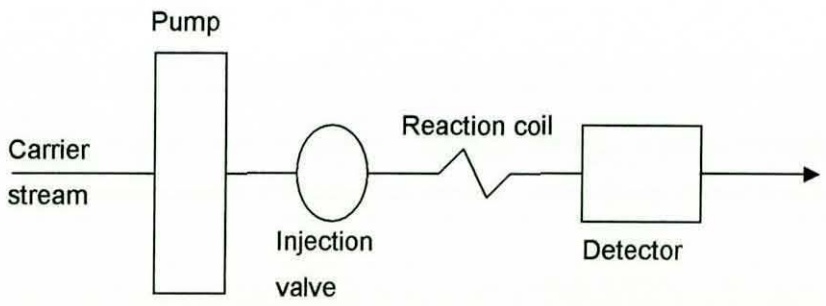

Figure 1.12 Schematic diagram of a single line FIA manifold

Usually, a FIA system consists of four components:

A **propelling unit,** which produces the flow of one or several solutions, either containing a dissolved reagent or merely acting as carriers. This function can be performed in various ways, for example by a pump, a gas-pressure system or even gravitation.

An **injection system,** which allows the reproducible insertion or introduction of an accurately measured sample volume into the flow without stopping it.

A **length of tubing**, along which the transport operation takes place, this is referred to as the reactor. Dispersion of the sample plug into the carrier or reagent takes place as the plug passes along the tube, also there may be chemical reactions occurring.

A **flow cell**, accommodated in a detector (e.g. photometer, fluorimeter, colorimeter) which transduces some property of the analyte into a signal to a recorder or a PC with a data handling package.

The flow emerging from the sensing system usually goes to waste, although it is sometimes recirculated through the peristaltic pump to achieve greater constancy of flow rate. The signal obtained from FIA techniques is transient. A typical FIA peak is shown in figure 1.13.

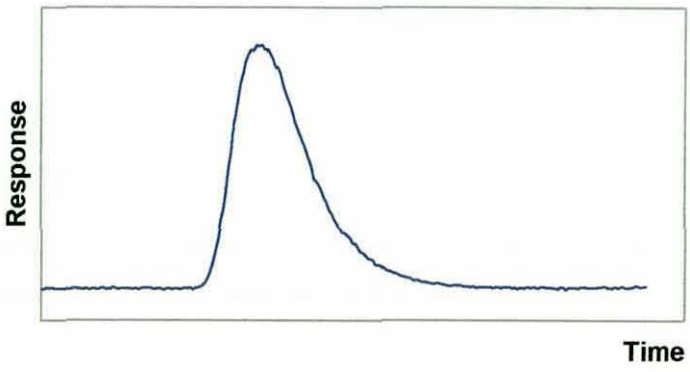

Figure 1.13 A typical FIA peak

The parameters of the peak shape are affected by the flow rate of the carrier, the injected volume, the length and bore of the manifold, the viscosity of the sample and carrier and the detector and recording system time constant.

In FIA, immediately after injection through the sampling valve, a sample zone is formed in the flow injection apparatus, which has a rectangular concentration profile. As it moves through the tubing, band broadening or dispersion takes place. If the sample dispersion is due to convection, the flow profile is characterised by a parabolic head and tail. This type of flow is characteristic of most flow injection systems. If this were the only mass transport process operating, the peak would have an infinitely long tail, as the velocity at the walls of the tubing is zero. Two additional mass transport processes are operating; molecular diffusion in the longitudinal direction (parallel to direction of flow). The longitudinal diffusion is small compared with the dispersion due to the flow velocity and can be ignored under the conditions of most flow injection experiments. Radial diffusion moves sample molecules to and from the tubing walls, where the radial flow velocity profile is zero towards the centre of the tube, where the mass flow velocity is at maximum. The net result of radial diffusion is that a peak with a finite peak width is obtained. Radial diffusion becomes more important as the residence time of the sample increases, at long residence times, primarily the radial diffusion process controls the dispersion product process and the peak shape assumes a symmetrical Gaussian shape.

Dispersion (D) is defined by equation

$$D = C_0 / C$$

Where: C_0 is the analyte concentration of the injected sample.

C is the peak concentration at the detector.

Dispersion is readily measured by injecting a dye solution of known concentration (C_0) and then measuring the absorbance in the flow cell. After calibration, C is calculated from Beer's law. Dispersion is influenced by the three interrelated and controllable variables: sample volume, tube length, and pumping rate.

1.4 ENZYMES

1.4.1 Introduction to enzymes

Enzymes are biological catalysts. They increase the rate of chemical reactions taking place within living cells without themselves suffering any overall change. The reactants of enzyme-catalysed reactions are termed substrates and each enzyme is quite specific in character, acting on a particular substrate or substrates to produce a particular product or products.

Enzymes are proteins. However, without the presence of a non-protein component called a cofactor, many enzyme proteins lack catalytic activity. When this is the case, the inactive protein component of an enzyme is termed the apoenzyme, and the active enzyme, including cofactor, the holoenzyme. The cofactor may be an organic molecule, when it is known as a coenzyme, or it may be a metal ion. Some enzymes bind cofactors more tightly than others. When a cofactor is bound so tightly that it is difficult to remove without damaging the enzyme it is sometimes called a prosthetic group.[68]

To summarize diagrammatically:

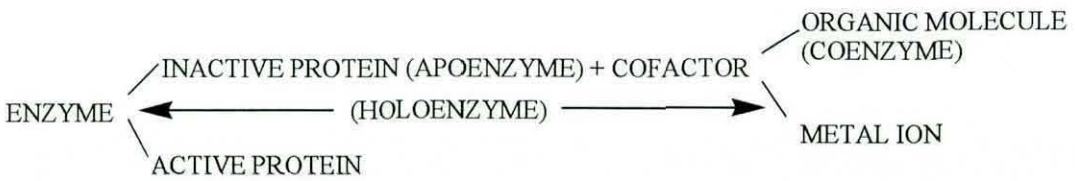

Enzymes are valuable analytical tools and offer sensitive and specific methods of quantitation for many substances. The increasing availability of highly purified enzyme preparations, both in solution and in immobilized forms permits the development of a wide range of methods.

Many sources of literature covering the structure function and basic concepts of enzymes are available for a more detailed discussion.[68-75]

1.4.2 Factors affecting enzyme activity

Several factors affect the rate at which enzymatic reactions proceed: temperature, pH, and the presence of any inhibitors or activators.

Like most chemical reactions, the rate of an enzyme-catalysed reaction increases as the temperature is raised to a maximum level, known as the optimum temperature. Activity then abruptly declines with further increase of temperature, normally due to denaturation of the enzyme.

Enzymes are affected by changes in pH. The most favourable pH – the point where the enzyme is most active – is known as the optimum pH. Extremes of pH generally result in complete loss of activity for most enzymes where activity may not be restored even after re-adjustment of the pH.

Enzyme inhibitors are substances that alter the catalytic action of the enzyme and consequently slow down, or in some cases, stop catalysis. Enzyme inhibition is discussed in more detail in section 1.6.

Activators are substances that increase the catalytic activity of an enzyme, are used in very small amounts and which, unlike coenzymes; do not participate in the enzyme reaction.

1.4.3 Free enzymes

Three different enzymes have been investigated in this work and thus a brief description of each is given below. An extremely comprehensive book covers databanks, name and history, activity and specificity, structural chemistry, preparation, biological aspects, and distinguishing features of enzymes known to date.[76,77]

1.4.3.1 Alkaline proteases

Alkaline proteases (AlkP, EC 3.4.24.31) are one of the most important groups of industrial enzymes produced commercially and are used in the detergent, protein, brewing, meat, photographic, leather, and dairy industries.[78] These enzymes offer advances over the use of conventional chemical catalysts for numerous reasons, for example they exhibit high catalytic activity, a high degree of substrate

specificity, can be produced in large amounts and are economically viable. One of the commercial applications of the enzymes is the possibility of using them to catalyse peptide synthesis and to resolve racemic mixtures of amino acids.[79] AlkP can be obtained from different sources such as bacteria, fungi, or certain insects. Brief properties of the enzymes are: enzyme type: serine protease, MW: 50,000, specificity: broad, pH: maximal activity at pH 11.0, additional information: type XXI protease.[77] AlkP is covered in more detail elsewhere.[80-82]

1.4.3.2 Alkaline phosphatase

Alkaline phosphatase (AP, EC 3.1.3.1) from bovine intestine mucosa is a homodimeric metalloenzyme, which hydrolyses non-specifically phosphate monoesters at alkaline pH with release of inorganic phosphate and alcohol.[83] AP is found in a variety of tissues and is particularly associated with bone mineralization, but its function and natural substrate are still unknown.[84] The increase in activity of AP can result in painful changes in the bones, hepatitis and tumerigenesis. Alternatively, it can be used as an indicator of normal physiological process such as pregnancy and bone growth. The enzyme is widely used in test systems used to diagnose various diseases, such as hyperparathyroidism, and productions of various therapeutic preparations.[85]

1.4.3.3 β-Galactosidases

β-Galactosidases (β-Gal, EC. 3.2.1.23) are widespread, in microorganisms, plants and animals tissues. This enzyme is responsible for degradation of galactosyl β-linkages in glycolipids, glycoproteins, polysaccharides, and such disaccharides as lactose. Several glycosidases have been purified and their specificities determined.[86-88] The enzyme from *Escherichia coli* (E.coli) is an ideal model enzyme for the study of glycosidases, which act on disaccharides.[89] β-Gal is a glycosidase enzyme with tetrameric structure and one active site per monomer, and its x-ray structure has been determined.[90] The mechanism of action of β-Gal has not been firmly established, but it is generally accepted that it involves a double displacement reaction in which the enzyme forms and hydrolyses a glycosyl enzyme intermediate via an oxocarbonium ion like transition state.[89]

Characteristics of β-Gal from E.coli [91] are MW: 540,000, composition: the enzyme is tetrameric, being composed of four identical subunits of 135000 daltons, each with an active site, which may be independently active. The enzyme is readily fragmented into small peptides. The amino acid analysis indicates approximately 1170 residues per subunit, and optimum pH: 6-8.

1.4.4 Enzyme kinetics

Experimental evidence shows that for many single-substrate enzyme-catalysed reactions a hyperbolic relationship exists between the velocity of the reaction, V and the substrate concentration [S] as shown in figure 1.14.

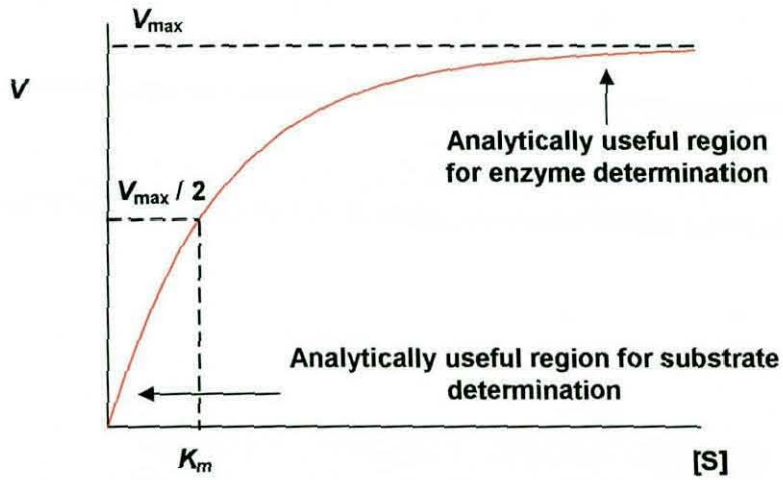

Figure 1.14 Dependence of initial velocity on substrate concentration for a single-substrate enzyme-catalysed reaction

The graph V versus [S] (figure 1.14) shows three distinct regions:

- At low substrate concentration the velocity of the reaction is directly related to the substrate concentration; this is the region of first order kinetics.
- At intermediate substrate concentration there is a big curve, where the velocity of the reaction increases more slowly with increase in the substrate concentration.

- At high substrate concentration V_{max} is attained and the observed velocity is independent of further addition of substrate; this is the region of zero order kinetics.

Kinetic models to explain these findings were proposed by Henri (1903) and Michaelis and Menten (1913). These were essentially similar, but Michaelis and Menten did a great deal of experimental work to give their work a sounder basis. The critical feature in their treatment is that a specific enzyme – substrate (ES) complex is a necessary intermediate in catalysis. The model proposed, which is the simplest one that accounts for the kinetic properties of many enzymes, is:

$$E + S \underset{k_{-1}}{\overset{k_1}{\rightleftharpoons}} ES \xrightarrow{k_2} E + P$$

where E = enzyme, S = substrate, ES = enzyme – substrate complex, and P = product. E combines with S to form ES with a rate constant of k_1. ES then has two fates. It can dissociate to E and S with a rate constant of k_{-1} or proceed to form P with a rate constant of k_2.

$$V = \frac{V_{max}[S]}{K_m + [S]} \qquad \text{(Eq.1.3)}$$

The equation 1.3 is Michaelis-Menten equation. It is a statement of the quantitative relationship between the velocity of the reaction V, the maximum velocity V_{max}, and the substrate concentration [S], all related through the Michaelis-Menten constant K_m.

The meaning of K_m is evident from the Michaelis-Menten equation. When [S] = K_m, then $V = V_{max} / 2$. Thus K_m is equal to a substrate concentration at which the reaction rate is half its maximal value.

The Michaelis-Menten equation gives a hyperbolic curve as shown in figure 1.14. This is not entirely satisfactory for the determination of V_{max} and K_m. Unless, after

a series of experiments, there are at least three consistent points on the plateau of the curve at different [S] values, then an accurate value of V_{max}, and hence of K_m cannot be obtained.

This problem was overcome by Lineweaver and Burk (1934) *without making any* fresh assumptions. They simply inverted the Michaelis-Menten equation thereby conveniently transforming it into a straight-line plot:

$$\frac{1}{V} = \frac{K_m}{V_{max}} \frac{1}{[S]} + \frac{1}{V_{max}} \qquad \text{(Eq.1.4)}$$

This is of the form y = mx + c, which is the equation of *a straight line graph; a plot* of y against x has a slope of m and intercept of c on the y-axis. As shown in figure 1.15, K_m and V_{max} can be read directly from the Lineweaver-Burk plot.

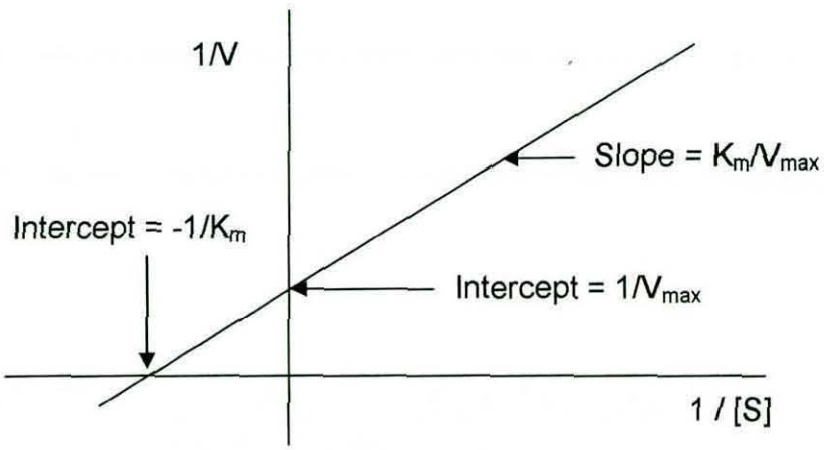

Figure 1.15 The Lineweaver-Burk plot

Numerous sources of literature are available that discuss enzyme kinetics in greater detail.[68,70]

1.4.5 Quenched over-labelled fluorigenic assays for proteolytic enzymes

Assays based on fluorigenic protein substrates, which are over-labelled by suitable fluorophores to such an extent that the dye is efficiently quenched by internal energy transfer in the protein conjugate, have also been employed in many

papers.[92,93] As shown in figure 1.16, upon protease digestion this internal energy transfer is abolished and the virtually non-fluorescent substrates release highly fluorescent dye-labelled peptides, the fluorescence intensity increases being proportional to enzyme activity. This type of protease assay removes the necessity for the separation of substrate from degradation products.

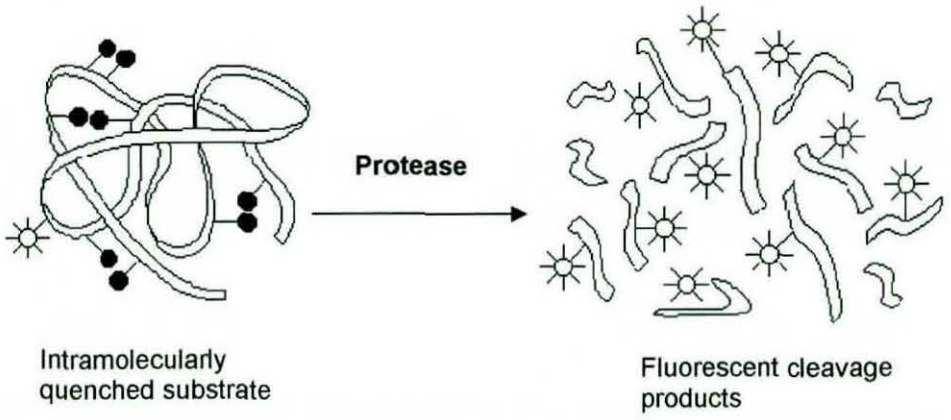

Figure 1.16 Schematic principle of an intramolecularly quenched protein substrate [57]

1.5 IMMOBILISED ENZYMES

The term 'immobilised enzyme' describes an enzyme that has been chemically or physically attached to a water-insoluble matrix, polymerised into a water-insoluble gel, or entrapped within a water-insoluble gel matrix or water-insoluble microcapsule resulting in reduced or complete loss of enzyme mobility. These immobilised enzymes retain their catalytic activity and can be used repeatedly and continuously.[94] The usage of binding enzymes onto solid materials goes back to 1916 when Nelson and Griffin [95] first immobilised invertase on charcoal and observed that the enzyme retained most of its activity over a long period of time. However, this work was largely ignored until the 1950s. Since then immobilisation of proteins in general and enzymes in particular, has been widely studied and the number of applications of immobilised enzymes is increasing. In addition, the application of immobilised enzymes to flow injection analysis systems allows the combination of immobilised enzymes in different arrangements to permit multi-

determination. Many sources of information can be found on the preparation, characteristics, and application of immobilised enzymes for more detailed reading. [96-102]

1.5.1 Why immobilise enzymes?

Immobilised enzymes offer many advantages over their solution analogues, some of which are listed below: [103]

- Low cost, they are economical as they can be used repeatedly and continuously
- Increased stability in storage and use against denaturing conditions such as high temperature, extreme pH, and extreme salt concentrations
- Ease of use as no enzyme solution preparation is required
- They do not contaminate the sample and insoluble enzymes can be easily recovered from the reaction medium in case of batch analysis, while in the case of continuous flow system; samples are made to pass through immobilised enzyme reactors, resulting in controlled product formation
- Rapid termination of reactions, especially in flow systems
- Less susceptibility to the normal activators and inhibitors of the enzyme, therefore much more useful, for complex analytical samples such as blood
- The possibility of simultaneous determinations, due to the greater variety of designs available for the use of immobilised enzymes in flow systems

1.5.2 Methods of immobilisation

Immobilised enzymes are classified by methods as given in figure 1.17.

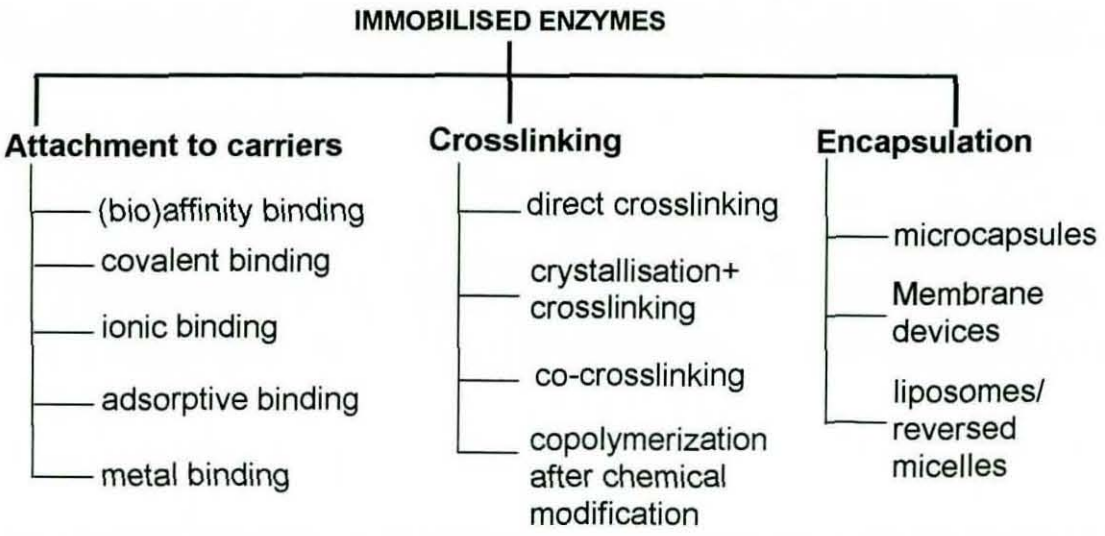

Figure 1.17 Classification of methods employed for enzyme immobilisation [96]

1.5.3 Immobilised enzyme support [94]

The support material can have a critical effect on the stability of the enzyme and the efficiency of enzyme immobilisation, although it is difficult to predict in advance which support will be most suitable for a particular enzyme. The most important requirements for a support material are that it must be insoluble in water, have a high capacity to bind enzyme, be chemically inert and be mechanically stable. The enzyme binding capacity is determined by the available surface area, both internal (pore size) and external (bead size or tube diameter), the ease with which the support can be activated and the resultant density of enzyme binding sites. The inertness refers to the degree of non-specific adsorption and the pH, pressure and temperature stability. In addition, the surface charge and hydrophilicity must be considered. The activity of the immobilised enzyme will also depend upon the bulk mass transfer and local diffusion properties of the system.

Due to the often-conflicting requirements of a good support, various materials have been used. At present there is not a universally recommended support, the final choice being a compromise for each particular enzyme and experimental system. The type of support can, however, be conveniently classified into one of three categories:

- Hydrophilic biopolymers based on natural polysaccharides such as agarose, dextran and cellulose.
- Lipophilic synthetic organic polymers such as nylon, polystyrene, polyacrylamide and bis-acrylamide/ azlactone copolymer.
- Inorganic materials such as controlled pore glass and iron oxide.

In this work UltraLink® Biosupport Medium was used and thus a brief description of it is given below.

1.5.3.1 UltraLink® biosupport medium [104]

Pierce UltraLink® biosupport medium is a preactivated, ready-to-use bead designed for use in affinity chromatography. These beads are composed of a bis-acrylamide/ azlactone copolymer that is slightly hydrophobic in its active forms and highly cross-linked. Because the azlactone functionality is copolymerised with the matrix material, the binding capacity is an integral part of the bead. This results in a high level of functionality throughout the porous bead matrix.

The support is provided in dry form and reacts rapidly with nucleophiles, which allows coupling to a wide range of proteins and small molecules. The beads average 50-80 microns in diameter with a very open architecture that provides both high surface area and high pore volume. Due to the rigid polymeric nature of this support, it has excellent utility in medium-to-low pressure chromatography applications.

The azlactone functionality of the UltraLink® biosupport medium couples nucleophiles on ligands via a ring reaction to attach the ligand to the support through stable covalent linkages (figure 1.18). For example, amino-functional byproduct as a result of the coupling reaction, therefore this coupling chemistry is extremely safe and easy to use.

Characteristics of UltraLink® biosupport medium are pH stability of matrix: 1-13, temperature stability: 4-40 °C, average particle size: 50-80 microns, pore size: 1000 Å, swell volume: 8 ml gel/g beads

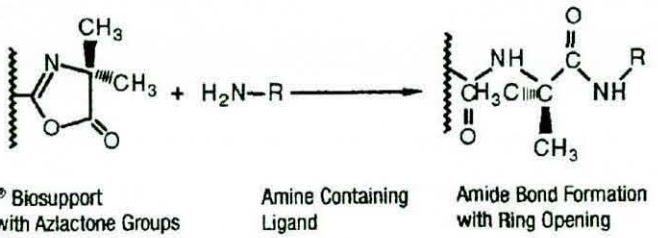

Figure1.18 Reaction of azlactone ring on UltraLink® Biosupport Medium with amine-containing ligand.

1.5.4 Changes in enzyme properties after immobilisation

Immobilisation of an enzyme results in a change in many of the physical kinetic properties of the corresponding soluble counterparts. This may be due to a considerable change in the microenvironment of the enzyme. Among the changes in physical properties, the storage and temperature stabilities are prominent. Numerous enzymes have been reported with an increase in long-term storage and thermal stability. Sulphite oxidase, which in the soluble form loses its activity rapidly (20% after six hours) at room temperature, when immobilised on controlled pore glass (CPG) shown no loss in activity for months in spite of continuous use at 25 °C.[105,106] This increase in stability may be due to the stabilisation of the native structure of enzyme. Immobilisation also has profound effect on the optimal pH. Depending on the nature of the carrier, the pH may shift towards a higher or lower value. Goldstein et al.[107] studied this phenomenon in detail. If the carrier used for immobilisation is negatively charged, then more positively charged ions, mainly H^+, will accumulate at the boundary layer between the carrier and surrounding solution. To compensate for that, the pH of the bulk solution has to be displaced towards more alkaline pH. If the carrier is positively charged the opposite may occur.

Enzyme kinetics and therefore reactivity are changed after immobilisation, possibly due to the placement of the enzyme in a new environment. The charge on the carrier may also contribute to change in the rate constants. Excellent discussions on this aspect are available.[108,109]

1.5.5 Analytical applications of immobilised enzymes

Immobilised enzymes have been used for a long time in industry for biotechnological purposes, and in clinical, food and environmental analysis. Many reviews [96,110] exist on their analytical applications. In a wide variety of applications, immobilised enzymes have been used in electrodes or in the form of enzyme reactors. A brief description of them is given below:

1.5.5.1 Immobilised enzyme electrodes

An immobilised enzyme electrode is an electrochemical sensor on whose surface is attached a thin layer of enzyme. The outer surface of the enzyme exposed to the analyte is covered with a semi permeable membrane to protect the enzyme and allow the passage of substrate and product. The electrode is dipped into the analyte solution, which is stirred continuously to speed up mass transfer and provide fast response. The principle of such an electrode is shown in figure 1.19.

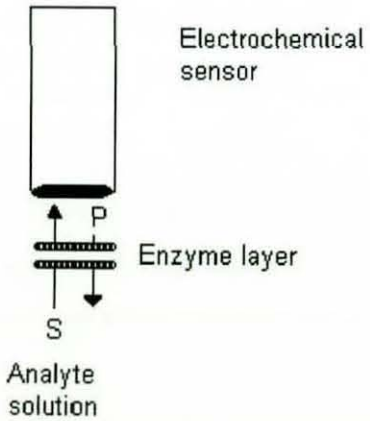

Figure 1.19 Principle of an immobilised enzyme electrode

When the enzyme electrode is immersed in a sample solution, the substrate diffuses into the enzyme layer, where it is converted into a product, which then diffuses out of the enzyme layer to the electrode. Since the conversion of substrate to product depletes the available concentration of substrate a concentration gradient of both substrate and product is formed. After some time (0.5-10 min) a steady state is reached where the rate of supply and rate of consumption of substrate and rate of transfer to the electrode becomes constant. Quantitative measurements either at steady state or during the initial stages of the reaction can be made.

Enzyme electrodes have been used for analysis of an analyte alone[105] or in a mixture.[111] These electrodes are very handy, easy to use and are cheap, but the disadvantages associated with their use are their long response and recovery times and their poor reproducibility.

1.5.5.2 Immobilised enzyme reactors

The reactors are columns holding immobilised enzymes on appropriate supports. Solutions carrying analyte can be made to pass through and react with enzyme, the enzyme being retained, while the product is carried to the detector. The advantage of these reactors is that almost any detector system can be used which can record the concentration of substrate, a product or coenzyme. Principally there are two types of reactors, packed-bed and open-tubular, both of which have been used successfully in flow systems. Jurkiewicz and Alegret[112] studied a comparison of flow injection analytical biosystems based on open-tube and packed-bed enzyme reactors with three different enzymes (urease, creatinin iminohydrolase and creatine aminohydrolase).

a) Packed-bed reactors

Packed-bed reactors are receiving much attention. Their use was previously avoided because of the pressure drop across the column, but nowadays with the introduction of inorganic supports like glass beads, that problem has disappeared. These supports do not swell on packing, so that the pressure drop is minimised. Such reactors are easily prepared by packing a column of fixed volume with

immobilised enzyme (figure1.20a). The unique advantage of a packed-bed reactor is its large surface area, thus it has the potential of providing a relatively larger number of immobilised enzyme molecules, therefore making possible the almost complete conversion of substrate into product.

b) Open-tubular reactors

Such reactors are comparatively difficult to construct. They are prepared by covalently immobilising enzymes onto the inner wall of tubing made of nylon or polyacrylamide (figure 1.20b). The advantages of open-tubular reactors are:

- Low pressure drop
- They are well suited for air-segmented analysers (autoanalysers).
- Blood samples do not block the reactors.
- Their commercial availability.

The problem associated with these reactors is the small amount of enzyme that can be attached to the inner wall of the tube owing to small surface area. Thus to achieve reasonable conversion of the substrate to product, a very long reactor would be required, which in turn would increase the dispersion.[113] Also radial mass transfers to the walls in an open tube with a flowing liquid may be prohibitively slow.

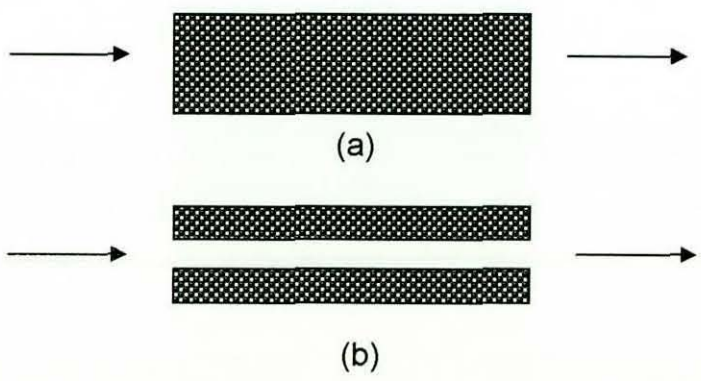

Figure 1.20 Immobilised enzyme reactors (a) packed-bed (b) open-tubular

1.5.6 Immobilised enzymes in FIA

Immobilised enzymes were introduced in a continuous flow system around 1974.[114] Since that time a variety of FIA methods using immobilised enzymes appeared, which shows their usefulness in many areas of application especially for the determination of enzyme substrates.[115,116]

Until 1988, of publications that appeared for the determination of substrates 30% of them dealt with glucose determination. This may be due to its clinical importance, as it is most frequently determined in clinical laboratories, or it may be due to the availability and cost of glucose oxidase, and perhaps also due to the high stability of this enzyme after immobilisation. Both areas (clinical and food) take advantage of high enzyme selectivity, so that enzymatic reactions can be applied to complex matrices like whole blood, serum, urine and all types of food and drinks.

As the knowledge of FIA is developing more interesting applications of immobilised enzymes appear. Starting from the determination of a single analyte by using a single immobilised column, and progressing towards the determination of five or six analytes [117] in a sample demonstrates the advances in enzymatic methods in FIA. Analysis of more than one analyte is made possible by placing more than one reactor in series or parallel like determination of ethanol and aldehyde by immobilised alcohol dehydrogenase and aldehyde dehydrogenase, placed parallel to each other and determination of glucose and sucrose by immobilised invertase and mutarotase placed in series.[118,119] A plug of analyte mixture is split into sub-plugs before transfer to enzyme reactors.

In spite of the high selectivity of enzymes for their substrates, sometimes interferences appear from the real samples e.g. blood and urine, in which ascorbic acid, uric acid and NH_3 may reduce the system applicability.

However, a system's selectivity can be increased in several ways:

- By the application of dialyser units or liquid chromatographic columns.[119]
- By using appropriate reactors, this can eliminate the interfering species. It may be enzyme reactors (e.g. use of immobilised ascorbate oxidase to eliminate interference of ascorbic acid in the determination of fructose).[120]

After the exploitation of the advantages of immobilised enzymes in conjunction with FIA for chemical analysis, the technique has also been extended to process analysis. Conventionally, most industrial analyses are carried out off-line and face problems like limited reliability, time consumption and extra labour to deal with large number of samples for analysis. FIA with immobilised enzyme reactors can give reliable determinations of analytes in media originating from food and fermentation.

The use of immobilised enzymes in FIA is not limited to the determination of enzyme substrates, but is also gaining attention for the determination of many enzyme inhibitors.

1.6 ENZYME INHIBITION

There are a variety of natural and synthetic compounds, which have the ability to inhibit specific enzymes and reduce or eliminate their catalytic activity. Drugs, metal ions and many other substrates are among such inhibitors.

Enzyme inhibiting processes may be divided into two main classes, reversible and irreversible, depending upon the manner in which the inhibitor (or inhibitor residue) is attached to the enzyme. Reversible inhibitors bind to an enzyme in a reversible fashion and can be removed by dialysis (or simply dilution) to restore full enzyme activity whereas irreversible inhibitors cannot be removed from an enzyme by dialysis. Sometimes it may be possible to remove an irreversible inhibitor from an enzyme by introducing another component to the reaction mixture, but this would not affect the classification of the original interaction.

1.6.1 Reversible inhibition

Reversible inhibition occurs if an inhibitor is bound non-covalently at the active site of the enzyme. Three distinct mechanisms of reversible inhibition are known and are recognized by the effect of substrate concentration on inhibition.

1.6.1.1 Competitive inhibition

In competitive inhibition, the inhibitor (I) may or may not be similar to the substrate, and attacks at the active site or close to the active site of the enzyme in a reversible fashion:

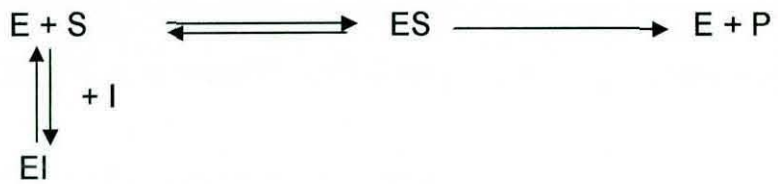

As shown above EI and ES complexes are formed and no ESI complex appears in this type of inhibition. A high concentration of substrate can overcome this inhibition by making the reaction process towards ES and then product formation.

The physical interpretation of competitive inhibition is that the inhibitor can reversibly bind with enzyme and compete with substrate for the binding site. Inhibitor can only bind with the free enzyme and not with the ES complex. By increasing the substrate concentration, inhibition decreases. From the kinetic expression it can be seen in figure 1.21a that in the presence of a competitive inhibitor the reaction reaches half of its maximum velocity at high substrate concentration i.e. the y-intercept of the Lineweaver-Burk plot remains the same and the value of K_m is increased, which is the characteristic of competitive inhibition.

1.6.1.2 Uncompetitive inhibition

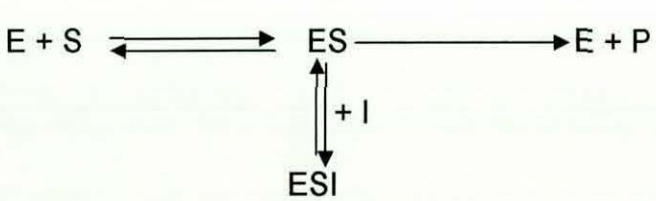

In uncompetitive inhibition, inhibitors only bind with the ES complex and not with the free enzyme. In this case a high concentration of substrate cannot reverse the inhibition, but increased substrate concentration increases the inhibition. In this case the rate of reaction cannot reach half of its maximum velocity i.e. the intercept and the value of K_m are decreased (figure 1.21b).

1.6.1.3 Noncompetitive inhibition

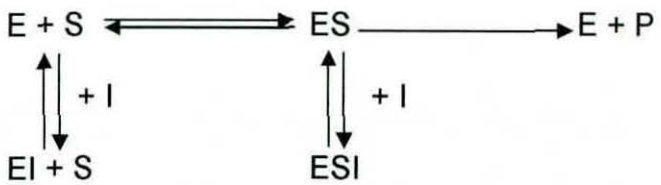

Noncompetitive inhibitors decrease the catalytic activity of an enzyme without influencing the binding relationship between the substrate and enzyme. It means that inhibitor and substrate can bind at the same site to an enzyme to form ES, EI and ESI complexes. Noncompetitive inhibition completely depends on the inhibitor concentration and is unaffected by the substrate concentration.

The Lineweaver-Burk plot is one way of visualizing the effect of inhibitors and determining the Michaelis-Menten constant, K_m and the maximum velocity, V_{max} from a set of measurements of velocity at different substrate concentrations. If $1/V$ is plotted against $1/[S]$, a straight line is obtained where the slope is equal to K_m/V_{max} and the y-intercept is equal to $1/V_{max}$. This method is usually used for distinguishing the type of inhibition. This information is used to select the appropriate type of plot needed to calculate the inhibition constant, K_i. The Lineweaver-Burk plots of three modes of reversible inhibition are shown in figure 1.21a, b, and c.

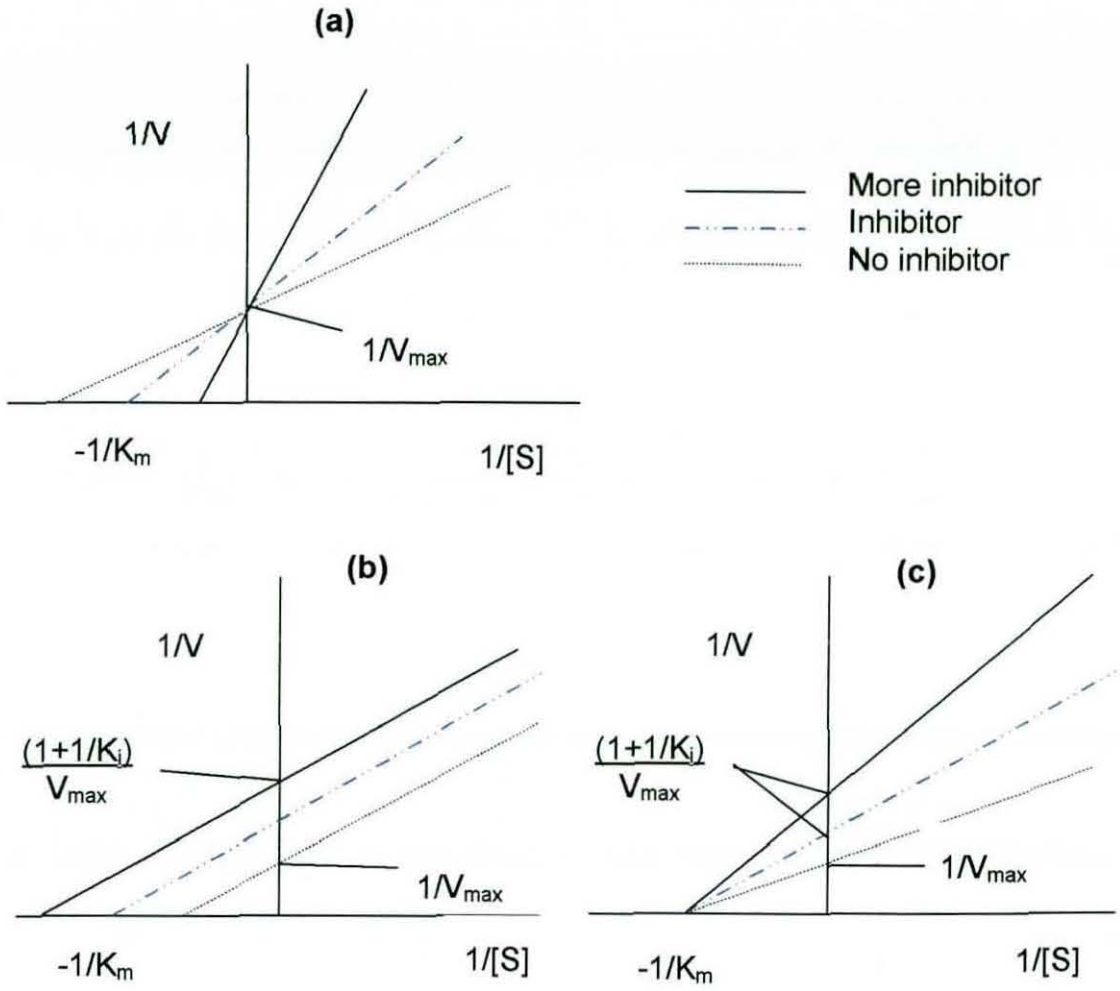

Figure 1.21 Lineweaver-Burk plot for different modes of reversible inhibition

where a, b, and c show competitive, uncompetitive and noncompetitive inhibition respectively

1.6.2 Irreversible inhibition

Irreversible inhibition occurs when an inhibitor binds to active site of the enzyme by an irreversible reaction and cannot subsequently dissociate from it. A covalent bond is usually formed and the inhibitor may act by preventing substrate binding or it may destroy some component of the catalytic site. In such type of inhibition the enzymatic activity cannot be reversed by dilution on dialysis.[121]

1.7 ENZYME INHIBITORS

In setting out to find new inhibitors of a particular enzyme, an early decision that must be made is where to look. Chemical synthesis of new compounds designed to be inhibitors of the enzyme probably is the most common approach. Random or selective screening of existing synthetic compounds can be a source of leads to new structural types of inhibitors. Extraction of naturally occurring inhibitors from animal tissues or plants has been another source.[122]

In this work some of inhibitors have been investigated and thus a brief description of each is given. Comprehensive accounts of different enzyme inhibitors can be found in excellent references.[123-125]

1.7.1 3-Nitrophenylboronic acid

3-nitrophenylboronic acid (3-NPBA) is a reversible competitive serine protease inhibitor with a molecular weight of 166.93 and acts as a transition state analogue. Saccharides have been shown to act as a 'co-inhibitor' in the boronic acid inhibition system.[126] Raghavendra and Prakash investigated the kinetics of inhibition of lipase by phenylboronic acid.[127] Investigation into the mechanism of binding of peptide boronic acids to proteases has been carried out.[128,129]

1.7.2 Vanadate

Vanadate has a wide variety of effects in biological systems. Vanadate has multiple biologic effects, including inhibition of alkaline phosphatases and protein tyrosine phosphatases. The biologic effects of vanadate are very diverse, depending on the target cell and the concentration of vanadate. Vanadate has been shown to activate certain signal transduction mechanisms.[130] In vitro vanadate has been shown to be a reversible inhibitor of phosphatases with a micromole/litre affinity.[131] This may arise because of the ability of vanadate to adopt a trigonal bipyramidal structure that mimics the transition state in phosphoryl transfer reactions.[132]

1.7.3 Phenylethyl β-D-thiogalactopyranoside

Phenylethyl β-D-thiogalactopyranoside (PETG) is a potent competitive inhibitor of β-galactosidase with K_i ranging from 0.94 - 2.5 μM.[133] PETG has a thiol group substituted for the hydroxyl linkage present in compounds that β-galactosidase normally hydrolyzes (figure 1.22).[134] PETG when present in a reaction would be expected to occupy the enzyme and thus inhibit its action on hydrolysable substrates such as FDG.

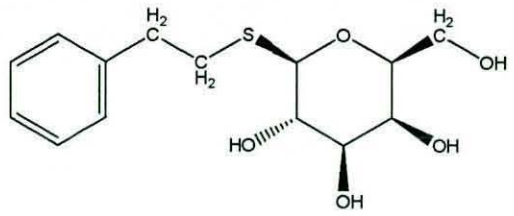

Figure 1.22 Molecular structure of phenylethyl β-D-thiogalactopyranoside

CHAPTER 2

CHEMOMETRICS: MULTIVARIATE CALIBRATION

2.1 WHAT IS CHEMOMETRICS?

A general definition of chemometrics is "the use of statistical and mathematical techniques to analyze chemical data".[135] The development of the discipline chemometrics is strongly connected with the use of computers in chemistry. The term chemometrics was introduced in 1972 by the Swede Svante Wold and the American Bruce R. Kowalski. The foundation of the International Chemometrics Society in 1974 led to the first description of this discipline. In the following years several conference series were organized, e.g. COMPANA (Computer applications in analytics), COBAC (Computer-based analytical chemistry) or CAC (Chemometrics in analytical chemistry). Some journals devoted special sections to papers on chemometric subjects. Later on novel chemometric journals were started, such as the Journal of Chemometrics (Wiley) and Chemometrics and Intelligent Laboratory Systems (Elsevier).[136]

The relationship of chemometrics to different disciplines is indicated in figure 2.1. On the left are the enabling sciences, mainly quite mathematical and not laboratory based. Statistics, of course, plays a major role in chemometrics. Computing is important as much of chemometrics relies on software. On the right are the main disciplines of chemistry that benefit from chemometrics. Analytical chemistry is probably the most significant area. Environmental chemists, biologists, food chemists as well as geochemists, chemical archaeologists, forensic scientists and so on depend on good analytical chemistry measurements and many routinely use multivariate approaches, and so need chemometrics to help interpret their data.

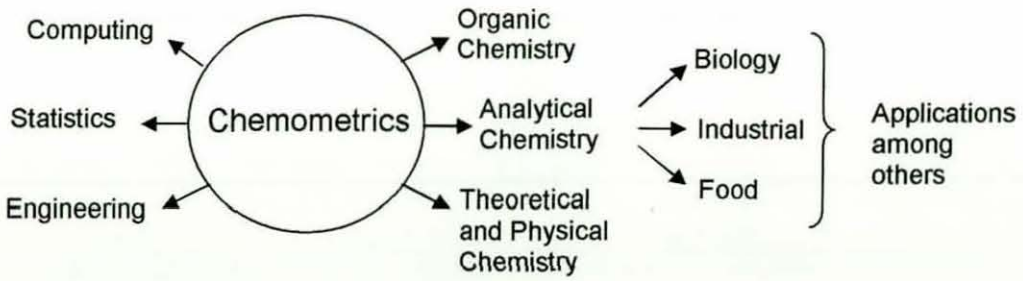

Figure 2.1 How chemometrics relates to other disciplines [137]

Chemometrics has been used to:

- Remove as much noise as possible from the data.
- Extract as much information as possible from the data.
- Use the information to learn how to make accurate predictions about unknown samples.

In order for this to work, two essential conditions must be met:

- The data must have information content.
- The information in the data must have some relationship with the property or properties which we are trying to predict.

The areas where chemometrics has been most successful, both in industry and in academia, according to all measures are the following:

- Multivariate calibration.
- Structure-(re)activity modelling.
- Pattern recognition, classification, and discriminant analysis.
- Multivariate process modelling and monitoring.

There are numerous sources of information on the theory of chemometrics and its applications.[135-140] Here only multivariate calibration will be considered in detail.

2.2 MULTIVARIATE CALIBRATION

The use of computers in the laboratory has enabled the adoption of a new approach to multicomponent determinations in complex samples by allowing the simultaneous processing of the vast amount of information provided by currently available instruments. Multivariate calibration methods, which rely on various mathematical algorithms, are being increasingly used to circumvent the problems posed by the presence of interferences, or spectral overlap.

Multivariate calibration is a general selectivity and reliability enhancement tool. It is applicable to the determination of major constituents as well as microcomponents and other qualities, and for a very wide range of instrument types. With multivariate calibration the need for sample preparation is greatly reduced. The reason is that selective input measurements are no longer needed — it is the output results that must be selective.

Multivariate calibration can thus stimulate the development of new analytical instruments and increase their analytical capacity and reliability. This extends the usefulness of quantitative methods in on-line industrial process control, analysis of intact biological or medical samples, etc.

2.2.1 Multivariate calibration decision tree [135]

The multivariate calibration decision tree (figure 2.2) is a guide to the selection of the appropriate multivariate calibration tool for a particular problem. Before discussing this tree, it is important to understand the distinction between linear and nonlinear approaches. In this chapter, only methods that estimate models that are linear in the parameters are discussed. Fortunately, these methods also tolerate some degree of nonlinear behaviour in the data.

In figure 2.2 there are two main branches for the multivariate methods: classical least squares (CLS) and inverse least squares (ILS). Deciding which method to employ is not always straightforward. The question posed is "Is the system simple and are all of the analytes known?" If the answer to this question is yes, CLS may be the best approach. If the answer is no, ILS is the best (or only) choice. The difficulty in applying the CLS approach is knowing if the system meets the assumptions inherent to the methods. CLS is applicable when all of the analytes are known and pure spectra can be obtained using either the direct or indirect methods. These systems typically have relatively few major components, few factors that affect the instrument response other than the concentration of the analytes of interest, and no significant interferences. It also must be possible to represent the mixture spectra as combinations of the pure spectra. If all these conditions hold, CLS has an advantage over the ILS methods in that it is generally easier to construct a calibration model. All that is required for the model are spectra of the pure components of interest.

Two CLS methods are available, direct (DCLS) and indirect (ICLS), where the difference is in how the pure spectra are obtained. If it is possible to isolate the pure analytes and directly measure the pure spectra, the DCLS method can be used. If the pure analytes cannot be isolated, it may be

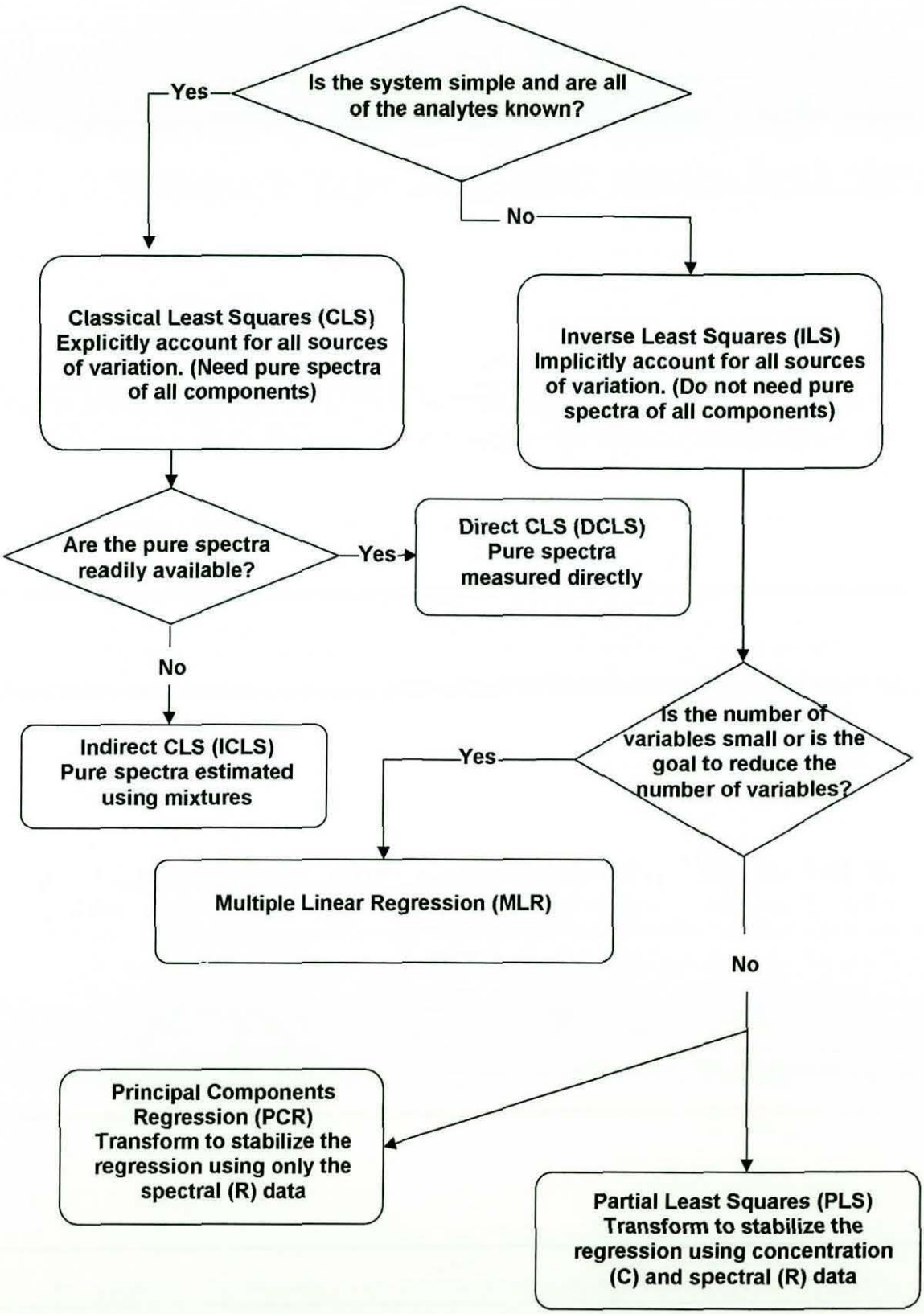

Figure 2.2 Multivariate calibration decision tree[135]

possible to obtain the pure spectra mathematically by using spectra of mixtures and the ICLS approach.

If the system is not simple, an inverse calibration method can be employed where it is not necessary to obtain the spectra of the pure analytes. The three inverse methods discussed later in this chapter include: multiple linear regression (MLR), principal components regression (PCR), and partial least squares (PLS). When using MLR on data sets found in analytical chemistry, variable selection is often required to make the matrix calculations possible and/or improve the stability of the calculations. It is therefore appropriate to use MLR when the number of variables is small, or in situations where a subset of measurement variables is desired. An example of the latter is when a full-wavelength instrument is used to perform a feasibility study, but where a filter instrument is to be purchased for economic or other reasons. It must be borne in mind that reducing the number of variables will almost always result in poorer error detection ability and less precise estimates. However, this may be outweighed by other factors.

Unlike MLR, PCR and PLS are methods that can be used without explicitly selecting variables. This is accomplished by transforming the measured variables (e.g. fluorescence spectra at many wavelengths) into new variables (often referred to as factors) that are used in the matrix calculations. The difference between PCR and PLS is in how this variable transformation is performed. Both PCR and PLS have good diagnostic tools and in general the results are similar. These methods are often preferred over MLR unless the number of variables is small or circumstances dictate the explicit reduction in the number of variables.

The basic questions that must be answered in deciding between these methods are found in the decision tree. The information found throughout this chapter also helps to reveal how these questions are best answered.

Quantification is an important task in fluorescence spectroscopy. Since fluorescence spectroscopy is an indirect measurement technique, calibration is usually required. Moreover, calibration is a fundamental step in the calculation of the unknown concentrations of compounds in spectroscopy. In calibration, indirect measurements are made from samples where the amount of analyte has been

pre-determined, usually by an independent assay or technique. These measurements, along with the pre-determined analyte concentrations, comprise a group known as the 'calibration set'. This set is then used to develop a model, albeit absolute or relative, that relates the concentration of analyte (y), to the measurements made by the instrument (x), via some evaluation function $f()$.

$$y = f(x) \qquad \text{(Eq.2.1)}$$

However, as with all chemical measurements there will always be some degree of systematic or random error, hence the calculated concentration is said to be an estimate of the actual concentration y, and is usually denoted $\hat{y}$ (the symbol $\hat{}$ above the term denotes its an estimate of the true value). So equation 2.1 should be correctly written as:

$$\hat{y} = f(x) \qquad \text{(Eq.2.2)}$$

Once the model has been constructed, it can then be used to predict the concentration of the analytes based on the measurements made from the new samples usually termed 'the new data set'. For absolute calibration methods, there tends to be a mathematical formula that relates x to y.

If the relationship between x and y is not obvious then determining the model can be very time consuming, and sometimes almost impossible to figure out. In these circumstances relative calibration methods can be used. Such calibration methods make assumptions on the underlying relationship between x and y. This is achieved by using some given examples of the x and y variables (calibration set), to estimate the parameters of the relationship.[141]

Univariate calibration is based on a single measurement. There are two possible approaches to univariate calibration. The first involves predicting a single concentration from absorbance at a single wavelength. The weakness of this is that it will fail if there are unknown interferences or completely overlapping spectra. An alternative is to predict the concentrations using a matrix of all concentrations. When there are more samples than variables, the approach is referred to as

multiple linear regression (MLR). If the number of variables is larger than the number of samples and the variables are linearly dependent or if they are highly correlated, the matrix is singular or nearly singular, which means that the computed regression coefficients are relatively imprecise. This collinearity can cause MLR to fail when applied to data sets containing highly correlated variables.[142] Another two common methods of calibrations include partial least squares (PLS) and principle component regression (PCR). Graphical representation of matrices of calibrations used in analytical chemistry is shown in figure 2.3.

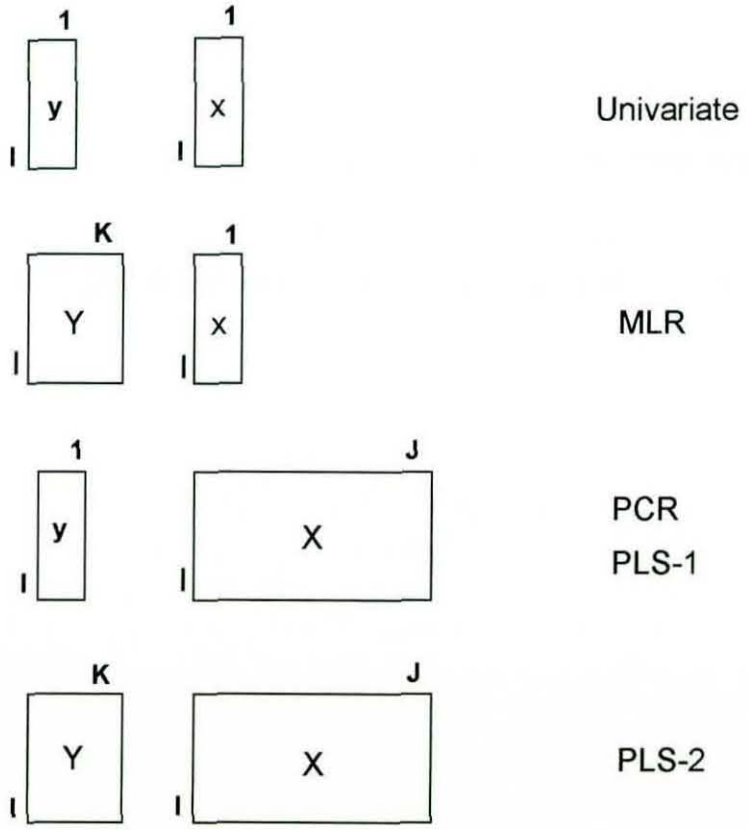

Figure 2.3 Graphical representation of matrices of calibrations used in analytical chemistry[142]

2.2.2 Principal component regression

The idea of principal component regression (PCR) is to form a model between a concentration of a compound and the principal components (PCs) of a data matrix, e.g. spectra. It differs from MLR in that the spectra are first reduced to a few orthogonal PCs. This means that even if there is a high correlation between wavelengths, PCR is nevertheless effective. PCR is performed using only one concentration vector at a time. When there is more than one concentration of interest, PCR is applied to each concentration vector separately.[137] The PCR can be implemented as a full spectrum calibration method. However, with PCR the spectral decomposition is performed slightly differently. PCR is a two-step multivariate calibration method in which the first step involves principal component analysis (PCA) being carried out on the data matrix, followed by a multiple linear regression (MLR) step.

There is plenty of literature on the methods of PCA and MLR.[143,144] Hotelling [145] first described PCA in 1933; however, Malinowski first introduced it into chemistry around the 1960's under the name of principal factor analysis. After 1970 a large number of chemical applications have been published and PCR has been successfully applied to the quantitative analysis of ultraviolet,[146,147] fluorescence,[148] near infrared,[149] and chromatographic [150] data.

The core of PCR is the PCA of the data matrix, and several algorithms for PCA are available. One of the most commonly used algorithms is the non-linear iterative partial least squares algorithm (NIPALS) and it computes sequentially the eigenvectors by order of explained variance. The algorithm has been described by many authors.[144,151]

2.2.3 Partial least squares

One of the most promising multivariate statistical methods to find application in chemistry is partial least squares (PLS) developed by Wold.[152] Certain Scandinavian and North American groups have based much of their development over the past two decades primarily on applications of the PLS algorithm. Since its introduction into chemometrics as a tool for solving regression problems with

linearly dependent predictor variables, PLS has become a common, if not standard regression method. It has been successfully applied to the quantitative analysis of ultraviolet,[153] fluorescence,[34,41] near infrared,[154] and chromatographic [155,156] data. Much work has gone into making clear its mathematical and statistical properties,[157-160] and several alternative algorithms have been proposed.[161,162] All these effects have helped to clarify the diverse aspects of PLS and shed light on what was once, by definition, only an algorithm.

Like PCR, the PLS algorithm can be implemented as a full spectrum calibration method which gives it many advantages such as; (1) potentially significant improvements in precision for estimating sample concentrations or properties from calibration spectral data, (2) useful information (contained in the loading vectors) that allows quantitative chemical interpretation of spectral features, and (3) the ability to calculate spectral residuals that can be used for efficient outlier detection diagnostics and further qualitative interpretation.

PLS is often presented as the major regression technique for multivariate data. An important feature of PLS is that it takes into account errors in both the concentration estimates and the spectra. A method such as PCR assumes that the concentration estimates are error free. Much traditional statistics rests on this assumption, which all errors are of the variables (spectra). If in medicine it is decided to determine the concentration of a compound in the urine of patients as a function of age, it is assumed that age can be estimated exactly, the statistical variation being in the concentration of a compound and the nature of the urine sample. Yet in chemistry there are often significant errors in sample preparation, for example accuracy of weighings and dilutions, and so the independent variable in itself also contains errors. Classical and inverse calibration force the user to choose which variable contains the error, whereas PLS assumes that it is equally distributed in both the x and c blocks.[137]

There are two main PLS algorithms, usually termed PLS-1 and PLS-2. The most widespread approach is often called PLS-1. Although there are several algorithms, the main ones due to Wold and Martens, the overall principles are fairly straightforward. An extension to PLS-1 was suggested some 20 years ago, often

called PLS-2. In PLS-1 one compound is modelled at a time, whereas in PLS-2 all known compounds can be included in the model simultaneously.

The concentration estimates are different when using PLS-2 compared with PLS-1. In this way PLS differs from PCR where it does not matter if each variable is modelled separately or all together. The reasons are rather complex but relate to the fact that for PCR the principal components are calculated independently of the c variables, whereas the PLS components are also influenced by both blocks of variables.[137]

In some cases PLS-2 is helpful, especially since it is easier to perform computationally if there are several c variables compared with PLS-1. Instead of obtaining many independent models, it can analyse all the data in one go. However, in many situations PLS-2 concentration estimates are, in fact, worse than PLS-1 estimates, so a good strategy might be to perform PLS-2 as a first step, which could provide further information such as which wavelengths are significant and which concentrations can be determined with a high degree of confidence, and then perform PLS-1 individually for the most appropriate compounds.[137]

The aim of this research is to quantify the individual components from a series of mixtures, thus the algorithm PLS-1 will only be discussed in detail here. The orthogonal PLS-1 method presented is that used by Marten and Næs,[163] and is used by the Unscrambler® software which was used throughout this research.

2.2.4 Orthogonal PLS-1 algorithm

To calculate the estimates of the model parameters, the number of relevant principal factors needs to be determined (factors that significantly affect the results, i.e. the number of components in the mixture, noise, etc.). It has been suggested that the number of factors should be higher than the number of phenomena expected, and those that do not contribute to the model should be removed later, thus allowing any unexpected phenomena to be modelled. The total number of factors used here will be denoted a (a = 1, 2...A).

To make the calculations easier, the calibration data is mean-centred. This is achieved by calculating the variance for each of the individual x and y variables.

$$\mathbf{X}_0 = \mathbf{X} - 1\overline{\mathbf{x}}' \qquad \text{(Eq.2.3)}$$

$$\mathbf{y}_0 = \mathbf{y} - 1\overline{\mathbf{y}} \qquad \text{(Eq.2.4)}$$

where **X** is a matrix containing the instrument response variables *j* for *i* samples $\{\mathbf{X}_{ij}\ i = 1,2....I\ j = 1,2....J\}$ and vector **y** contains the concentrations of a particular analyte in the samples $\{y_i\}$

For each of the variables in $\mathbf{X}_0$ its projection in the X-space has direction and length. These two parameters are usually known as spectral loadings and scores and are denoted **p** and **t** respectively. So theoretically,

$$\mathbf{X}_{a-1} = \mathbf{t}_a\mathbf{p}_a' + \mathbf{E} \qquad \text{(Eq.2.5)}$$

where **E** is the X-residual error matrix. However, in PLS the **t** scores tend to be orthogonal to each other, whereas the spectral loadings **p**, tend to be non-orthogonal.[39] Hence, there is no guarantee that the spectral loadings (or rather the scores formed by the projection) are suitable for predicting y. To solve this problem a set of loading weights are used (denoted w_i) that are orthogonal to each other. They express how the information in each X-variable relates to the variation in y. The loading weights also can be used to calculate the **t** scores from the **X** matrix so that the decomposition of the data is orthogonal. So equation 2.5 can be rewritten as:

$$\mathbf{X}_{a-1} = \mathbf{t}_a\mathbf{w}_a' + \mathbf{E} \qquad \text{(Eq.2.6)}$$

However, the loading weights are usually scaled to a length of 1 to avoid any scaling ambiguities, using the scaling factor s, where:

$$s = \frac{1}{\sqrt{(\mathbf{y}_{a-1}'\mathbf{X}_{a-1}\mathbf{X}_{a-1}'\mathbf{y}_{a-1})}} \qquad \text{(Eq.2.7)}$$

This is so their lengths can be interpreted as well as their direction. The variables with large loading weights are of importance when it comes to predicting y. Therefore the loading weights need to maximize the scaled covariance between $\mathbf{X}_{a-1}$ and $\mathbf{y}_{a-1}$ such that:

$$\mathbf{X}_{a-1} = \mathbf{y}_{a-1}\mathbf{w}_a' + \mathbf{E} \qquad \text{(Eq.2.8)}$$

The loading weights can be estimated using the following formula:

$$\hat{\mathbf{w}}_a = s\mathbf{X}_{a-1}'\mathbf{y}_{a-1} \qquad \text{(Eq.2.9)}$$

Now that the loading weights have been estimated, the **t** scores can be estimated using equation 2.6. The least squares solution is:

$$\hat{\mathbf{t}}_a = \mathbf{X}_{a-1}\hat{\mathbf{w}}_a \qquad \text{(Eq.2.10)}$$

Substituting $\hat{\mathbf{t}}_a$ back into equation 2.6 gives,

$$\mathbf{X}_{a-1} = \mathbf{X}_{a-1}\hat{\mathbf{w}}_a'\hat{\mathbf{w}}_a + \mathbf{E} \qquad \text{(Eq.2.11)}$$

which is equivalent to,

$$\mathbf{X}_{a-1} = \mathbf{X}_{a-1} + \mathbf{E} \qquad \text{(Eq.2.12)}$$

since $\hat{\mathbf{w}}_a'\hat{\mathbf{w}}_a$ is equal to 1.

The spectral loadings can now be estimated using equation 2.5. The least squares solution is (where $\hat{\mathbf{p}}_a$ is an estimate of $\mathbf{p}$):

$$\hat{\mathbf{p}}_a = \mathbf{X}_{a-1}' \frac{\hat{\mathbf{t}}_a}{\hat{\mathbf{t}}_a' \hat{\mathbf{t}}_a} \qquad \text{(Eq.2.13)}$$

Substituting $\hat{\mathbf{p}}_a$ back into equation 2.5 gives:

$$\mathbf{X}_{a-1} = \mathbf{X}_{a-1} \frac{\hat{\mathbf{t}}_a \hat{\mathbf{t}}_a'}{\hat{\mathbf{t}}_a \hat{\mathbf{t}}_a'} + \mathbf{E} \qquad \text{(Eq.2.14)}$$

which is equivalent to equation 2.12 because:

$$\frac{\hat{\mathbf{t}}_a \hat{\mathbf{t}}_a'}{\hat{\mathbf{t}}_a \hat{\mathbf{t}}_a'} = 1$$

Vector $\mathbf{y}_{a-1}$, can also be broken down in to chemical loadings and scores. The chemical loading is usually denoted q and is a scalar because only one y variable is calculated in this PLS-1 algorithm. So $\mathbf{y}_{a-1}$ can be written as:

$$\mathbf{y}_{a-1} = \hat{\mathbf{t}}_a q_a + \mathbf{f} \qquad \text{(Eq.2.15)}$$

So using the least squares solution (where $\hat{q}_a$ is an estimate of q_a):

$$\hat{q}_a = \frac{\mathbf{y}_{a-1}' \hat{\mathbf{t}}_a}{\hat{\mathbf{t}}_a' \hat{\mathbf{t}}_a} \qquad \text{(Eq.2.16)}$$

Substituting back into equation 2.15 gives:

$$\mathbf{y}_{a-1} = \mathbf{y}_{a-1}' + \mathbf{f} \qquad \text{(Eq.2.17)}$$

So from equations 2.5 and 2.15 the **X** and **y** residual matrix and vector can now be estimated respectively.

$$\hat{\mathbf{E}} = \mathbf{X}_{a-1} - \hat{\mathbf{t}}_a \hat{\mathbf{p}}_a' \qquad \text{(Eq.2.18)}$$

$$\hat{\mathbf{f}} = \mathbf{y}_{a-1} - \hat{\mathbf{t}}_a \hat{q}_a \qquad \text{(Eq.2.19)}$$

If a equals A then the model parameters $\hat{\mathbf{c}}$ and $\hat{c}_0$ can be estimated. However, if a does not equal A, then a should be increased by one and the values for $\hat{\mathbf{t}}_a, \hat{\mathbf{p}}_a, \hat{\mathbf{w}}_a$ and $\hat{q}_a$ should be re-calculated using the new values for $\mathbf{X}_{a-1}$ and $\mathbf{y}_{a-1}$ where:

$$\mathbf{X}_{a-1} = \hat{\mathbf{E}} \quad \text{and} \quad \mathbf{y}_{a-1} = \hat{\mathbf{f}}$$

Once the number of relevant factors has been determined the model parameters $\hat{\mathbf{c}}$ and $\hat{c}_0$ can be estimated using the following formulas:

$$\hat{\mathbf{c}} = \hat{\mathbf{W}}(\hat{\mathbf{P}}'\hat{\mathbf{W}})^{-1}\hat{\mathbf{q}} \qquad \text{(Eq.2.20)}$$

and $$\hat{c}_0 = \bar{y} - \bar{\mathbf{x}}'\hat{\mathbf{c}} \qquad \text{(Eq.2.21)}$$

The matrices $\hat{\mathbf{W}}$ and $\hat{\mathbf{P}}$ represent the combined loading weights and spectral loading vectors respectively, estimated from each of the relevant factors, i.e. $\hat{\mathbf{W}} = \{\hat{\mathbf{w}}_1, \hat{\mathbf{w}}_2, \ldots \hat{\mathbf{w}}_A\}$ and $\hat{\mathbf{P}} = \{\hat{\mathbf{p}}_1, \hat{\mathbf{p}}_2, \ldots \hat{\mathbf{p}}_A\}$. The vector $\hat{\mathbf{q}}$ represents the combined chemical loadings for all the relevant factors, i.e. $\hat{\mathbf{q}} = \{\hat{q}_1, \hat{q}_2, \ldots\ldots \hat{q}_A\}$.

Once the model parameters $\hat{\mathbf{c}}$ and $\hat{c}_0$ have been estimated any further x_j variables from the new data set can be used to predict y using the formula:

$$\hat{y} = \hat{c}_0 + \mathbf{x}'\hat{\mathbf{c}} \qquad \text{(Eq.2.22)}$$

2.3 UNSCRAMBLER SOFTWARE

The Unscrambler is developed and published by CAMO ASA, created in the mid-1980's. Harald Martens and the Norwegian Food Research Institute originally developed the software and tailor-made it for the modelling, prediction and classification of multivariate data. It has been used for chemometrics and process analysis within the food and drink industries, chemical industries, pharmaceutical industries, process industries and research and development. The software is a general software package for multivariate calibration and prediction by use of the PLS-1, PLS-2, PCR and MLR algorithms. It also carries out statistical tests on the models generated, to check their validity. The methods give adequate solutions where traditional multiple regression fails owing to multi-colinearity problems.[164]

The following are the five basic types of problems which can be solved using the software:

- Design experiments, analyze effects and find optima.
- Find relevant variation in one data matrix.
- Find relationships between two data matrices.
- Predict the unknown values of a response variable.
- Classify unknown samples into various possible categories.

There is much literature on various aspects of the Unscrambler software.[164-170]

2.4 VALIDATION

When generating a calibration model it is very important to carry out validation tests on the data set to ensure that any future predictions made from it are accurate and reliable. In general to validate a model means to see how well it will perform on any new data and estimate the uncertainty of predictions made upon that data. If the uncertainty is reasonably low, then the calibration model can be considered to be valid.

The best way of evaluating a model is prediction testing, or test set validation, with an independent data set that is not used in the calibration model. Test set

validation tends to be used on large numbers of samples (usually 50 or more) and divides the data set into two global sets called the calibration set and the test set. The calibration set contains the samples used to compute the calibration model and the samples in the test set are predicted from this model and compared to their actual values. However, this method is very inefficient with regards to samples (usually the test set contains 25% to 50% of the total data set) and the test samples are not used for calibration.

Other alternative methods of validation that have been widely used include cross validation and leverage correction.

2.4.1 Cross validation

Cross validation has been referred to as a cunning technique to make up for the shortage of data and permits the testing of a calibration model without having a test set. There are a number of cross validation methods including full cross validation and segmented cross validation.

Full cross validation (FCV) is a method that leaves out one sample at a time, the concentration of this sample being calculated from the calibration model generated by the other samples. This method improves the relevance and power of the analysis because all the samples are tested individually. However, using this method does have its drawbacks because it can be very time consuming and sensitive to unique samples (outliers), which would give a validation model significantly different from that of the calibration model. However, such findings could be useful in detecting outlying samples in the calibration set.

An alternative method is segmented cross validation, which leaves out a whole group of samples at a time. This method is faster but the segments must contain unique information i.e. samples that are considered replicates of each other should not be present in different segments. This method is also sensitive to clusters in the calibration set e.g. if all the samples in the segment are very different from the others then there will be an excessive prediction error for this segment.

So how is the uncertainty of a calibration model measured when using the different cross validation methods? The simplest way and most efficient measure of uncertainty on future predictions is the root mean squared error of prediction (RMSEP) and is calculated using the following formula:

$$\text{RMSEP} = \sqrt{\frac{\sum_{n}^{N}(\hat{y}_n - y_n)^2}{N}} \qquad \text{(Eq.2.23)}$$

where $\hat{y}_n$ is the predicted concentration of sample n, y_n is the actual concentration of sample n, and **N** is the total number of samples (minus the omitted sample). This value gives the average uncertainty that can be expected when predicting the concentration of the samples, and because the square root is taken the units are the same as y. The lower the RMSEP value the more valid the model (zero being the ideal value).

2.4.2 Leverage correction

Leverage correction (LC) can be used for projection methods such as PLS and PCR, but should only be used in early stages of analysis. This is because for such methods it gives more 'optimistic' results than the other validation methods. It especially affects the PLS algorithm because of the way in which the scores are estimated. The PLS components are more dependent upon the information in y thus the residuals f_n (equation 2.26) for the calibration samples are much too small and cannot be fully corrected by the denominator $1-h_n$. The leverage (h_n) is calculated in the space spanned by the correct number of relevant factors. Thus,

$$h_n = \frac{1}{N} + \sum \frac{c_{na}^2}{\mathbf{s}_a' \mathbf{s}_a} \qquad \text{(Eq.2.24)}$$

where $\mathbf{s}_a$ are the orthogonal score vectors, c_{na} is the regression factor for prediction sample *n*, **N** is the total number of calibration samples, and a is the factor number. The leverage of a sample describes its actual contribution to the

calibration model. A leverage value close to zero indicates that the corresponding sample had very little influence on the calibration model.

The equation for calculating RMSEP for LC is based on an equation that is valid for multiple linear regression, thus can only give an approximation for PLS and PCR. Leverage correction is an approximation to cross validation that enables prediction residuals to be estimated without actually performing any prediction. The predicted residuals in full cross validation [164] are equal to:

$$f_{n(cv)} = \frac{f_n}{1-h_n} \qquad \text{(Eq.2.25)}$$

where f_n is the predicted residual for sample *n* and h_n is the leverage for sample *n*. Thus, the equation to calculate the RMSEP (LC) is equal to,

$$\text{RMSEP(LC)} = \sqrt{\sum_{n}^{N} \frac{f_n^2/(1-h_n)^2}{N}} \qquad \text{(Eq.2.26)}$$

where N is the number of samples. The lower the RMSEP the more valid the model (zero being the ideal value).

2.4.3 Residual variance

The residual variance can be calculated for both x and y data (x being the spectral data and y being the concentration of the analyte that the spectral data represent); however, it is the residual y variance that is of interest here. The Unscrambler software calculates the residual variance for each factor in one of two ways, depending upon which validation method was chosen,

Leverage Correction

$$\text{RV(LC)} = \frac{1}{d}\sum_{n=1}^{N} \frac{(\hat{y}_n - \bar{y}_n)^2}{(1-h_n)} \qquad \text{(Eq.2.27)}$$

Cross Validation

$$RV(CV) = \frac{1}{d}\sum_{n=1}^{N}(\hat{y}_n - \bar{y}_n)^2 \qquad \text{(Eq.2.28)}$$

where d is the number of degrees of freedom, n is the number of samples and h_n is the leverage value. The Unscrambler also calculates the total residual variance (TRV) (usually termed factor 0):

$$TRV = \frac{1}{N}\sum_{a}^{A} RV_a \qquad \text{(Eq.2.29)}$$

where a is the factor number and N is the total number of calibration samples. Using the TRV value, the percentage of explained variance can be calculated and is a good way of seeing how much of the variance in y is explained by the model.

There are two kinds of residual variances that can be observed using the Unscrambler and these are the calibration variance and the validation variance. The calibration variance is based on fitting the calibration data to the calibration model, whereas the validation variance is obtained by testing the data that have not been used to build the model. From these two variances it is possible to see if the model describes the new data well.

CHAPTER 3

MATERIALS, INSTRUMENTATION AND GENERAL PROCEDURES

3.1 MATERIALS AND INSTRUMENTATION

3.1.1 Reagents

Table 3.1 Reagents and Suppliers

Substance	Supplier
Buffer reagents	
10X Phosphate buffer	Molecular Probes
Sodium carbonate, anhydrous	Sigma
Sodium dihydrogen orthophosphate	Fisher Scientific UK
Sodium hydrogen carbonate	Fisher Scientific UK
Sodium phosphate, dibasic anhydrous	Sigma
Trizma base	Sigma
Trizma hydrochloride	Sigma
Enzymes	
β-galactosidase grade VI: from *Escherichia coli*	Sigma
Protease type XXI: from *Streptomyces griseus*	Sigma
Alkaline phosphatase type I-S: from Bovine intestine mucosa	Sigma
Fluorophores and fluorigenic substrates	
BODIPY®493/503,SE	Molecular Probes
BODIPY®FL, SE	Molecular Probes
Fluorescein isothiocyanate isomer I	Sigma
Fluorescein di-β-D-galactopyranoside (FDG)	Molecular Probes
Fluorescein di-phosphate (FDP)	Molecular Probes

Substance	Supplier
Immobilisation supports	
UltraLink® Biosupport Medium	Pierce
Inhibitors	
Phenylethyl thiogalactoside (PETG)	Sigma
3-Nitrophenylboronic acid	Sigma
Sodium orthovanadate	Sigma
Other reagents	
Bicinchoninic acid	Sigma
Copper (II) sulphate pentahydrate 98%	Sigma
Dimethyl sulphoxide (DMSO), anhydrous	Sigma
Ethanolamine	Fisher Scientific UK
Sodium chloride	Sigma
Sodium azide	Sigma
N,N-Dimethylformamide	Fluka
Ethanol	Fluka
Methanol	Fluka
Protein	
α-Casein: from bovine milk	Sigma

All chemicals were analytical reagent grade

3.1.2 Balances

Electronic balance, Precisa 620C, two decimal places.....Precisa

Electronic balance, Precisa 40SM-200A, four decimal places.....Precisa

Electronic balance, Adventurer, four decimal places.....Ohaus

3.1.3 Cells

Quartz fluorescence cell (3500 µl volume, 1 cm light path) .....Hellma

Quartz UV cell (3500 µl volume, 1 cm light path) .....Hellma

Flow cell UV and fluorescence, 25 µl volume.....Hellma

1.5 mm X 1.5 mm light path

3.1.4 Chromatographic columns and frits

PD-10 column ..... Amersham Pharmacia Biotech UK

Glass column 3.0 x 1.5 cm (105 mm bed volume).....Omnifit

Glass column 3.0 x 2.5 cm (170 mm bed volume).....Omnifit

Glass column 3.0 x 5.0 cm (350 mm bed volume).....Omnifit

Frits (2 micron).....Omnifit

3.1.5 Flow system equipment

Injection valves (manual with 25 µl, 50 µl and 75 µl sample loop).....Omnifit

Peristaltic pump (Gilson minipuls 3) .....AD Instruments

Pump tubing 0.8 mm I.D..... Elkay

Sterile Syringe, 1ml (BD Plastipak).....Fisher Scientific

3.1.6 Pipettes

Automatic adjustable pipettes: P100, 200, 1000, and 5000 ..... Anachem

3.1.7 pH Meter

Bench pH meter model PHA 230 .....Whatman

pH meter model 220.....Corning

3.1.8 Spectrometers

Model F-4500 Fluorescence Spectrophotometer .....Hitachi

UV/Visible Spectrometer .....Unicam Analytical Systems

3.1.9 Temperature control

Water bath (0 – 99 °C, ± 0.1 °C) ..... Grant

3.1.10 Other equipments

Centrifuge, model Z 2000A.....Hermle

Micro centrifuge, model 320.....Quickfit

Roller bed, model Spiramix 10.....Denley

3.2 GENERAL PROCEDURES

3.2.1 Water purification

All solutions were prepared using triply deionised water (18.2 MΩ), purified by a Maxima ultra pure water system (USF Elga Ltd.).

3.2.2 Buffer preparation

Buffers were prepared in triply deionised water throughout. Tris-HCl, carbonate and phosphate buffers have been used during the experimental work.

3.2.3 pH measurement

pH measurements were carried out using the pH meter, with a pH range of 0.00 to 14.00 and an accuracy of ± 0.01 pH. The instrument was calibrated with high-resolution buffer solutions at pH 4.00, 7.00, and 10.00, ± 0.005, before use.

3.2.4 Mass determination

Weighing measurements were carried out on three balances depending on the weighing range needed.

3.2.5 Pipetting

Pipetting was carried out using Gilson (supplied by Anachem) variable volume automatic pipettes.

3.2.6 Fluorescence measurement

The Hitachi F-4500 Fluorescence Spectrophotometer was used in this study. The spectrophotometer mainframe has a xenon lamp light source, the beam of which is incident on the excitation monochromator. The beam after wavelength selection with the excitation monochromator (λ_{ex}) is irradiated onto the sample cell. Light emitted from the sample in the form of fluorescence (λ_{em}) then passes through the emission monochromator (which is at right angles to the incident light) to remove any light that is not at the emission wavelength. The intensity of fluorescence is detected via a red-sensitive photomultiplier tube (R928F). Instrument parameters are shown in appendix C.

3.2.7 Absorbance measurement

Absorbance measurements were carried out on a Unicam 8700 Series UV/ Visible spectrometer using buffer solution to obtain a baseline.

3.2.8 Flow system measurement

Flow system measurements were made using the basic set-up shown in figure 4.10, and variations thereof. Buffer solution was pumped using a peristaltic pump, and injections of substrate and enzyme inhibitor into the flowing stream were made using a manual sample injection valve fitted with 25, 50 or 75 µl sample loops. A manual 6-port rotary valve was used to direct the main flow stream into a reactor where assay components were captured. The reactor was situated in a thermostatted water bath to enable the reactions to occur at a defined temperature. The rotary valve was then again switched to direct the assay components back into the main stream. This flowed through a fluorescence flow cell situated in the Hitachi F-4500 fluorescence detector to measure the fluorescence intensity and then through to waste.

3.2.9 General dye: protein conjugation procedure

Dye-protein conjugation procedures varied depending on the reaction conjugation times, concentrations of dye and protein, conjugation buffer, stop solution,

separation column/methods, etc. The following are the procedures, according to the Molecular Probes guidelines.[57]

3.2.9.1 FITC- α-casein and BODIPY® 493/503- α-casein conjugates

FITC- α-casein and BODIPY® 493/503- α-casein conjugates were prepared according to the following method.

- 2 mg/ml α-casein was prepared by dissolving 2 mg α-casein in 1 ml 0.1 M carbonate buffer pH 8.4.
- 1 mg FITC and BODIPY® 493/503 were dissolved each dye in DMSO at 10 mg/ml.
- The FITC and BODIPY® 493/503 solutions were added to 2 mg/ml α-casein solutions. The total volume for each dye was made up to 2.5 ml with 0.1 M carbonate buffer pH 8.4.
- The solutions were incubated for 2 hours in dark vials with continuous stirring at room temperature.
- *Two PD-10 Sephadex G25 columns were equilibrated with 25 ml* 0.1 M phosphate buffer pH 7.2. Each conjugate was passed through the PD-10 column in order to remove unconjugated dye from the conjugate.
- For each reaction conjugate, 3.5 ml 0.1 M phosphate buffer pH 7.2 was added to the PD-10 column in order to elute the conjugate. *Aliquots of* conjugate were stored in black vials in the freezer.

3.2.9.2 BODIPY® FL- α-casein conjugates

BODIPY® FL- α-casein conjugates were prepared according to the following method.

- 2 mg/ml α-casein was prepared by dissolving 2 mg α-casein in 1 ml 0.1 M carbonate buffer pH 8.4.
- Amount of BODIPY® FL required for 5:1, 10:1, 20:1 and 40:1 reaction mixture ratios of BODIPY® FL- α-casein were calculated by multiplying the

number of moles of α-casein by the molecular weight of BODIPY® FL followed by multiplying by the ratio.

- The BODIPY® FL solution was made up by dissolving the require amount of BODIPY® FL in DMSO at 10 mg/ml.
- For each reaction mixture ratio conjugate, the BODIPY® FL solution was added to a 2 mg/ml α-casein solution. The total volume was made up to 2.5 ml with 0.1 M carbonate buffer pH 8.4.
- The solutions were incubated for 2 hours in dark vials with continuous stirring at room temperature.
- PD-10 Sephadex G25 columns were equilibrated with 25 ml 0.1 M phosphate buffer pH 7.2. The conjugates were passed through the columns in order to remove unconjugated dyes from the conjugates.
- Elution buffer was prepared by diluting the 10X PBS stock pH 7.2, which contains 2 mM sodium azide, and 10 fold in deionised water.
- For each reaction conjugate, 3.5 ml of the elution buffer was added slowly until the conjugate had been eluted. Aliquots of the conjugate were stored in black vials in the freezer.

3.2.9.3 Final dye: protein ratio or degree of labelling calculations

- A portion of the conjugates was diluted so that the maximum absorbance was 0.5 to 1.5 AU. The absorbance of the conjugate solution at 280 nm and at the dye maximum wavelength (A_{280} and A_{max}) was measured in a cuvette with a 1 cm pathlength.
- The concentration of protein in mg/ml was determined;

$$A_{protein} = A_{280} - A_{max}\,(CF)$$

$$CF = A_{280\ free\ dye} / A_{max\ free\ dye}$$

CF is a correction factor, and the CF values for used fluorophores are listed in table 1.3.

- The protein concentration was calculated assuming 1.4 $A_{protein}$ units = 1 mg/ml (this may not be true for all proteins).
- Final dye: protein (D: P) ratios or degree of labelling (DOL) were calculated. The ratios were the average numbers of dye molecules coupled to each protein molecules.

$$D: P = (A_{max} \times MW) / ([protein] \times \varepsilon_{dye})$$

MW = the molecular weight of the protein

ε_{dye} = the extinction coefficient of the dye at its absorbance maximum and protein concentration is in mg/ml

Calculation of dye: protein ratio assumes that the absorption properties (λ, ε) of both the dye and the protein were not changed when they combine (this may not be true).

3.2.10 Immobilisation of enzyme onto Pierce UltraLink biosupport medium

The enzymes were immobilised onto Pierce UltraLink biosupport medium according to the manufacturer's instructions.[104] 0.125 g of UltraLink were weighed out. A solution of enzyme in 2 ml cold (4°C) 0.1 M phosphate buffer pH 7.2 with 0.6 M Sodium citrate was added to the dry beads and the solution vortexed, followed by gentle rotation on a roller bed for 2 hours at room temperature. The solution was then filtered to remove unbound enzyme from the beads and this filtrate was kept in order to determine the amount of enzyme not coupled to the beads, using the BCA assay. A quench solution of 2.5 ml 3.0 M ethanolamine pH 9.0 was then added to the beads to block unreacted azlactone sites, vortexed and gently rotated on a roller bed for 2.5 hours at room temperature. The beads were then separated from the quench solution by filtration and resuspended in 2.5 ml 0.1 M phosphate buffer pH 7.2 followed by vortexing and gentle rotation for 15 minutes. Buffer was removed and the beads were resuspended in 2.5 ml 1.0 M NaCl to remove non-specifically attached protein. The solution was vortexed and rotated for 15 minutes after which the NaCl was removed and the beads resuspended in 0.1 M phosphate buffer pH 7.2, the solution vortexed and gently

rotated for 15 minutes followed by removing the buffer. This last step was repeated and the beads stored in 0.1 M phosphate buffer pH 7.2 at 4°C.

3.2.11 Bicinchoninic acid (BCA) assay for determination of protein concentration

The BCA assay [171] was used to determine the amount of enzyme immobilised on to the UltraLink biosupport medium. This method was used to determine the protein concentration in solution before and after the immobilisation. It was adopted as the use of Triton® X-100 surfactant in the bead production may have interfered with an assay using absorbance at 280 nm for the measurement of uncoupled enzyme. Both the standard protocol (room temperature for 2 hours, working range 20-200 µg/ml) and the enhanced protocol (60 °C for 30 minutes, working range 5-250 µg/ml) were used according to the PIERCE BCA reagent manufacturer's instructions.[172]

3.2.12 Preparation of Fluorescein di-galactoside (FDG) solution

FDG was prepared according to the following method.[58] FDG is susceptible to hydrolysis and only minimally soluble in aqueous solutions. To minimize hydrolysis and facilitate solution preparation, first the FDG was added to a 1:1 mixture of DMSO/ethanol – the FDG should readily dissolve. Then the resulting FDG solution was gradually added to an appropriate volume of ice-cold water to make an 8:1:1 water/DMSO/ethanol solution. This stock solution was faint yellow in colour. The 20 nM stock solution was divided into aliquots containing sufficient substrate for a single set of experiments and stored in brown vials in the freezer.

3.2.13 Preparation of Fluorescein di-phosphate (FDP) solution

FDP solution was prepared according to the following method.[59] A 5000 µg/ml stock solution of FDP was prepared by dissolving the entire content of the bottle in 0.1 M pH 7.8 Tris-HCl buffer. Background fluorescence of FDP samples is primarily due to fluorescein monophosphate. If not used immediately, the stock solution has to be promptly divided into aliquots containing sufficient substrate for a single set of experiments and stored in brown vials in the freezer.

CHAPTER 4

SINGLE LABELLED SUBSTRATE ENZYME AND ENZYME INHIBITION SCREENING ASSAYS

4.1 INTRODUCTION

During screening for promising drug candidates, hundreds of thousands of compounds need to be assayed. The aim of these experiments was therefore to develop a simple, sensitive and efficient method for assaying enzyme and enzyme inhibitor activity that would facilitate the testing of large numbers of samples using High Throughput Screening (HTS).

The application of fluorogenic substrates, which are non- or weakly fluorescent but are converted by an appropriate enzyme to a highly fluorescent product, is widespread in biochemical analysis.[173] Such methods combine the amplification effects of the catalytic enzyme action with the high sensitivity of fluorescence spectrometry. Some applications are straightforward enzyme assays, while in others the enzyme is a label through which other reactions such as immunoassays are monitored.[174]

4.2 SINGLE ENZYME SCREENING ASSAYS IN STATIC SYSTEM

4.2.1 Determination of dye to protein ratios of conjugate substrates

Four Bodipy FL-α-casein conjugates were prepared as described in section 3.2.9.2 using fluorophore:protein reaction mixture molar ratios of 5:1, 10:1, 20:1 and 40:1. Reaction mixture ratios greater than these caused precipitation of the conjugates. Final D: P ratios were calculated using the method given in section 3.2.9.3. Reaction mixture ratios and calculated final dye: protein molar ratios are given in table 4.1.

Table 4.1 Initial reaction mixture and calculated final dye: protein ratios for Bodipy FL-α-casein conjugates

Initial reaction mixture ratio of dye: protein	**Final dye: protein ratio**
5:1	1.05:1
10:1	2.37:1
20:1	5.72:1
40:1	-

As would be expected, as the amount of dye in the reaction mixture was increased relative to the protein concentration, a concomitant increase was seen in the final D: P ratio. As this ratio was increased, it might be expected that the suitability of the substrate as a quenched protease substrate would also have increased. Unfortunately due to the difference between the absorbance values of the 280nm and the maximum wavelength of the Bodipy FL- α-casein conjugates, it was impossible to strike a balance and obtain accurate absorbance values. Moreover, the 40:1 ratio conjugates seemed to be less stable than others. Therefore, the 20:1 ratio was used in all subsequent work.

4.2.2 Effect of excitation wavelength on the emission spectra of Bodipy FL-α-casein-AlkP, FDG-β-Gal and FDP-AP

Using excitation and emission bandwidths of 10 nm and solutions of Bodipy FL-α-casein-AlkP, FDG-β-Gal and FDP-AP in a standard 3 ml quartz cuvette, emission spectra were taken using a variety of excitation wavelengths. Figure 4.1 shows that the optimum excitation wavelength of Bodipy FL-α-casein-AlkP, FDG-β-Gal and FDP-AP was 490 nm. The optimum emission wavelengths of Bodipy FL-α-casein-AlkP, FDG-β-Gal and FDP-AP were around 512 nm, 515 nm and 516nm respectively, giving a Stokes shifts of just 22 nm, 25 nm and 26 nm respectively.

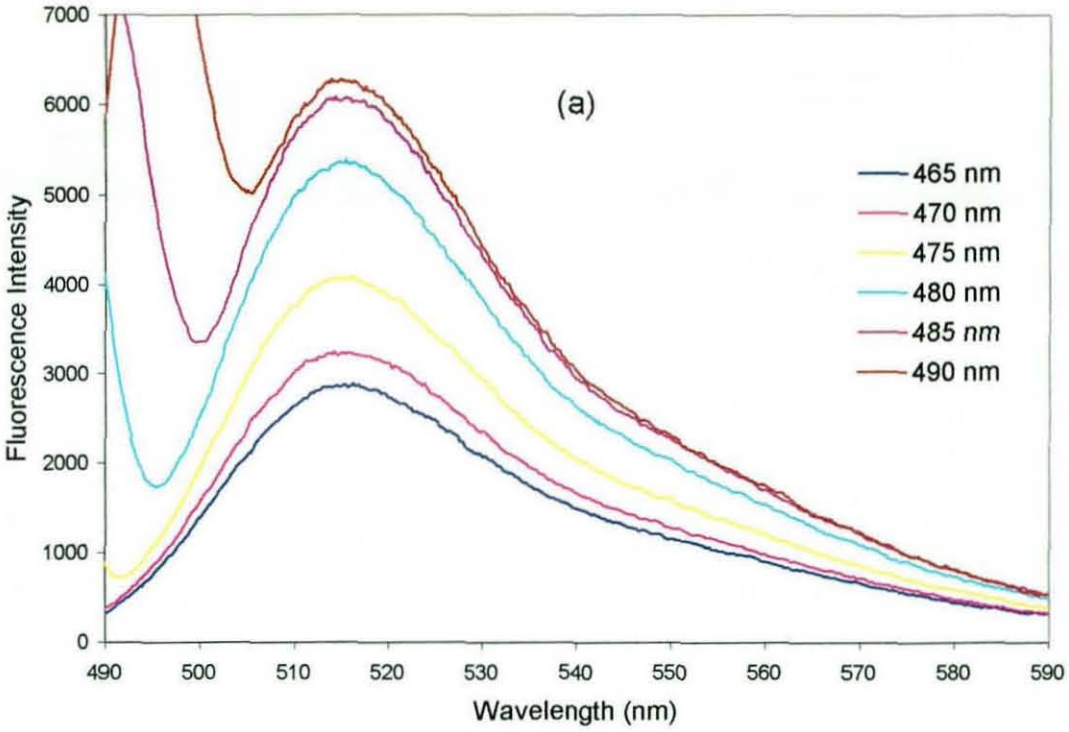
(a)
Fluorescence Intensity
Wavelength (nm)
465 nm
470 nm
475 nm
480 nm
485 nm
490 nm
0
1000
2000
3000
4000
5000
6000
7000
490
500
510
520
530
540
550
560
570
580
590

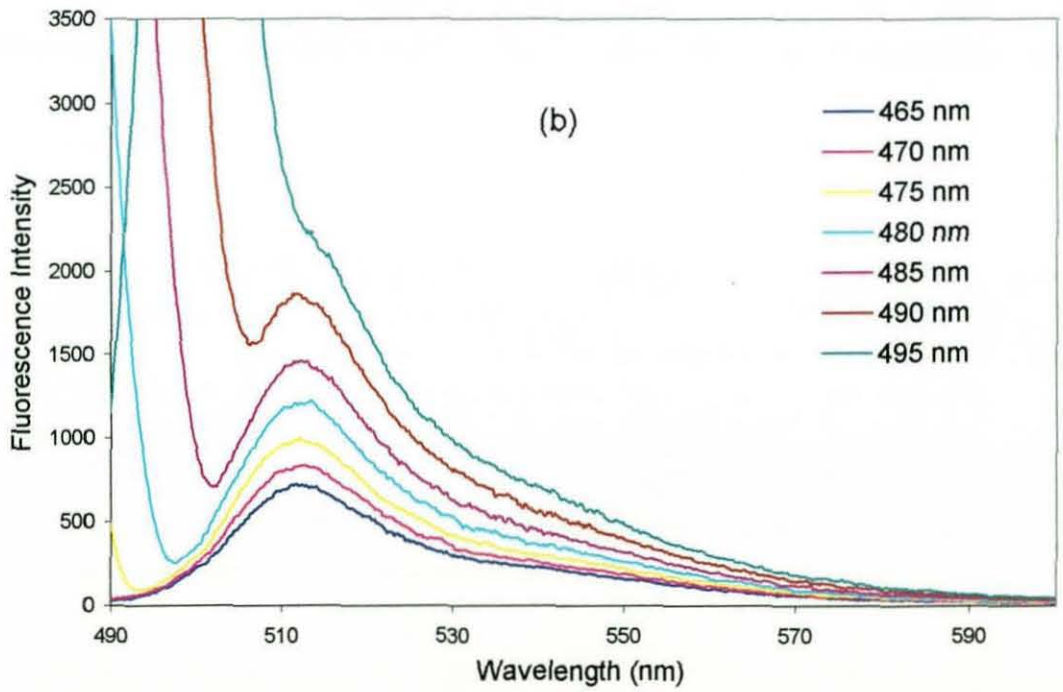
(b)
Fluorescence Intensity
Wavelength (nm)
465 nm
470 nm
475 nm
480 nm
485 nm
490 nm
495 nm
0
500
1000
1500
2000
2500
3000
3500
490
510
530
550
570
590

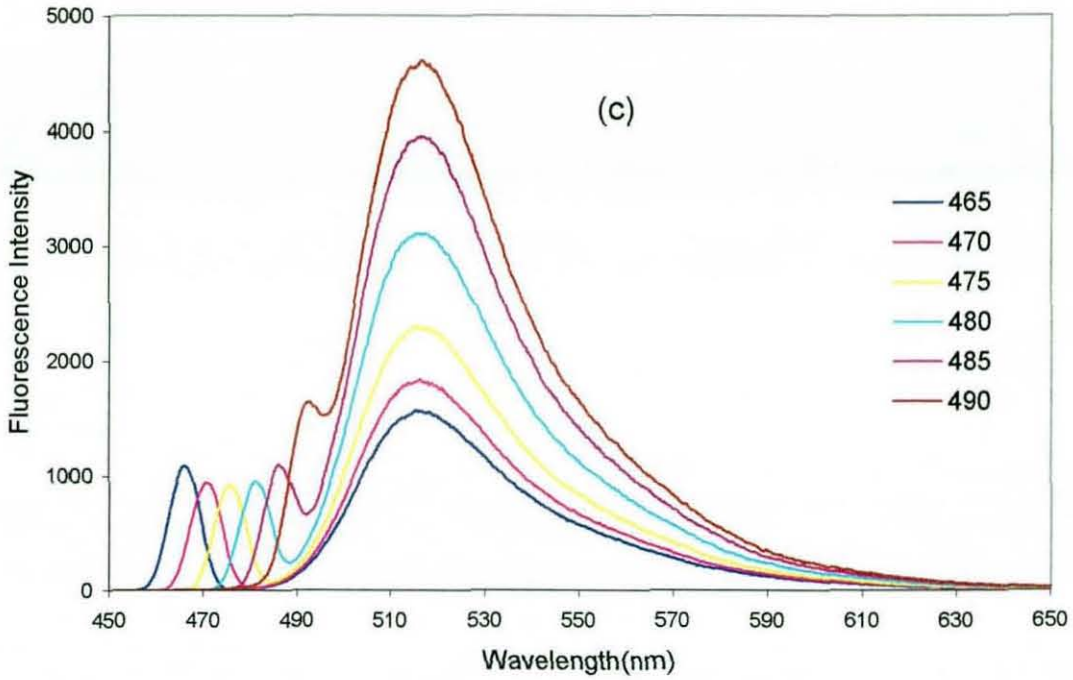

Figure 4.1 Effect of excitation wavelength on the emission spectrum of Bodipy FL-α-casein-AlkP (a), FDG-β-Gal (b) and FDP-AP (c)

Figure 4.1 Illustrates the increasing interference from the scatter peak on the emission peak as the excitation wavelength was increased to the optimum excitation wavelength. The use of the optimal excitation wavelengths of 490 nm for Bodipy FL-α-casein-AlkP, FDG-β-Gal and FDP-AP was therefore not practical because the Stokes shift was so small. Although a loss in fluorescence intensity was seen with lower excitation wavelengths, decreasing the sensitivity of the enzyme assays, a balance between sensitivity and interference was required and a sub-optimal wavelength of 480 nm was chosen for use in all subsequent experiments.

4.2.3 Enzyme assays in a static system

4.2.3.1 Optimisation of Enzyme assay conditions

Fluorescence measurements were made for the enzyme assays using a Hitachi F-4500 fluorescence spectrophotometer with excitation and emission bandwidths of 10 nm and an excitation wavelength of 480 nm. The F-4500 was switched on and allowed to stabilise for 1 hour before fluorescence readings were taken. Static measurements were carried out in a standard quartz fluorescence cuvette. Descriptions of Bodipy FL, FDG, FDP, AlkP, β-Gal and AP are given in chapter 1.

The substrates were subjected to enzyme digestion, the fluorescence intensity of the digested substrates then being compared with that of the undigested substrates (blank). Incubation time, buffer concentration, enzyme concentration, temperature, pH and concentration of substrate were optimised univariately.

The assay parameters studied and optimum conditions found for Bodipy FL-α-casein-AlkP, FDG-β-Gal and FDP-AP are shown in table 4.2

Table 4.2 Assay parameters studied and optimum conditions for various enzyme and substrates in a static system

Assay parameters	Bodipy FL-α-casein-AlkP		FDG-β-Gal		FDP-AP	
	Range studied	Optimum	Range studied	Optimum	Range studied	Optimum
Incubation time, minutes	0-35	5	0-35	10	0-35	5
[Enzyme], μg/ml	0-10	8	0-20	15	0-10	8
[Substrate], μg/ml	0-5	4	0-1.5	1.5	0-1	0.5
Temperature, °C	25-40	37	25-40	37	25-40	37
pH	7.5-9.5	8.5	5.0-9.0	7.5	8.0-9.5	9.0
Buffer	PBS,CA	PBS	PBS,CA	PBS	PBS,CA	CA
[Buffer], mM	10-100	10	10-100	10	10-100	10

CA = Carbonate and PBS = Phosphate

The effect of assay parameters will be shown in detail only for the FDG-β-Gal as it was found that similar trends were observed with all three substrate-enzyme pairs.

As optimisation experiments will be discussed in detail for the assays carried out in a flowing system, the optimisation experiments for the assay conditions for FDG-β-Gal are only summarised. The results are shown below in figure 4.2 - 4.6

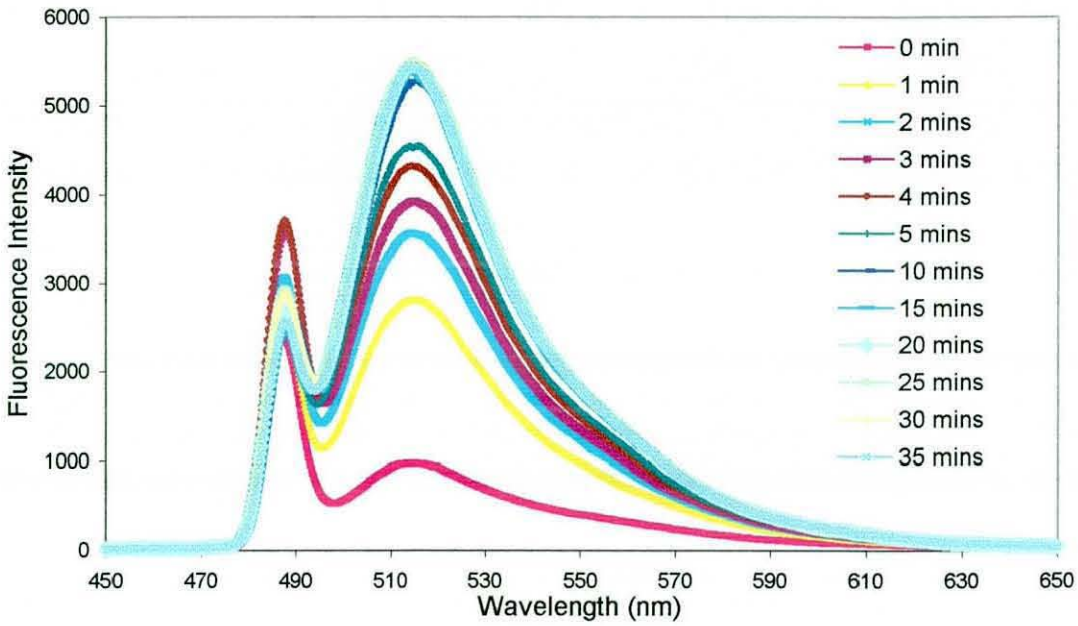

Figure 4.2 Influence of incubation time on FDG-β-Gal

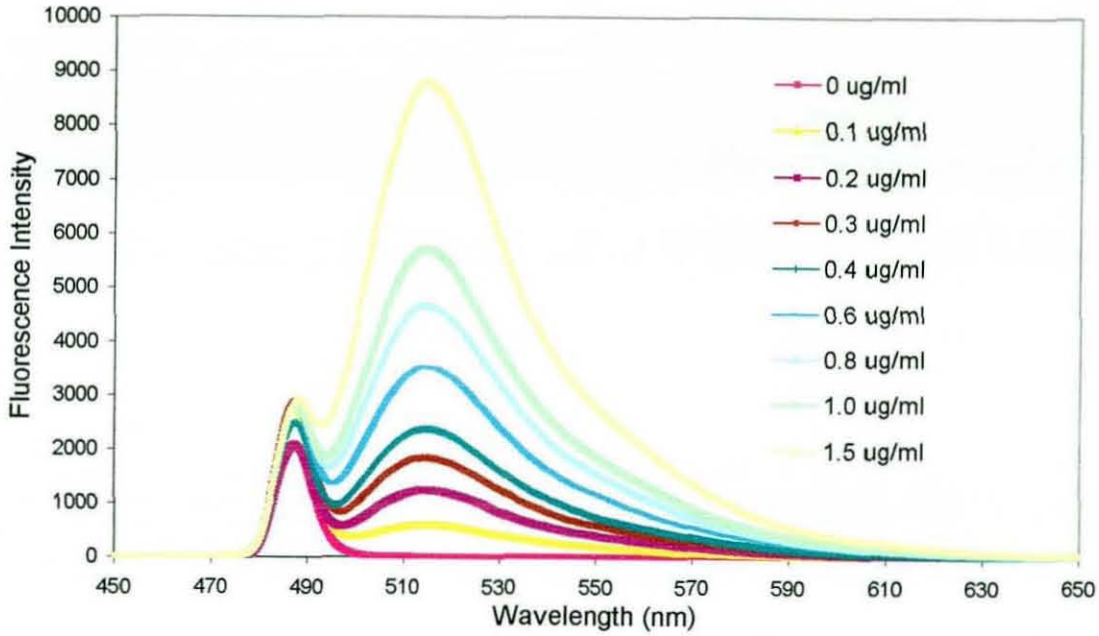

Figure 4.3 Influence of FDG concentration on FDG-β-Gal

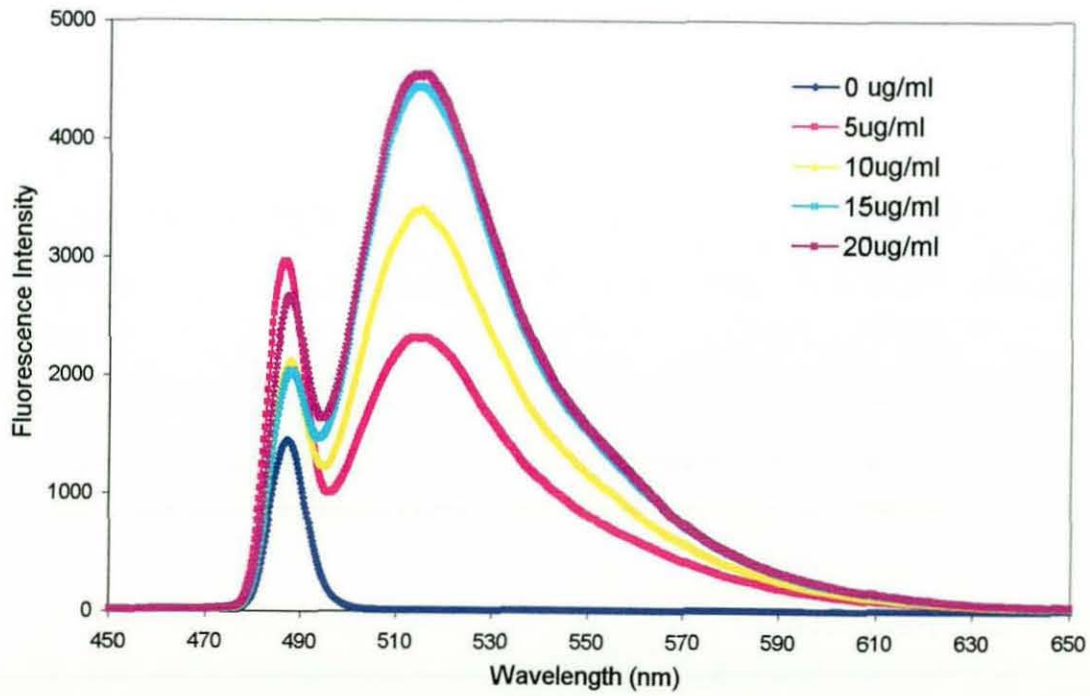

Figure 4.4 Influence of β-Gal concentration on FDG-β-Gal

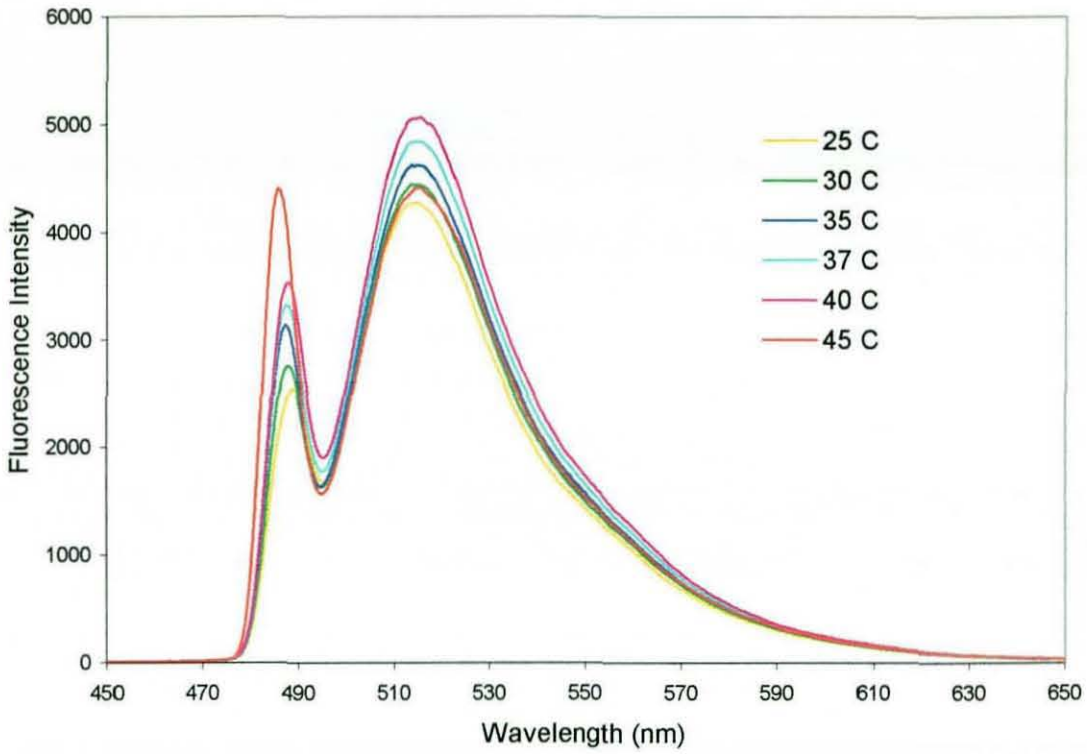

Figure 4.5 Influence of temperature on FDG-β-Gal

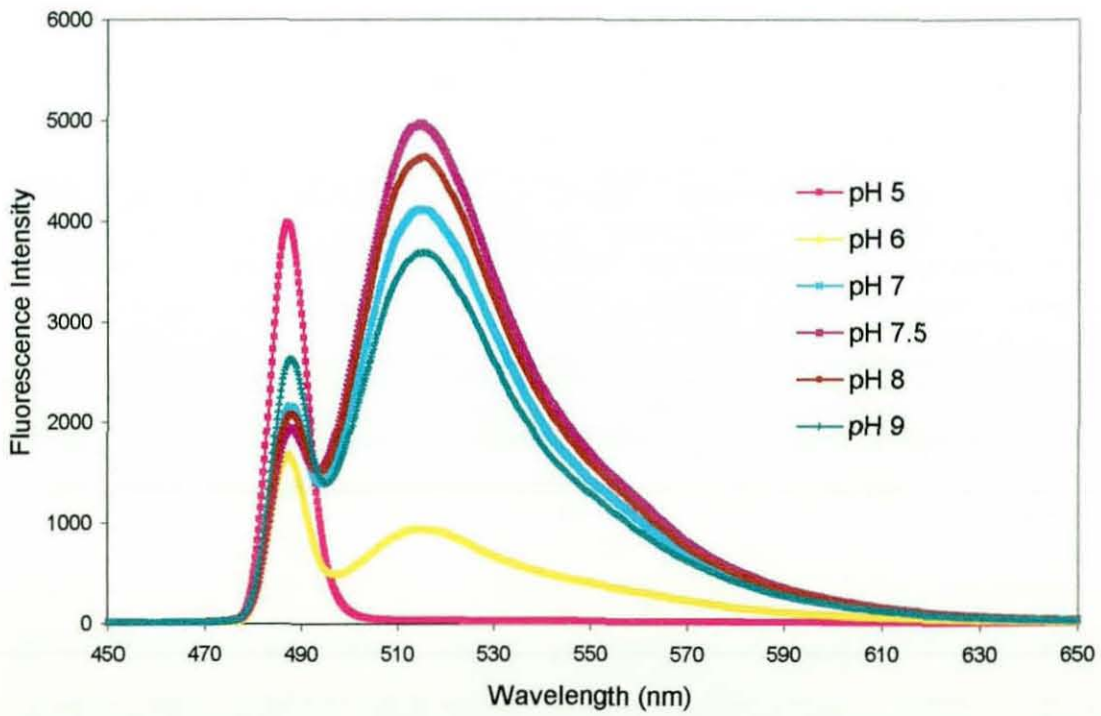

Figure 4.6 Influence of pH on FDG-β-Gal

Under the optimised conditions given in table 4.2, Bodipy FL-α-casein, FDG and FDP were incubated with AlkP, β-Gal and AP, respectively. As shown in figure 4.7-4.9, the fluorescence of Bodipy FL-α-casein, FDG and FDP increases dramatically after enzymatic digestion, indicating that Bodipy FL-α-casein, FDG and FDP are promising as fluorigenic substrates.

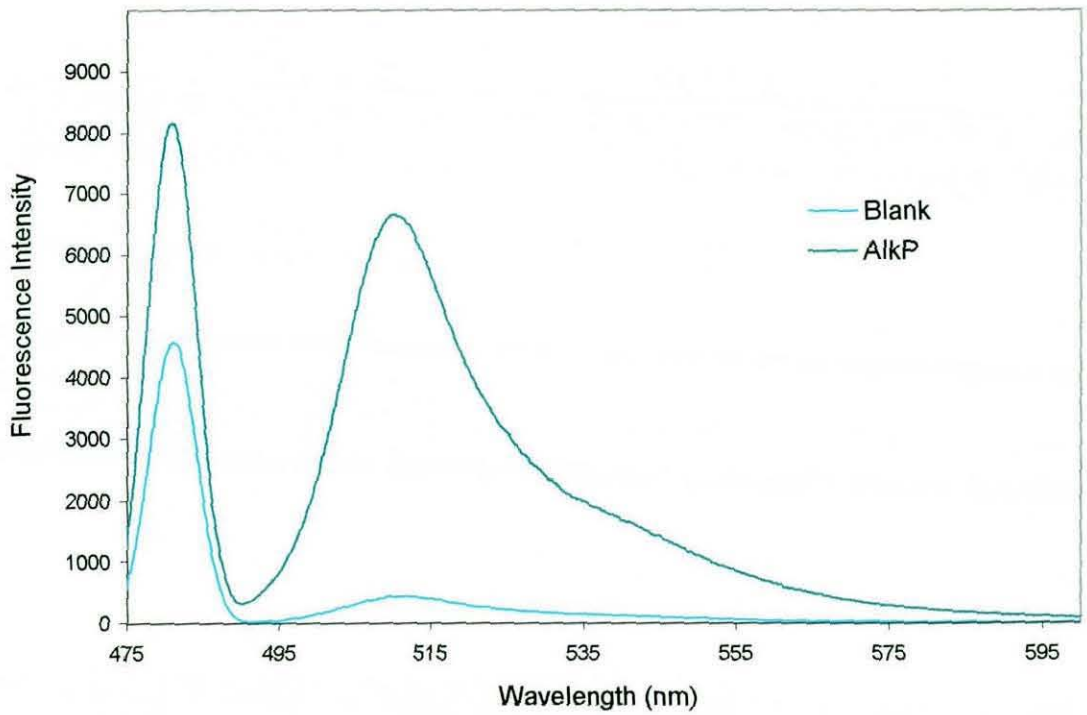

Figure 4.7 Fluorescence emission spectra showing enhancement seen upon incubation of Bodipy FL-α-casein with AlkP

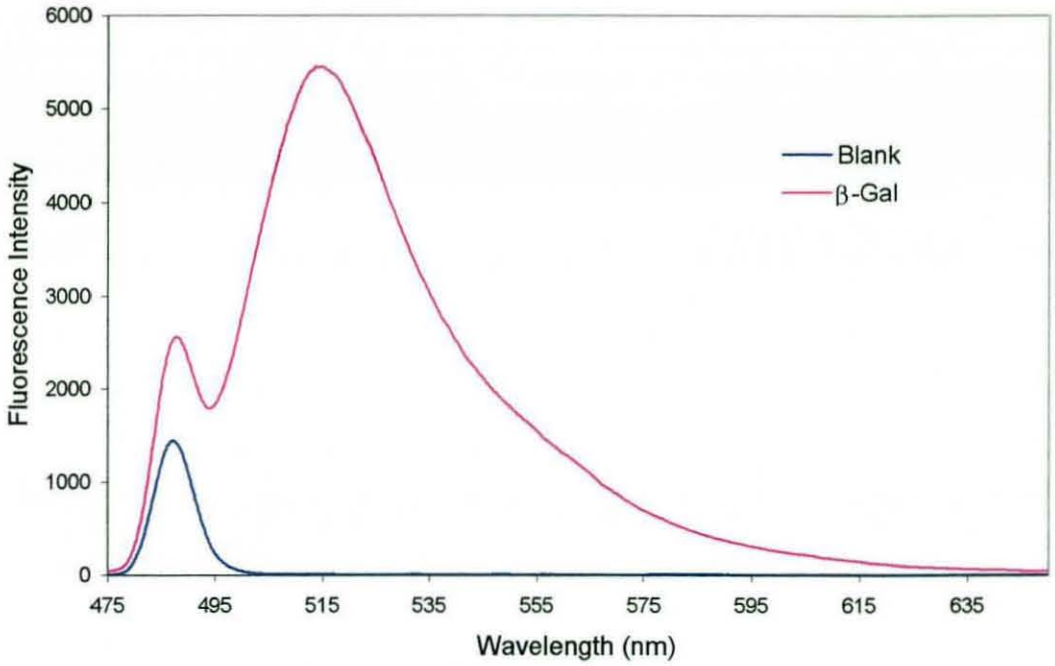

Figure 4.8 **Fluorescence emission spectra showing enhancement seen upon incubation of FDG with β-Gal**

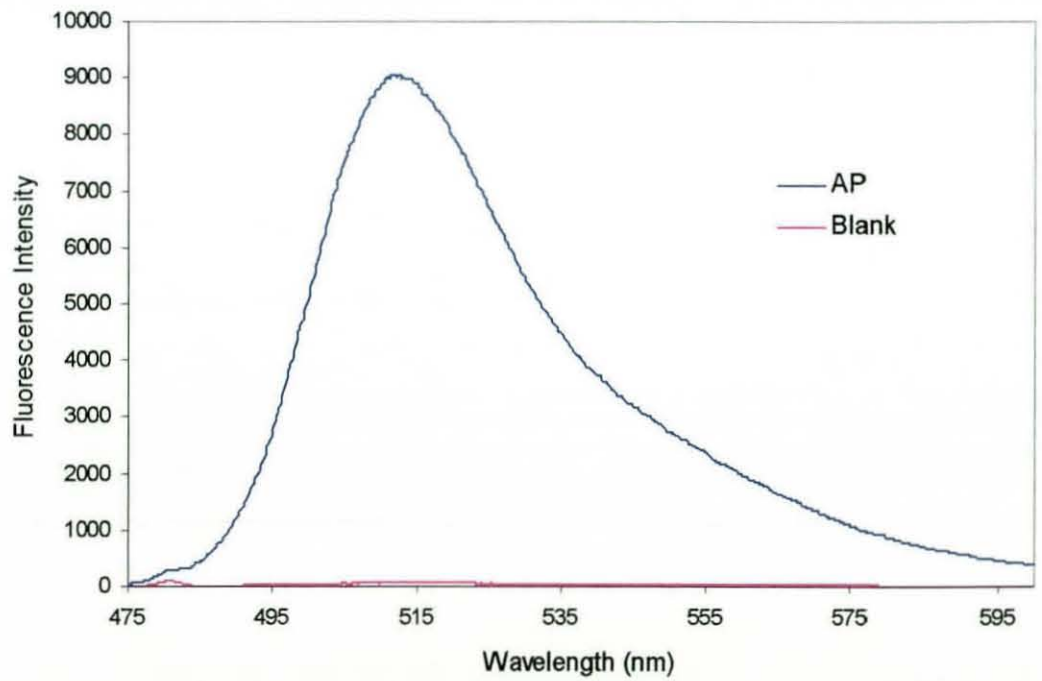

Figure 4.9 **Fluorescence emission spectra showing enhancement seen upon incubation of FDP with AP**

4.3 ENZYME IMMOBILISATION ON ULTRALINK BIOSUPPORT MEDIUM

Enzymes were immobilised on UltraLink biosupport medium. The immobilisation procedure is given in 3.2.10. The immobilised enzymes were packed in enzyme columns and incorporated into the flow injection system (figure 4.10). The hydrolysis products of Bodipy FL-α-casein, FDG and FDP reacted with AlkP, β-Gal and AP, respectively were monitored fluorimetrically at 514 nm, using the F-4500 detector. The immobilised enzymes were stored in PBS buffer (0.1 M, pH 7.2) at 4 °C when not in use. When the stability of the immobilised enzymes on UltraLink was tested it was found that the immobilised enzymes could be used for over 500 injections with around 90% capacity, and that the enzyme reactors preserved their activity for at least two months.

Enzyme concentrations and sodium citrate concentrations for immobilisation of AlkP, β-Gal and AP were optimised univariately.

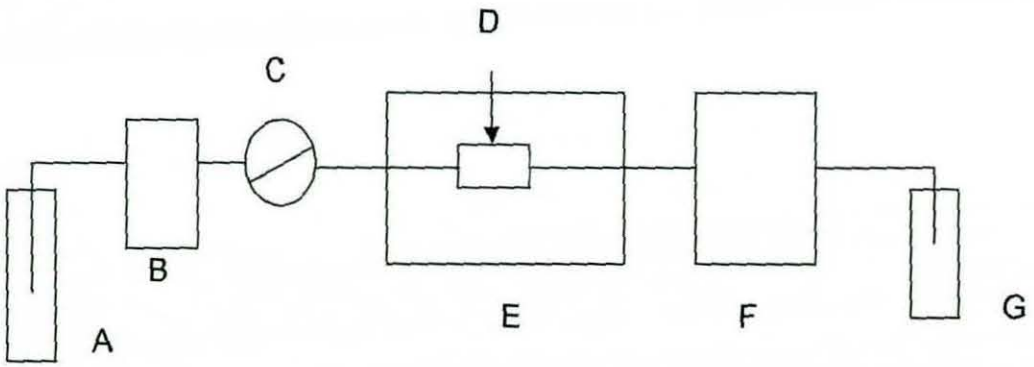

Figure 4.10 Manifold for flow injection enzyme and enzyme inhibition assays

(A = Buffer, B = Peristaltic pump, C = Injection valve, D = Enzyme reactor, E = Thermostatted water bath, F = Fluorescence detector and G = waste)

As it was found that similar trends were observed with all three conjugate-enzyme pairs, only the effect of assay parameters on the FDG-β-Gal will be described in detail here.

4.3.1 Effect of enzyme concentration

The effect of enzyme concentration on the immobilisation of β-Gal was examined over the range 10-80 mg/g of dry beads. As shown in figure 4.11, the percentage coupling efficiency of β-Gal was around 80% over the whole range of concentrations studied.

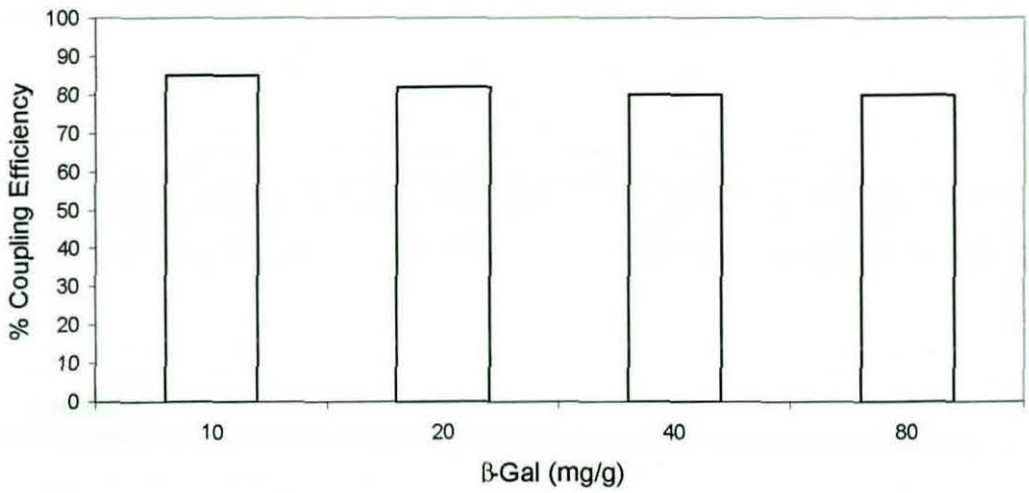

Figure 4.11 Influence of β-Gal concentration on immobilisation on UltraLink Biosupport Medium

4.3.2 Effect of salt concentration in the coupling buffer

The addition of salts to the coupling buffer may or may not enhance the amount of ligand covalently attached to the UltraLink biosupport medium, regardless of the pH of the coupling buffer. Salts could be added to the coupling buffer if they were compatible with the ligand. β-Gal was coupled to the UltraLink beads in PBS buffers pH 7.5. To the buffer were added different salt (sodium citrate) concentrations. The most efficient coupling for this enzyme was found to be at 0.6 M Sodium citrate or greater (figure 4.12).

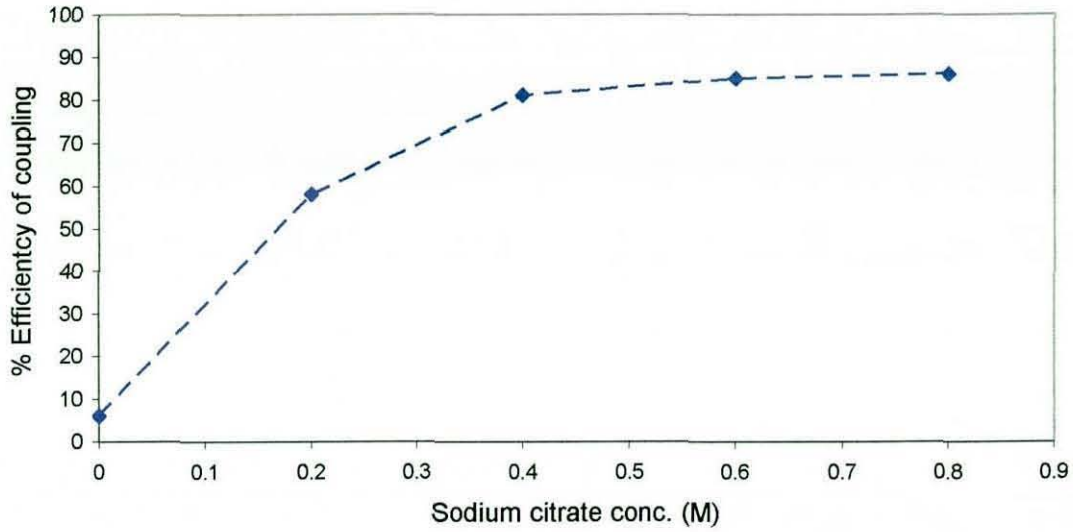

Figure 4.12 Effect of sodium citrate concentration on coupling for β-Gal

4.4 ENZYME ASSAYS IN A FLOWING SYSTEM

Fluorescence measurements were made using an F-4500 fluorescence spectrophotometer with excitation and emission bandwidths of 10 nm and time scans were performed with excitation and emission wavelengths of 480 nm and 514 nm respectively. Flow system measurements were carried out using the set - up shown in figure 4.10

Assay conditions for Bodipy FL-α-casein-AlkP, FDG-β-Gal and FDP-AP were optimised. The effects of the following parameters on the enzyme assays were studied:

- pH
- Buffer
- Buffer concentration
- Temperature
- Enzyme concentration
- Flow rate
- Enzyme reactor volume

- Substrate volume

The assay parameters studied, and optimum conditions found, for each conjugate-enzyme pair is shown below in table 4.3.

Table 4.3 Assay parameters studied and optimum conditions for various enzymes and substrates in a flow system

Assay parameters	Bodipy FL-α-casein-AlkP		FDG-β-Gal		FDP-AP	
	Range studied	Optimum	Range studied	Optimum	Range studied	Optimum
pH	7.0-9.5	9.0	7.0-9.0	8.0	7.5-9.5	8.5
Buffer	PBS, CA	PBS	PBS, CA	PBS	PBS, CA	CA
[Buffer], μM	10-100	20	10-100	20	10-100	20
Temperature,°C	25-45	37	25-45	37	25-45	37
[Enzyme], mg/g	5-100	100	5-40	20	5-100	80
Flow rate, ml/min	0.5-3.0	1.0	0.5-3.0	1.0	0.5-3.0	1.0
Enzyme reactor volume, μl	150-350	170	150-350	170	150-350	170
Substrate volume, μl	25-75	50	25-75	50	25-75	50

4.4.1 Effect of pH

The effect of pH on the activity of FDG-β-Gal was investigated. A pH range from 7.0 – 9.0 in 0.5 increments was investigated using PBS buffer. As shown in figure 4.13, pH affected the reaction rate insignificantly. However, a pH optimum of 8.0 was seen for FDG-β-Gal. Soluble β-Gal shown pH optimum at 7.5 (figure 4.6), which is shifted to 8.0 when the enzyme was immobilised. This may be attributed to the new environment for the enzyme and changes in its kinetic properties after it was immobilised.

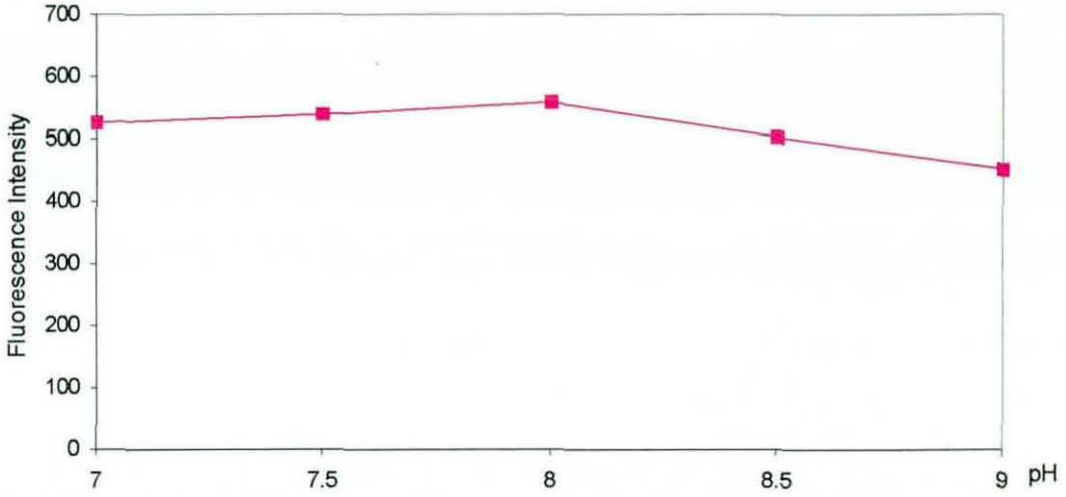

Figure 4.13 Effect of pH on the activity of FDG-β-Gal

4.4.2 Effect of buffer concentration

The effect of PBS buffer concentration on the extent of product formation was optimised. A concentration range of 10 mM – 100 mM was studied and as shown in figure 4.14, the buffer concentration had little effect on the activity of β-Gal on FDG. The greatest increase in intensity was observed with 10 mM PBS buffer. At higher buffer concentrations a gradual drop in the reaction rate occurred. A 20 mM PBS buffer concentration was chosen as a compromise between sensitivity and maximum buffering capacity.

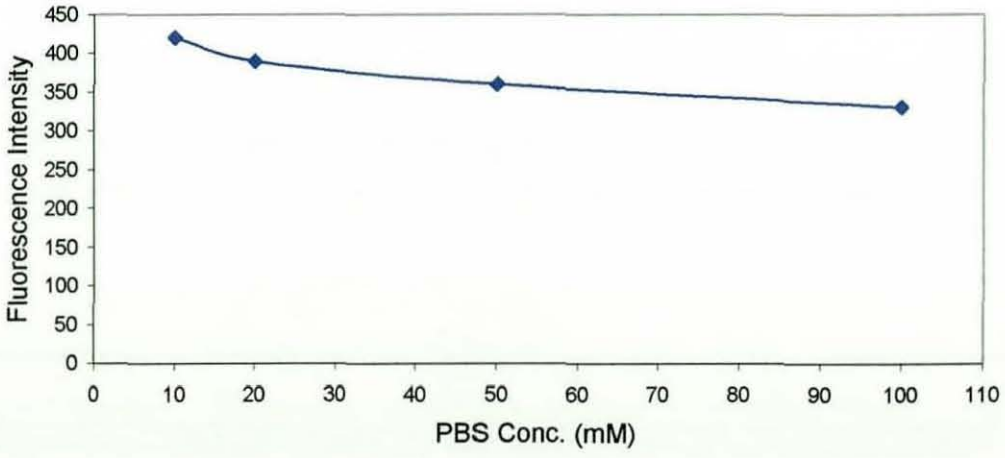

Figure 4.14 Effect of buffer concentration on the activity of β-Gal

4.4.3 Effect of temperature

The effect of temperature on the activity of FDG-β-Gal was examined over the range 25 - 45°C using a thermostatted water bath. As shown in figure 4.15, there was an increase in the reaction rate as the temperature was increased from 25°C to 40°C. Above 40°C an irreversible fall in the activity due to the denaturation of the immobilised enzyme was observed. As a result, subsequent investigations were carried out at 37°C in order to ensure a long lifetime for the enzyme reactor.

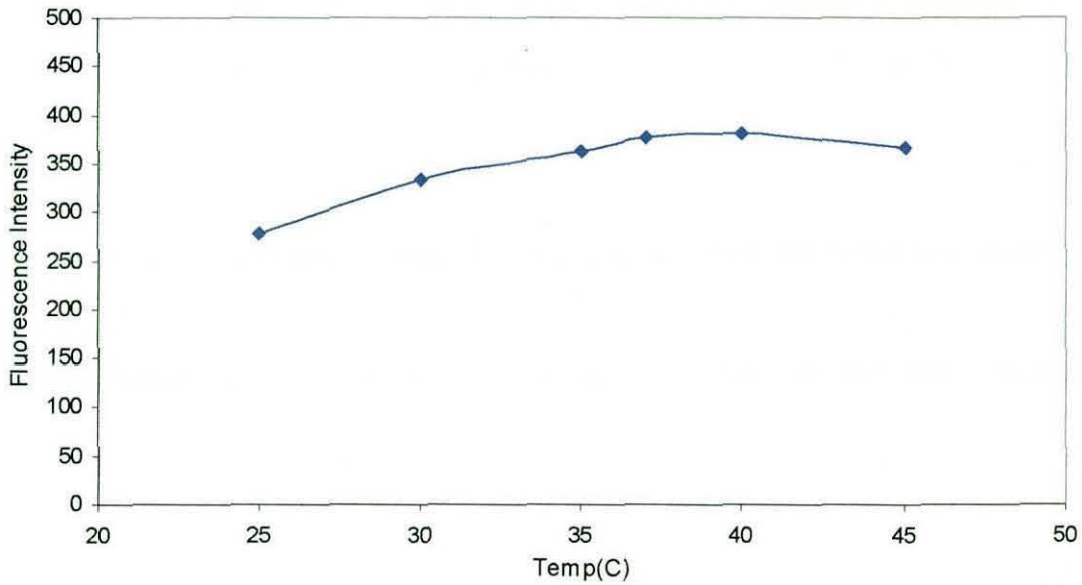

Figure 4.15 Effect of temperature on the activity of β-Gal

4.4.4 Effect of enzyme concentration on the reaction rate

Due to the high level of azlactone functionality, proteins couple with high coupling efficiency (around 80%) to the UltraLink biosupport medium over a wide range of concentrations. β-Gal concentration was varied between 10 and 40 mg/g dry beads. It can be seen from figure 4.16 that there was some increase in the reaction rate as the enzyme concentration was substantially increased. However, it was only slightly increased from 20 to 40 mg/g dry beads. Probably, the maximum coupling capacity has been reached at 40 mg β-Gal bound per gram of dry beads.

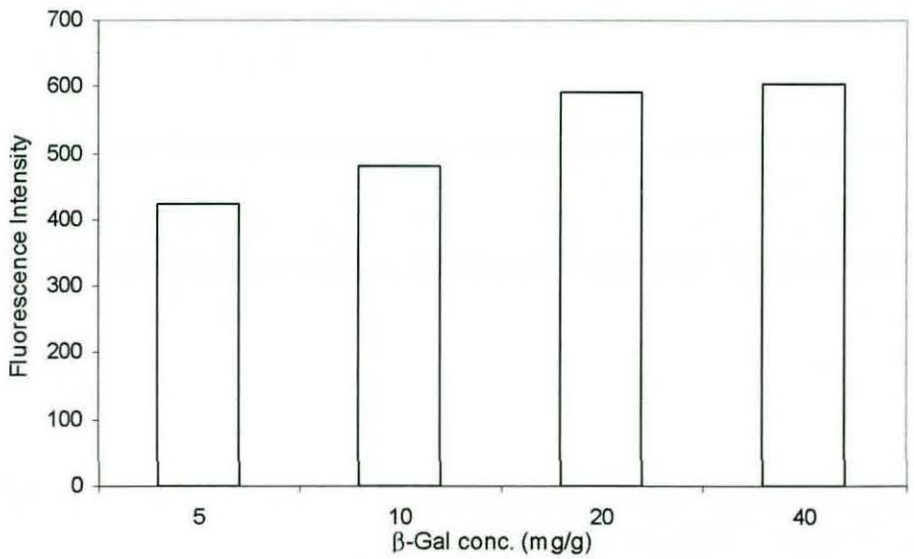

Figure 4.16 Influence of β-Gal concentrations on the formation of product

4.4.5 Influence of the enzyme reactor volume

The sensitivity of the β-Gal for FDG was investigated by using a set of three columns (150, 170 and 350 μl bed volume). As can be seen in figure 4.17, enzyme reactor volume did not greatly affect the sensitivity for using peak height, perhaps because of the higher dispersion effect of longer reactors. Measuring the peak area, the enzyme reactor volume had a marked effect on the sensitivity of β-Gal for FDG. In practice, however, using peak height was more convenient and less time consuming. Therefore the 170 μl bed volume was used for further studies.

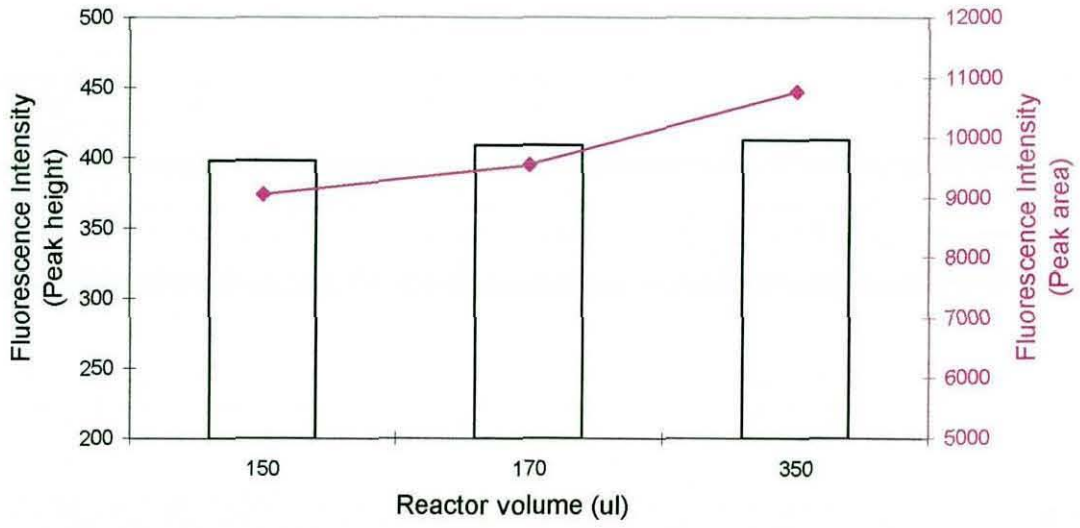

Figure 4.17 Effect of the enzyme reactor volume

4.4.6 Effect of flow rate

The flow rate effect was also examined for the optimum response from 0.5 – 3.0 ml/min. It was observed that increasing the flow rate from 0.5 – 1 ml/min slightly increases the fluorescence signal peak height, probably due to dispersion effect. However, flow rates above 1.0 ml/min resulted in a gradual fall in the enzymatic activity because of the decreased residence time of the sample in the system (figure 4.18). Therefore, a flow rate of 1.0 ml/min was used.

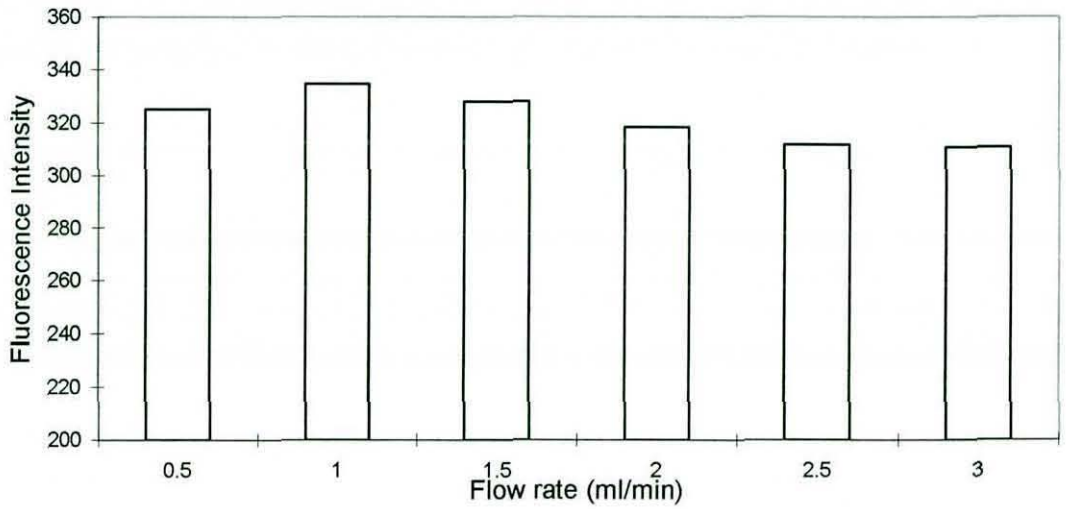

Figure 4.18 Effect of flow rate on the response of FDG-β-Gal

4.4.7 Effect of substrate volume

The effect of substrate volume was investigated for the optimum response from 25 – 75 μl. From figure 4.19, it was observed that increasing the substrate volume from 25 to 50 μl the fluorescence signal peak height dramatically increases. However, a substrate volume at 75 μl produced only a slight further increase in fluorescence. Thus, a substrate volume of 50 μl was used for further experiments.

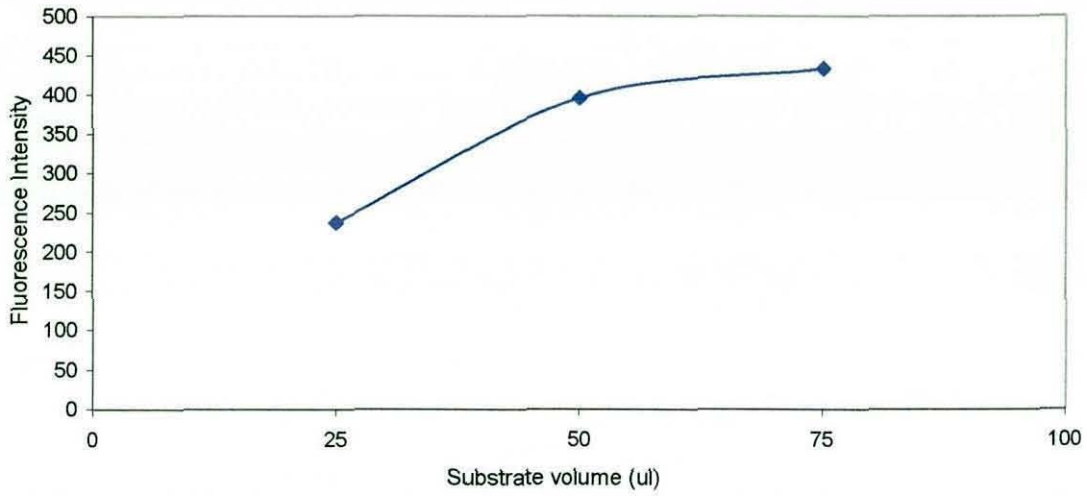

Figure 4.19 Effect of substrate volume on the response of FDG-β-Gal

4.4.8 Calibration graphs for Bodipy FL-α-casein-AlkP, FDG-β-Gal and FDP-AP

To evaluate the quantitative range, various concentrations of Bodipy FL-α-casein, FDG and FDP were injected into the flow injection system (figure 4.10), under the optimal conditions in table 4.3. The fluorescence intensity of the products of the enzymatic reaction increased with increasing concentration of the substrates indicating that the enzymatic system appeared to be working. Typical calibration graphs for Bodipy FL-α-casein, FDG and FDP was shown in figure 4.20. A linear relationship between fluorescence intensity, and Bodipy FL-α-casein, FDG and FDP concentrations was in the range of 0.5-8 μg/ml, 0.1-10 μg/ml and 0.02-10 μg/ml, respectively. The coefficient of determination was 0.9995 for Bodipy FL-α-casein, 0.9989 for FDG and. 0.9993 for FDP.

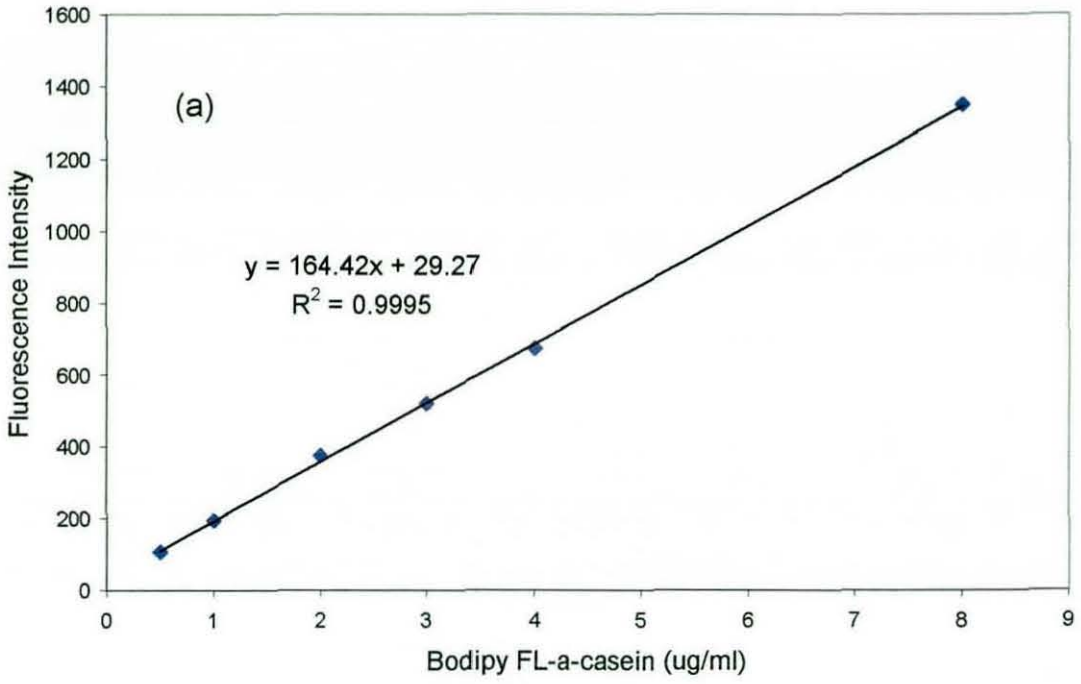
(a)
y = 164.42x + 29.27
R^2 = 0.9995
Fluorescence Intensity
Bodipy FL-a-casein (ug/ml)
0
200
400
600
800
1000
1200
1400
1600
0
1
2
3
4
5
6
7
8
9

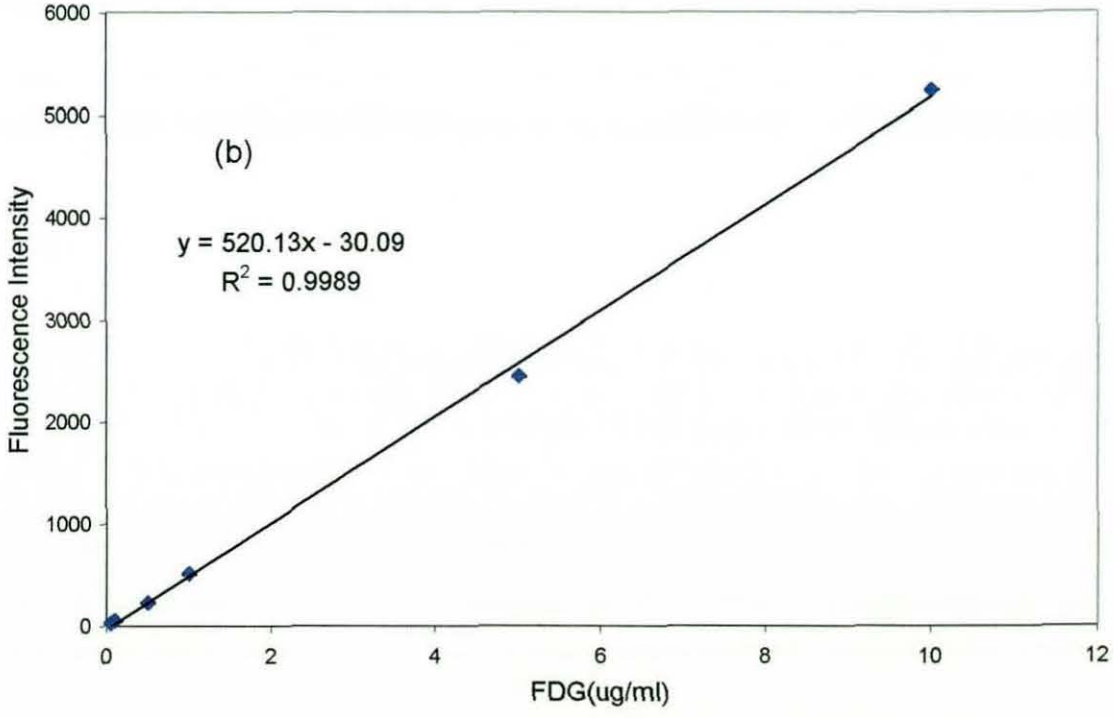
(b)
y = 520.13x - 30.09
R^2 = 0.9989
Fluorescence Intensity
FDG(ug/ml)
0
1000
2000
3000
4000
5000
6000
0
2
4
6
8
10
12

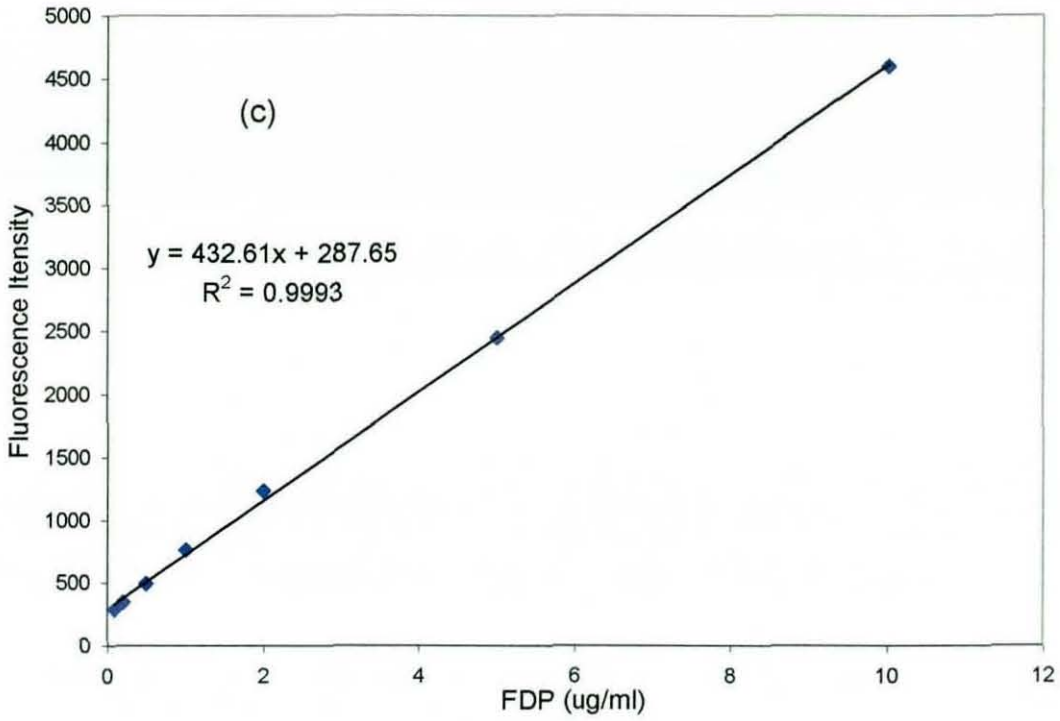

Figure 4.20 Influence of substrate concentration on the production of Bodipy FL-α-casein-AlkP (a), FDG-β-Gal (b) and FDP-AP (c) in a flow system

4.5 ENZYME INHIBITION ASSAYS

The inhibition of immobilised AlkP, β-Gal and AP by 3-nitrophenyl boronic acid (3-NPBA), phenylethyl thiogalactoside (PETG) and sodium vanadate (VI) respectively was investigated. The percent inhibition (%I) was calculated as follows:

$$\%I = 100 (A_0 - A_I) / A_0$$

where A_0 and A_I are the responses in the absence and presence of the inhibitor, respectively.

4.5.1 Enzyme reactivation

Along with the optimization process to obtain a sensitive method for enzyme inhibitor determination, attention must also be given to the rapid recovery of the enzyme activity so that the reactors can be reused. As a first step, the possibility of continuously passing buffer solution through the column to displace the inhibitor

was studied. Then the activity of the column was checked by injecting the substrate. It was found that 3-NPBA, PETG and VI could be displaced by the buffer and enzyme activity regenerated, around 1-3 min being required for 100% reactivation. The rate of reactivation after 3-NPBA, PTEG and VI inhibition actually depended on the degree of inhibition. 80% inhibited enzyme was fully reactivated in 2-3 min, which was checked by consecutive injections of the substrate after treatment with the inhibitor.

4.5.2 Inhibition of β-Gal by PETG

There are numerous sources of information on the inhibition of β-Gal.[175,176] In the present work attempts were made to evaluate the inhibitory effect of PETG on immobilised β-Gal in a flow system. The previously optimised conditions were checked. In addition the volume and concentrations of inhibitor were also examined. An increase in the volume and concentration of PETG increased the rate of inhibition of β-Gal (table 4.4). No significant change in the level of inhibition was observed by varying the other conditions. Therefore, all the conditions used for the inhibition of the enzyme were as previously described, with the exception of the volume of PETG (50 μl). The mixtures (inhibitor and substrate) were injected into the flowing system containing the enzyme reactor and then the response was measured. The results are shown in figure 4.21. The effect of PETG on the inhibition of β-Gal was evaluated by varying the inhibitor concentration with constant substrate concentration. As can be seen in figure 4.21, 80% inhibition was obtained with 20 μg/ml PETG.

Table 4.4 Effect of the volume and concentration of PETG on % inhibition of β-Gal

Volume of PETG, μl	25	50
% Inhibition	59	68

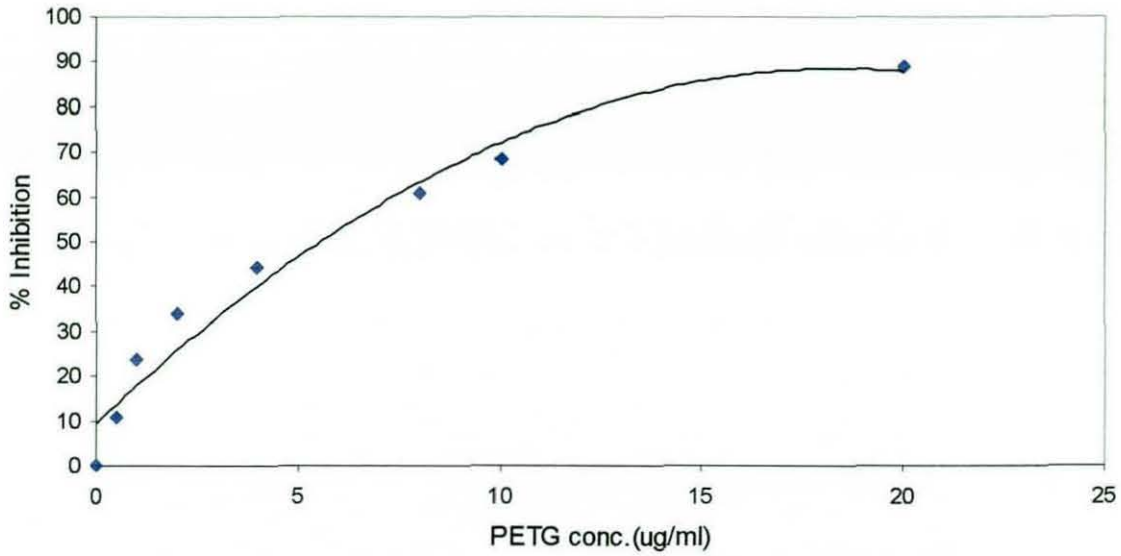

Figure 4.21 Inhibition of β-Gal by PETG determined with FDG at 37 °C

4.5.3 Inhibition of AlkP by 3-NPBA

Trigonal boron compounds contain a vacant 2p orbital which easily reacts as a Lewis acid with nucleophiles such as alkoxides and imidazoles to give a tetrahedral adduct.[177] The extended boronic acids are among the most potent reversible protease inhibitors yet developed. These compounds are similar to the peptide aldehydes in their apparent function as transition state analogues, but they appear to be very selective for serine proteases. In the current study attempts to develop an inhibition based assay for AlkP by 3-NPBA using Bodipy FL-α-casein as a substrate were made. This assay was performed in the same conditions as described earlier.

Standard solutions of 3-NPBA were mixed with the substrate prior to injection into the flow system. The concentrations of the inhibitor were between 0-5 μg/ml. As shown in figure 4.22, 3-NPBA efficiently inactivated the enzyme between 0.5 and 5.0 μg/ml

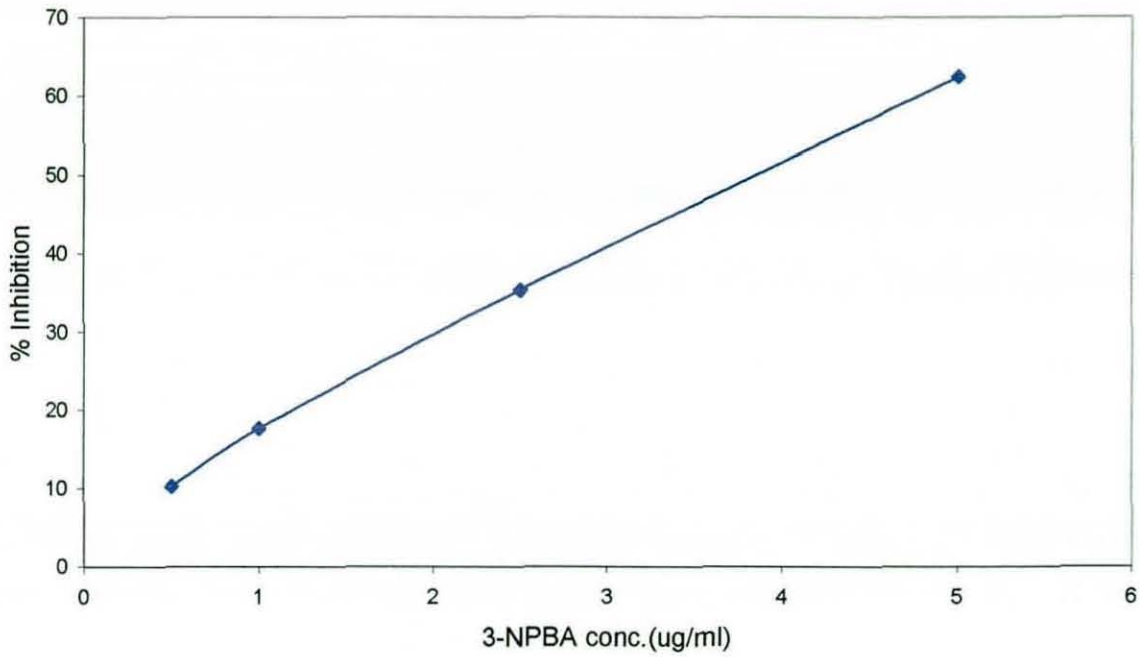

Figure 4.22 Inhibition of AlkP by 3-NPBA determined with Bodipy FL-α-casein at 37 °C

4.5.4 Inhibition of AP by VI

Vanadate (VO_4^{3-}) is a reversible phosphatase inhibitor. Vanadate is a phosphate analog and is generally thought to bind as a transition state analog to the phosphoryl transfer enzymes that it inhibits, since it can easily adopt a trigonal bipyramidal structure.[131] In the present study attempts to develop an inhibition based assay for AP by VI using FDP as a substrate were made. This assay was performed under the same condition as described earlier. The mixtures (inhibitor and substrate) were injected in the flowing system through the enzyme reactor and then the response was measured. The results are shown in figure 4.23. The effect of VI on the inhibition of AP was evaluated by varying the inhibitor concentration with constant substrate concentration. As can be seen in figure 4.23, 80% inhibition was obtained with 2.0 μg/ml VI.

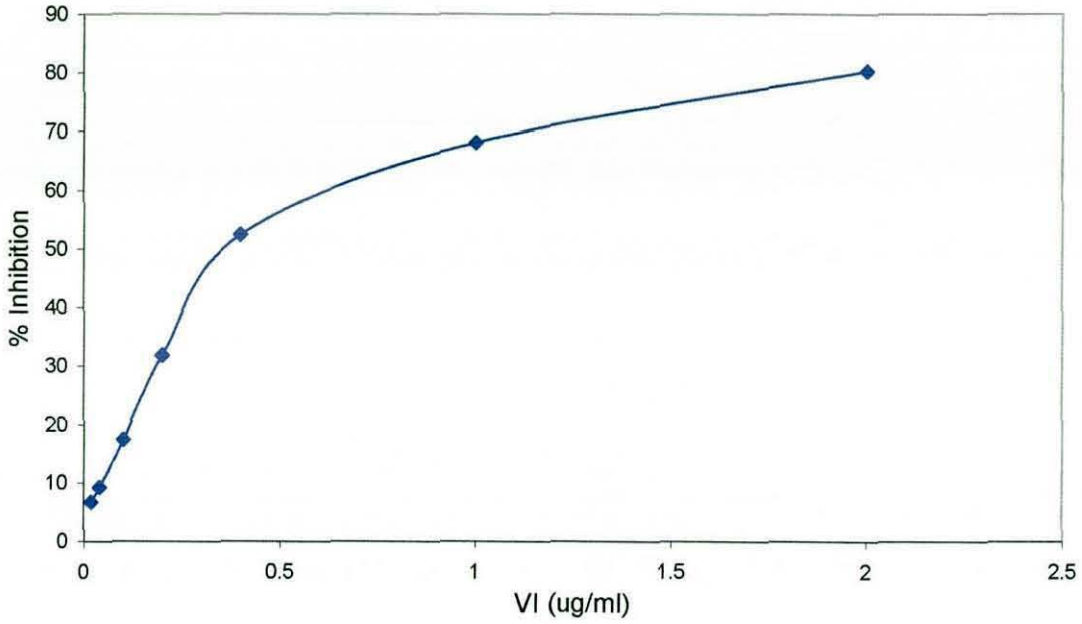

Figure 4.23 Inhibition of AP by VI determined with FDP at 37 °C

4.6 CONCLUSIONS AND DISCUSSION

Fluorimetric methods have proven to be safe, rapid and sensitive techniques to determine enzyme activity. The availability of a suitable fluorigenic substrate is critical to the success of fluorimetric determination of enzyme activities. Fluorigenic substrates usually practical convenience, and higher sensitive in enzymatic assays than their chromogenic counterparts.[178] Such methods combine the amplification effects of the catalytic enzyme action with the high sensitivity of fluorescence spectrometry and flow injection analysis. The procedure does not require any process such as separation, precipitation or centrifugation.

In this work the enzymes AP, AlkP and β-Gal were immobilised on UltraLink media. The enzyme reactor was placed in a flow injection system (figure 4.10). In order that an assay with optimum sensitivity could be constructed, the experimental conditions such as buffer (type, pH and concentration), temperature, flow rate, enzyme concentration, volume of substrate and volume of enzyme reactors, under which enzyme activities could be achieved were investigated (figure 4.13-4.19). The results obtained show identical trends for all the enzymes.

Increasing temperature had a positive influence on the enzymatic reaction; however, temperatures over 40 °C produced denaturation of the biocatalyst. The flow rate finally selected (1.0 ml/min) was appropriate for the reaction. Higher flow rates decreased the analytical signal due to a shorter on line substrate-enzyme contact time.

The enzymes exhibited a maximum response at pH 8.0-9.0 in flow systems. All the soluble enzymes showed pH optima which were shifted by 0.5pH units when the enzymes were immobilised. This may be attributed to the new environment for the enzymes and change in their kinetic properties after they were immobilised. Using enzymes with optimum activities at alkaline pH is ideal for the detection of the fluorescent products, especially fluorescein (pK_a = 7.9).

The activities of enzymes gradually decreased with increasing buffer concentration (10-100 mM), probably due to an increase in ionic strength.

In the optimum conditions (table 4.3) it was possible to obtain good calibration linearity over the range 0.5-8 μg/ml, 0.1-10 μg/ml and 0.02-10 μg/ml for Bodipy FL-α-casein ($y = 164.42x + 29.27$, $r^2 = 0.9995$), FDG ($y = 520.13x - 30.09$, $r^2 = 0.9989$) and FDP ($y = 432.61x + 287.65$, $r^2 = 0.9993$), respectively (figure 4.20). The relative standard deviation for 10 successive injections was 1.07–2.39%.

3-NPBA, PETG and VI, in this work were determined by their inhibitory effect on immobilised, AlkP, β-Gal and AP, respectively in a flow injection system and continuous reuse of the immobilised enzymes with little loss of enzyme activity. The previously optimised conditions were used for this investigation. The method is rapid (allowing around 15-25 measurements to be made per hour) and economic. The inhibition of AP, AlkP and β-Gal with the inhibitors at μg/ml levels was achieved.

This approach offers the potential to determine the concentration of two or more analytes in a single sample which could be used for the simultaneous detection. In addition, it may be possible to extend this concept to the development of more rapid simultaneous assays.

CHAPTER 5

MULTIPLEX SCREENING ENZYME INHIBITION ASSAYS

5.1 INTRODUCTION

The aim of these experiments was to investigate multiplex screening enzyme inhibition assays in a flow injection analysis system based on the use of immobilised enzyme reactors, such that the system would allow the determination of more than one inhibitor in the same assay.

The need to improve productivity is imperative for drug discovery companies. One strategy is: test more discover more. The availability therefore of a simple, sensitive, and efficient method for the simultaneous determination of immobilised enzymes and their inhibitors would be of much use in the high throughput screening of candidate drug molecules. This set-up would allow a much higher throughput accompanied by cost advantages.

An excellent review discusses the determination of two or more species in the same sample with a single flow injection analysis system.[179]

5.2 FLUORESCENCE SPECTRA OF BODIPY FL-α-CASEIN, FDP AND FDG

A comparison of the fluorescence spectra of Bodipy FL-α-casein-AlkP, FDP-AP and FDG-β-Gal are shown in figure 5.1.

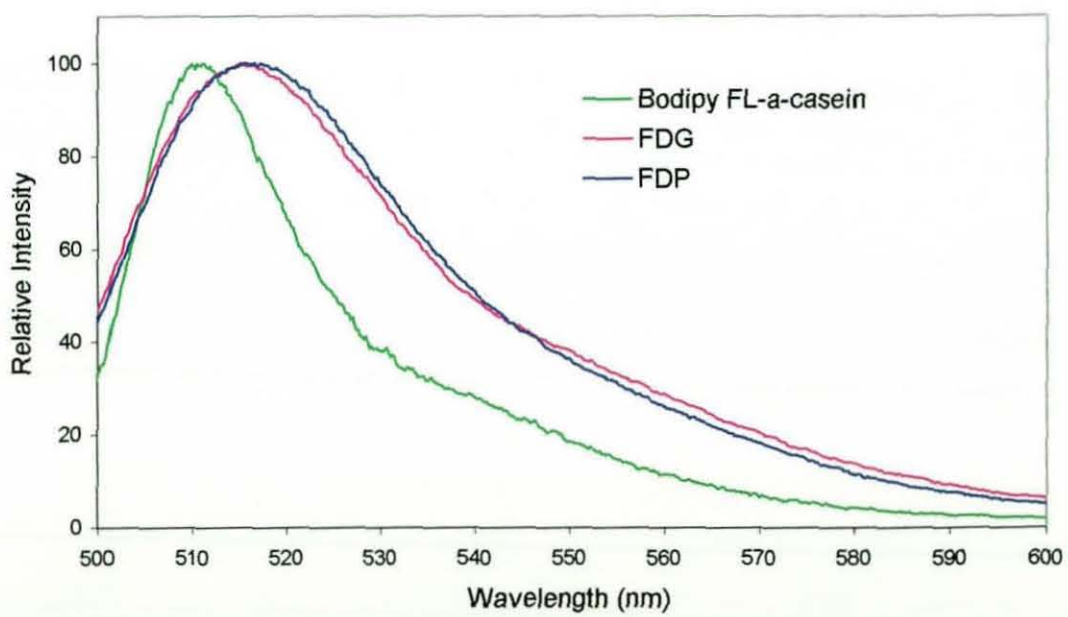

Figure 5.1 Emission spectra of Bodipy FL-α-casein-AlkP, FDP-AP and FDG-β-Gal

From the result it can be seen that the emission spectra of Bodipy FL-α-casein-AlkP, FDP-AP and FDG-β-Gal are extremely overlapped, their fluorescence spectra are similar, especially when they are at the same intensity. Therefore, it is difficult to analyse these two or three analytes using conventional fluorescence spectroscopy. However, the problem of overlapping spectra can be overcome by using chemometric techniques (in chapter 6) or using time-dependent separation of flow injection analysis. Here the latter method was investigated.

5.3 INVESTIGATION OF SIMULTANEOUS ASSAYS BY A FLOW-INJECTION METHOD BASED ON THE USE OF IMMOBILISED ENZYME REACTORS

Fluorescence measurements were made using a F-4500 fluorescence spectrophotometer with excitation and emission bandwidths of 10 nm. Time scans were performed with excitation and emission wavelengths of 480 nm and 514 nm respectively for FDG and FDP as well as Bodipy FL-α-casein. All optimised conditions previously described in chapter 4 were used.

As a starting point for the assays, it was decided that the simplest approach would be a dual assay using one buffer system. As was shown in table 4.3, the optimum pHs and buffers for AlkP, β-Gal and AP were different. However, the best compromise of pH for FDG-β-Gal and Bodipy FL-α-casein-AlkP in a dual assay system is PBS, pH 8.0, for FDG-β-Gal and FDP-AP is CA, pH 8.0, and for Bodipy FL-α-casein-AlkP and FDP-AP is CA, pH 8.5.

The ideal set-up for a simple assay was to flow buffer slowly through two enzyme reactors, each containing a different immobilised enzyme, as shown in figure 5.2. A substrates solution would be injected and the fluorescence detected through the time-dependent separation of the peaks emerging from each of the reactors by having different lengths of flow tubing between the enzyme reactors and the detector.

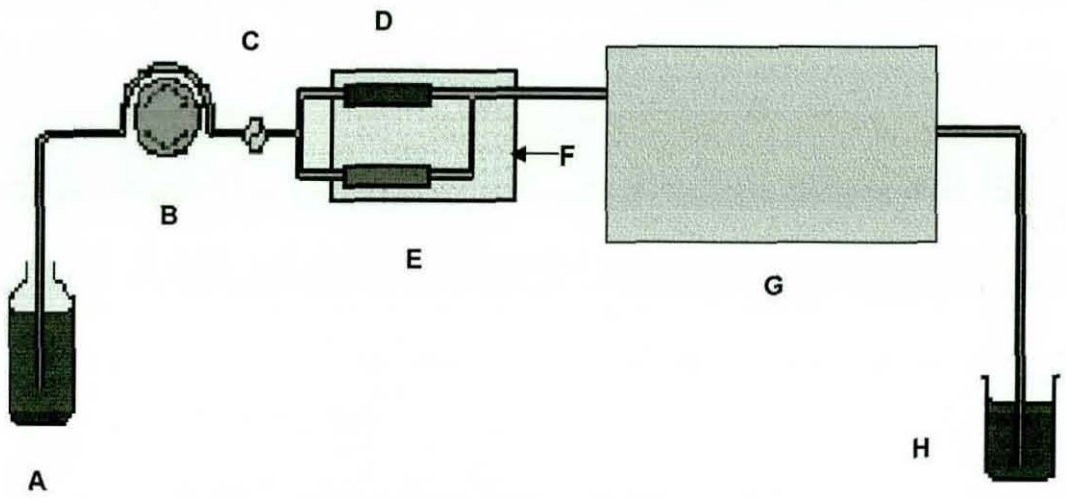

Figure 5.2 Schematic of flow injection analysis system for dual assay
(A = buffer, B = peristaltic pump, C = injection valve, D = enzyme reactor 1, E = enzyme reactor 2, F = thermostatted water bath, G = fluorescence detector and H = waste

Immobilised enzyme was packed into Omnifit glass columns with a bore of 3 mm, and a length of 2.5 cm corresponding to reactor volume of 175 μl. Aluminium frits with 2 μm pores were used at both ends to prevent leakage of the UltraLink media. The appearance of the enzyme reactors is shown in figure 5.3. Columns were packed by mounting the columns vertically, and connecting the bottom of the column to a peristaltic pump that allowed suction of loaded UltraLink through the top end of the column downwards. The glass column was then incorporated into the flowing system and clamped vertically in the water bath. Buffer was flowed upwards through the column, which was opposite to the direction of packing. This ensured maximum contact of the buffer with the UltraLink and tighter packing.

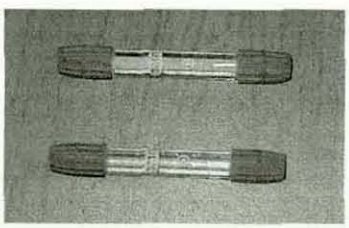

Figure 5.3 Appearance of the enzyme reactors
(top – packed glass column, bottom – empty glass column)

5.3.1 Investigation of interference between the substrates and enzymes

Interference caused between components in the system is an important consideration in a mixture for simultaneous assays. To determine the interference the following methods were used:

In a static system, dual assays of Bodipy FL-α-casein-AlkP and FDG-β-Gal, FDP-AP and FDG-β-Gal, as well as Bodipy FL-α-casein-AlkP and FDP-AP were investigated. The concentrations of chemicals were kept constant, but the combinations of the components were varied. The resulting changes in fluorescence intensities were considered. The results showed that there was no interference amongst the components in the experiments. Only the result of the experiment for Bodipy FL-α-casein-AlkP and FDG-β-Gal was shown in figure 5.4.

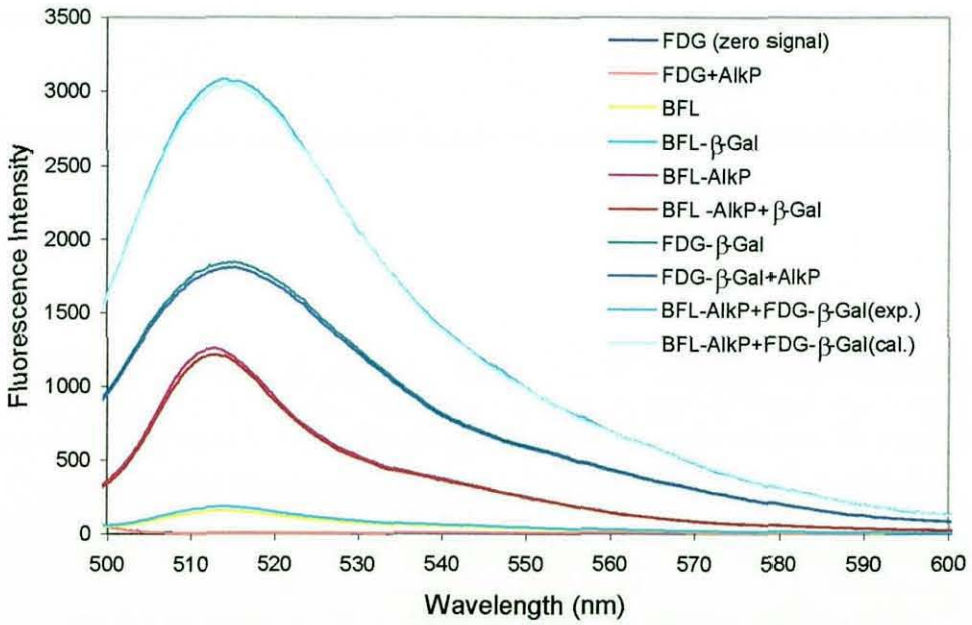

Figure 5.4 Interference of Bodipy FL-α-casein-AlkP and FDG-β-Gal

5.3.2 Determination of length of flow tubing required for separation of peaks

As the principle behind the dual-determination assay was to inject two substrates with or without inhibitors and detect the two peaks of products by time-dependent separation, it was important to determine the length of tubing required to cause such a separation. The tubing that was used for the experiments was Omnifit Teflon tubing with an internal diameter of 0.8 mm. A minimum length of tubing was required for the shorter length section so that the fluorescence spectra (which appear as a rapid pulse) actually recorded would be as sharp as possible. The appearance of actual layout and the length of flow tubing used are shown in figure 5.5 (b). A length of 15 cm. was used between the first Y junction to both reactors. This was chosen so that the assay components would flow through the thermostatted water bath. For the shorter length section, a 5 cm. length was used between the reactor and the second Y junction as this was the minimize distance. Using this length of tubing, the time between injection and detection of the first peak was around 9 seconds at flow rate 1.2 ml/min.

A longer length of tubing of 50 cm. for the second reactor was firstly added. However, using this length was too short for peak separation. In order for a separation of the peaks to occur the first peak has to return to the baseline first, so sufficient time must be allowed for this to occur. A length of 200 cm. was then added. This length was long enough to separate the two peaks which were properly resolved.

Photos are shown in figure 5.5 (a) and (b) depicting the actual set-up of this flow system in our laboratory

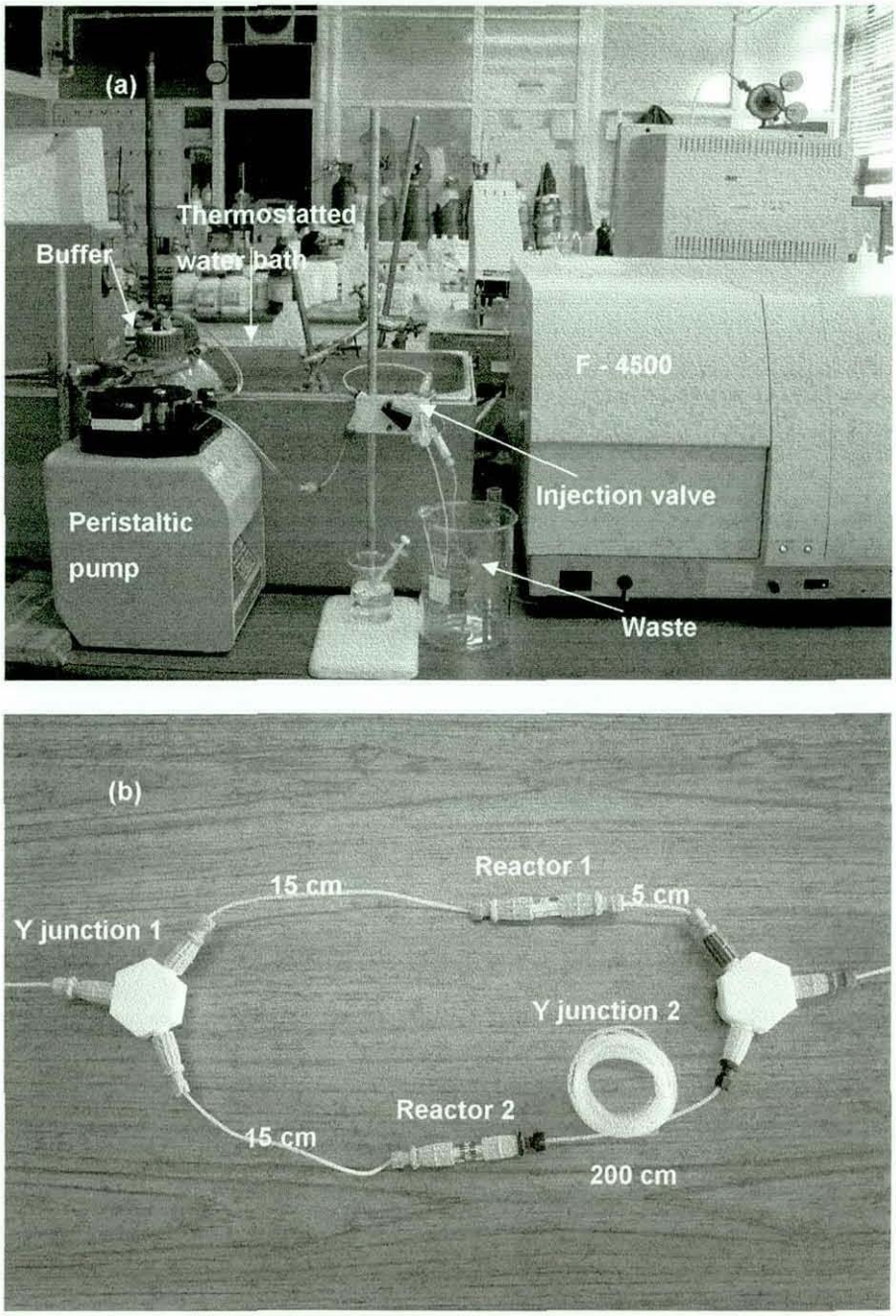

Figure 5.5 (a) and (b) – Actual layout and equipment used for flow analysis enzyme and enzyme inhibition assays

5.3.3 Effect of flow rate

The flow velocities of the buffer stream should be considered so that in the complete system there would be sufficient residence time for the sample in the enzyme reactors and any risk that tight packing of the column material might lead to increased back-pressure would be minimized.

The effect of the flow rate on the response to Bodipy FL-AlkP and FDP-AP were investigated in the range of 0.5-1.5 ml/min. The result showed that the response decreased with increasing flow rate up to 1.5 ml/min. The choice of flow rate involves a compromise between sensitivity and sample output rate as well as a risk of tight packing. A flow rate of 1.2 ml/min was chosen for further experiments, considering its relatively high response and the short sample output time.

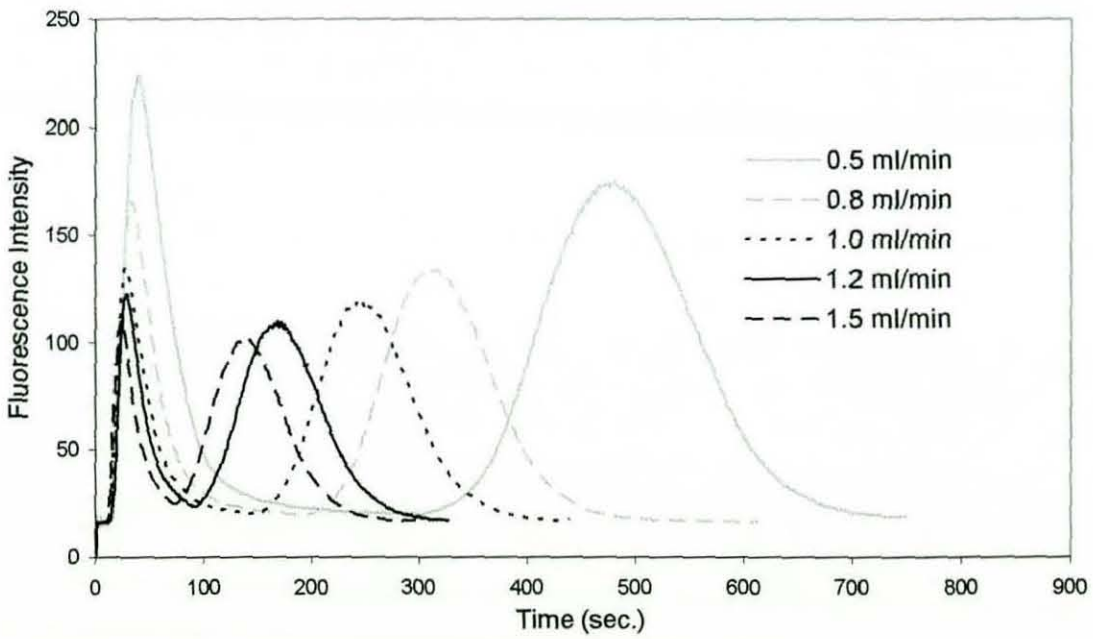

Figure 5.6 Effect of flow rate on dual Bodipy FL-AlkP and FDP-AP assay

5.3.4 Simultaneous FDG and Bodipy FL-α-casein using immobilized β-Gal and AlkP reactors

In order to establish a simple dual enzyme assay standard mixtures of Bodipy FL-α-casein (0-10 μg/ml) and FDG (0-5 μg/ml) were injected through a manual injection valve (50 μl each) into the flow system shown in figure 5.2 and figure 5.5. The sample was split into two parts using a Y-connector and then passed into the AlkP and β-Gal reactors. Product from the enzyme reactor with the shorter distance to the F-4500 was detected first. Then product from the enzyme reactor with the longer distance to the F-4500 was detected second.

A typical flow injection analysis response of the products obtained by the two enzyme system was shown in figure 5.7. The calibration graphs obtained for FDG ($y = 182.1x - 1.1489$, $r^2 = 0.9962$) and for Bodipy FL-α-casein ($y = 72.504x + 9.1279$, $r^2 = 0.9990$) showed good linearity in the range investigated as shown in figure 5.8. These results demonstrate that the system can successfully be used for dual-analyte assays.

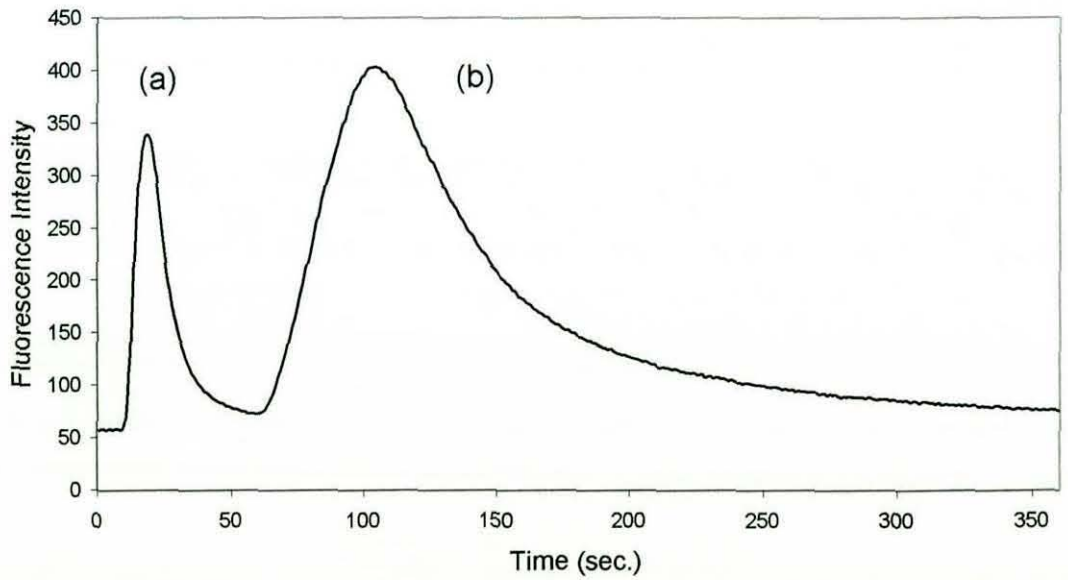

Figure 5.7 Typical flow injection analyses obtained by Bodipy FL-α-casein and FDG using a dual enzyme system, (a) AlkP and (b) β-Gal

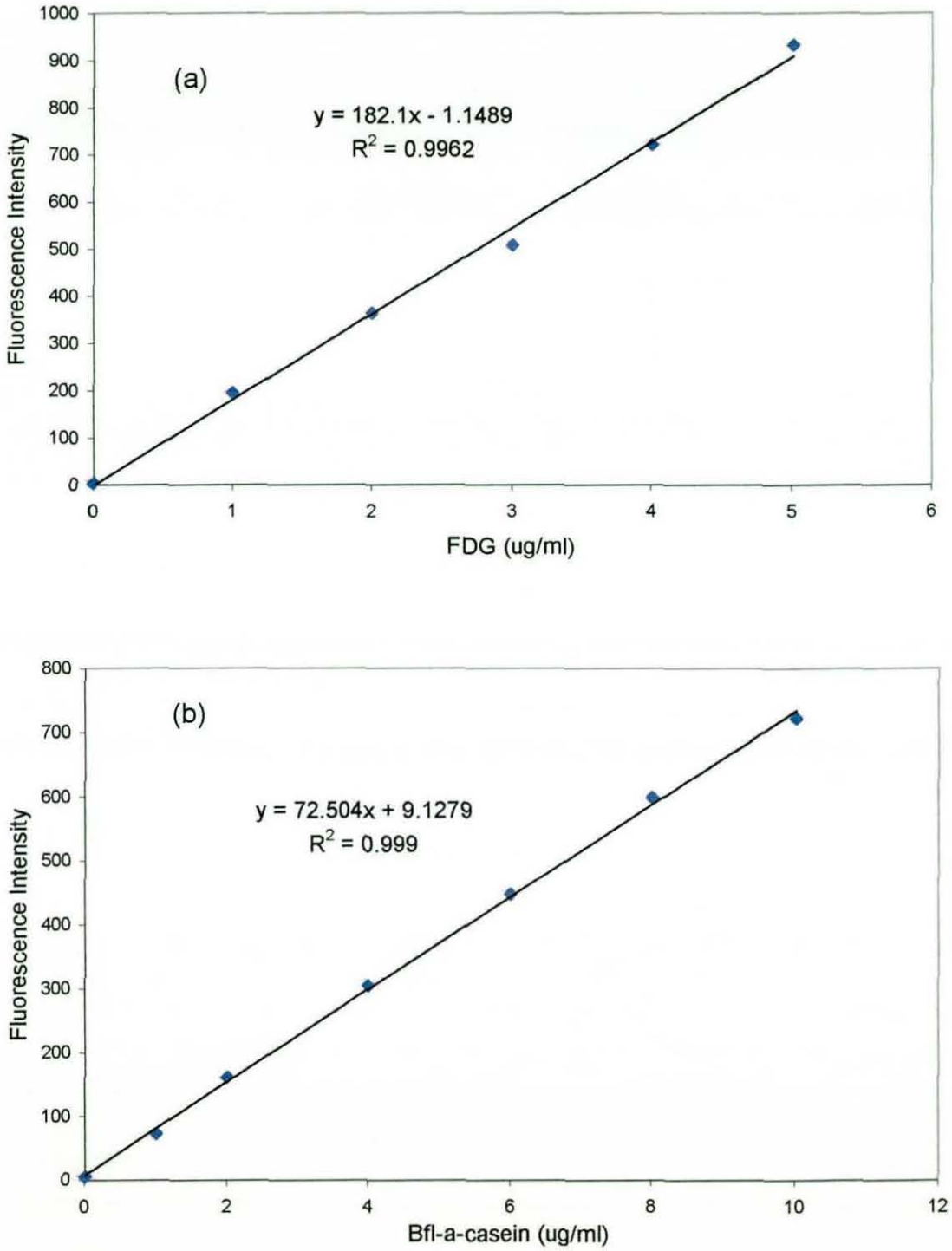

Figure 5.8 Calibration graph for (a) FDG and (b) Bodipy FL-α-casein using a dual enzyme system

5.3.5 Simultaneous FDG and FDP using immobilized β-Gal and AP reactors

Standard mixtures of FDG (0-5 μg/ml) and FDP (0-5 μg/ml) were injected. The typical flow injection analysis responses of the products was obtained by the immobilized β-Gal and AP enzyme reactor system (figure 5.9). The good calibration linearity was shown over the range investigated as shown in figure 5.10. For FDG, y = 149.86x – 4.076, r^2 = 0.9984, and for FDP, y = 227.21x + 75.172, r^2 = 0.9978. Therefore, the system can be used for dual-analyte assays successfully.

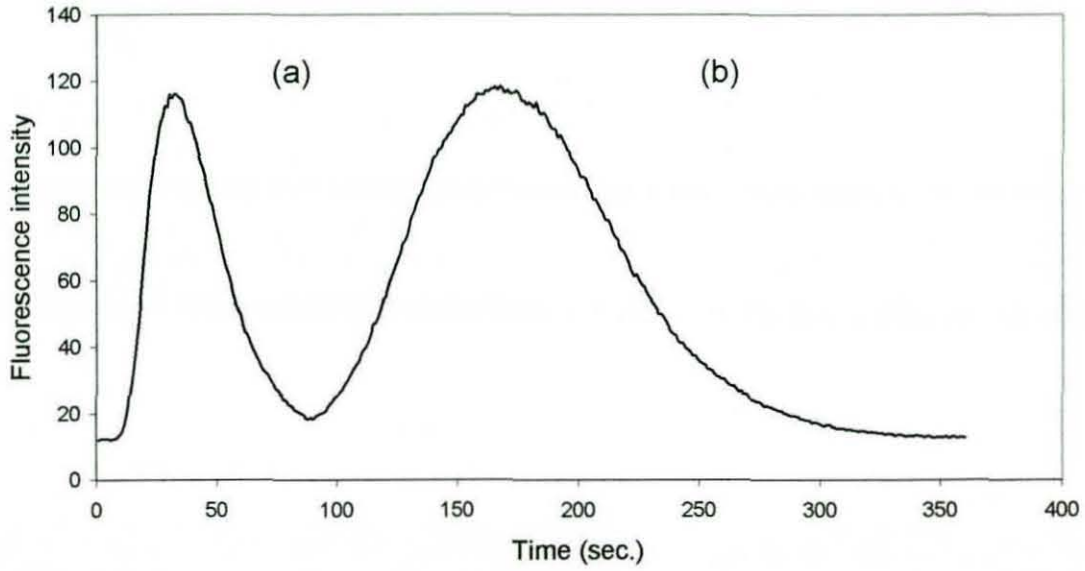

Figure 5.9 Typical flow injection analyses obtained by FDG and FDP using a dual enzyme system, (a) β-Gal and (b) AP

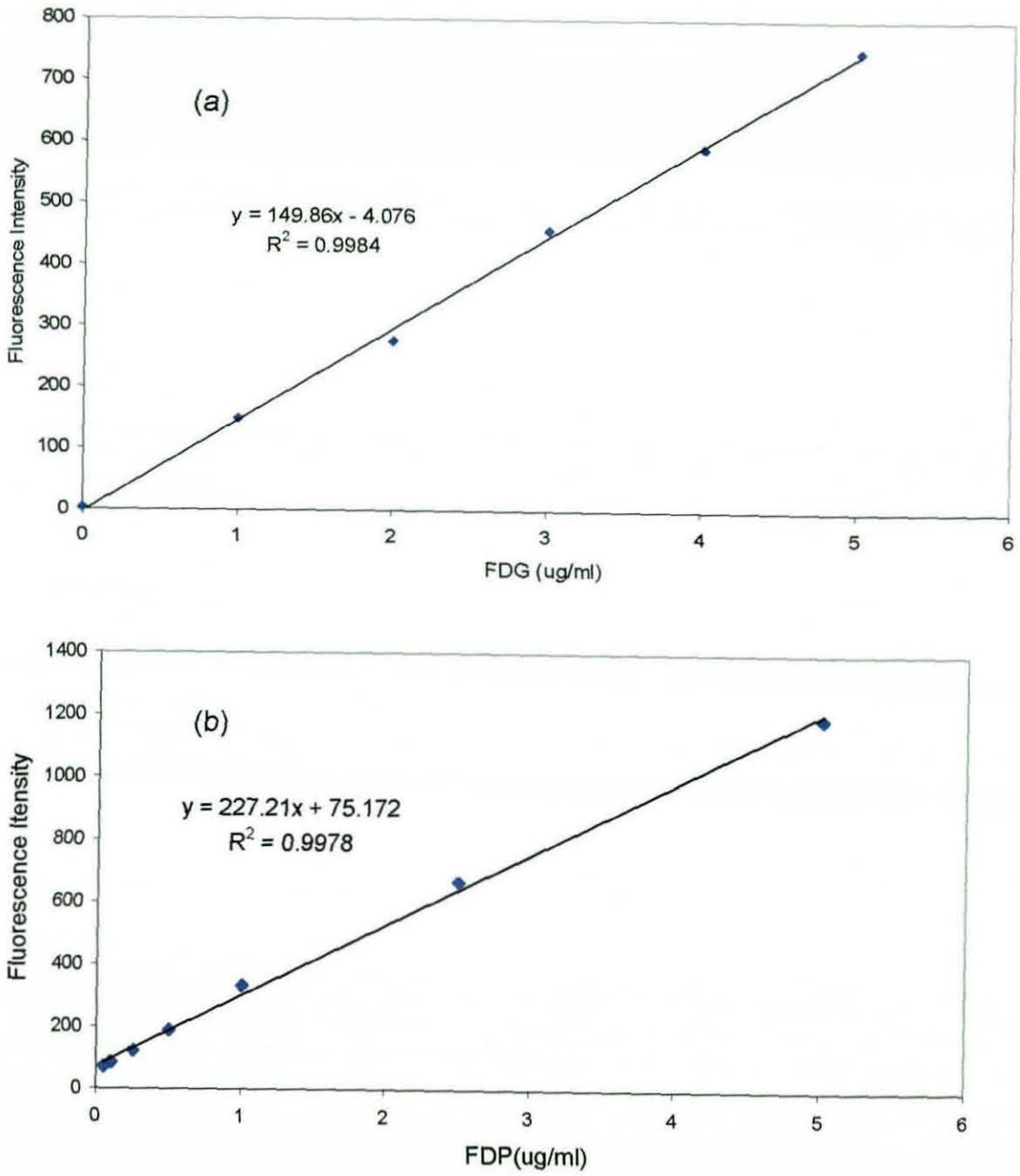

Figure 5.10 Calibration graph for (a) FDG and (b) FDP using a dual enzyme system

5.3.6 Simultaneous Bodipy FL-α-casein and FDP using AlkP and AP

Standard mixtures of Bodipy FL-α-casein (0.5-10μg/ml) and FDP (0.01-5μg/ml) were injected. The typical flow injection analysis responses of the products was obtained by the immobilized AlkP and AP enzyme reactor system (figure 5.11),

and calibration graphs, which gave the good linearity in the range investigated, are shown in figure 5.12. For Bodipy FL-α-casein, y = 33.909x + 1.46, r^2 = 0.9985, and for FDP, y = 284.92x + 104.84, r^2 = 0.9997. Therefore, the system can be used for dual-analyte assays successfully.

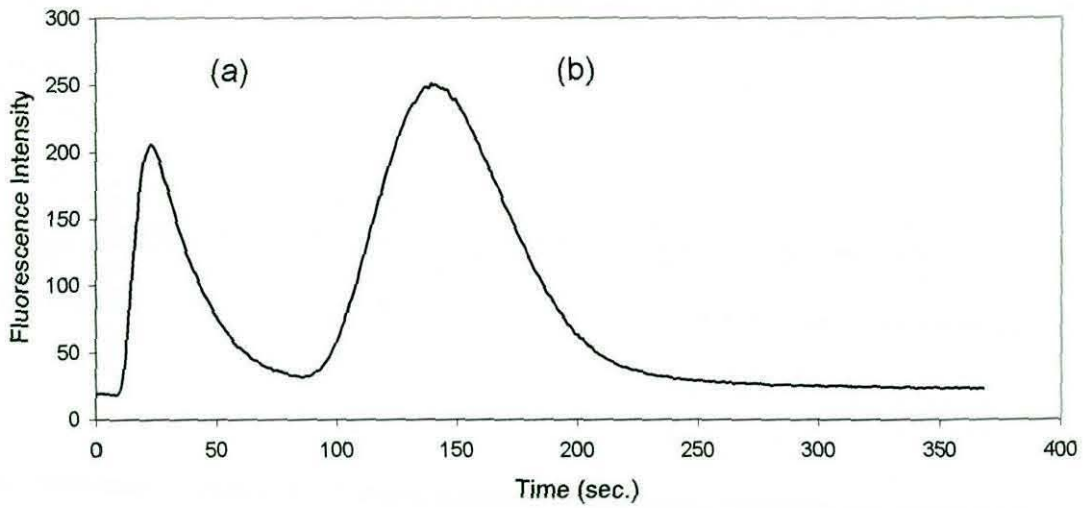

Figure 5.11 Typical flow injection analyses obtained by Bodipy FL-α-casein and FDP using a dual enzyme system, (a) AlkP and (b) AP

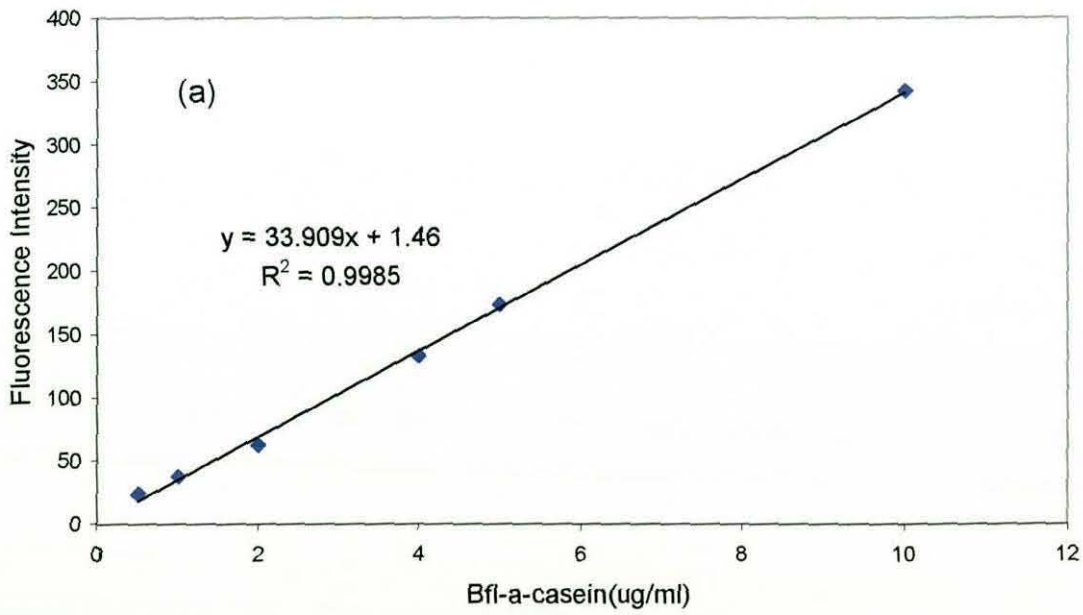

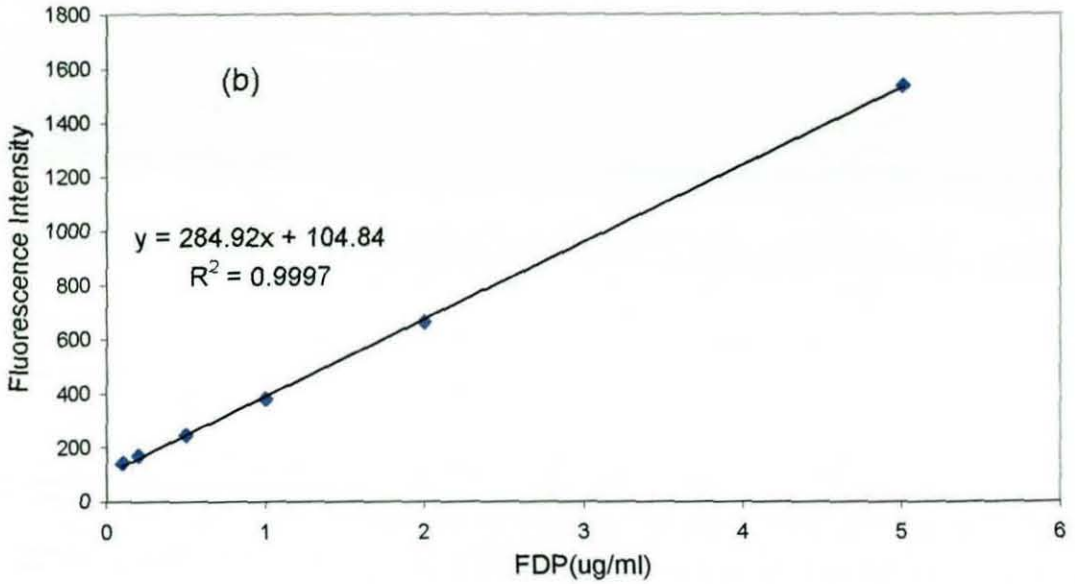

Figure 5.12 Calibration graph for (a) Bodipy FL-α-casein and (b) FDP using a dual enzyme system

5.4 INVESTIGATION OF SIMULTANEOUS SCREENING FOR DUAL ENZYME INHIBITORS BY USING IMMOBILISED ENZYME REACTORS

Fluorescence measurements were made using a F-4500 fluorescence spectrophotometer with excitation and emission bandwidths of 10 nm. Time scans were performed with excitation and emission wavelengths of 480 nm and 514 nm respectively for FDG-β-Gal and FDP-AP as well as Bodipy FL-α-casein-AlkP. In chapter 4, the inhibition in all cases, using 3-NPBA, PETG and VI, was shown to be highly reversible.

The set-up for a simple assay is shown in figure 5.2. All the conditions used for these experiments were as previously described. The buffer was flowed slowly through two enzyme reactors, each containing different immobilised enzyme, as substrates / inhibitors solution would be injected and the fluorescence detected through the time-dependent separation of the peaks emerging from each of the reactors by having different lengths of flow tubing between the enzyme reactors and the detector. For the complete displacement of the inhibitors the carrier buffer

was passed through the enzyme reactors for 2 minutes. Injecting the substrate solution at intervals checked the activity of the enzyme reactors.

5.4.1 Effects of Dimethyl sulphoxide on components in the system

Dimethyl sulphoxide (DMSO) is an important solvent for small molecule (MW. < 500 Da) studies as it provides a nearly universal approach for the solubilisation of small molecules. Because of its physicochemical properties, high solvent power, low chemical reactivity and relatively low toxicity, DMSO has become the solvent of choice for sample storage and handling in the pharmaceutical industry, particularly in the initial stages of high-throughput screening where storage of candidate molecules in DMSO is routine.

The effects of DMSO on protein structure and function are extremely varied. When used as a co-solvent at high concentration DMSO has great potential to give misleading results in bioavailability measurements, by acting as a permeation enhancer, or even an inhibitor.[180]

The effect of DMSO on substrates (Bodipy FL-α-casein, FDG and FDP), enzymes (AlkP, β-Gal and AP) and inhibitors (3-NPBA, PETG and VI) for the simultaneous determination of dual enzyme inhibitors by using immobilised enzyme reactors was investigated in static system. Similar trends were observed with all experiments, so only the effect of DMSO on FDP-AP with / without VI inhibitor is shown here (figure 5.13). Addition of DMSO (0-5%) had relatively little effect, but at 10% had great effect. However, DMSO had similar effects whether the inhibitor was present or not.

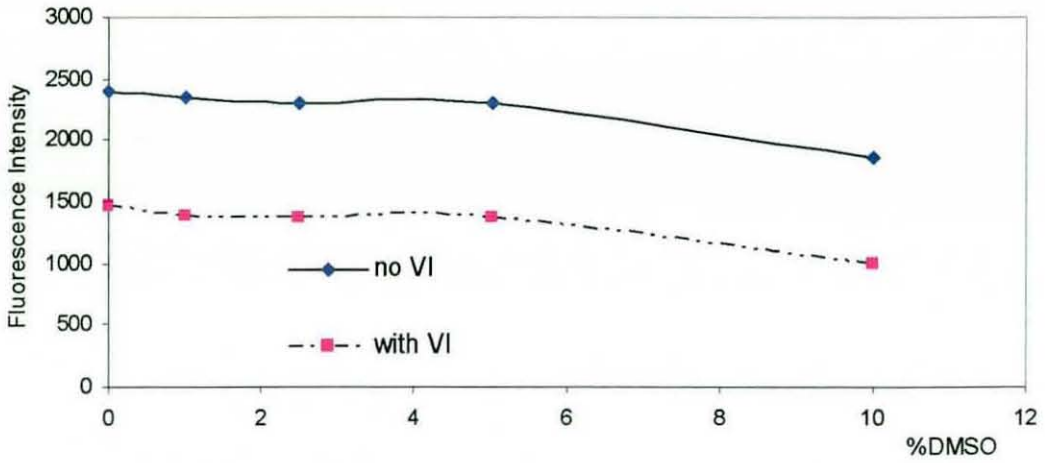

Figure 5.13 Effect of DMSO on FDP-AP with/ without VI

5.4.2 Investigation of simultaneous screening for PETG and 3-NPBA by using immobilised β-Gal and AlkP enzyme reactors

Based on preliminary investigations, a model assay for measuring the inhibitory effect of PETG and 3-NPBA on β-Gal and AlkP reactors respectively was studied. The standard solutions of PETG and 3-NPBA, mixed with the substrate solutions (Bodipy FL-α-casein and FDG) were injected into the flow system (figure 5.2).

The result (figure 5.14) shown that there were interactions in the system, probably because boronic acids have a covalent and reversible interaction with monosaccharides in water.[181] The interaction of the boronic acids with diols is illustrated in figure 5.15. Therefore this system is not suitable for simultaneous enzyme inhibitors assay with the 20 mM PBS buffer, pH 8.0.

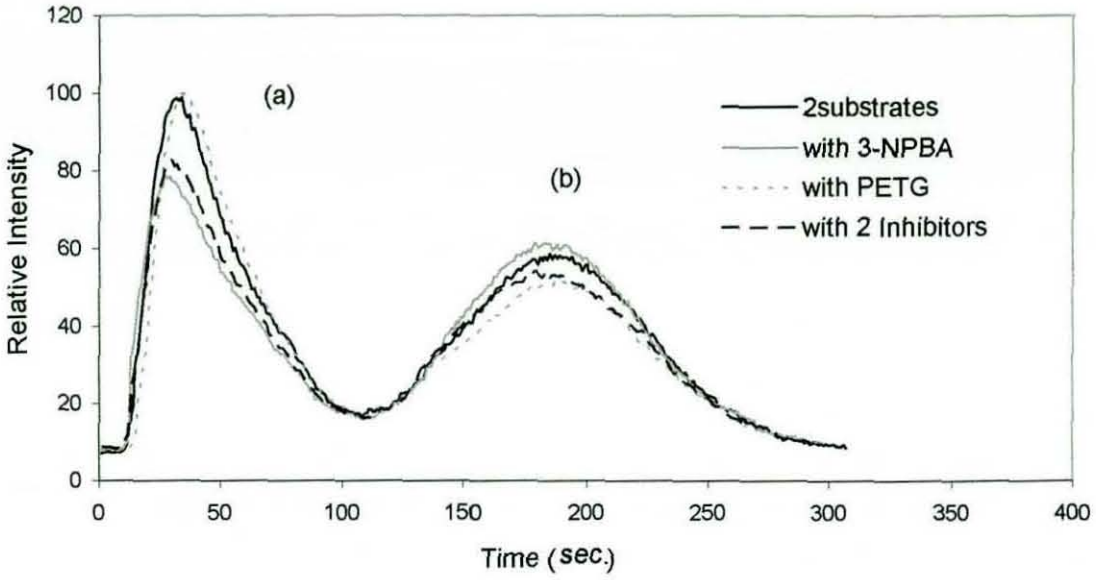

Figure 5.14 **FIA peaks for Bodipy FL-α-casein and FDG with 3-NPBA and PETG, using AlkP (a) and β-Gal (b) reactors**

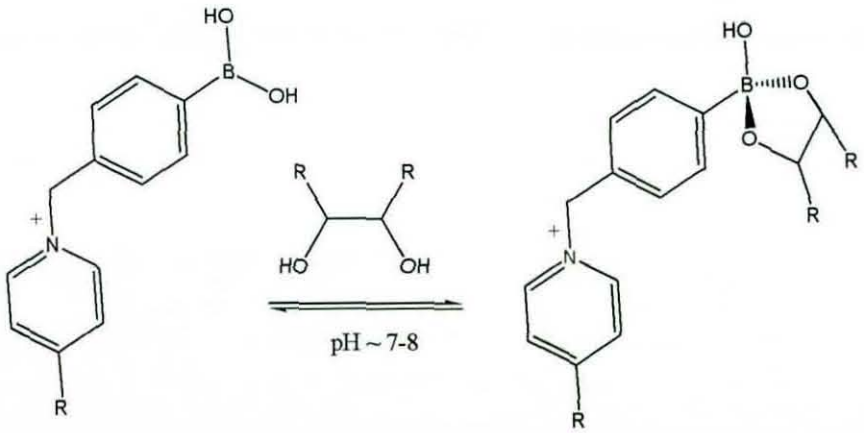

Figure 5.15 **Interaction between phenyl boronic acid and sugar at near neutral pH[181]**

5.4.3 Investigation of simultaneous screening for PETG and VI inhibitors by using immobilised β-Gal and AP enzyme reactors

A series of standard mixtures, which contain substrates (FDG and FDP) and inhibitors (PETG and VI) at various concentrations were treated under optimised conditions with β-Gal and AP enzyme reactors in the flow system (figure 5.2). The

FIA response increased rapidly just after injection of the sample and returned to baseline within about 2 min for the first peak and within 4 min for the second peak. Percentage inhibition against inhibitor concentration was plotted for each of the inhibitors. The calibration curves are given in figure 5.16. For PETG, the calibration graph showed good linearity over the range 0.02-0.5 µg/ml with $y = 76.689 + 13.55$, $r^2 = 0.9931$, and for VI, the linearity showed over the range 0.05-0.3 µg/ml with $y = 138.7 + 7.79680$, $r^2 = 0.9978$. The limit of detection (DL) was calculated using the equation: $DL = 3S.D._B/m$, where $S.D._B$ is the standard deviation of the blank (pure substrates solution) and m is the slope of the calibration curve (obtained by IUPAC criterion). The limit of detection for these inhibitors was 0.02 µg/ml (PETG) and 0.01 µg/ml (VI). These results demonstrate that the system can successfully be used for multiplex screening assays.

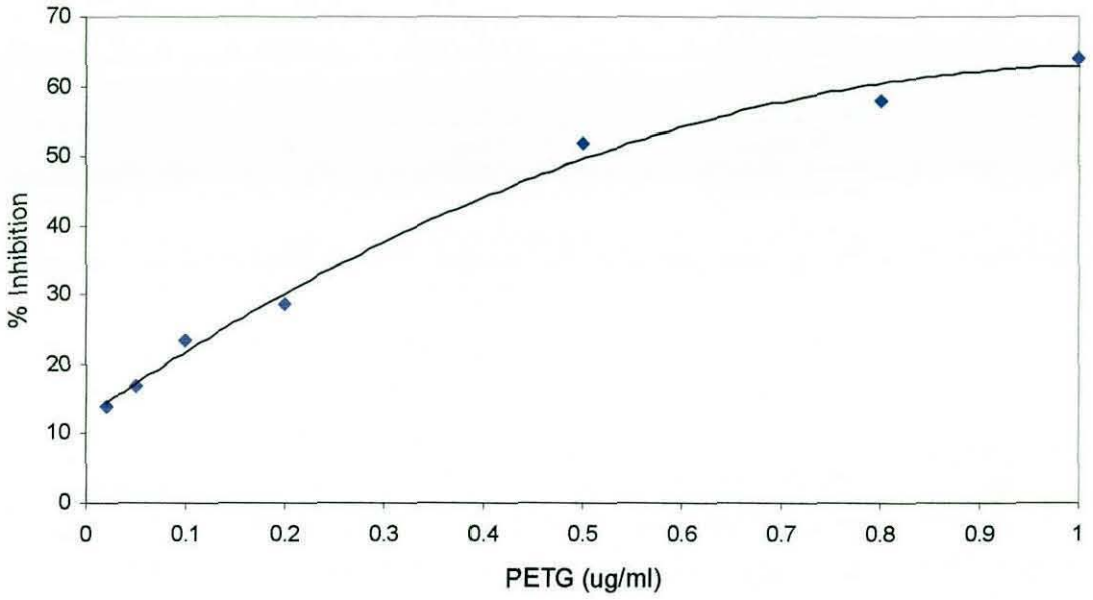
70
60
50
40
30
20
10
0
% Inhibition
0
0.1
0.2
0.3
0.4
0.5
0.6
0.7
0.8
0.9
1
PETG (ug/ml)

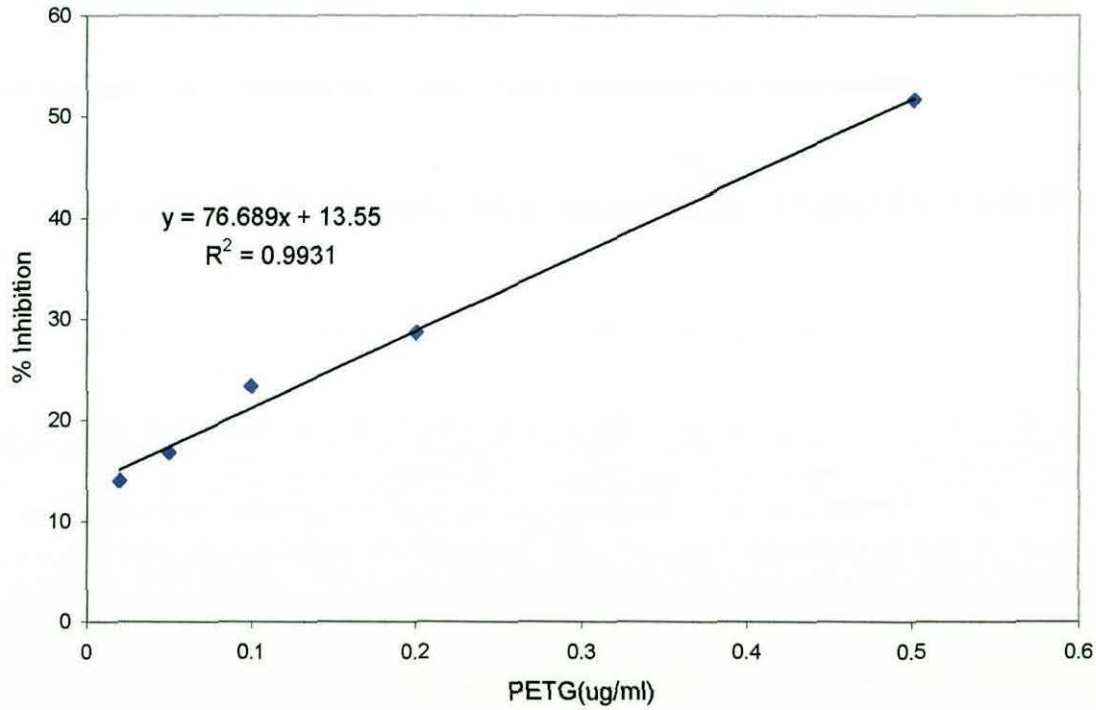
60
50
40
30
20
10
0
% Inhibition
y = 76.689x + 13.55
R2 = 0.9931
0
0.1
0.2
0.3
0.4
0.5
0.6
PETG(ug/ml)

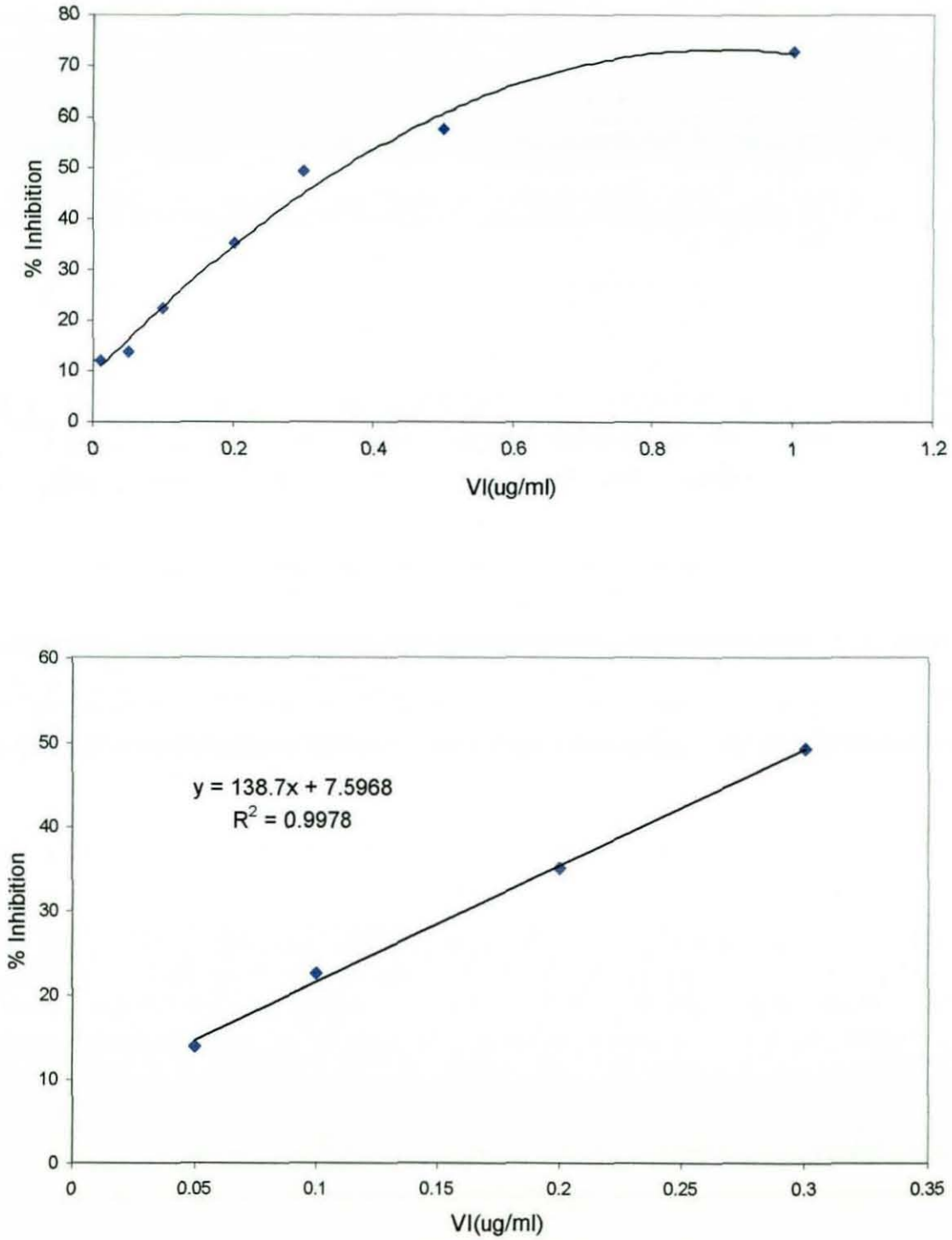

Figure 5.16 Calibration graph for PETG and VI using a dual enzyme system

5.4.4 Investigation of simultaneous screening for 3-NPBA and VI by using immobilised AlkP and AP enzyme reactors

A series of standard mixtures, which contain a constant concentration of substrates (Bodipy FL-α-casein and FDP) mixed with 3-NPBA and VI at various concentrations were treated under optimised conditions with AlkP and AP enzyme reactors in the flow system (figure 5.2). The calibration curves are given in figure 5.17. The good linearity shown over the range 0.01-0.2 µg/ml ($y = 226.56x + 5.3469$, $r^2 = 0.9954$) for VI, and 1-5 µg/ml ($y = 8.7081x + 3.6727$, r^2 0.9956) for 3-NPBA. The limit of detection for VI was 0.02 µg/ml, and for 3-NPBA was 0.78 µg/ml. These results demonstrate that the system can successfully be used for multiplex screening assays.

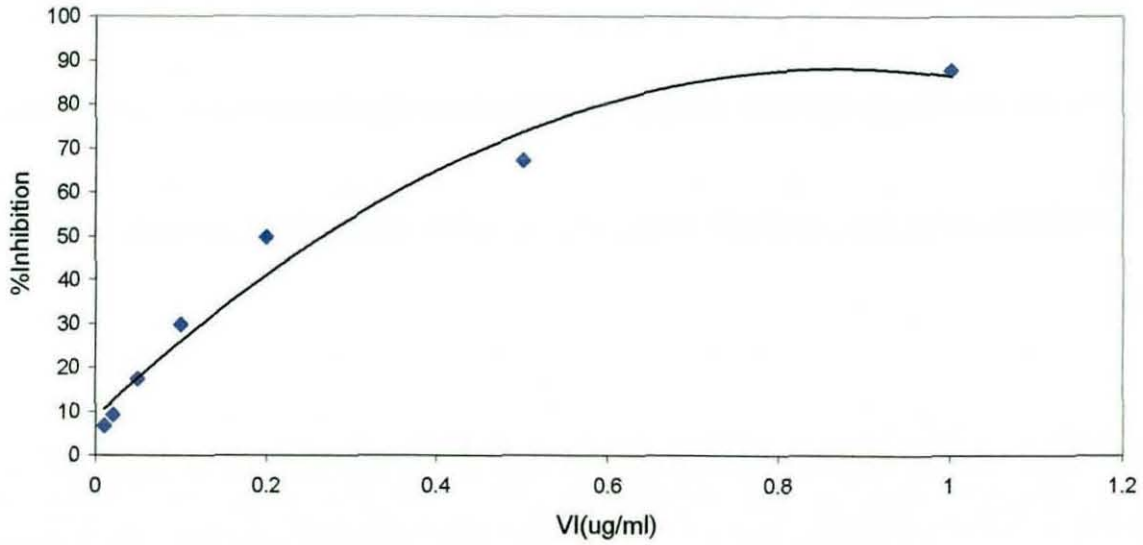

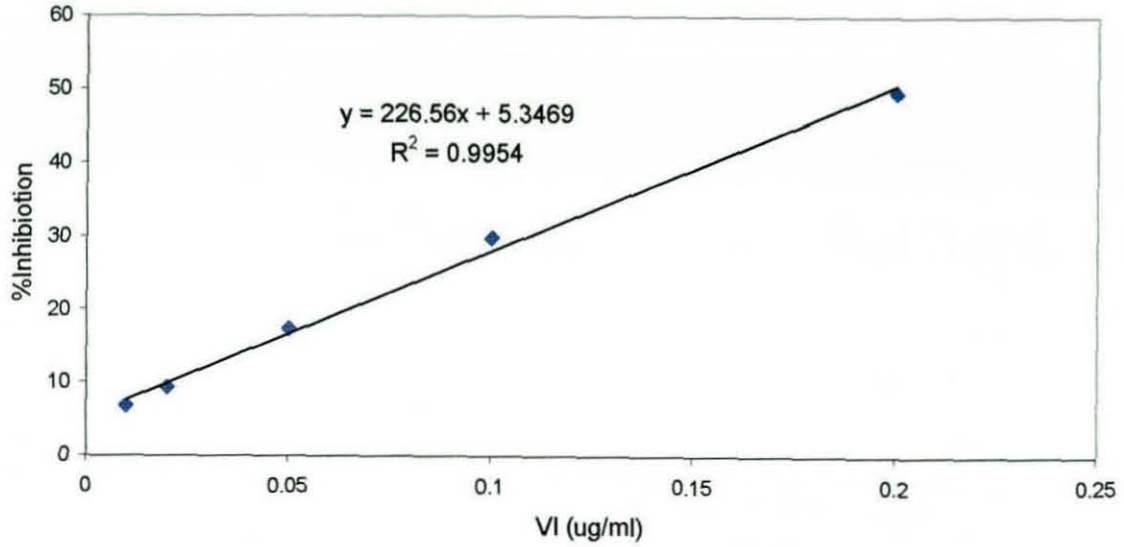
y = 226.56x + 5.3469
R^2 = 0.9954
%Inhibiotion
VI (ug/ml)
0
10
20
30
40
50
60
0
0.05
0.1
0.15
0.2
0.25

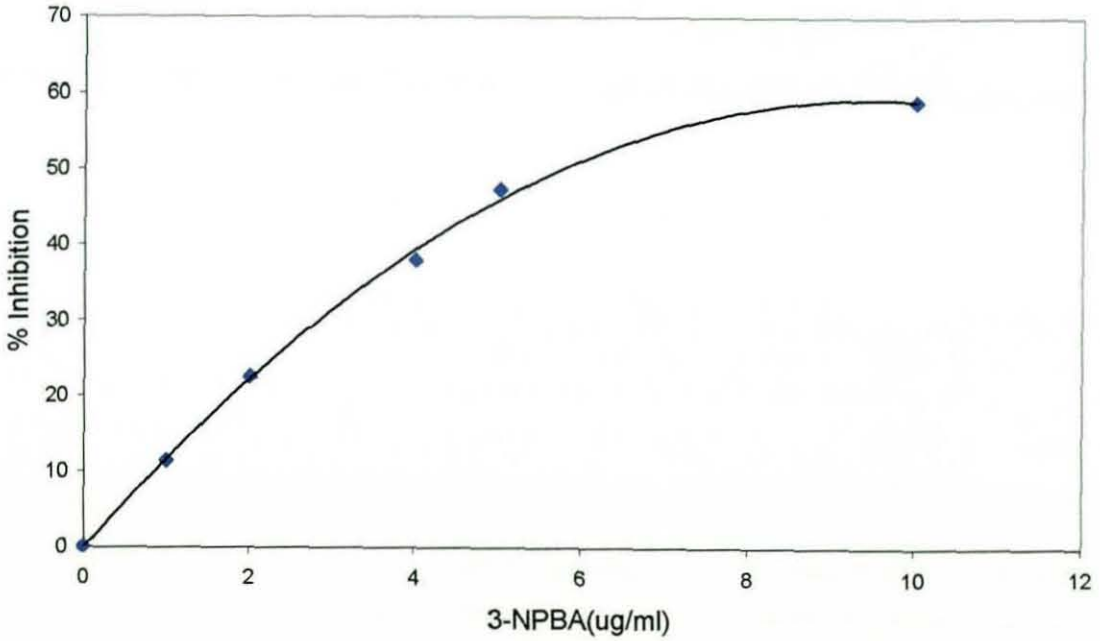
% Inhibition
3-NPBA(ug/ml)
0
10
20
30
40
50
60
70
0
2
4
6
8
10
12

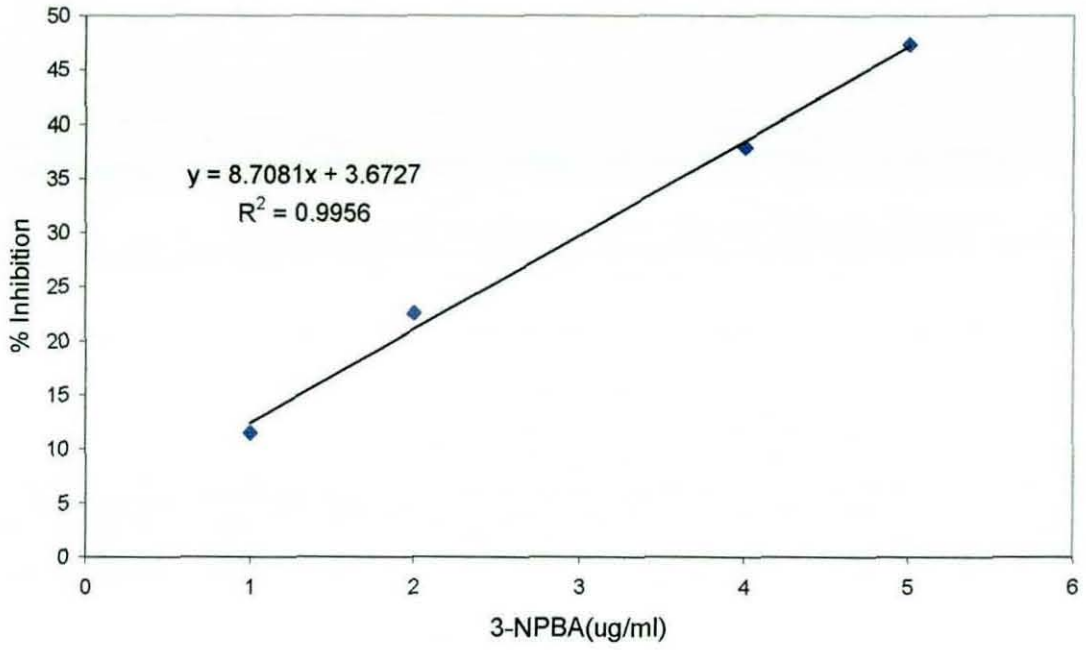

Figure 5.17 Calibration graph for 3-NPBA and VI using a dual enzyme system

5.5 CONCLUSIONS AND DISCUSSION

The suitability of applying the fluorigenic substrates to multiplex enzyme inhibitor assays, using flow injection analysis and immobilised enzyme reactors in parallel, has been investigated.

From a comparison of the fluorescence spectra of Bodipy FL-α-casein-AlkP, FDP-AP and FDG-β-Gal (figure 5.1) can be seen that all three emission spectra are strongly overlapped. Therefore, using time-dependent separation of flow injection analysis method was used to overcome the problem.

The interference amongst components (substrates and enzymes) in the system was also investigated. The results (figure 5.4) showed that there was no interference among these components. Therefore all these components could be used in the mixtures for dual simultaneous assays.

A simple flow-injection system for dual assays, using one buffer is described that incorporates small glass reactors each containing different immobilised enzymes as shown in figure 5.2 and 5.5. Two-substrate / inhibitor solution would be injected and the fluorescence detected through the time-dependent separation of the fluorescence peaks by having different lengths of flow tubing between the enzyme reactors and the F-4500 detector.

For optimisation of the total FIA system, one of the parameters would be the flow rate of the buffer stream because this affects the residence time of the sample in the enzyme reactors and thus the amplification as well as compression of the supports in the reactors. From the result shown in figure 5.6, a flow rate of 1.2 ml/min was chosen for all experiments.

Another important parameter for optimisation based on the dual-determination assay, using the flow injection system (figure 5.2) is the length of flow tubing required for separation of peaks. The length of flow tubing should be a judicious compromise between efficient separations and acceptable dispersion of the injected sample solution. The optimal lengths of flow tubing are shown in figure 5.5(b).

However, the minimal length of tubing that was required for a good separation of the two peaks was not ideal. The length of 200 cm. had to be coiled for placement in the water bath. This set-up would be much more applicable to a miniaturised system where such long lengths would not be needed.

Based on these studies, a model assay was developed to demonstrate the dual simultaneous assay concept.

The suitability of Bodipy FL-α-casein, FDP and FDG as substrates in the dual enzyme inhibition assays has also been demonstrated. The inhibition of AlkP, AP and β-Gal with 3-NPBA, VI and PETG, respectively at μg/ml levels was achieved. However, based on the preliminary investigations, an assay for measuring the inhibitory effect of PETG and 3-NPBA on β-Gal and AlkP reactor showed the result that the approach was not suitable for dual simultaneous enzyme inhibition assay

since there were some interactions amongst the components. Probably due to 3-NPBA interacted with galactoses from FDG and PETG.

The dual fluorogenic assays that have been described here took at most 2 minutes for the first analyte and around 4 minutes for the second inhibitor.

Using the optimal conditions, the calibration graphs for VI and 3-NPBA or PETG were constructed with AP and AlkP or β-Gal immobilised reactors (figure 5.16 – 5.17). The limits of detection were also determined for each of the inhibitors. The calculated limits of detection for each inhibitor using the substrates (Bodipy FL-α-casein and FDP) and immobilised AlkP and AP enzyme reactors were 0.78 μg/ml for 3-NPBA and 0.02 μg/ml for VI. For the system using the substrates (FDG and FDP) and immobilised β-Gal and AP enzyme reactors, the calculated limits of detection for each inhibitor were 0.02 μg/ml for PETG and 0.01 μg/ml for VI inhibitor.

In conclusion, the application of the dual enzyme inhibition assays in the FIA system, using immobilised enzyme reactors is a rapid, simple (does not require any process such as separation, precipitation or centrifugation) and sensitive method for the assay of enzyme inhibitors, essential requirements for screening assays.

CHAPTER 6

MULTIPLEX SCREENING ENZYME INHIBITION ASSAYS USING CHEMOMETRICS

6.1 INTRODUCTION

Spectrofluorimetry has been widely used to determine analytes in such disparate fields as clinical, biomedical and environmental analysis on account of its high selectivity, sensitivity and relatively low cost. However, the analytes usually exhibit broad spectral bands that tend to overlap when the sample contains several components; this entails the use of prior separation procedures or highly specific methods, both of which result in increased analysis times and cost. There is thus a continuing need to improve existing methods, not only to improve their selectivity and detection limits, but also to expedite analysis. This challenge has been met by using many techniques, such as variable-angle fluorescence spectroscopy[182] and synchronous fluorescence spectroscopy.[183,184] Nevertheless, assays of complex mixtures by spectrofluorimetry are practically impossible in many cases. This is due to the high number of sample components and extensive spectral overlapping.

From the system described in chapter 5 it is possible to quantify two enzyme inhibitors with dye-protein labelled substrates which have strongly overlapping spectra, using flow injection fluorimetry and time-dependent separation of the peaks, with different lengths of flow tubing between the enzyme reactors and the detector. However, problems may arise when using peak height or peak area to quantify more than two components using this system.

The problem of overlapping spectra can be overcome by using multivariate calibration techniques as described in chapter 2. Such techniques would enable a reliable and accurate prediction of the analytes concentration without using either peak height or peak area. Recently, multivariate calibration methods seem to be the techniques showing the best performance in terms of complex mixture resolution. Spectrofluorimetry has benefited from their introduction and several applications to pharmaceutical preparations, containing many active compounds and excipients having spectra in the same region, have been reported.[185,186] The application of these techniques to spectral data offers the advantage of speeding up complex system resolution, without tedious preliminary separation steps.

Among the various multivariate approaches applied to multicomponent analysis, principal component regression (PCR) and partial least-squares regression (PLS)

have been successfully adopted in many applications. PCR and PLS are factor analysis methods which establish a relationship between matrices of chemical data. PLS-1 and PCR have been found to give very similar results when used for concentration predictions in some mixtures.[187,188] However, in contrast to this De Jong [159] and Ragno [189] discovered that PLS-1 gave better predictions than PCR, especially in the case of an extensive spectral overlap. Therefore, in this work only PLS-1 was employed.

Multivariate calibration methods, however, do depend on the quality of the samples and variables obtained from the samples. This is because there needs to be an accurate and reliable interpretation of the calibration results before any predictions can be made. Thus validation methods need to be employed to check the validity of the calibration model. If the validation model differs significantly from the calibration model then any predictions from it may be unreliable. Also, in order to optimise the calibration model further, selection of the correct number of relevant principal factors, variables and removing any outlying samples, all need to be carried out first.

The aim of this work was to evaluate the potential of PLS-1 for the analysis of dual enzyme inhibitors by a flow-injection fluorimetry method with immobilised enzyme reactors, and also to use the method to study ternary mixtures with strongly overlapping spectra

6.2 THE INVESTIGATION OF DUAL SCREENING ENZYME INHIBITIONS USING A FLOW-INJECTION METHOD AND CHEMOMETRIC METHODS

6.2.1 Procedure

Fluorescence measurements were made using a F-4500 fluorescence spectrophotometer with excitation and emission bandwidths of 10 nm. Time scans were performed with excitation and emission wavelengths of 480 nm and 514 nm respectively for Bodipy FL-α-casein-AlkP and FDP-AP. The single-channel manifold set-up for a simple assay as shown in figure 4.10 was used. All the conditions used for these experiments were as previously described in section

5.4.4. The buffer (CA at pH 8.5) was flowed at a rate of 1.2 ml/min through two enzyme reactors containing AlkP and AP in series (figure 6.1). Samples (substrates/inhibitors, containing Bodipy FL-α-casein 4 µg/ml, FDP 0.5 µg/ml, 3-NPBA between 1 and 5 µg/ml, and VI between 0.05 and 0.45 µg/ml) were injected and the fluorescence measured. Full spectra (495 to 594 nm) were recorded 22 seconds after injection, the flow being stopped manually. Spectral data were saved in ASCII files and then converted to Excel® files before analysis using the Unscrambler software. All plots obtained from the software show calibration data in red and validation data in green. The concentration ranges were selected from the established linear calibration range for each compound. The optimised calibration models, calculated using PLS-1 and full cross validation (FCV) were applied to analyze the spectra of the samples, and calculate the concentrations of 3-NPBA and VI in the mixtures.

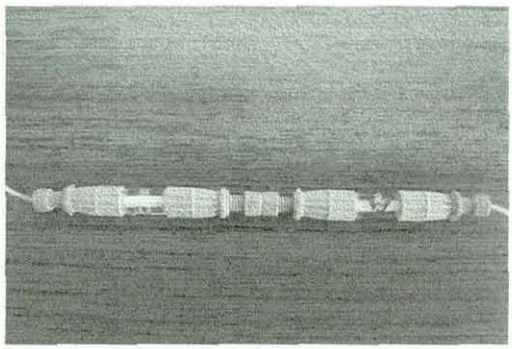

Figure 6.1 AlkP and AP enzyme reactors in series

6.2.2 Results and discussion

6.2.2.1 PLS treatment of spectrofluorimetric data

A calibration set of 13 samples was studied at wavelengths between 495 and 594 nm at 1nm interval (100 data points). In table 6.1 the compositions of binary mixtures used in the calibration matrices are summarized, and a diagrammatic representation of the mixture design is shown in figure 6.2.

Table 6.1 Concentration data used in the calibration set for determination of 3-NPBA and VI

Sample	Concentration of 3-NPBA, µg/ml	Concentration of VI, µg/ml
1	3	0.25
2	5	0.45
3	4	0.15
4	1	0.05
5	5	0.25
6	1	0.45
7	5	0.05
8	3	0.45
9	3	0.05
10	2	0.15
11	1	0.25
12	2	0.35
13	4	0.35

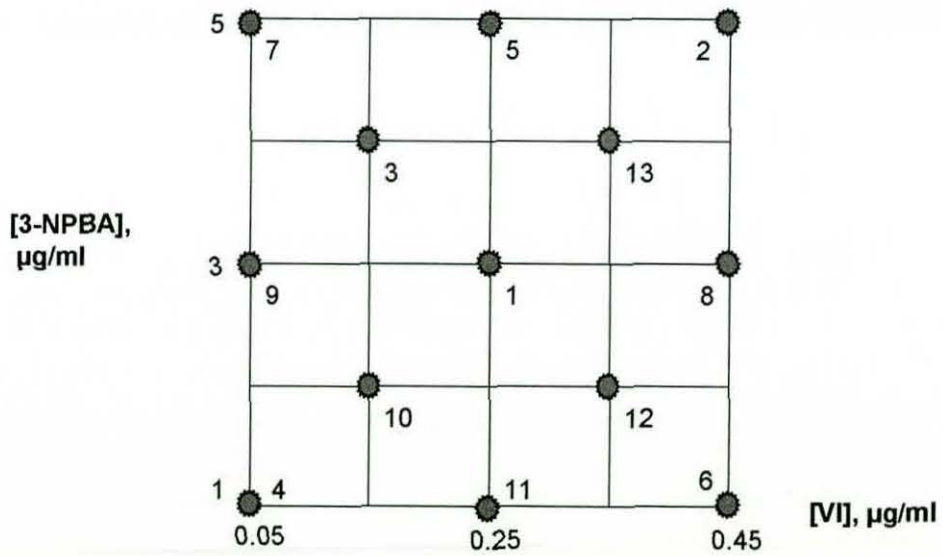

Figure 6.2 Mixture design for the binary mixtures used in the data set for the PLS-1 method. The concentrations of the different mixtures are given in table 6.1

An appropriate choice of the number of principal components, or factors, is necessary for the correct performance of PLS-1. The number of factors should be properly selected in order to avoid both over-fitting – which would result in accurate calibration but poor predictions – and under-fitting, which would lead to increased robustness but again, at the expense of impaired predictions: several criteria have been recommended for selecting the optimum number.[163] Here the residual Y variance value was employed to select the optimum number of principal components (PCs). Full cross validation consists of systematically removing each of the observations in turn and using the remaining observations for construction of latent factors and their regression. PLS calibration was performed on the 13 calibration spectra: 12 spectra were used and the concentrations of the analytes in the sample left out were predicted. This process was repeated 13 times until each calibration sample had been left out once. The plots of scores, the root mean square error (RMSE), residual Y validation variance, and the correlation coefficient (r) obtained when plotting predicted versus measured concentrations for each component are included to give an indication both of the average error in the analysis and the quality of fit of all the data. (figure 6.3 and 6.4).

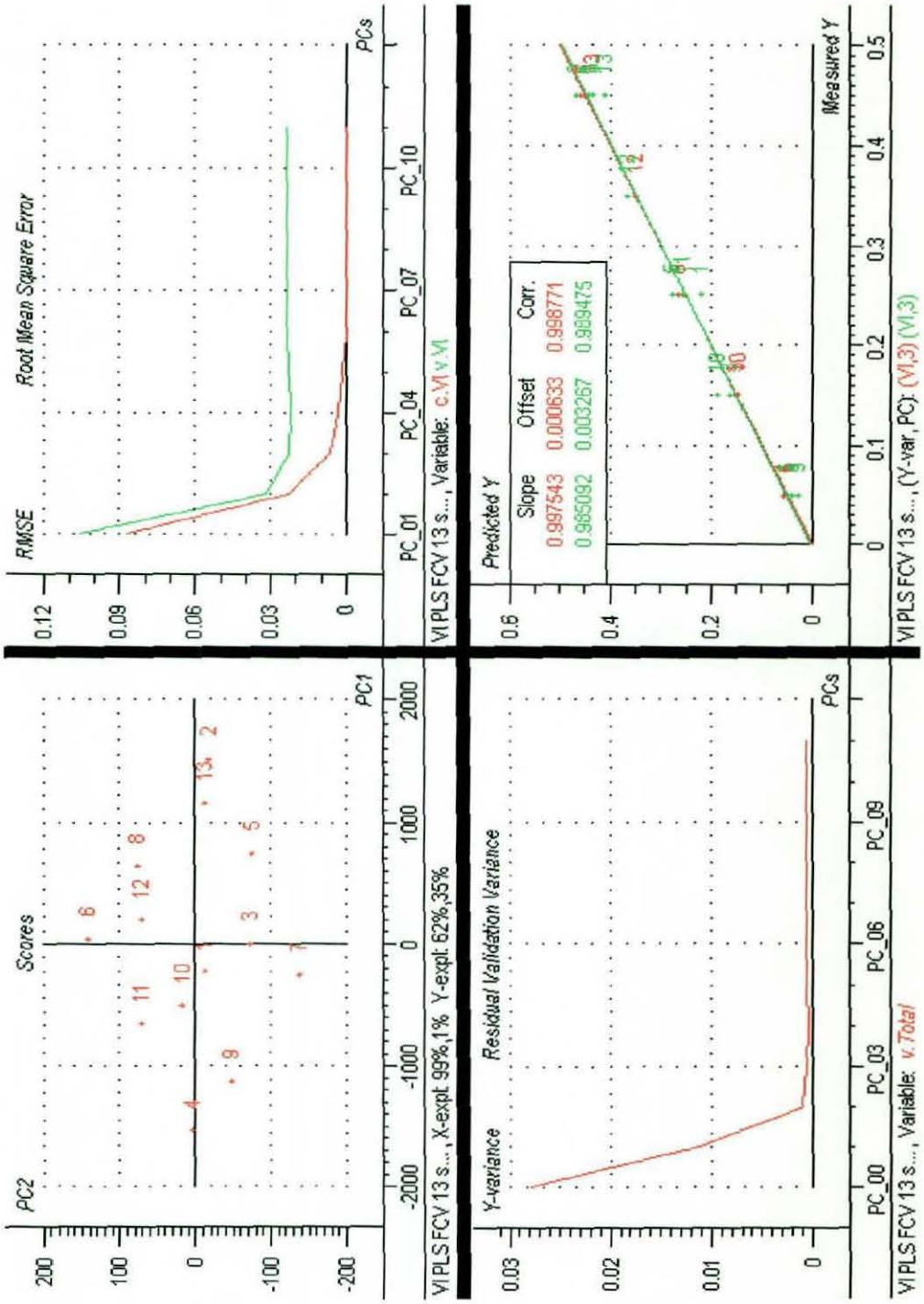

Figure 6.3 The analysis plots of calibration set for VI using PLS-1 and FCV

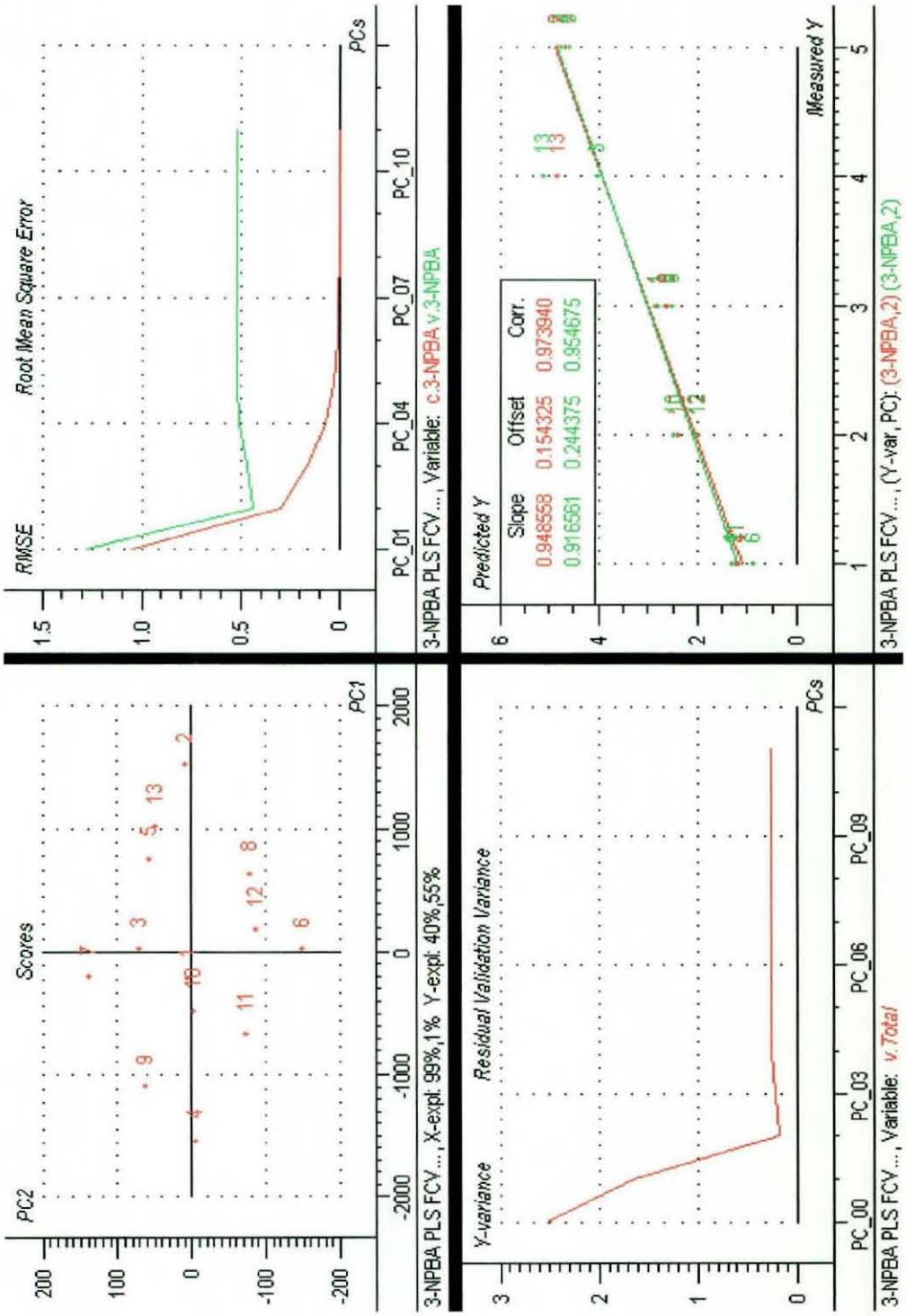

Figure 6.4 The analysis plots of calibration set for 3-NPBA using PLS-1 and FCV

From figure 6.3, the score plots for the VI calibration set using PLS-1 and FCV show that all the samples fell within the average pattern for the x data. The residual Y validation variance plot showed the optimum number of PCs is three, so this was used for prediction. The RMSE plot at 3 PCs is fairly small (0.006 for RMSE of calibration, RMSEC, and 0.02 for RMSE of validation, RMSEP). The r-value was 0.998771. Therefore the calibration set gave a good PLS-1 model; no outlying samples had to be removed.

However, figure 6.4 showed that for the 3-NPBA the r-value was only 0.97394. From the plot of predicted versus measured concentrations sample 13 in the calibration set was rather far away from the straight line. Moreover the RMSE plot showed quite high values (0.29 for RMSEC and 0.44 for RMSEP). From figure 6.5, it is clear that the residual Y variance of sample 13 differed significantly from the other samples. This sample could be classed as influential outlier, so it was removed from the calibration set. When the plots were recalculated (figure 6.6), the score plots showed that all the samples fell within the average pattern for the x data. The residual Y validation variance plot showed that the optimum number of PCs was two, so this was used for prediction. The RMSE plot at 2 PCs was also better (0.17 for RMSEC and 0.26 for RMSEP). Moreover, the r-value was higher (0.990833). This means that the corrected calibration set gave a satisfactory PLS-1 model for the predictions, with no further outlying samples to be considered.

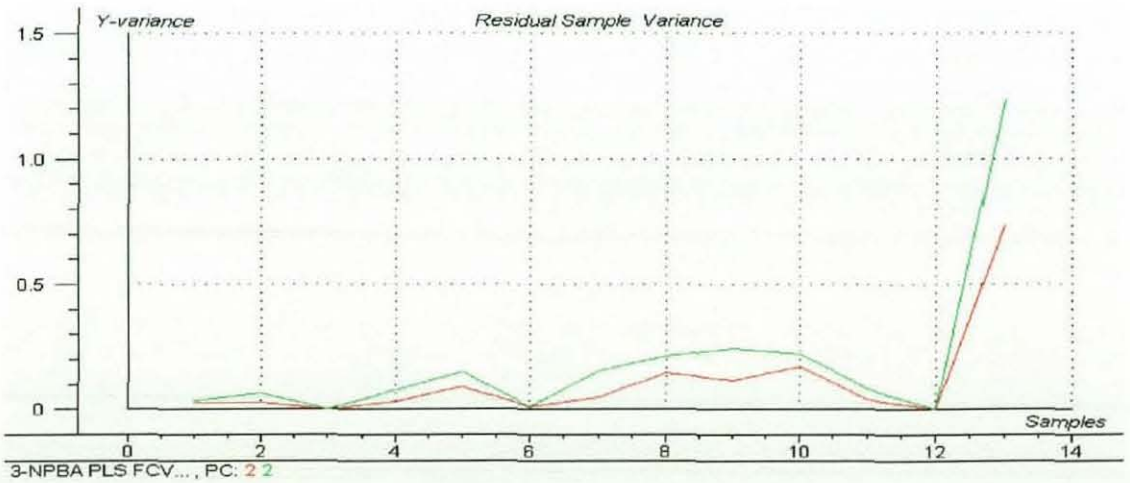

Figure 6.5 The residual sample variance plot for outlier checking of 3-NPBA calibration set using PLS-1 and FCV

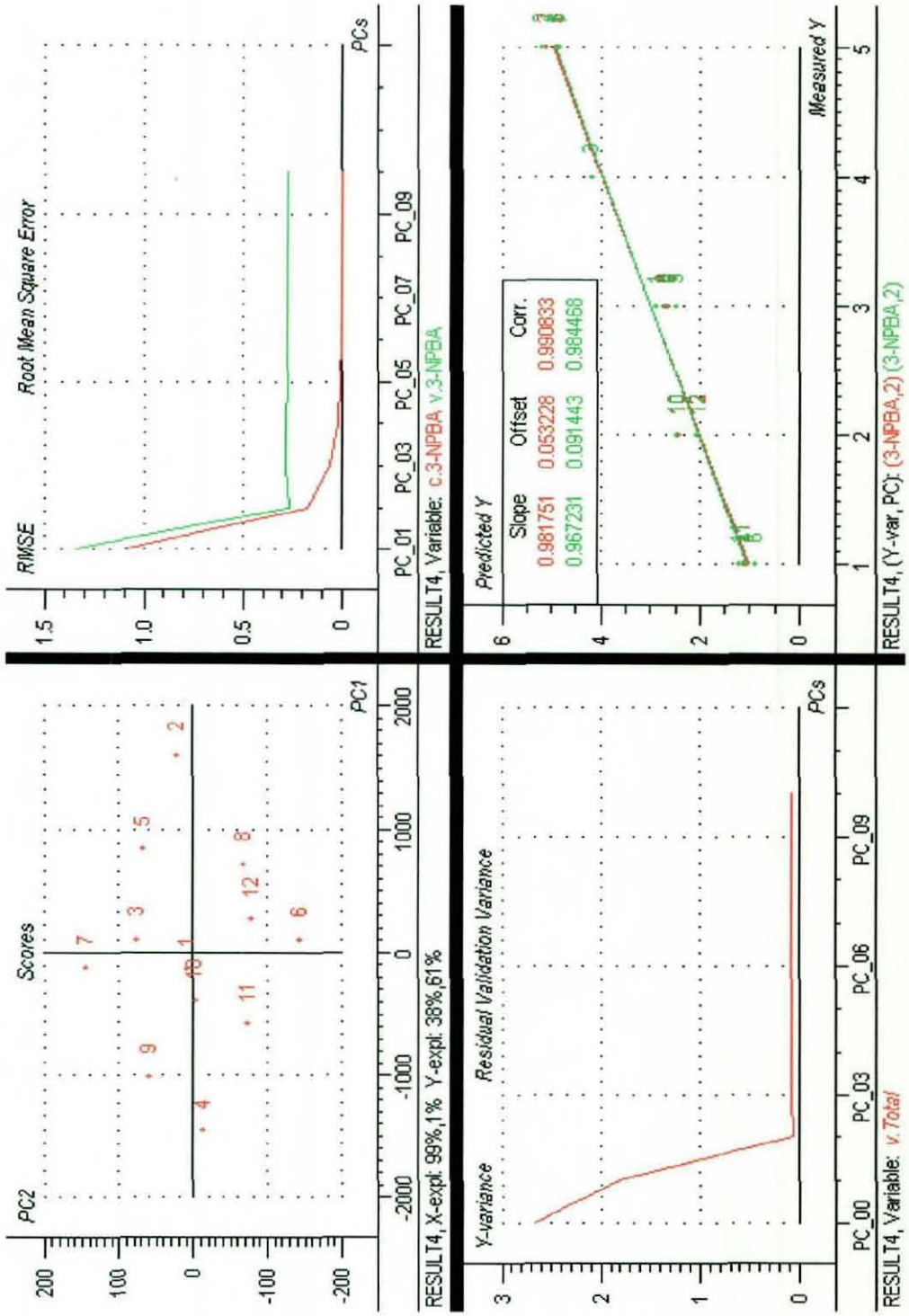

Figure 6.6 The analysis plots of calibration set without the outlying sample for 3-NPBA using PLS-1 and FCV

6.2.2.2 Prediction and deviations

In order to test the performance of the proposed method, it was applied to the determination of artificial mixtures containing various concentrations of the two compounds at µg/ml levels. The above-mentioned model was used to predict the concentration of the analytes in 10 synthetic mixtures (new data set in table 6.2).

Table 6.2 Concentration data used in the new data set for determination of 3-NPBA and VI

Sample	Concentration of 3-NPBA, µg/ml	Concentration of VI, µg/ml
1	3	0.25
2	5	0.45
3	4	0.15
4	5	0.25
5	1	0.45
6	2	0.35
7	5	0.05
8	4	0.35
9	2	0.25
10	4	0.45

A full analysis of the results can be seen in table 6.3. Results are summarized in figure 6.7. As can be seen, the actual and predicted values were consistent for most of the mixtures tested. All the predicted concentrations were 98–113% and 90-105% of their actual concentrations for 3-NPBA and VI respectively. A large deviation value might suggest that the predicted sample is different from those that were used to make the calibration model. The deviation values were within 10% for 3-NPBA, except sample 5 (23%) and within 10% for VI, except sample 7 (34%). The large deviation value might be due to signals from components in considerable excess, which tend to engulf the other peaks, making it difficult for the software to predict the concentrations. The multivariate calibration techniques look for changes in the x-data matrix and if one of the analyte peaks is much bigger than another or others, no significant spectral change may be observed. Hence it would be hard for the PLS-1 to predict the amount of the engulfed peak. The results can be considered satisfactory keeping in mind the strong spectral

overlap between Bodipy FL-α-casein-AlkP and FDP-AP (figure 5.1), and given that the aim of this research is to develop screening methods.

Table 6.3 A full analysis for 3-NPBA and VI with FCV for the PLS-1 model

Sample	[Actual], µg/ml		[Predicted], µg/ml		% Deviation		% Recovery	
	3-NPBA	VI	3-NPBA	VI	3-NPBA	VI	3-NPBA	VI
1	3.00	0.25	2.97	0.25	9.2	7.5	99.0	100.8
2	5.00	0.45	4.94	0.46	4.5	3.6	98.8	102.2
3	4.00	0.15	3.99	0.15	5.9	10.1	99.9	99.3
4	5.00	0.25	4.91	0.26	4.3	6.3	98.3	105.2
5	**1.00**	**0.45**	1.13	0.44	**23.1**	3.7	113.4	100.4
6	2.00	0.35	1.96	0.35	10.2	5.0	98.0	100.3
7	**5.00**	**0.05**	5.09	0.04	4.7	**34.4**	101.8	89.8
8	4.00	0.35	4.09	0.36	5.4	4.4	102.3	103.1
9	2.00	0.25	2.06	0.25	9.9	8.6	102.9	100.8
10	4.00	0.45	4.11	0.42	5.8	3.7	102.8	96.4

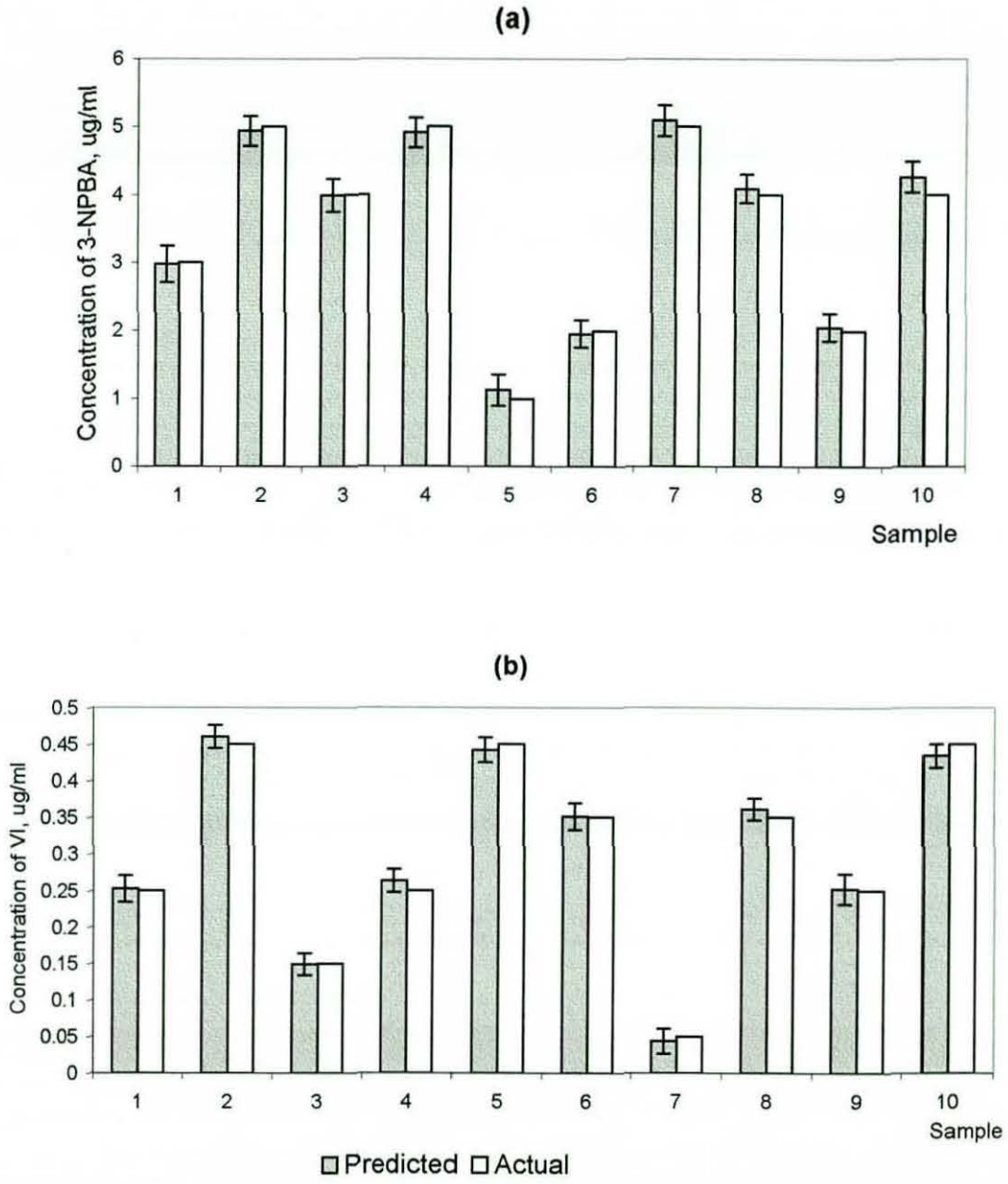

Figure 6.7 **A comparison of the predicted results using PLS-1 and FCV with the actual results for the new data set: (a) 3-NPBA and (b) VI**

6.2.2.3 Variable (data point) selection

Many methods have been published that look at variable selection.[190,191] Having uninformative variables in the data must lead to less precision (higher variance due to imbedded error[192]) and also a higher bias in the eigenvalues.[193] Elimination of such variables in the data matrix must in theory improve the overall model and result in better predictions. However, from the findings in section 6.2.2.2 the problem of uninformative variables seems to be irrelevant because of the good predictions. The software suggests that only a small percentage (<1%) of the 293 data points for each sample do not ideally fit the model, too few to have any significant effect on the overall calibration model. The spectra of the calibration standards cover the whole spectral range of interest, so the chances of there being any uninformative section of variables in this data are very small. Thus, no further data manipulation was carried out on these results.

6.2.2.4 Noise addition

Contrary to the other transformations in the software, adding noise to the data would decrease the precision of the analysis. This is exactly the purpose of the transformation: include some additive or multiplicative noise in the variables, see how this affects the model, and check how the model would perform if it was used for predictions based on noisier new data e.g. from real samples. In previous work (section 6.2.2.1), the PLS-1 model gave satisfactory predictions for the new data sets, but here we check how well the model predicts for samples which are noisier by 3% than the original sample sets. All the optimum conditions and the compositions of the calibration set and new data set in the previous work were used. The calibration set spectra with 3% noise added are shown in figure 6.8.

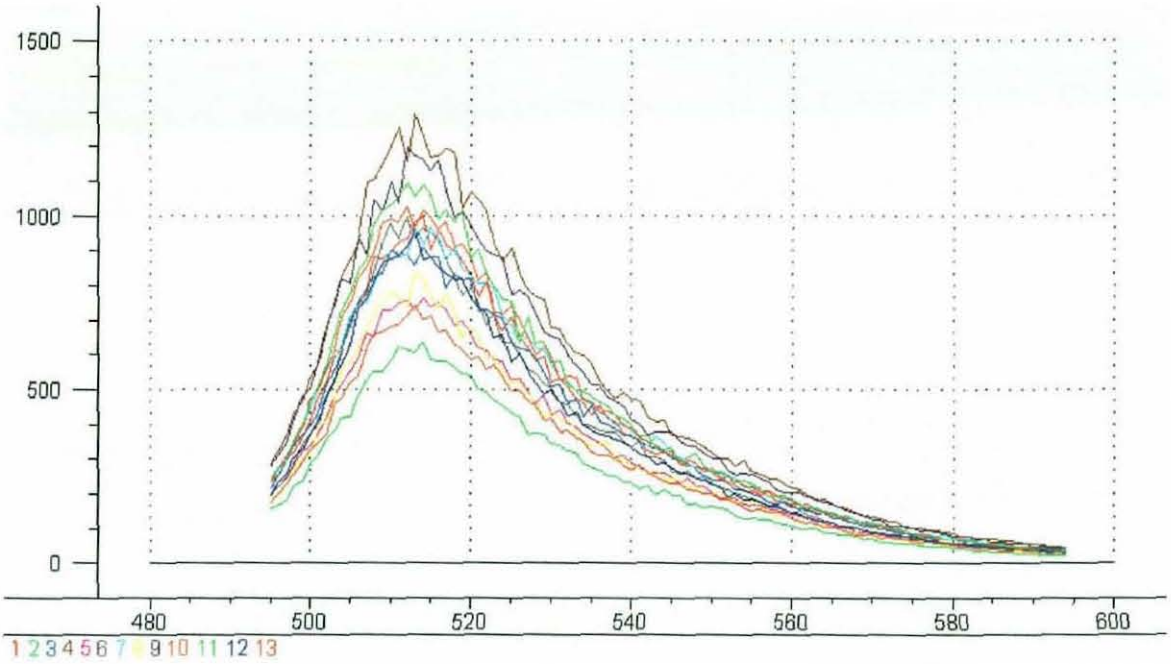

Figure 6.8 The calibration set spectra with 3% noise adding

The plots of scores, the root mean square (RMSE), residual Y validation variance, and the correlation coefficient (r) obtained when plotting predicted versus measured concentration for each component are included to give an indication both of the average error in the analysis and the quality of fit of all data (figure 6.9 and 6.10).

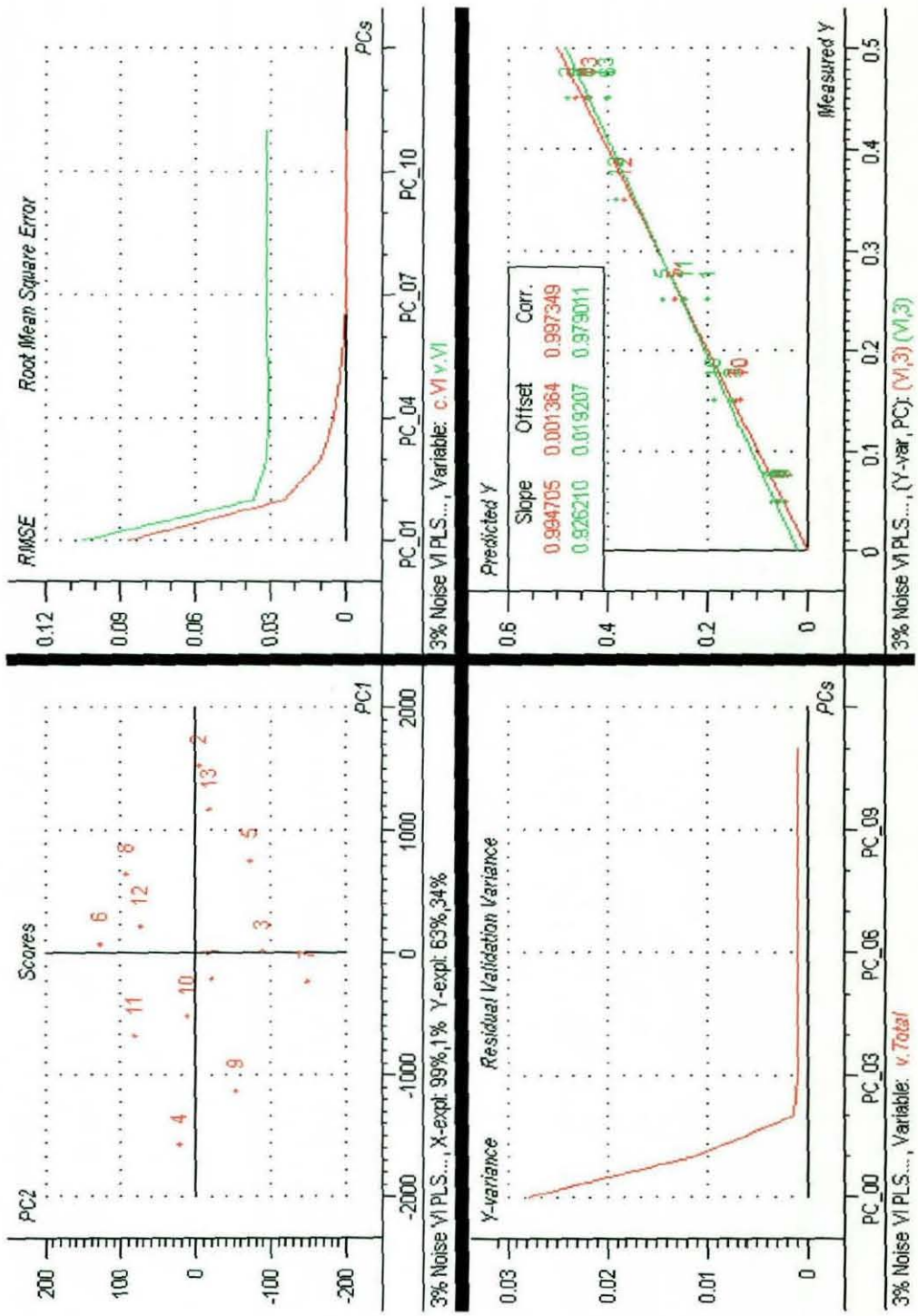

Figure 6.9 The analysis plots of calibration set with 3% noise for VI using PLS-1 and FCV

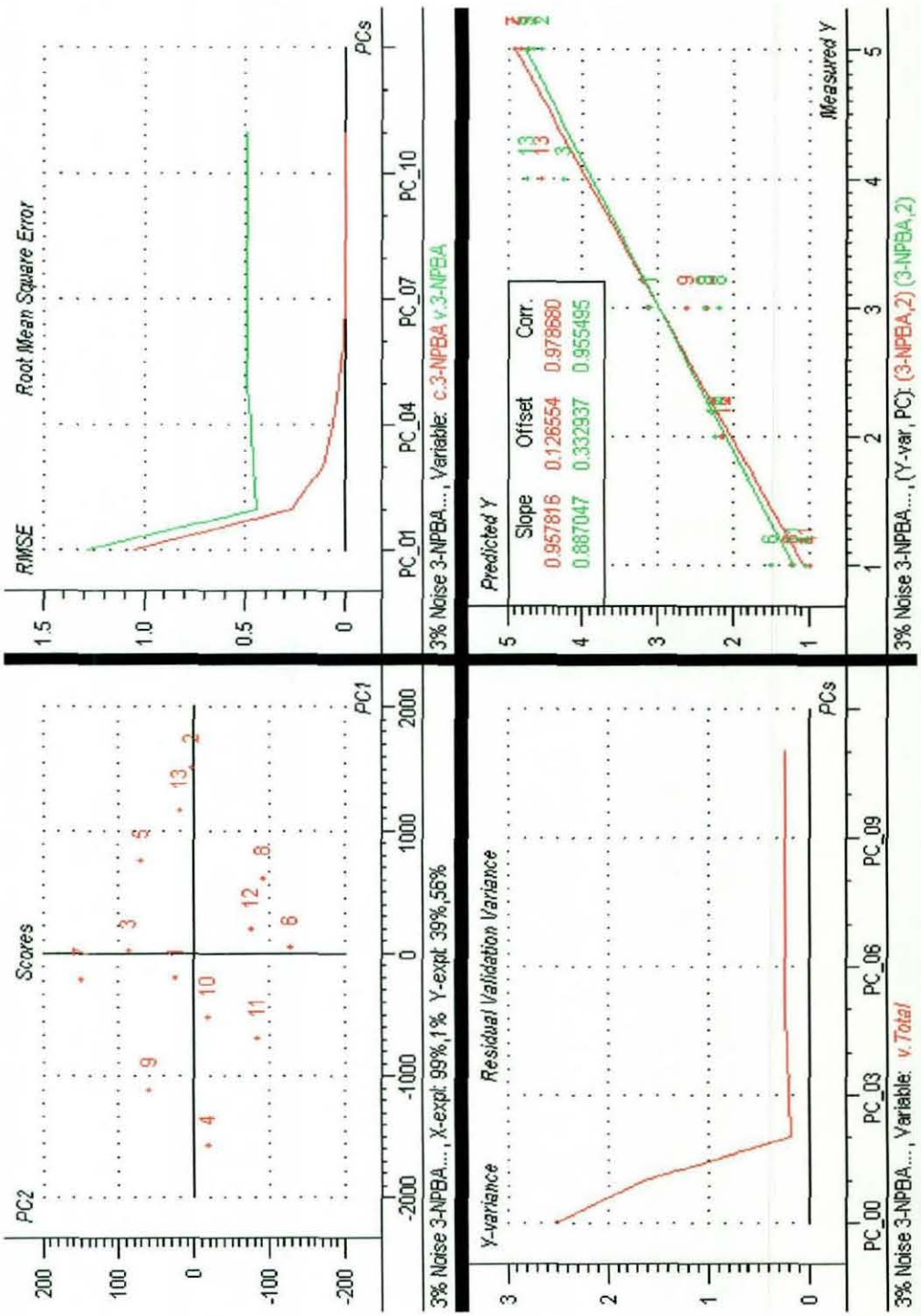

Figure 6.10 The analysis plots of calibration set with 3% noise for 3-NPBA using PLS-1 and FCV

From figure 6.9, the score plots for the VI data showed that all the samples fell within the average pattern for the x data. The residual Y validation variance plot showed the optimum number of PCs at three, so this was used for prediction. The RMSE plot at 3 PCs was fairly small (0.01 for RMSEC and 0.03 for RMSEP). And the r-value was 0.997349. Thus the calibration set gave a good PLS-1 model, with no outlying samples to be removed.

However, in figure 6.10 (3-NPBA data) the r-value was only 0.976680 and from the plot of predicted versus measured concentrations it can be seen that two samples (8 and 13 in the calibration set) were rather far away from the straight line. Moreover the RMSE plot showed quite high values (0.26 for RMSEC and 0.44 for RMSEP). From figure 6.11, it is clear that the residual Y variance values of sample 8 and 13 differ significantly from the other samples. Also sample 9 obviously differs from the rest. These samples could therefore be classed as influential outliers, so they were removed from the calibration set and the plots were recalculated. The results were better (figure 6.12): the score plots showed that all of the samples fell within the average pattern for the x data. The residual Y validation variance plot showed the optimum number of PCs at two, so this was used for prediction: the RMSE plot was then much improved (0.11 for RMSEC and 0.26 for RMSEP) and the r-value was higher (0.996724). So the corrected calibration set gave a satisfactory PLS-1 model for the prediction, and no further outlying samples were considered.

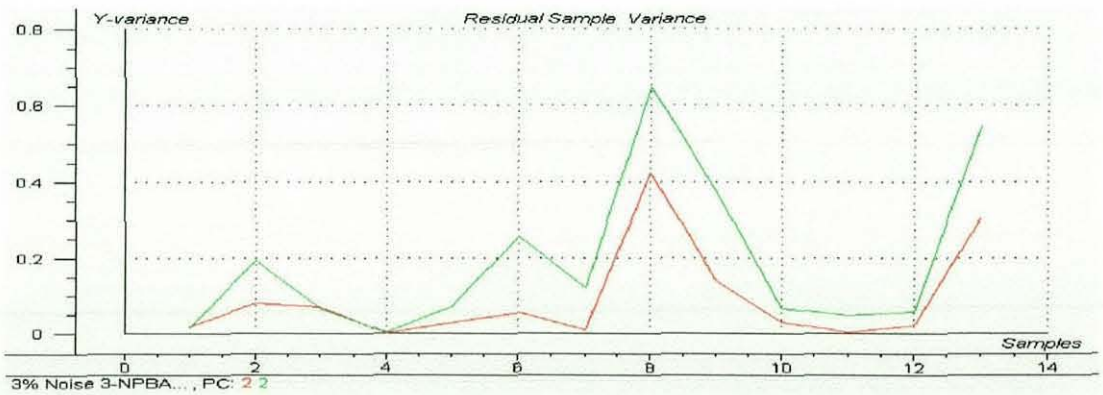

Figure 6.11 The residual sample variance plot for outlier checking of 3-NPBA calibration set with 3% noise adding using PLS-1 and FCV

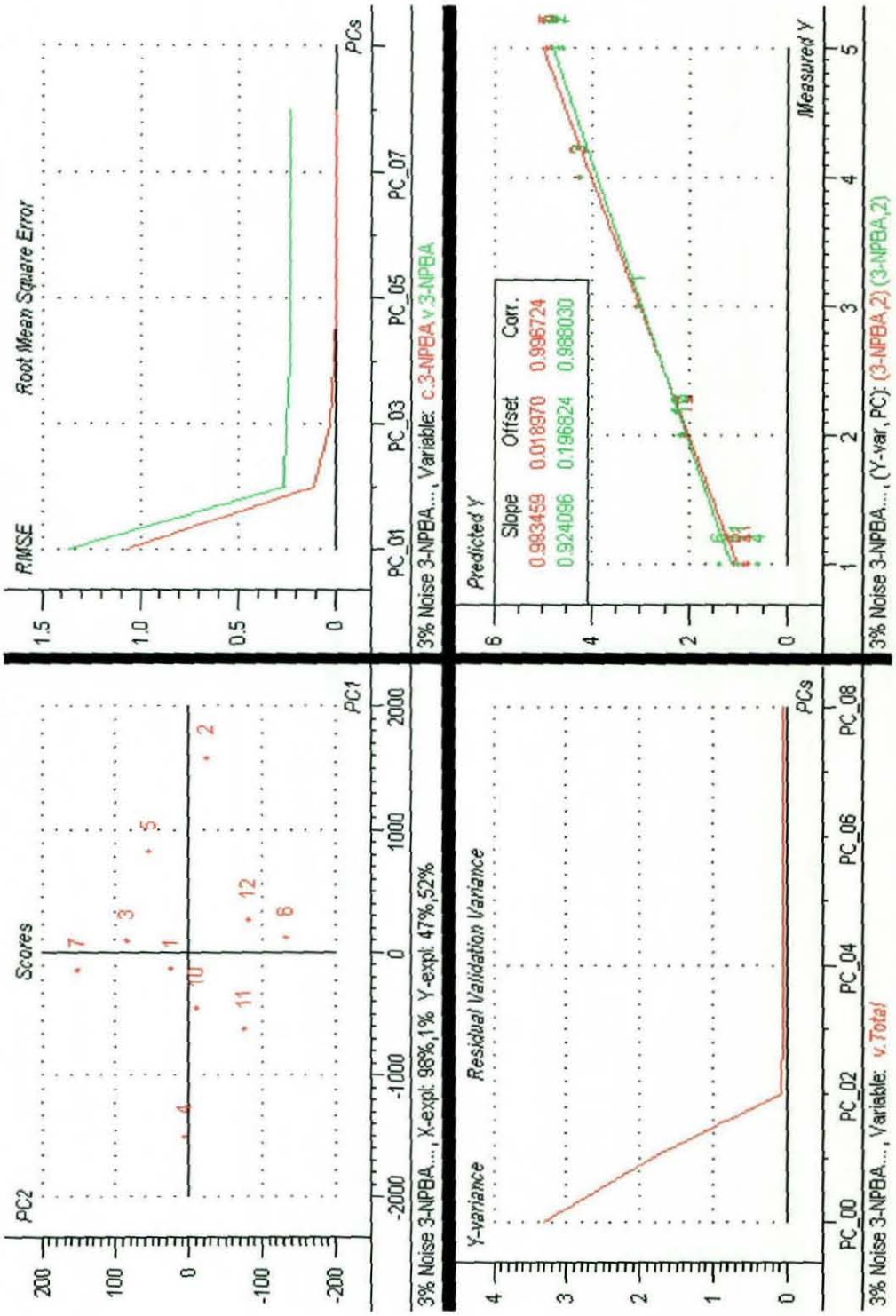

Figure 6.12 The analysis plots of calibration set (without outlying samples) with 3% noise adding for 3-NPBA using PLS-1 and FCV.

In order to test the performance of the proposed method, it was applied to the determination of artificial mixtures containing various concentrations of the two compounds at µg/ml levels. The above-mentioned model was used to predict the concentrations of the analytes in 10 synthetic mixtures (new data set in table 6.2).

A full analysis of the results can be seen in table 6.4, and the results are summarized in figure 6.13. As can be seen, the amounts added and found were consistent for most of the mixtures tested. All the predicted concentrations were 87-106% and 87-106% of their actual concentrations for 3-NPBA and VI respectively. A large deviation value might suggest that the predicted sample is different to those that were used to make the calibration model. The percentage deviations were within 13% for 3-NPBA, except sample 5 (24.5%) and within 16% for VI, except sample 7 (49.9%). This could be attributed to the fact that the concentration of 3-NPBA was the lowest level (1 µg/ml), while the concentration of VI was the highest level (0.45 µg/ml) for sample 5, but vice versa for sample 7. Thus the method may be difficult to apply if the target analyte peak is engulfed by another.

Table 6.4 A full analysis for 3-NPBA and VI with FCV for the PLS-1 model with 3% Noise adding

Sample	[Actual], µg/ml		[Predicted], µg/ml		% Deviation		% Recovery	
	3-NPBA	VI	3-NPBA	VI	3-NPBA	VI	3-NPBA	VI
1	3.00	0.25	2.94	0.24	8.6	11.1	97.8	97.2
2	5.00	0.45	4.93	0.46	4.7	4.8	98.6	103.1
3	4.00	0.15	3.99	0.14	5.4	15.6	99.8	95.3
4	5.00	0.25	4.74	0.26	4.2	8.8	94.7	106.0
5	**1.00**	**0.45**	0.87	0.44	**24.5**	5.6	87.2	98. 2
6	2.00	0.35	2.05	0.37	11.2	6.5	102.3	105.1
7	**5.00**	**0.05**	4.69	0.04	7.8	**49.9**	93.8	87.4
8	4.00	0.35	4.13	0.36	6.5	7.1	103.4	103.4
9	2.00	0.25	2.11	0.26	13.0	11.0	105.5	103.6
10	4.00	0.45	4.23	0.41	6.5	6.3	105.7	90.7

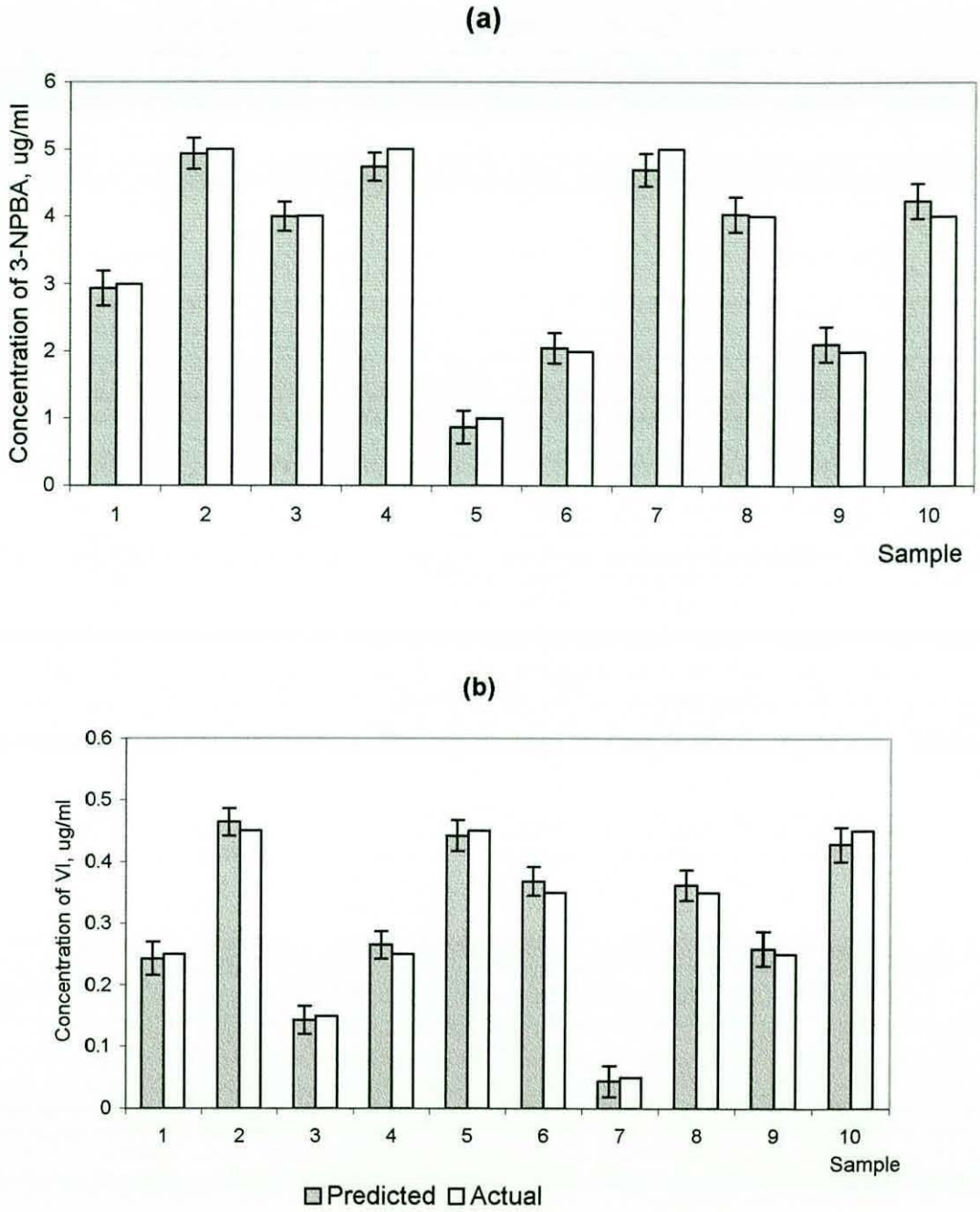

Figure 6.13 **A comparison of the predicted results using the 3% noise adding, PLS-1 and FCV with the actual results for the validation set: (a) 3-NPBA and (b) VI**

6.3 THE INVESTIGATION OF TERNARY ANALYTE MIXTURES WITH STRONGLY OVERLAPPING SPECTRA FOR MULTIPLEX SCREENING

The aim of this study was to demonstrate the practicability of the PLS-1 method for three strongly overlapping fluorescence spectra. The final aim could be multiplex screening enzyme inhibition assays using chemometric methods. The three conjugates used were Bodipy FL-α-casein conjugate, Bodipy 493/503-α-casein conjugate, and FITC-α-casein conjugate (hereafter referred to as Bodipy FL conjugate, Bodipy 493 conjugate, and FITC conjugate, respectively). From figure 6.14, the fluorescence emission maxima of Bodipy FL conjugate, Bodipy 493 conjugate, and FITC conjugate are 511 nm, 512 nm and 519 nm respectively. It is clear that the emission peaks of the three conjugates overlap significantly, and a mixture of the three conjugates gave only one major peak. This is a preliminary study of the application of PLS-1 to such heavily overlapping spectra.

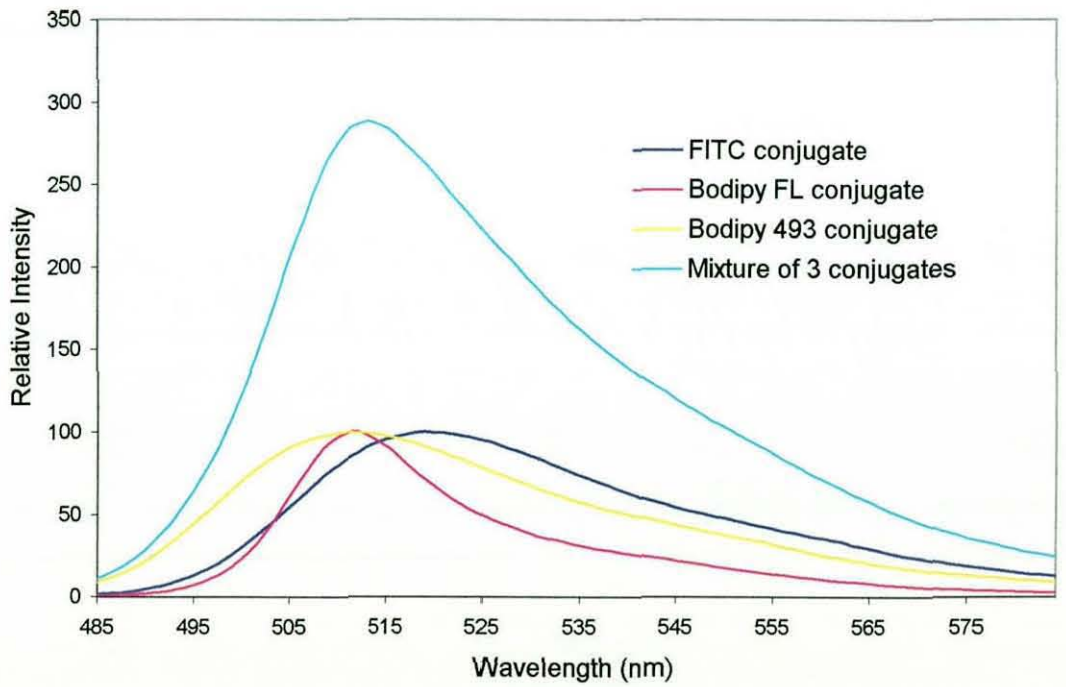

Figure 6.14 Fluorescence emission spectra of Bodipy FL conjugate, Bodipy 493 conjugate, FITC conjugate and a mixture of the three conjugates

6.3.1 Procedure

PBS buffer (0.02 M, pH 9.0) was used throughout. The three conjugate solutions (Bodipy FL conjugate, Bodipy 493 conjugate, and FITC conjugate) were prepared by the methods given in section 3.2.9, then diluted to give similar fluorescence intensities and kept in dark bottles.

Various samples were then prepared from the above solutions. The calibration set comprised 25 samples (table 6.5) and the new data set 20 samples (table 6.6). The samples were all selected within the linear calibration range for each compound. Fluorescence measurements were made using the F-4500 fluorescence spectrometer with excitation and emission bandwidths of 10 nm. The time scan mode was used with excitation and emission wavelengths of 470 nm and 513 nm, respectively. The flow system in figure 4.10 was used. Each sample was injected (50 µl) into a stream of buffer flowing at 1.2 ml/min. Once the flow was stopped (after 21 seconds), fluorescence spectra over the range 490 -584 nm were recorded with an excitation wavelength of 470 nm. Spectral data were saved in ASCII files and then converted to Excel® files before analysis using the Unscrambler software. The PLS-1 optimised model and FCV method were applied to analyze the spectra of the samples, and calculate the concentrations of the 3 analytes in the mixtures.

Table 6.5 The composition of the calibration set for ternary mixtures

Sample	FITC conjugate, ml	Bodipy FL conjugate, ml	Bodipy 493 conjugate, ml
1	0.6	0.2	0.2
2	0.2	0.2	1.0
3	0.2	1.0	0.4
4	1.0	0.4	1.0
5	0.4	1.0	0.6
6	1.0	0.6	0.4
7	0.6	0.4	0.4
8	0.4	0.4	0.8
9	0.4	0.8	1.0
10	0.8	1.0	0.8
11	1.0	0.8	0.6
12	0.8	0.6	1.0
13	0.6	1.0	1.0
14	1.0	1.0	0.2
15	1.0	0.2	0.8
16	0.2	0.8	0.2
17	0.8	0.2	0.6
18	0.2	0.6	0.8
19	0.6	0.8	0.8
20	0.8	0.8	0.4
21	0.8	0.4	0.2
22	0.4	0.2	0.4
23	0.2	0.4	0.6
24	0.4	0.6	0.2
25	0.6	0.6	0.6

Table 6.6 The composition of the new data set for ternary mixtures

Sample	FITC conjugate, ml	Bodipy FL conjugate, ml	Bodipy 493 conjugate, ml
1	1	0.4	1
2	0.4	1.0	0.6
3	0.6	0.6	0.4
4	0.2	1.0	1.0
5	0.4	0.8	1.0
6	0.8	1.0	0.8
7	1.0	0.8	0.6
8	0.6	1.0	1.0
9	1.0	1.0	0.2
10	0.2	0.8	0.2
11	0.8	0.2	0.6
12	0.2	0.6	0.8
13	0.2	0.2	1.0
14	0.6	0.8	0.8
15	0.8	0.8	0.4
16	0.2	0.4	0.6
17	1.0	1.0	1.0
18	0.2	1.0	0.2
19	1.0	0.2	0.2
20	1.0	0.2	1.0

6.3.2 Results and discussion

6.3.2.1 PLS-1 treatment of fluorescence data

A calibration set of 25 emission spectra was taken between 490 and 584 nm at 1 nm intervals (95 data points). The plots of scores, the RMSE, the residual Y validation variance, and the correlation coefficient (r) obtained are shown in appendix E, figures E-1 to E-3, and a summary of the statistical parameters of the calibration set is shown in table 6.7.

Table 6.7 Summarisation of statistical parameters of 3 analytes with PLS-1 and FCV

Analyte	Optimum principal component, PC	RMSE		Slope	Offset	Correlation coefficient, r
		RMSEC	RMSEP			
FITC conjugate	3	0.03	0.039	0.986411	0.008153	0.993182
BFL conjugate	3	0.023	0.030	0.992044	0.004774	0.996014
B493 conjugate	4	0.028	0.040	0.988033	0.007180	0.993998

From figure 6.15, it is clear that the residual Y variance of sample 8 (FITC conjugate calibration set), sample 3 (BFL conjugate calibration set), and sample 3 (B493 conjugate calibration set) differ significantly from the other samples. These samples could therefore be classed as influential outliers, so they were removed from the calibration set and the plots were recalculated. The improved results shown in appendix E, figures E-4 to E-6. The summary of the statistical parameters of the corrected calibration set is shown in table 6.8. It demonstrates that the modified calibration set gave a satisfactory PLS-1 model for the prediction.

Table 6.8 Summarisation of statistical parameters of 3 analytes with PLS-1 and FCV without outliers

Analyte	Optimum principal *component*, PC	RMSE		Slope	Offset	Correlation coefficient, *r*
		RMSEC	*RMSEP*			
FITC conjugate	3	0.018	0.024	0.995034	0.003021	0.997514
BFL conjugate	3	0.016	0.022	0.995692	0.002513	0.997844
B493 conjugate	4	0.014	0.021	0.997013	0.001817	0.998505

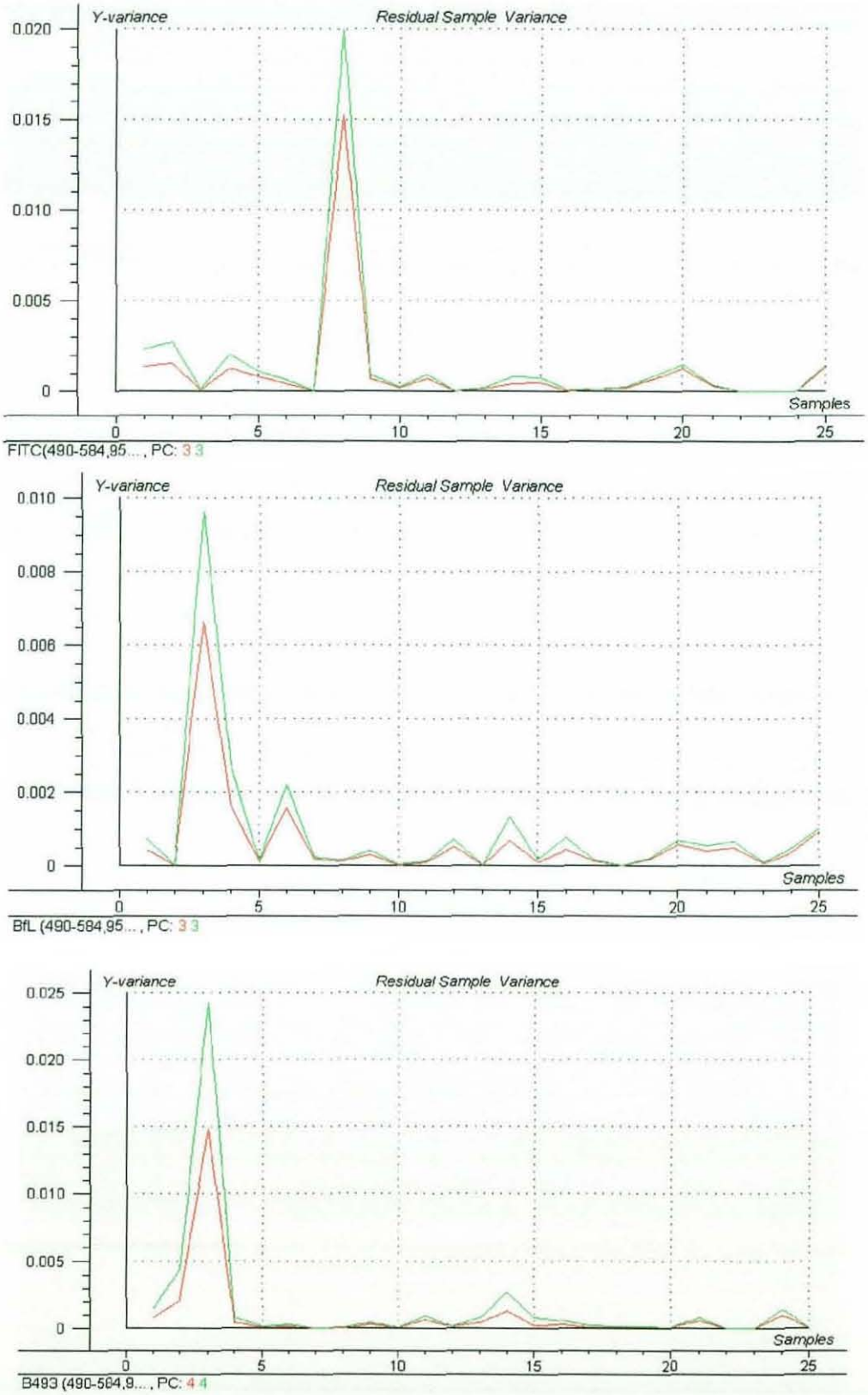

Figure 6.15 The residual sample variance plot for outlier checking of 3 conjugates calibration set using PLS-1 and FCV: (a) FITC conjugate, (b) BFL conjugate, and (c) B493 conjugate

6.3.2.2 Prediction and deviations

In order to test the performance of the proposed method, it was applied to the determination of artificial mixtures containing various amounts of the three conjugates. The above-mentioned model was used to predict the concentration of the analytes in 20 synthetic mixtures (new data set in table 6.6).

A full analysis of the results can be seen in table 6.9. Results are summarised in figure 6.16. As can be seen the actual and predicted amounts were consistent for most of the mixtures tested. All the predicted values were 91-106%, 90-108%, and 91-110% of the actual amounts for FITC, BFL, and B493 conjugate respectively. The deviation values were within 10% for all conjugates. The results can be considered satisfactory for screening purposes.

Table 6.9 A full analysis for 3 conjugates prediction set with FCV for the PLS-1 model

Sample	Actual, ml			Predicted, ml			% Deviation			% Recovery		
	FITC	BFL	B493	FITC	BFL	B493	FITC	BFL	B493	FITC	BFL	B493
1	1.0	0.4	1.0	1.03	0.37	1.00	2.9	6.7	1.8	103.2	92.0	99.9
2	0.4	1.0	0.6	0.42	0.98	0.61	4.7	1.7	2.8	106.2	97.7	101.1
3	0.6	0.4	0.4	0.59	0.38	0.39	2.8	3.7	3.5	99.2	96.2	98.5
4	0.2	1.0	1.0	0.18	0.97	1.01	9.5	2.9	3.3	91.0	96.6	101.0
5	0.4	0.8	1.0	0.41	0.81	1.00	4.2	1.8	1.8	103.7	100.8	99.7
6	0.8	1.0	0.8	0.82	0.99	0.8	2.0	1.4	2.0	102.0	99.0	100.0
7	1.0	0.8	0.6	0.98	0.81	0.62	1.6	1.7	3.1	97.9	101.2	104.0
8	0.6	1.0	1.0	0.61	0.99	0.99	2.5	1.4	1.8	101.0	99.4	99.5
9	1.0	1.0	0.2	0.99	1.02	0.18	2.0	1.8	9.0	99.4	102.2	91.0
10	0.2	0.8	0.2	0.2	0.80	0.20	8.0	1.7	8.0	99.5	100.6	102.0
11	0.8	0.2	0.6	0.78	0.22	0.61	2.6	9.5	3.0	97.7	108.5	101.0
12	0.2	0.6	0.8	0.2	0.59	0.81	6.5	2.0	1.7	98.5	98.3	101.0
13	0.2	0.2	1.0	0.18	0.18	1.04	7.5	6.0	3.6	91.5	90.5	104.3
14	0.6	0.8	0.8	0.57	0.81	0.82	2.8	2.0	2.2	94.5	100.7	102.8
15	0.8	0.8	0.4	0.77	0.82	0.40	2.8	2.6	4.2	96.0	102.3	100.7
16	0.2	0.4	0.6	0.18	0.4	0.62	8.0	4.0	2.8	92.0	100.0	103.5
17	1.0	1.0	1.0	1.01	0.92	0.96	3.7	1.5	3.6	101.1	97.9	96.4
18	0.2	1.0	0.2	0.19	1.00	0.22	8.5	1.6	9.5	95.0	100.3	109.5
19	1.0	0.2	1.0	0.95	0.21	0.19	3.3	4.0	6.2	95.4	106.5	93.5
20	1.0	0.2	1.0	0.98	0.21	1.01	1.2	5.5	1.3	97.9	106.5	101.2

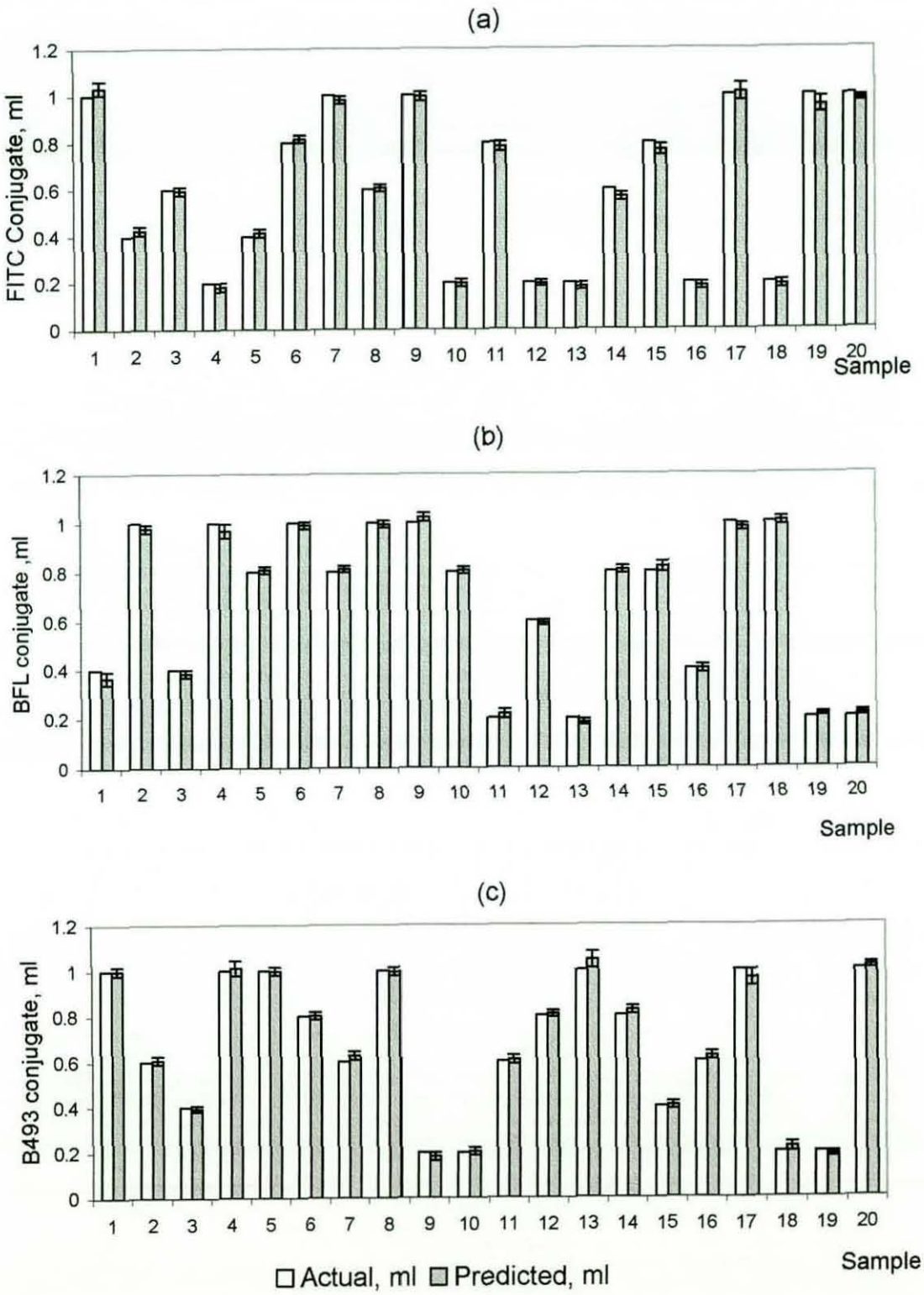

Figure 6.16 **A comparison of the predicted results using PLS-1 and FCV with actual results for the new data set: (a) FITC conjugate, (b) BFL conjugate, and (c) B493 conjugate**

6.4 CONCLUSIONS

The system developed in this chapter is a simple design that could be dramatically improved with a flow system designed to be automatic rather than manual: this might reduce the experimental error considerably. Having an automatic injection and timing procedure to capture the spectral data would also improve the data analysis step because the input data would be more accurate, hence the output information will be better.

However, despite all the technical problems, and taking into consideration any other experimental errors such as dilution errors etc., the multiplex screening systems using flow injection and multivariate calibration seem a promising approach. The predictions were relatively good for both dual and ternary analyte assays, suggesting that such a system could be used as part of a screening process for target analytes. Therefore, the findings of this chapter show that multiplex screening using enzyme inhibition, fluorescence detection and multivariate calibration is valid, and if improved further could bring many benefits in drug discovery applications.

CHAPTER 7

CONCLUSIONS AND FUTURE WORK

7.1 CONCLUSIONS

The application of flow injection fluorescence spectroscopic assays to the simultaneous determination of two or more components has been challenging for many years. Fluorescence enzyme assays are well known as analytical methods in clinical chemistry and other fields, being sensitive, safe, and easy to use and available in a variety of formats. The immunoassays normally used in industry or research now are still mostly single assays, i.e. each assay is only able to analyse one analyte. However, in many cases dual- or multi-analyte assays would be much more valuable with the advantages of increased information content, savings in time and costs, and the elimination of some sources of sampling variance. Amongst all the labels used in immunoassays, only fluorescent groups offer realistic prospects of practicable multi-analyte assays.

Enzymes are being used to an ever-increasing extent in automated assays in analytical chemistry and biochemistry. This is clearly indicated by the dramatic increase in the number of papers being published in this area and by the large range of commercial instrumentation that has become available in recent years.

The main advantage of enzymes as reagents in analytical chemistry is their specificity and extreme sensitivity. Disadvantages are their high cost especially when continuous flow, automated systems are employed and relative instability. These general limitations on enzymes as catalysts have been minimised to a great extent by the technique of immobilisation.

The two main objectives of this investigation were to develop new fluorescence methods for the rapid and sensitive multi-analyte determinations of enzymes inhibitors using flow injection analysis, and to investigate the use of chemometric methods to determine whether it was feasibible to develop the simultaneous determination of the multiple analytes. These objectives were set with the intention that the final system could easily be reduced to a miniaturised scale (although miniaturisation was not one of the key objectives of this research). In addition, these assays were aimed at a high throughput screening application.

To a large extent the aims of the project have been successfully fulfilled.

The use of a single excess-labelled substrate has been the successful fluorescence method for the determination of enzymes inhibitors. A substrate utilising α-casein labelled with BODIPY dye has been synthesised. This substrate has been shown to be a suitable intramolecularly quenched conjugate for the determination of enzymes inhibitors in flow-based screening programmes. The flow-based procedure that has been described is particularly well suited to the high throughput screening of candidate drug molecules.

Pierce UltraLink biosupport medium was investigated and was shown to be extremely promising as a support in these assays. Enzymes, namely alkaline phosphatase (AP), alkaline protease (AlkP) and β-galactosidase (β-Gal) were immobilised on UltraLink successfully. The enzyme reactor was placed in a flow injection system (figure 4.10). In order that an assay with optimum sensitivity could be constructed, the experimental conditions such as buffer (type, pH and concentration), temperature, flow rate, enzyme concentration, volume of substrate and volume of enzyme reactors, under which enzyme activities could be achieved were investigated.

The single and dual screening assays based on flow injection analysis methodology, with immobilised enzyme reactors to analyse enzyme inhibitors have been investigated successfully. 3-Nitrophenylboronic acid (3-NPBA), phenylethyl β-D-thiogalactopyranoside (PETG) and sodium vanadate (VI), were determined by their inhibitory effect on immobilised, AlkP, β-Gal and AP, respectively in a flow injection system, with continuous reuse of the immobilised enzymes. The previously optimised conditions were used for this investigation. The inhibition of AP, AlkP and β-Gal with the inhibitors at μg/ml levels was achieved.

The fluorescence spectra of Bodipy FL-α-casein-AlkP, FDP-AP and FDG-β-Gal (figure 5.1) are strongly overlapped. Therefore, a time-dependent flow injection analysis method was used to analyse them simultaneously. The flow-injection system for dual assays used one buffer and incorporated small glass reactors containing different immobilised enzymes as shown in figures 5.2 and 5.5. Two-substrate / inhibitor solutions were injected and the fluorescence detected through

the time-dependent separation of the fluorescence peaks by having different lengths of flow tubing between the enzyme reactors and the detector.

The suitability of Bodipy FL-α-casein, FDP and FDG as substrates in dual enzyme inhibition assays has also been demonstrated. The inhibition of AlkP, AP and β-Gal by 3-NPBA, VI and PETG, respectively at μg/ml levels was achieved. But preliminary investigations of a dual assay for measuring the inhibitory effect of PETG and 3-NPBA on β-Gal and AlkP respectively showed that there were difficulties because of some interactions between the two reaction systems.

The application of the dual enzyme inhibition assays in the FIA system, using immobilised enzyme reactors provides a rapid, simple (does not require any process such as separation, precipitation or centrifugation) and sensitive method for the assay of enzyme inhibitors, essential requirements for screening assays.

The dual determination capabilities of the system were even further enhanced by using the multivariate techniques partial least squares, PLS-1. Analysis using three fluorophores by flow injection fluorescence spectroscopy and a multivariate calibration method has been examined. However, the technique did have its problems when resolving significantly overlapping signals as seen in chapter 6.

The system also suffered from reproducibility problems that were due to a variety of reasons. The main reason was the use of manual operations during the experimental procedures such as injecting the sample and collecting the data. This was a significant problem when trying to capture the whole spectrum at a particular time (one shot) because timing is vital in order to get the maximum signal: if the spectra are captured too early or too late this affected the statistical analysis of the data and therefore resulted in poor predictions. The technique of partial least squares looks for patterns in the spectral data and if any changes occur in the spectra that are not due solely to concentration it affects the overall calibration model: as always the output data is only as good as the input data.

Overall; however, despite all these technical issues the predictions and deviation values of both dual and triple component analysis looked very promising and suggest such systems could be used as a major screening method.

7.2 FUTURE WORK

Multi-determination allows a higher throughput and thus is extremely important in a future development of the labelled substrates for high throughput screening. The work that was carried out showed that UltraLink Biosupport Medium was extremely promising as a support for enzyme immobilisation. The enzyme reactor containing this support could be integrated into the dual inhibition assays described in section 5. Using the enzymes and inhibitors from the assays described in chapter 5, numerous other set-ups are possible. Figure 7.1 illustrates just a couple of examples of possible set-ups out of the many combinations that are possible. Much more work can therefore be carried out in the area of multiplex determination.

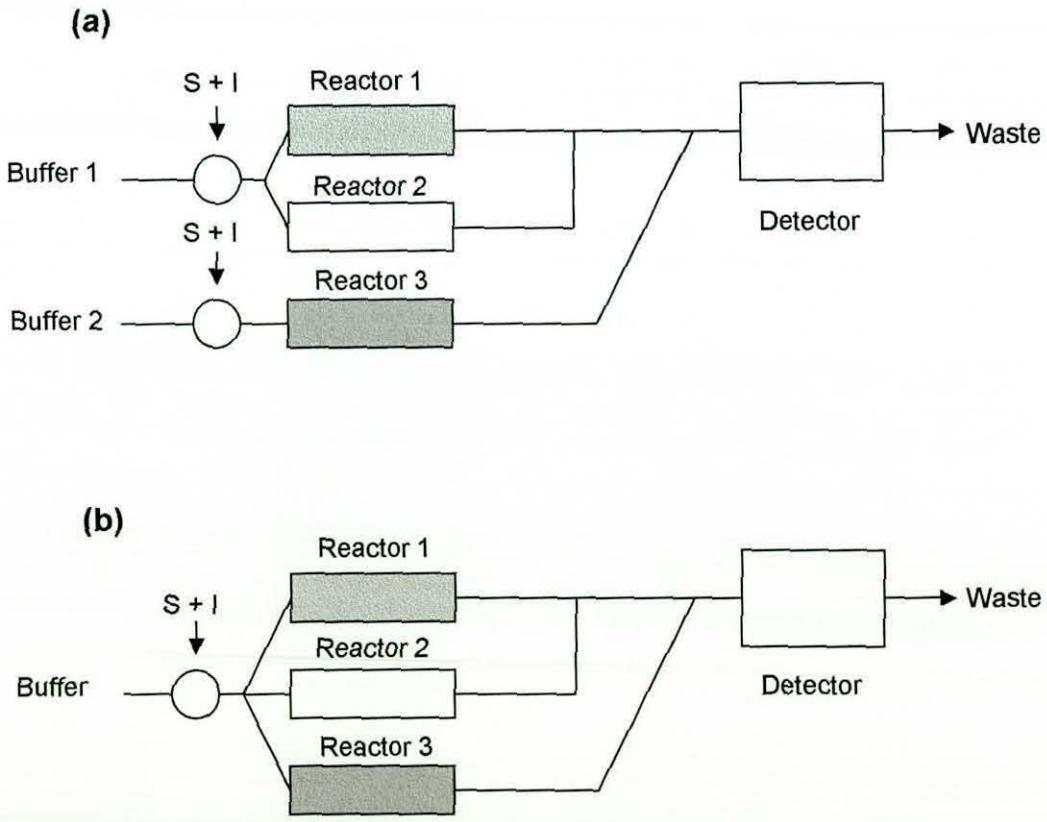

Figure 7.1 Possible set-ups for multi-determination assays

However, although parallel channels allow multi-determinations, which in turn produces a greater throughput of samples, the current macro-system has limitations. It would be impractical to keep paralleling up because of the amount of tubing that would be required. Space requirements would also increase, as well as the cost associated with high reagent consumption. This macro system therefore becomes limiting. The designs of such assays are much more suited to miniaturised assay formats, and hence a discussion of the transferral of these enzyme inhibition assays to a miniaturised system is given. Many discussions on the general concepts and techniques of the technology can be found.[194-196] Using a chip-based system, the ability to manufacture a set-up with many parallel channels is much simpler than with a macro system. Many parallel channels of different lengths would be easily manufactured in such a system, allowing the determination of two or more activities in nanolitre volumes using time separation. The small amounts of sample and reagents required in such systems are much better suited to the small amounts of compounds synthesised by combinatorial methods, allowing a better connection of combinatorial chemistry to HTS.

Modern microfabrication technology has had a great impact on the miniaturisation of analytical laboratory methods. Networks of coupled channels for sample concentration, mixing, dilution, reaction, etc. can be easily fabricated on a compact microchip.[197-200] A simple method integrating an immobilised enzyme reactor into a microchip electrophoresis device was developed.[194] Enzyme immobilisation was performed by drying a drop of dissolved nitrocellulose (NC) on a glass surface, and adsorbing enzyme on to the reconstituted NC membrane. The glass plate carrying the enzyme was incorporated into a polydimethylsiloxane chip on which the separation channel was fabricated (figure 7.2).

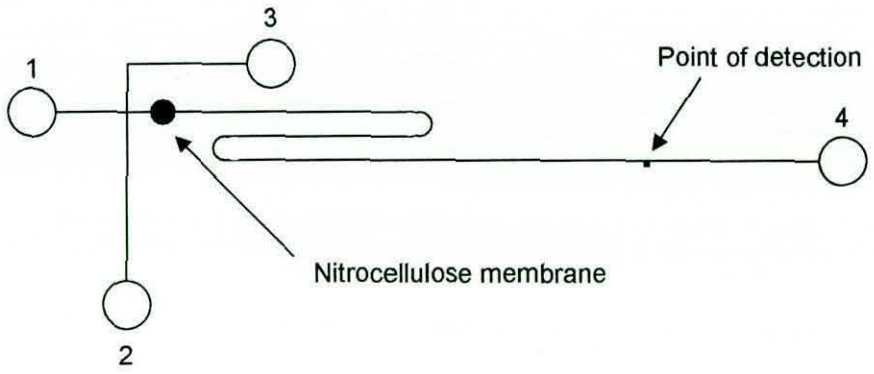

Figure 7.2 Schematic diagram showing the set-up of the microchip [194]
Reservoirs: (1) sample, (2) buffer anode, (3) sample waste, and (4) buffer cathode

The advantage of this method is the ability to change easily the position and size of the reactor within the device. A β-galactosidase reaction was demonstrated with fluorescein di-β-galactopyranoside. Enzyme kinetics and inhibition of the β-galactosidase using fluorescein mono-β-galactopyranoside and 2-phenylethyl β-galactoside, respectively, were also studied.

Microfabricated devices with integral heaters were described, which can be used for heterogeneous catalysis reactions.[201] Banu et. al.[202] reported a device designed to permit the in situ packing of a section of channel with enzyme immobilised on to controlled pore glass (CPG). The chip design is shown in figure 7.3. It was fabricated from glass and polydimethylsiloxane and to prevent dead volumes, had dedicated channels for packing the reactor. The device had the advantage of simplicity, the flow through enzyme reactor channel being just a widened section of the analyte channel. The system is suitable for both hydrodynamic and electro-osmotic pumping, and is designed such that when the packing is exhausted it can be repacked. The device was used with two enzymes of different molecular masses, alkaline phosphatase and xanthine oxidase for the assay of p-nitrophenyl phosphate and hypoxanthine with spectrophotometric detection at 405 and 470 nm, respectively. The limits of detection were 5 and 8 μM, respectively.

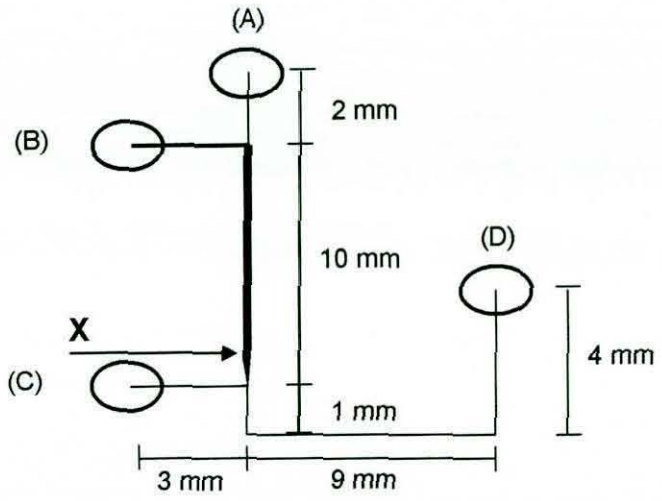

Figure 7.3 The chip design, showing the channel configuration[202]

The four circles represent the location of the reservoirs. X is where the channel depth changes. The enzyme reactor where the CPG is packed is represented by the portion of thick black line along the channel A-D

A potentially tricky part of the design of a miniaturised system would be the excitation of the fluorophore and subsequent detection. Detection of fluorescence on a chip is described briefly in many papers.[203-205] These methods would require much thought and planning in order to develop multiplex miniaturised systems for the determination of enzymes and their inhibitors.

For the chemometrics approach, future work should involve improving the flow injection system components to obtain more reliable and reproducible results, especially by automation of the sample injection and timing. Better software to capture and transform the data and the use of statistical software approaches to help resolve overlapping peaks more accurately should also be studied. In this work results were put into the Unscrambler software by initial data importation into Microsoft Excel®, and then arranging them appropriately on the spreadsheet before transferring them to the Unscrambler. With large data matrices this was time consuming, and increased the possibility of introducing errors into the data. The Unscrambler does provide another mode which can import the data as ASCII files from any instrument directly into the software with little input from the user. This might save time and minimise errors from converting the data. Another

approach is to look more deeply into variable selection methods that remove irrelevant variables and therefore reduce the size of the data matrices. This in turn speeds up calculations and increases accuracy.

The Unscrambler software also found it difficult to predict particular analytes when they were in the presence of other analytes that were in large molar excess. This was especially true when there was considerable overlap between the signals such that one of the peaks engulfed another. However this problem may be difficult to solve when using PLS-1 algorithms in any software. Therefore, other multivariate methods need to be investigated such as neural networks [206,207] etc., to see if they give better predictions. Also, investigating other software packages such as SIMCA-p [208], Matlab [209], etc might be worthwhile.

REFERENCES

(1) Dickson, M., and Gagnon, J. P. Key factors in the rising cost of new drug discovery and development. *Natural Review Drug Discovery* **2004**, *3*, 417-429.

(2) Giersiefen, H., Hilgenfeld, R., and Hillisch, A. Modern methods of drug discovery: an introduction. In *Modern Methods of Drug Discovery*; Hillisch, A., and Hilgenfeld, R. Ed.; Birkhauser Verlag: Germany, 2003; pp 1-18.

(3) Williams, M., and Malick, J. B. Drug Discovery and Development; The Humana, Inc.: New Jersey, 1987.

(4) Hillisch, A., and Hilgenfeld, R. *Modern Methods of Drug Discovery*; Birkhauser Verlag: Berlin, 2003.

(5) Patrick, G. L. *An Introduction to Medical Chemistry*; Oxford University Press: Oxford, 1995; 336.

(6) Drews, J. Drug discovery: a historical perspective. *Science* **2000**, *287*, 1960-1964.

(7) Couvreur, P., Braguer, D. J. A., Duchene, D., Engels, J. W., Kerr, D. J., Krogsgaard-Larsen, P., Meijer, D. K., Paoletti, R., and Wagner, E. Contribution of academic research to discovery and developmant of medicines: current status and future opportunities. *Phamaceutical Sciences* **2005**, *24*, 245-252.

(8) Dimasi, J. A., Hansen, R. W. and Grabowski, H. G. The price of innovation: new estimates of drug development costs. *Journal of Health Economy* **2003**, *22*, 151-185.

(9) Koh, H.-L., Yau, W. P., Ong, P. S., and Hegde, A. Current trends in modern pharmaceutical analysis for drug discovery. *Drugdiscoverytoday* **2003**, *8*, 889-897.

(10) Oldenburg, K. R. Current and future trends in high throughput screening for drug discovery. *Annual Report Medical Chemistry* **1998**, *33*, 301-311.

(11) Fox, S., Farr-Jones, S., and Yund, M. A. High throughput screening for drug discovery: continually transitioning into new technologies. *Journal of Biomolecular Screening* **1999**, *4*, 183-186.

(12) Copeland, R. A. Review: mechanistic considerations in high-throughput screening. *Analytical Biochemistry* **2003**, *320*, 1-12.

(13) Silverman, L., Campbell, R., and Broach, J. R. New assay technologies for high-throughput screening. *Current Opinion in Chemical Biology* **1998**, 2, 397-403.

(14) Sittampalam, G. S., Kahl, S. D., and Janzen, W. P. High-throughput screening: advances in assay technologies. *Current Opinion in Chemical Biology* **1997**, *1*, 384-391.

(15) Kumar, R. S., and Clark, D. S. High-throughput screening of biocatalytic activity: applications in drug discovery. *Current Opinion in Chemical Biology* **2006**, *10*, 162-168.

(16) Diamandis, E. P., and Christopoulos, T. K. Simultaneous Multianalyte Immunoassays. In *Immunoassay*; Kricka, J. L. Ed.; Academic Press, Inc.: London, 1996; pp Chapter 18.

(17) Deshpande, S. S. *Enzyme Immunoassays: from Concept to Product Development*; Chapman & Hall: New York, 1996.

(18) Galvez, A. M., Mateo, J. V. G. G., Calatayud, J. M. Simultaneous dissolution profiles of two drugs in pharmaceutical formulations by an FIA manifold. *Journal of Phamaceutical and Biomedical Analysis* **2002**, *27*, 1027-1030.

(19) Becker, T. M., and Schmidt, H. L. New ways of enzymatic two-substrate determinations in flow injection systems. *Analytica Chimica Acta* **2000**, *421*, 7-18.

(20) Parsons, R. G., Kowal, R., LeBlond, D., Yue, V. T., Neargarder, L., Bond, L., Garcia, D., Slater, D., and Rogers, P. Multianalyte assay system developed for drugs of abuse. *Clinical Chemistry* **1993**, *39*, 1899-1903.

(21) Buechler, K. F., Moi, S., Noar, B., McGrath, D., Villela, J., Clancy, M., Shenhav, A., Colleymore, A., Valkirs, G., Lee, T., Bruni, J. F., Walsh, M., Hoffman, R., Ahmuty, F., Nowakowski, M., Buechler, J., Mitchell, M., Boyd, D., Stiso, N., and Anderson,R. Simultaneouse detection of seven drugs of abuse by the Triage panel for drugs of abuse. *Clinical Chemistry* **1992**, *38*, 1678-1684.

(22) Kakabakos, S. E., Christopoulos, T. K., and Diamandis, E. P. Multianalyte immunoassay based on spatially distinct fluorescent areas quantified by laser excited solid-phase time-resolved fluorometry. *Clinical Chemistry* **1992**, *38*, 338-342.

(23) Pulgarin, J. A. M., Molina, A. A., and Lopez, P. F. Direct analysis of amiloride and triamterene mixtures by fluorescence spectrometry using partial-least squares calibration. *Analytica Chimica Acta* **2001**, *449*, 179-187.

(24) Bos, M., Bos, A., and van der Linden, W. E. Processing of signals from an ion-elective electrode array by a neural network. *Analytica Chimica Acta* **1990**, *233*, 31-39.

(25) Yao, T., Takashima, K., and Nanjyo, Y. Simultaneous determination of orthophosphate and total phosphates(inorganic phosphates plus purine nucleotides) using a bioamperometric flow-injection system made up by a 16-way switching valve. *Talanta* **2003**, *60*, 845-851.

(26) Matsue, T., Aoki, A., Ando, E., and Uchida, I. Multichannel electrochemical detection system for flow analysis. *Analytical Chemistry* **1990**, *62*, 407-409.

(27) Spohn, U., Van der Pol, J., Eberhardt, R., Joksch, B., and Wandrey, Ch. An automated system for multichannel flow-injection analysis. *Analytica Chimica Acta* **1994**, *292*, 281-292.

(28) O'Haver, T. C. Derivative and wavelength modulation spectrometry. *Analytical Chemistry* **1979**, *51*, 91A-100A.

(29) Murillo, J. A., Alanon, A., Fernandez, P., Munoz, A., Munoz de la Pena, A., and Espinosa-Mansilla, A. Simultaneous determination of nafcillin and

methicillin by different fluorimetric techniques using partial least-squares calibration. *Analyst* **1998**, *123*, 1073-1077.

(30) Petidier, A., Rubio, S., Gomez-Hens, A., and Valcarcel, M. Simultaneous and direct determination of pyridoxal, pyridoxal-5'-phosphate, and pyridoxic acid in serum by derivative synchronous fluorescence spectroscopy. *Analytical Biochemistry* **1986**, *157*, 212-220.

(31) Lindberg, W., Persson, J. A., and Wold, S. Partial least-squares method for spectrofluorimetric analysis of mixtures of humic acid and ligninsulfonate. *Analytical Chemistry* **1983**, *55*, 643-648.

(32) Sjostrom, M., Lindberg, S. W. W., and Martens, J. A. P. H. A multivariate calibration problem in analytical chemistry solved by partial least-squares models in latent variables. *Analytica Chimica Acta* **1983**, *150*, 61-70.

(33) Wang, Z. P., Qian, Y. H., Chen, G. S., and Cheng, K. L. Studies on simultaneous fluorescence-spectrophotometric determination of ultratrace niobium(V), tantalum(V), and zirconium(IV) using partial least-squares algorithm. *Microchemical Journal* **1998**, *60*, 271-281.

(34) Wang, Z. P., Shi, L. L., Chen, G. S., and Cheng, K. L. Multivariate spectrofluorimetry of ultra trace zirconium(IV) and hafnium(IV) assisted by several chemometrics methods. *Talanta* **2000**, *51*, 315-326.

(35) Hernandez, O., Martin, E., Jimenez, F., Jimenez, A. I., and Arias, J. J. Use of partial least-squares regression for multicomponent determinations based on kinetic spectrofluorimetric data. Simultaneous determination of canrenone and spironolactone in urine. *Analyst* **2000**, *125*, 1159-1165.

(36) Damiani, P. C., Borraccetti, M. D., and Olivieri, A. C. Direct and simultaneous spectrofluorometric determination of naproxen and salicylate in human serum assisted by chemometric analysis. *Analytica Chimica Acta* **2002**, *471*, 87-96.

(37) Armas, G., Miro, M., Estela, J. M., and Cerda, V. Simultaneous determination of fluorophores with overlapped spectra by sequential injection analysis coupled to variable angle scanning fluorescence

spectrometry and multivariate linear regression algorithms. *Analytica Chimica Acta* **2002**, *471*, 173-186.

(38) Billa, E., Pastou, A., Monties, B., Romero, J., and Koukios, E. G. Multivariate chemometric analysis of the fluorescence spectra of eucalyptus wood. *Industrial Crops and Products* **2000**, *11*, 187-196.

(39) Norgaard, L. A multivariate chemometric approach to fluorescence spectroscopy. *Talanta* **1995**, *42*, 1305-1324.

(40) Luis, M. L., Fraga, J. M. G., Jimenez, A. I., Jimenez, F., Hernandez, O., and Arias, J. J. Application of PLS regression to fluorimetric data for the determination of furosemide and triamterene in pharmaceutical preparations and triamterene in urine. *Talanta* **2004**, *62*, 307-316.

(41) Martos, N. R., Diaz, A. M., Navalon, A., Paya, I. D. O., and Vallvey, L. F. C. Simultaneous spectrofluorimetric determination of (acetyl) salicylic acid, codeine and pyridoxine in pharmaceutical preparations using partial least-squares multivariate calibration. *Journal of Phamaceutical and Biomedical Analysis* **2000**, *23*, 837-844.

(42) Wiberg, K., Sterner-Molin, A., and Jacobsson, S. P. Simultaneous determination of albumin and immunoglobulin G with fluorescence spectroscopy and multivariate calibration. *Talanta* **2004**, *62*, 567-574.

(43) Bright, F. V. Bioanalytical applications of fluorescence spectroscopy. *Analytical Chemistry* **1988**, *60*, 1031A-1039A.

(44) Skoog, D. A., and Leary, J. J. Fluorescence, Phosphorescence, and Chemiluminescence Spectroscopy. In *Principles of Instrumental Analysis*; Fourth ed.; Saunders College Publishing: Florida, 1992; pp Chapter 9.

(45) Lakowicz, J. R. *Principles of Fluorescence Spectroscopy*; Second ed.; Kluwer Academic/ Plenum Publishers: New York, 1999.

(46) Soper, S. A., Warner, I. M., and McGown, L. B. Fluorescence, phosphorescence, and chemiluminescence spectrometry. *Analytical Chemistry* **1998**, *70*, 477R-494R.

(47) Fletcher, K. A., Fakayode, S. O., Lowry, M., Tucker, S. A., Neal, S. L., Kimaru, I. W., McCarroll, M. E., Patonay, G., Oldham, P. B., Rusin, O., Strongin, R. M., and Warner, I. M. Molecular fluorescence, phosphorescence, and chemiluminescence spectrometry. *Analytical Chemistry* **2006**, *78*, 4047-4068.

(48) Hill, S. J., Chenery, S., Dawson, J. B., Evans, E. H., Fisher, A., Price, W. J., Smith, C. M. M., Sutton, K. L., and Tyson, J. F. Advances in atomic emission, absorption, and fluorescence spectrometry, and related techniques. *Journal of Analytical Atomic Spectrometry* **2000**, *15*, 763-805.

(49) Valeur, B., and Brochon, J. C. New Trends in Fluorescence Spectroscopy: Applications to Chemical and Life Sciences; Springer-Verlag Berlin Heidelberg: New York, 2001.

(50) Willard, H. H., Merritt, L. L., Dean, J. A., and Settle, F. A. Fluorescence and Phosphorescence Spectrophotometry. *Instrumental Methods of Analysis*; Seventh ed.; Wadsworth, Inc.: California, 1988; pp Chapter 8.

(51) Guilbault, G. G. Principles of luminescence spectroscopy luminescent determination of clinically and agriculturally important samples. *Pure and Applied Chemistry* **1985**, *57*, 495-514.

(52) Karoui, R., Mazerolles, G. and Dufour, E. Spectroscopic techniques coupled with chemometric tools for structure and texture determinations in dairy products. *International Dairy Journal* **2003**, *13*, 607-620.

(53) Sigma-Aldrich Company Ltd. Product Information: fluorescein isothiocyanate-isomer I. Accessed via https://www.sigmaaldrich.com/sigma/product, 10 July 2005.

(54) Kang, H. C. Dibenzopyrromethene boron Difluoride Dyes. *US patent 5* **1995**, *433*, 896.

(55) Johnson, I. D., Kang, H. C., and Haugland, R. P. Fluorescent membrane probes incorporating dipyrromethene boron difluoride fluorophores. *Analytical Biochemistry* **1991**, *198*, 228-237.

(56) Karolin, J., Johansson, B. A., Strandberg, L., and Ny, T. Fluorescence and absorption spectroscopic properties of dipyrromethene boron difluoride (BODIPY) derivatives in liquids, lipid membranes, and proteins. *Journal of the American Chemical Society* **1994**, *116*, 7801-7806.

(57) Molecular Probes Inc. Amines-reactive probes. Accessed via www. probes.com, 30 September 2002.

(58) Molecular Probes Inc. Product information: fluorescein digalactoside (F-1179). **2003**.

(59) Molecular Probes Inc. Product information: alkaline and acid phosphatase substrates: FDP, MUP, DiFMUP and DDAO phosphate. **2002**.

(60) Haugland, R. P. *The Handbook: A Guide to Fluorescent Probes and Labelling Technologies*; Tenth ed.; Invitrogen Corp.: USA, 2005; Chapter 10.

(61) Ruzica, J., and Hansen, E. H. Flow injection analysis. *Analytical Chemistry* **2000**, *March*, 212A-217A.

(62) Gubitz, G., and Shellum, C. Flow-injection immunoassays: review. *Analytical Chimica Acta* **1993**, *283*, 421-428.

(63) Yaqoob, M., and Nabi, A. Flow-injection method for the determination of serine using immobilized enzyme. *Talanta* **2000**, *55*, 1181-1186.

(64) Karlberg, B., and Pacey, G. E. *Flow Injection Analysis: A Practical Guide*; Elsevier Science Publishers B.V.: Amsterdam, 1989.

(65) Trojanowicz, M. *Flow Injection Analysis: Instrumentation and Applications*; Royal Press (S) Pte. Ltd.: Singapore, 2000.

(66) Valcarcel, M., and Luque de Castro, M. D. *Flow-Injection Analysis: Principles and Applications*; Ellis Horwood Limited: Sussex, 1987.

(67) Ruzica, J., and Hansen, E. H. Flow injection analysis, part 1: a new concept of fast continuous flow analysis. *Analytica Chimica Acta* **1975**, *78*, 145-157.

(68) Palmer, T. *Understanding Enzymes*; Third ed.; Ellis Harwood: Sussex, 1991.

(69) Holme, D. J., and Peck, H. *Analytical Biochemistry*; Third ed.; Pearson Education Limited: Essex, 1998; Chapter 8.

(70) Lehninger, A. L., Nelson, D. L., and Cox, M. M. Enzymes. *Principles of Biochemistry*; Second ed.; Worth Publishers Inc.: New York, 1997; pp 198-239.

(71) Stryer, L. *Biochemistry*; Fourth ed.; W.H.Freeman and Company: New York, 1995; Chapter 8.

(72) Meisenberg, G., and Simmons, W. H. *Medical Biochemistry*; Mosby, Inc.: Missouri, 1998; Chapter 4.

(73) Price, N. C., and Stevens, L. *Fundamentals of Enzymology: The Cell and Molecular Biology of Catalytic Proteins*; Third ed.; Oxford University Press Inc.: New York, 1999.

(74) Bugg, T. *An Introduction to Enzyme and Coenzyme Chemistry*; Blackwell Science Ltd.: Oxford, 1997.

(75) Chaplin, M. F., and Bucke, C. *Enzyme Technology*; Cambridge University Press: Cambridge, 1990.

(76) Barrett, A. J., Awlings, N. D., and Woessner, J. F., eds. *Handbook of Proteolytic Enzymes*; Academic Press: London, 1998.

(77) Purich, D. L., and Allison, R. D. *The Enzyme Reference: A Comprehensive Guide to Enzyme Nomenclature, Reactions, and Methods*; Academic Press: California, 2002; 929.

(78) Kalisz, H. M. Microbial proteinases. *Advance Biochemical Engeneering Biotechnology* **1988**, *36*, 1-65.

(79) Chen, S. T., chen, S. Y., Hsiao, S. C., and Wang, K. T. Kinetic resolution of N-protected amino acid esters in organic solvents catalysed by a stable industrial alkaline protease. *Biotechnology Letter* **1991**, *13*, 773-778.

(80) Anwar, A., and Saleemuddin, M. Alkaline proteasees: review. *Bioresource Technology* **1998**, *64*, 175-183.

(81) Beshay, U. Production of alkaline protease by *Teredinobacter turnirae* cells immobilised in Ca-alginate beads. *African Journal of Biotechnology* **2003**, *2*, 60-65.

(82) Moreira, K. A., Porto, T. S., Teixeira, M. F. S., Porto, A. L. F., and Filho, J. L. L. New alkaline protease from *Nocardiopsis sp.*: partial purification and characterization. *Process biochemistry* **2003**, *39*, 67-72.

(83) Bortolato, M., Besson, F., and Roux, B. An infrared study of the thermal and pH stabilities of the GPI-alkaline phosphatase from bovine intestine. *Biochemical and Biophysical Research Communications* **2002**, *292*, 874-879.

(84) McCarroll, N. A. Bone disorders (osteoporosis). *Analytical Chemistry* **1993**, *65*, 388R-395R.

(85) Schreiber, W. E., and Sadro, L. C. Agarose gel patterns of alkaline phosphatase isoenzymes before and after treatment with neuraminidase. *American Journal of Clinical Pathology* **1988**, *90*, 181-186.

(86) Bunting, P. S., and Laidler, K. J. Kinetic studies on solid-supported beta-galactosidase. *Biochemistry* **1972**, *11*, 4477-4483.

(87) Juers, D. H., Heightman, D., Vasella, A., McCarter, J. D., Mackenzie, L., Withers, S. G., and Matthews, B. W. A structural view of the action of *Escherichia coli (lacZ)* beta-galactosidase. *Biochemistry* **2001**, *40*, 14781-14794.

(88) Ladero, M., Santos, A., Garcia, J. L., and Garcia-Ochoa, F. Activity over lactose and ONPG of a genetically engineered beta-galactosidase from *Escherichia Coli* in solution and immobilized: kinetic modelling. *Enzyme and Microbial Technology* **2001**, *29*, 181-193.

(89) McCarter, J. D., Adam, M. J., and Withers, S. G. Binding energy and catalysis: fluorinated and deoxygenated glycosides as mechanistic probes of Escherichia coli (lacZ) beta-galactosidase. *Journal of Biochemistry* **1992**, *286*, 721-727.

(90) Jacobson, R. H., Zhang, X. J., DuBose, R. F., and Matthews, B. W. Three-dimensional structure of beta-galactosidase from E. coli. *Nature* **1994**, *369*, 761-766.

(91) WBC. Manual Page: Galactosidase, B., Accessed via www.worthington-biochem.com/BG/default.html, 30 October 2003.

(92) Jones, L. J., Upson, R. H., Haugland, R. P., Panchuk-Voloshina, N., Zhou, M., and Haugland, R. P. Quenched BODIPY dye-labeled casein substrates for the assay of protease activity by direct fluorescence measurement. *Analytical Biochemistry* **1997**, *251*, 144-152.

(93) Homer, K. A., and Beighton, D. Fluorometric determination of bacterial protease using fluorescein isothiocyanate-labeled proteins as substrates. *Analytical Biochemistry* **1990**, *191*, 133-137.

(94) Worsfold, P. J. Classification and chemical characteristics of immobilized enzymes. *Pure and Applied Chemistry* **1995**, *67*, 597-600.

(95) Nelson, J. M., and Griffin, E. G. Adsorption of Invertase. *Journal of American Chemical Society* **1916**, *38*, 1109-1115.

(96) Tischer, W., and Wedekind, F Immobilized enzymes: methods and applications. *Topics in Current Chemistry* **1999**, *200*, 96-126.

(97) Rao, S. V., Anderson, K. W., and Bachas, L. G. Fundamental review: oriented immobilization of proteins. *Mikrochimica Acta* **1998**, *128*, 127-143.

(98) Zaborsky, O. *Immobilized Enzymes*; CRC Press: Ohio, 1974.

(99) Liang, J. F., Li, Y. T., and Yang, V. C. Biomedical application of immobilized enzymes. *Journal of Pharmaceutical Sciences* **2000**, *89*, 979-990.

(100) Bayramoglu, G., Yilmaz, M. and Arica, M. Y. Immobilization of a thermostable alpha-amylase onto reactive membranes: kinetics characterization and application to continuous starch hydrolysis. *Food Chemistry* **2004**, *84*, 591-599.

(101) Farag, A. M., and Hassan, M. A. Review: purification, characterization and immobilization of a keratinase from *Aspergillus Oryzae*. *Enzyme and Microbial Technology* **2004**, *34*, 85-93.

(102) Luque de Castro, M. D., and Cases, M. V. Simultaneous determination in flow injection analysis: a review. *Analyst* **1984**, *109*, 413-419.

(103) D'Souza, S. F. Immobilized enzymes in bioprocess. *Current Science* **1999**, *77*, 69-79.

(104) PIERCE Instructions: UltraLink™ Biosupport Medium; Pierce Chemical Company: USA, 1999; pp 1-12.

(105) Olsson, B., Lundback, H., and Johansson, G. Theory and application of diffusion-limited amperometric enzyme electrode detection in flow injection analysis of glucose. *Analytical Chemistry* **1986**, *58*, 1046-1052.

(106) Masoom, M., and Townshend, A. Flow-injection determination of sulphite and assay of sulphite oxidase. *Analytica Chimica Acta* **1986**, *179*, 399-405.

(107) Goldstein, L., Leven, Y., and Katckalski, E. A Water-insoluble polyanionic derivative of trypsin II: effect of the polyelectrolyte carrier on the kinetic behavior of the bound trypsin. *Biochemistry* **1964**, *3*, 1913-1919.

(108) Chambert, R., and Petit-Glatron, M. F. Immobilisation of levansucrase on calcium phosphate gel strongly increases its polymerase activity. *Carbohydrate Research* **1993**, *244*, 129-136.

(109) Guinn, R. M., Blanch, H. W., and Clark, D. S. Effect of a water-miscible organic solvent on the kinetic and structural properties of trypsin. *Enzyme and Microbial Technology* **1991**, *13*, 320-326.

(110) Kuswandi, B., Andres, R., and Narayanaswamy, R. Optical fibre biosensors based on immobilised enzymes. *Analyst* **2001**, *126*, 1469-1491.

(111) Scheller, F., and Renneberg, R. Glucose-eliminating enzyme electrode for direct sucrose determination in glucose-containing samples. *Analytica Chimica Acta* **1983**, *152*, 265-269.

(112) Jurkiewicz, M., Alegret, S., and Fabregas, E. Comparison of flow injection analytical biosystems based on open-tube and packed-bed enzyme reactors. *Analytica Chimica Acta* **1998**, *370*, 47-58.

(113) Snyder, L. R. Continuous-flow analysis: present and future. *Analytica Chimica Acta* **1980**, *114*, 3-18.

(114) Mizutani, F., and Tsuda, K. Amperometric determination of cholinesterase with use of an immobilized enzyme electrode. *Analytica Chimica Acta* **1982**, *139*, 359-362.

(115) Tsukatani, T., and Matsumoto, K. Flow-injection fluorometric quantification of succinate in foodstuffs based on the use of an immobilized enzyme reactor. *Analytica Chimica Acta* **2000**, *416*, 197-203.

(116) Hassan, S. S. M., Mahmoud, W. H., Elmosallamy, A. F., and Othman, A. H. M. Determination of metformin in pharmaceutical preparations using potentiomery, spectrofluorimetry and UV-visible spectrophotometry. *Analytica Chimica Acta* **1999**, *378*, 299-311.

(117) Matsumoto, K., Matsubara, H., Hamada, M., Ukeda, H., and Osajima, Y. Simultaneous determination of glucose, ethanol and lactate in alcoholic beverages and serum by amperometric flow injection analysis with immobilized enzyme reactors. *Journal of Biotechnology* **1990**, *14*, 115-126.

(118) Masoom, M., and Townshend, A. Simultaneous determination of sucrose and glucose in mixtures by flow injection analysis with immobilized enzymes. *Analytica Chimica Acta* **1985**, *171*, 185-194.

(119) Lazaro, F., Luque de Castro, M. D., and Valcarcel, M. Individual and simultaneous determination of ethanol and acetaldehyde in wines by flow injection analysis and immobilized enzymes. *Analytical Chemistry* **1987**, *59*, 1859-1863.

(120) Matsumoto, K., Hamada, O., Ukeda, H., and Osajima, Y. Amperometric flow injection determination of fructose with an immobilized fructose 5-dehydrogenase reactor. *Analytical Chemistry* **1986**, *58*, 2732-2734.

(121) Williams, A. *Introduction to the Chemistry of Enzyme Action*; McGraw-Hill Publishing Company Limited: London, 1969.

(122) Fuller, R. W., and Steranka, L. R. Drug Discovery at the Enzyme Level. *Drug Discovery and Development*; Humana Press: New Jersey, 1987; pp 177-198.

(123) Barrett, A. J., Salvesen and G., eds. *Proteinase Inhibitors*; Elsevier Science Publishers BV (Biomedical Division): New York, 1986.

(124) Salvesen, G., and Nagase, H. Inhibition of Proteolytic Enzymes. *Proteolytic Enzymes-A Practical Approach*; University Press: Oxford, 1989.

(125) Laskowski, M., Jr., and Kato, I. Protein inhibitors of proteinases. *Annual Review Biochemistry* **1980**, *49*, 593-626.

(126) Suenaga, H., Yamamoto, H., and Shinkai, S. Screening of boronic acids for strong inhibition of the hydrolytic activity of alpha-chymotrypsin and for sugar sensing associated with a large fluorescence change. *Pure and Applied Chemistry* **1996**, *68*, 2179-2186.

(127) Raghavendra, M. P., and Prakash, V. Phenylboronic acid-a potent inhibitor of lipase from *Oryza sativa*. *Journal of Agricultural and Food Chemistry* **2002**, *50*, 6037-6041.

(128) Kettner, C. A., Bone, R., Agard, D. A., and Bachovchin, W. W. Kinetic properties of the binding of alpha-lytic protease to peptide boronic acids. *Biochemistry* **1988**, 27, 7682-7688.

(129) Bachovchin, W. W., Wong, W. Y. L., Farr-Jones, S., Shenvi, A. B., and Kettner, C. A. Nitrogen-15 NMR spectroscopy of the catalytic-triad histidine of a serine protease in peptide boronic acid inhibitor complexes. *Biochemistry* **1988**, *27*, 7689-7697.

(130) Wenzel, U. O., Fouqueray, B., Biswas, P., Grandaliano, G., Choudhury, G. G., and Abboud, H. E. Activation of mesangial cells by the phosphatase inhibitor vanadate. *Journal of Clinical Investigation* **1995**, *95*, 1244-1252.

(131) Huyer, G., Liu, S., Kelly, J., Moffat, J., Payette, P., Kennedy, B., Tsaprailis, G., Gresser, J., and Ramachandran, C. Mechanism of inhibition of protein-tyrosine phosphatases by vanadate and pervanadate. *Journal of Biological Chemistry* **1997**, *272*, 843-851.

(132) Cuncic, C., Detich, N., Ethier, D., Tracey, A. S., Gresser, M. J., Ramachandran, C. Vanadate inhibition of protein tyrosine phosphatases in Juekat cells. *Journal of Biological Inorganic Chemistry* **1999**, *4*, 354-359.

(133) Choi, J. H., Choe, Y. S., Lee, K. H., Choi, Y., Kim, S. E., and Kim, B. T. Synthesis of radioiodine-labeled 2-phenylethyl 1-thio-b-galactopyranoside for imaging og LacZ gene expression. *Carbohydrate Research* **2003**, *338*, 29-34.

(134) BIO-TEX Instruments, I. Application Note: Kinetic Analysis of b-Galactosidase Activity Using the PowerWavw 200 in Conjunction with KC4 Data Reduction Software; Accessed via www.biotek.com, 10 July 2005.

(135) Beebe, K. R., Pell, R. J., and Seasholtz, M. B. *Chemometrics: A Practical Guide*; John Wiley & Sons, Inc.: Canada, 1998; 413.

(136) Otto, M. *Chemometrics: Statistics and computer Application in Analytical Chemistry*; Wiley-vCH: Weinheim, 1999; Chapter 1.

(137) Brereton, R. G. *Chemometrics: Data Analysis for the Laboratory and Chemical Plant*; John Wiley & Sons Ltd.: Sussex, 2003.

(138) Gabrielsson, J., Lindberg, N.-O., and lundstedt, T. Multivariate methods in pharmaceutical applications: Review. *Journal of Chemometrics* **2002**, *16*, 141-160.

(139) Haswell, S. J., and Walmsley, A. D. Chemometrics: the issues of measurement and modelling. *Analytica Chimica Acta* **1999**, *400*, 399-412.

(140) Lavine, B. K., and Workman, J. Jr. Chemometrics. *Analytical Chemistry* **2002**, *74*, 2763-2770.

(141) Thomas, E. V. Adaptable multivariate calibration models for spectral applications. *Analytical Chemistry* **2000**, *72*, 2821-2827.

(142) Demir, C., and Brereton, G. Multivariate calibration on designed mixtures of four pharmaceuticals. *Analyst* **1998**, *123*, 181-189.

(143) Jackson, J. E. *A Users Guide to Principal Components*; John Wiley and Sons, Inc.: New York, 1991.

(144) Malinowski, E. R. *Factor Analysis in Chemistry*; Third ed.; John Wiley and Sons, Inc.: New York, 2002.

(145) Hotelling, H. Analysis of a complex of statistical variables into principal components. *Journal of Education Psychology* **1933**, *24*, 417-441.

(146) Cloarec, O., Gonzalez, C., Touraud, E., and Thomas, O. Improvement of UV spectrophotometry methodology for the determination of total polycyclic aromatic compounds in contaminated soils. *Analytica Chimica Acta* **2002**, *453*, 245-252.

(147) Gallego, J. M. L., and Arroyo, J. P. Spectrophotometric resolution of ternary mixtures of dexamethasone, polymyxin B and trimethoprim in synthetic and pharmaceutical formulations. *Analytica Chimica Acta* **2001**, *437*, 247-257.

(148) Guiteras, J., Beltran, J. L., and Ferrer, R. Quantitative multicomponent analysis of polycyclic aromatic hydrocarbons in water samples. *Analytica Chimica Acta* **1998**, *361*, 233-240.

(149) Otsuka, M., Kato, F., and Matsuda, Y. Determination of indomethacin polymorphic contents by chemometric near-infrared spectroscopy and conventional powder X-ray diffractometry. *Analyst* **2001**, *126*, 1578-1582.

(150) Verdu-Andres, J., Herraez-Hernandez, R., and Campins-Falco, P. Analysis of enantiomers giving partially overlapped peaks by using different treatments of the chromatographic ultraviolet signals: quantification of pseudoephedrine enantiomers. *Journal of Chromatography A* **2001**, *930*, 95-107.

(151) Geladi, P., and Kowalski Partial least-squares regression: a tutorail. *Analytica Chimica Acta* **1986**, *185*, 1-17.

(152) Wold, H. Partial Least Squares. *Encyclopedia of statistical Sciences, Vol. 6*; Wiley: New York, 1985; pp 581-591.

(153) Collado, M. S., Mantovani, V. E., Goicoechea, H. C., and Odivieri, A. C. Simultaneous spectrophotometric-multivariate calibration determination of several components of ophthalmic solutions: phenylephrine, chloraphenicol, antipyrine, methylparaben and thimersal. *Talanta* **2000**, *52*, 909-920.

(154) Eustaquio, A., Graham, P., Jee, R. D., Moffalt, A. C., and Trafford, A. D. Quantification of paracetamol in intact tablets using near infrared transmittance spectroscopy. *Analyst* **1998**, *123*, 2303-2306.

(155) Frenich, A. G., Vidal, J. L. M., Parrilla, P., and Galera, M. M. Resolution of folpet, procymidone and triazophos in high-performance liquid chromatography-diode array detection by using partial least squares calibration to cross-sections of spectrochromatograms. *Journal of Chromatography A* **1997**, *778*, 183-192.

(156) Casal, V., Martin-Alvarez, P. J., and Herraiz, T. Comparative prediction of the retention behavior of small peptides in several reverse-phase high-performance liquid chromatography columns by using partial least squares and multiple linear regression. *Analytica Chimica Acta* **1996**, *326*, 77-84.

(157) Manne, R. Analysis of two partial-least-squares algorithms for multivariate calibration. *Chemometrics and Intelligent Laboratory Systems* **1987**, *2*, 187-197.

(158) Phatak, A., and Jong, S. D. The geometry of partial least squares. *Journal of Chemometrics* **1997**, *11*, 311-338.

(159) De Jong, S. Short communication: PLS fits closer than PCR. *Journal of Chemometrics* **1993**, *7*, 551-557.

(160) Lang, P. M., and Kalivas, V. H. A global perspective on multivariate calibration methods. *Journal of Chemometrics* **1993**, *7*, 153-164.

(161) Rannar, S., Lindgren, F., Geladi, P., and Wold, S. A PLS kernel algorithm for data sets with many variables and fewer objects, part 1: theory and algorithm. *Journal of Chemometrics* **1994**, *8*, 111-125.

(162) Lindberg, W., Geladi, P., and Wold, S. The kernel algorithm for PLS. *Journal of Chemometrics* **1993**, *7*, 45-59.

(163) Martens, H., and Naes, T. *Multivariate Calibration*; john Wiley & Sons Ltd.: Chichester, 1989.

(164) CAMO ASA *User manual: The Unscrambler*; CAMO ASA: Norway, 1998.

(165) Vries, S. D., and Braak, C. J. F. T. Prediction error in partial least squares regression: a critique on the deviation used in The Unscrambler. *Chemometrics and Intelligent Laboratory Systems* **1995**, *30*, 239-245.

(166) Hoy, M., Steen, K., and Martens, H. Review of partial least aquares regression prediction error in Unscrambler. *Chemometrics and Intelligent Laboratory Syatems* **1998**, *44*, 123-133.

(167) Tysso, V. UNSCRAMBLER, an interactive program for multivariate calibration and prediction. *Chemometrics and Intelligent Laboratory Systems* **1987**, *2*, 239-243.

(168) Foulk, S. The Unscrambler. *American Laboratory* **1988**, *20*, 10.

(169) Norgaard, L. Unscrambler:software review. *Journal of Chemometrics* **2000**, *14*, 45-46.

(170) Acedo-Valenzuela, M.-I., and Galeano-Diaz, T. Response surface methodology for the optimisation of flow-injection analysis with in situ solvent extraction and fluorimetric assay of tricyclic antidepressants. *Talanta* **2005**, *66*, 952-960.

(171) Smith, P. K., Krohn, R. I., Hermanson, G. T., Mallia, A. K., Gartner, F. H., Provenzano, M. D., Fujimoto, E. K., Goeke, N. M., Olson, B. J., and Klenk, D. C. Measurement of protein using bicinchoninic acid. *Analytical Biochemistry* **1985**, *150*, 76-85.

(172) PIERCE BCA protein assay kit instructions. **2002**.

(173) Robinson, D. The fluorimetric determination of beta-glucosidase: its occurrence in the tissues of animals, including insects. *Journal of Biochemistry* **1956**, *62*, 39-44.

(174) Burd, J. F., et al. Specific Protein-Binding Reactions Monitored By Enzymatic Hydrolysis Of Ligands-Fluorescent Dye Conjugates. *Analytical Biochemistry* **1977**, *77*, 56-67.

(175) Dubost, E., Tschamber, T. and Streith, J. Increasing the inhibitory potency of L-arabino-imidazolo-[1,2]-piperidinose towards b-D-Glucosidase and b-D-galactosidase. *Tetrahedron Letters* **2003**, 3667-3670.

(176) Pessela, B. C. C., Mateo, C., Fuentes, M., Vian, A., Garcia, J. L., Carrascosa, A. V., Guisan, J. M., and Fernandez-Lafuente, R. The immobilization of a thermophilic b-galactosidase on sepabeads supports decreases product inhibition complete hydrolysis of lactose in daily products. *Enzyme and Microbial Technology* **2003**, *33*, 199-205.

(177) Bone, R., Frank, D., Kettner, C. A., and Agard, D. A. Structural analysis of specificity: alpha-lytic protease complexes with analogues of reaction intermediates. *Biochemistry* **1989**, *28*, 7600-7609.

(178) Guilbault, G. G. Fluorescence in Enzymology. *Practical Fluorescence*; Marcel Dekker: New York, 1990; pp 683.

(179) Kuban, V. Simultaneous determination of several components by flow injection analysis. *Critical Reviews in Analytical Chemistry* **1992**, *23*, 15-53.

(180) Farfield Sensors Quantifying the Effects of Dimethyl Sulphoxide (DMSO) on Protein Structure using Dual Polarisation Inferometry. *Accessed via http://www.azonano.com/Details.asp?ArticleID=1536#_References, 30 March 2006.*

(181) DiCesare, N., Pinto, M. R., Schanze, K. S., and Lakowicz, J. R. Saccharide detection based on the amplified fluorescence quenching of a water-soluble poly(phenylene ethynylene) by a boronic acid functionalized benzyl viologen derivative. *Langmuir* **2002**, *18*, 7785-7787.

(182) Sanchez, F. G., Gutierrez, A. F., and Blanco, C. C. Variable-angle scanning fluorescence spectrometry for the simultaneous determination of three diuretic drugs. *Analytica Chemica Acta* **1995**, *306*, 313-321.

(183) Garcia, L., Blazquez, S., San Andres, M. P., and Vera, S. Determination of thiamine, riboflavin and pyridoxine in pharmaceuticals by synchronous fluorescence spectrometry in organized media. *Analytica Chimica Acta* **2001**, *434*, 193-199.

(184) Perez Ruiz, T., Martinez Galera, C., and Tomas, V. Simultaneous determination of propranolol and pindolol by synchronous spectrofluorimetry. *Talanta* **1998**, *45*, 969-976.

(185) Andrew, K. N., and Worsfold, P. J. Comparison of multivariate calibration techniques for the quantification of model process streams using diode-array spectrophotometry. *Analyst* **1994**, *119*, 1541-1546.

(186) Nevado, J. J. B., Flores, J. R., Llerena, M. J. V., and Farinas, N. R. Simultaneous spectrophotometric determination of tartrazine, patent blue V, and indigo carmine in commercial products by partial least squares and principal component regression methods. *Talanta* **1999**, *48*, 895-903.

(187) Thomas, E. V., and Haaland, D. M. Comparison of multivariate calibration methods for quantitative spectral analysis. *Analytical Chemistry* **1990**, *62*, 1091-1099.

(188) El-Gindy, A., Emara, S., and Mostafa, A. Application and validation of chemometrics-assisted spectrophotometry and liquid chromatography for the simultaneous determination of six-component pharmaceuticals. *Journal of Pharmaceutical and Biomedical Analysis* **2006**, *41*, 421-430.

(189) Ragno, G., Loele, G., and Risoli, A. Multivariate calibration techniques applied to the spectrophotometric analysis of one-to-four component systems. *Analytica Chimica Acta* **2004**, *512*, 173-180.

(190) Centner, V., Massart, D. L., Noord, O. E., Jong, S., Vandeginste, B. M., and Sterna, C. Elimination of Uninformative variables for multivariate calibration. *Analytical Chemistry* **1996**, *68*, 3851-3858.

(191) Alsberg, B. K., Kell, D.B., and Goodacre, R. Variable selection in discriminant partial least squares analysis. *Analytical Chemistry* **1998**, *70*, 4126-4133.

(192) Faber, N. M., Meinders, M. J., Geladi, P., Sjostrom, M., Buydens, L. M. C., and Kateman, G. Random error in principal component analysis. Part II: Application of theoretical predictions to multivariate problems. *Analytica Chimica Acta* **1995**, *304*, 273-283.

(193) Faber, N. M., Meinders, M. J., Geladi, P., Sjostrom, M., Buydens, L. M. C., and Kateman, G. Random error bias in principal component analysis Part I: Derivation of theoretical predictions. *Analytica Chemica Acta* **1995**, *304*, 257-271.

(194) Park, S. S., Cho, S. I., Kim, M. S., Kim, Y. K., and Kim, B. G. Integration of on-column immobilized enzyme reactor in microchip electrophoresis. *Electrophoresis* **2003**, *24*, 200-206.

(195) Effenhauser, C. S., and Manz, A. Miniaturizing a whole analytical laboratory down to chip size. *American Laboratory* **1994**, *September*, 15-18.

(196) Figeys, D., and Pinto, D. Lab-on-a-chip: a revolution in biological and medical sciences. *Analytical Chemistry* **2000**, 330A-335A.

(197) Burns, M. A., Johnson, B. N., Brahmasandra, S. N., Handique, K., Webster, J. R., Krishman, M., sammarco, T. S., Man, P. M., Jones, D., Heldsinger, D., Mastrangelo, C. H., and Burke, D. T. An integrated nanoliter DNA analysis device. *Science* **1998**, 282, 484-487.

(198) Liu, J., Hansen, C., and Quake, S. R. Solving the "world-to-chip" interface problem with a microfluidic matrix. *Analytical Chemistry* **2003**, *75*, 4718-4723.

(199) Hadd, A. G., Raymond, D. E., Halliwell, J. W., Jacobson, S. C., and Ramsey, J. M. Microchip device for performing enzyme assays. *Analytical Chemistry* **1997**, *69*, 3407-3412.

(200) Hayes, M. A., Polson, N. A., Phayre, A. N., and Garcia, A. A. Flow-based microimmunoassay. *Analytical Chemistry* **2001**, *73*, 5896-5902.

(201) McCreedy, T. Microfabricated reactors for on-chip heterogeneous catalysis. *Analyst* **2001**, *126*, 21-23.

(202) Banu, S.; Greenway, G. M.; McCreedy, T.; Shaddick, R. Microfabricated bioreactor chips for immobilised enzyme assays. *Analytica Chimica Acta* **2003**, *486*, 149-157.

(203) Chiem, N., and Harrison, D. J. Microchip-based capillary electrophoresis for immunoassays: analysis of monoclonal antibodies and theophilline. *Analytical Chemistry* **1997**, *69*, 373-378.

(204) Hadd, A. G., Jabobson, S. C., and Ramsey, J. M. Microfluidic assays of acetylcholinesterase inhibitors. *Analytical Chemistry* **1999**, *71*, 5206-5212.

(205) Lu, Q., Callahan, J. H., and Collins, G. E. The selective detection of uranium (VI) on a microchip using a derivatized 4-sulfonic calix [6] arene. *Chemical Communications* **2000**, *19*, 1913-1914.

(206) Deshpagne, F., and Massart, D. L. Neural networks in multivariate calibration. *Analyst* **1998**, *123*, R157-R178.

(207) Li, Q., Yao, X., Chen, X., Liu. M., Zhang, R., Zhang, X., and Hu, Z. Application of artificial neural networks for the simultaneous determination of a mixture of fluorescent dyes by synchronous fluorescence. *Analyst* **2000**, *125*, 2049-2053.

(208) Umetrics Multivariate data analysis. **1998**, Accessed via http://www.umetrics.com, 8 November 2002.

(209) Mathworks Matlab 6.5. **2002**, Accessed via http://www.mathworks.com, 8 November 2002.

(210) Hitachi *Instruction Manual: Model F-4500 Fluorescence Spectrophotometer*, 1991; Chapter 2.

APPENDICES

APPENDIX A

Supplier names and addresses

Supplier name	Address
Amersham Pharmacia Biotech UK, Ltd.	Amersham Place Little Chalfont Buckinghamshire HP7 9NA,UK
Anachem, Ltd.	20 Charles Street Luton, Bedfordshire LU2 0EBG,UK
Elkay Laboratory Products (UK), Ltd.	Unit4, Marlborough Mews Crockford Lane Basingstoke, Hampshire RG24 8NA, UK
Fisher Scientific UK	Bishop Meadow Road Loughborough Leicestershire LE11 5RG, UK
Grant Instruments (Cambridge), Ltd.	29 Station Road Shepreth, Royston Herefordshire SG8 6PZ, UK

Supplier name	Address
Hellma (England), Ltd.	Cumberland House 24-28 Baxter Avenue Southend-on-Sea Essex SS2 6HZ, UK
Hitachi Scientific Instruments	7 Ivanhoe Road Hogwood Industrial Estate Finchampstead Berkshire RG40 4QQ, UK
Molecular Probes, Inc.	Cambridge Bioscience 24-25 Signet Court Newmarket Road Cambridge CB5 8LA, UK
Ohaus UK, Ltd.	64 Boston Road Beaumont Leys Leicester LE4 1AW, UK
Omnifit, Ltd.	2 College Park Coldhams Lane Cambridge CB1 3HD, UK

Supplier name	Address
Precisa Balances Ltd.	4 Vermont Place Tongwell, Milton Keynes, Buckinghamshire MK15 8JA, UK
Sigma-Aldrich Company, Ltd.	Fancy Road Poole Dorset BH12 4QH, UK
Unicam Limited	York Street Cambridge CB1 2PX, UK
Whatman International Ltd.	St Leonard's Road 20/20 Maidstone Kent ME16 0LS, UK

APPENDIX B

Appearance of the model F-4500 fluorescence spectrophotometer (Hitachi) located in our laboratory

Figure B-1 Appearance of the F-4500 in our laboratory

APPENDIX C

Block diagram of the layout of the model F-4500 fluorescence spectrophotometer (Hitachi)

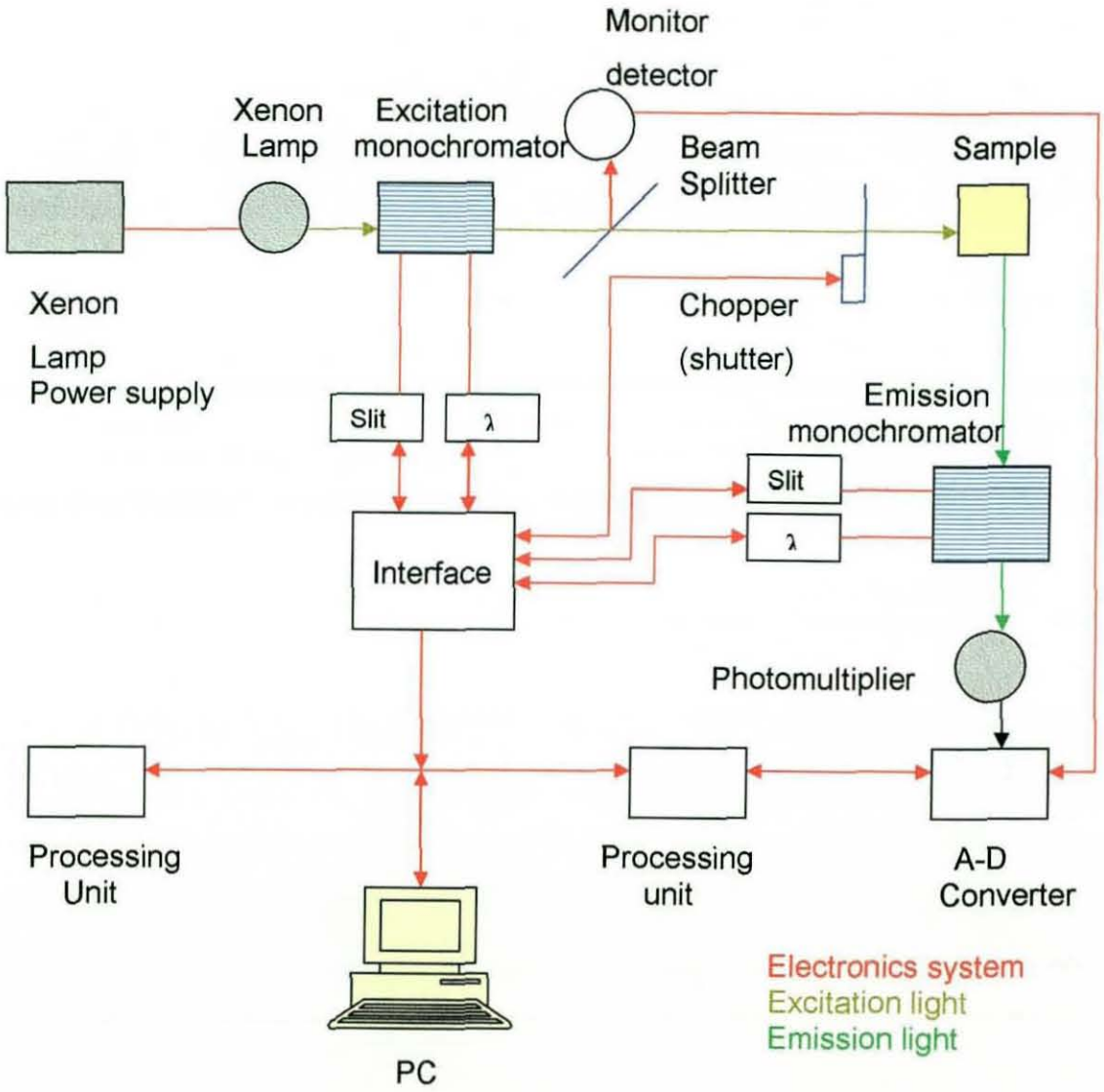

Figure C-1 Internal block diagram of the F-4500 [210]

APPENDIX D

Instrument specifications for the Hitachi F-4500 fluorescence spectrophotometer

Table D-1 Instrument parameters of the F-4500[210]

Parameters	Specifications
Light source	150 W Xenon lamp
Monochromators	Excitation: 200 – 600 nm
	Emission: 200 – 900 nm
Excitation slit width	1.0, 2.5, 5.0, and 10.0 nm
Emission slit width	1.0, 2.5, 5.0, 10.0, and 20.0 nm
Scanning speed	15, 60, 240, 1200, 2400, 12000, and 300000 nm / min
Wavelength accuracy	± 2.0 nm
Response	0.004, 0.01, 0.05, 0.1, 0.5, 2.0, and 8.0 seconds
PMT Voltage	400, 700, and 950 V

APPENDIX E

Analysis plots of the calibration set for 3 conjugates with PLS-1 and FCV

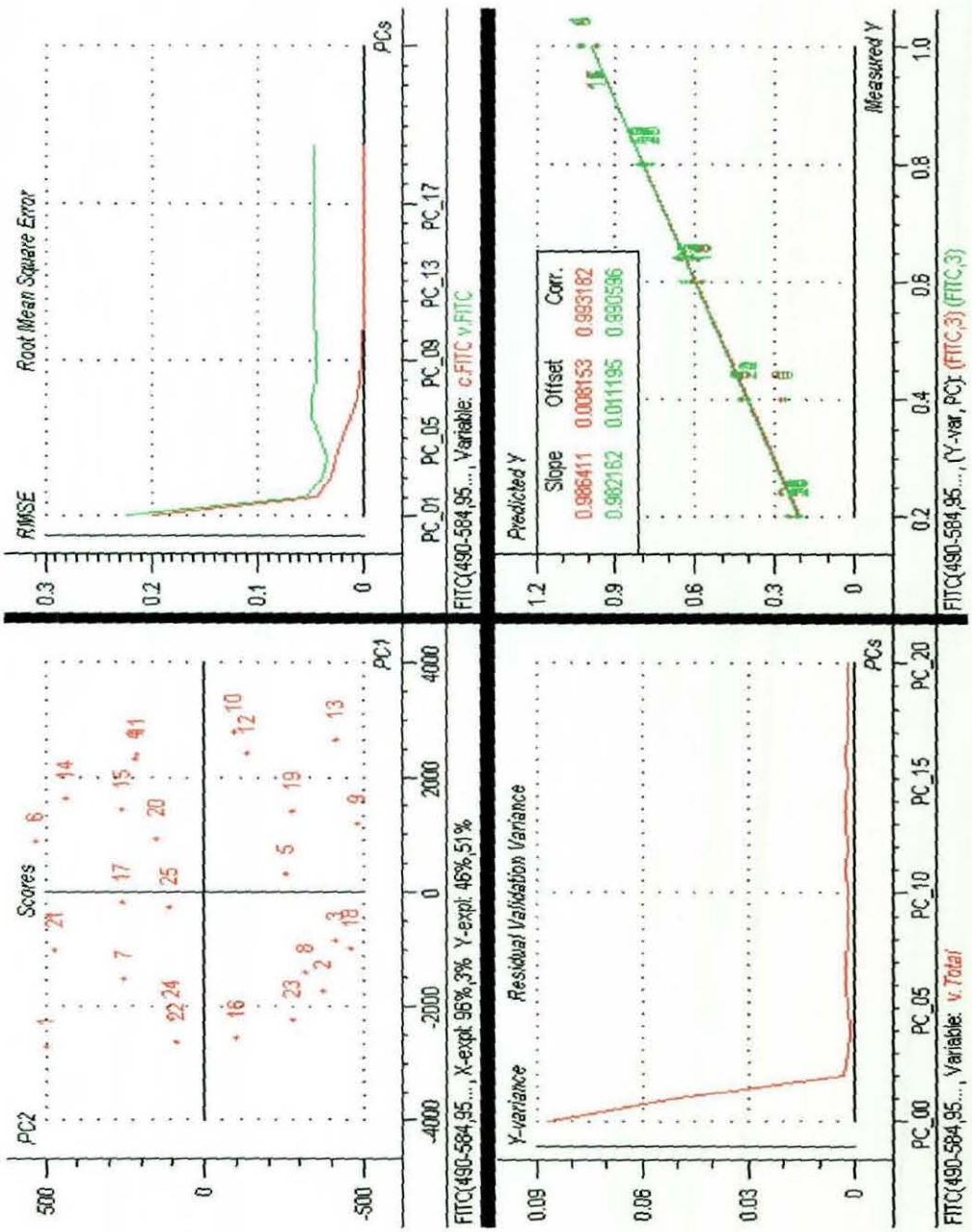

Figure E-1 The analysis plots of calibration set for FITC conjugate using PLS-1 and FCV

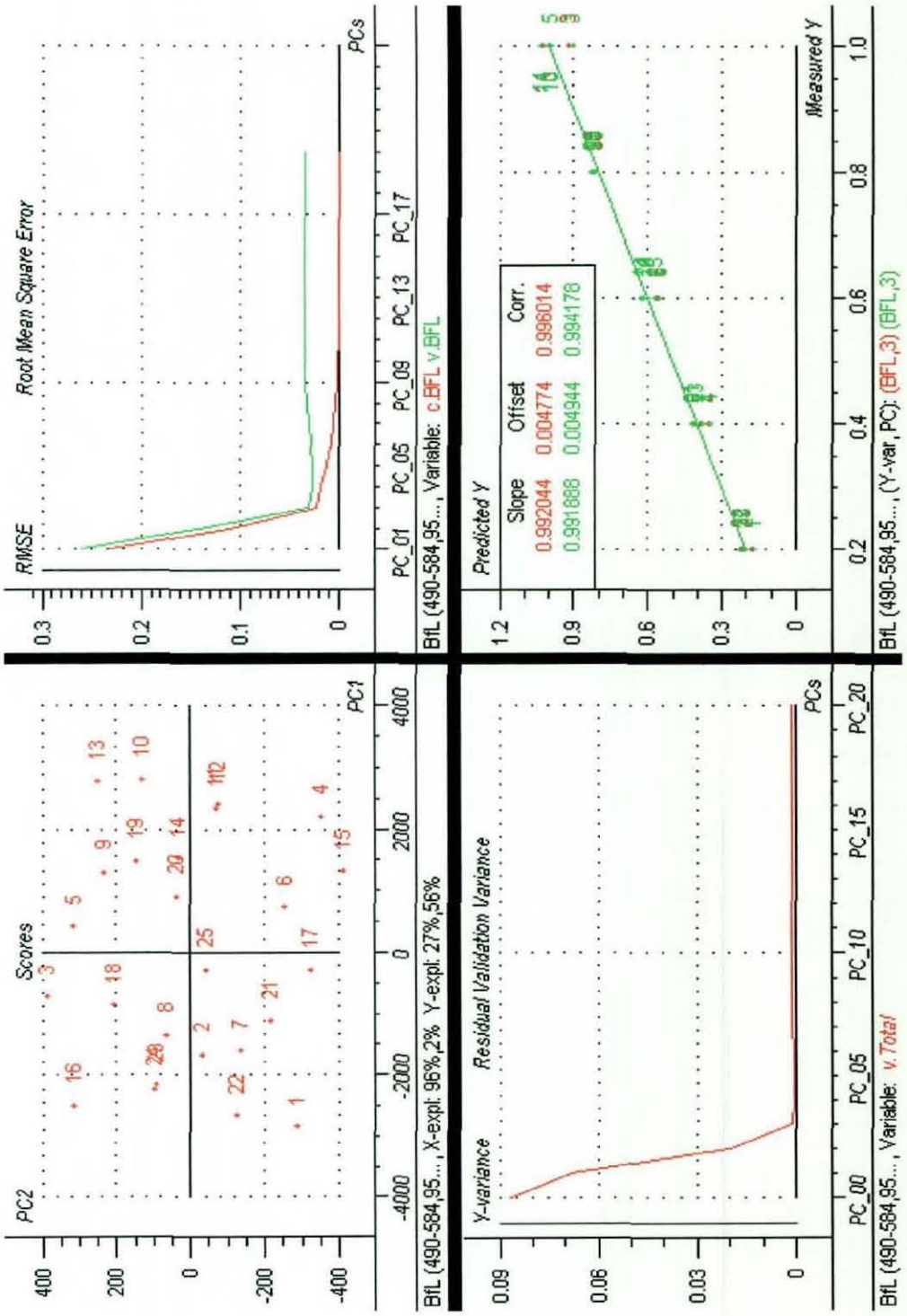

Figure E-2 The analysis plots of calibration set for BFL conjugate using PLS-1 and FCV

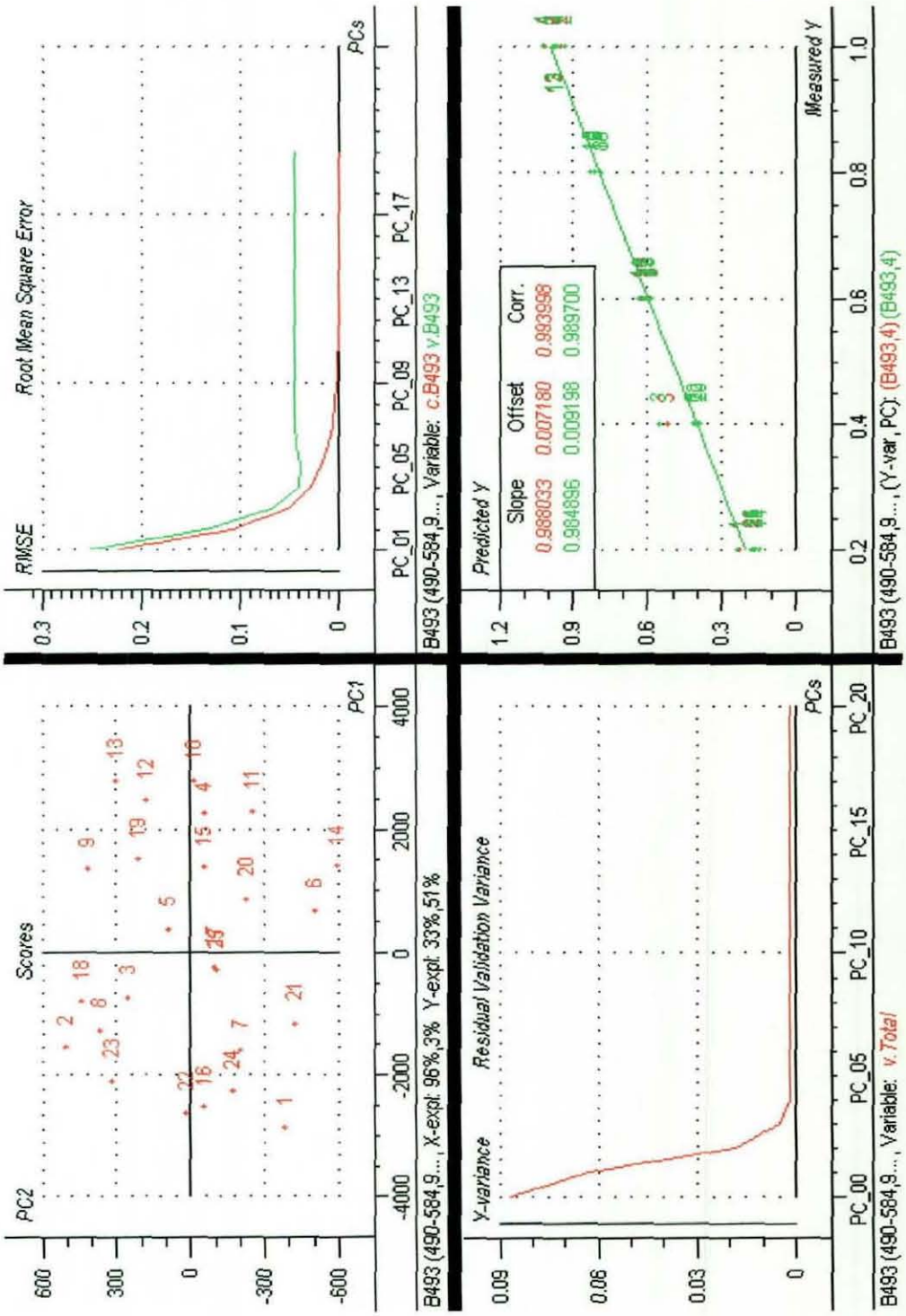

Figure E-3 The analysis plots of calibration set for B493 conjugate using PLS-1 and FCV

Analysis plots of the calibration set for 3 conjugates with PLS-1 and FCV without outlier

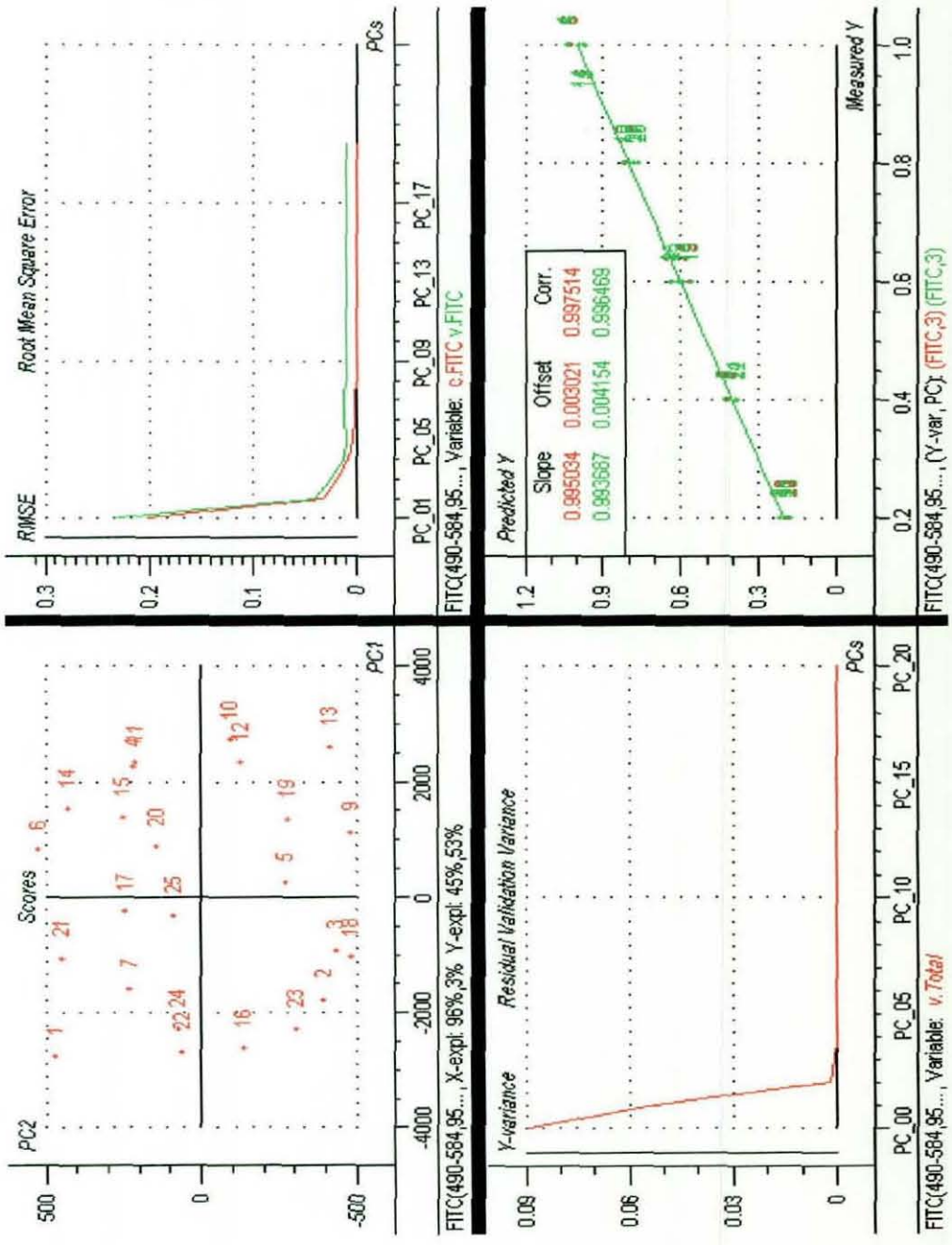

Figure E-4 The analysis plots of calibration set for FITC conjugate using PLS-1 and FCV without outlier

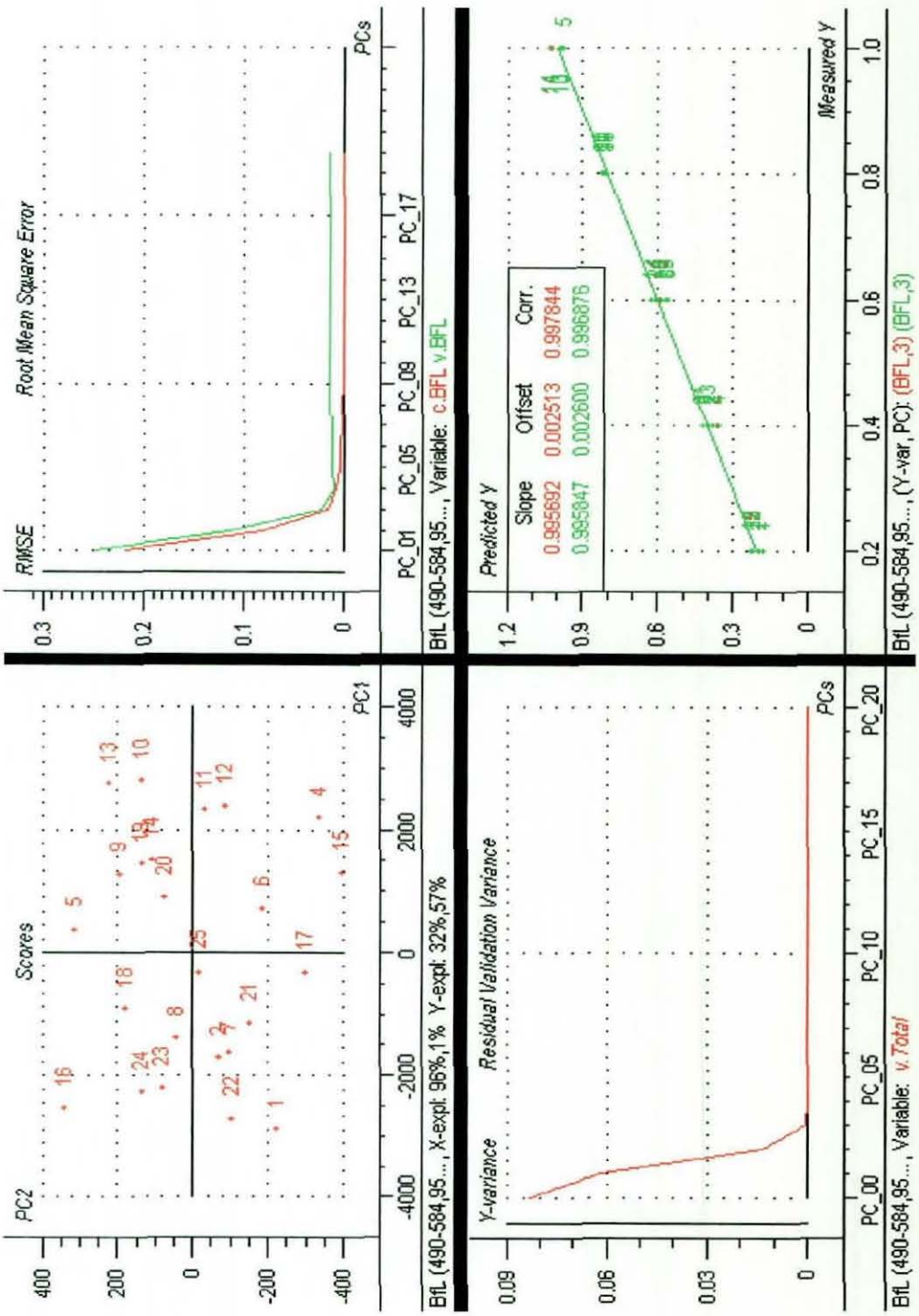

Figure E-5 The analysis plots of calibration set for BFL conjugate using PLS-1 and FCV without outlier

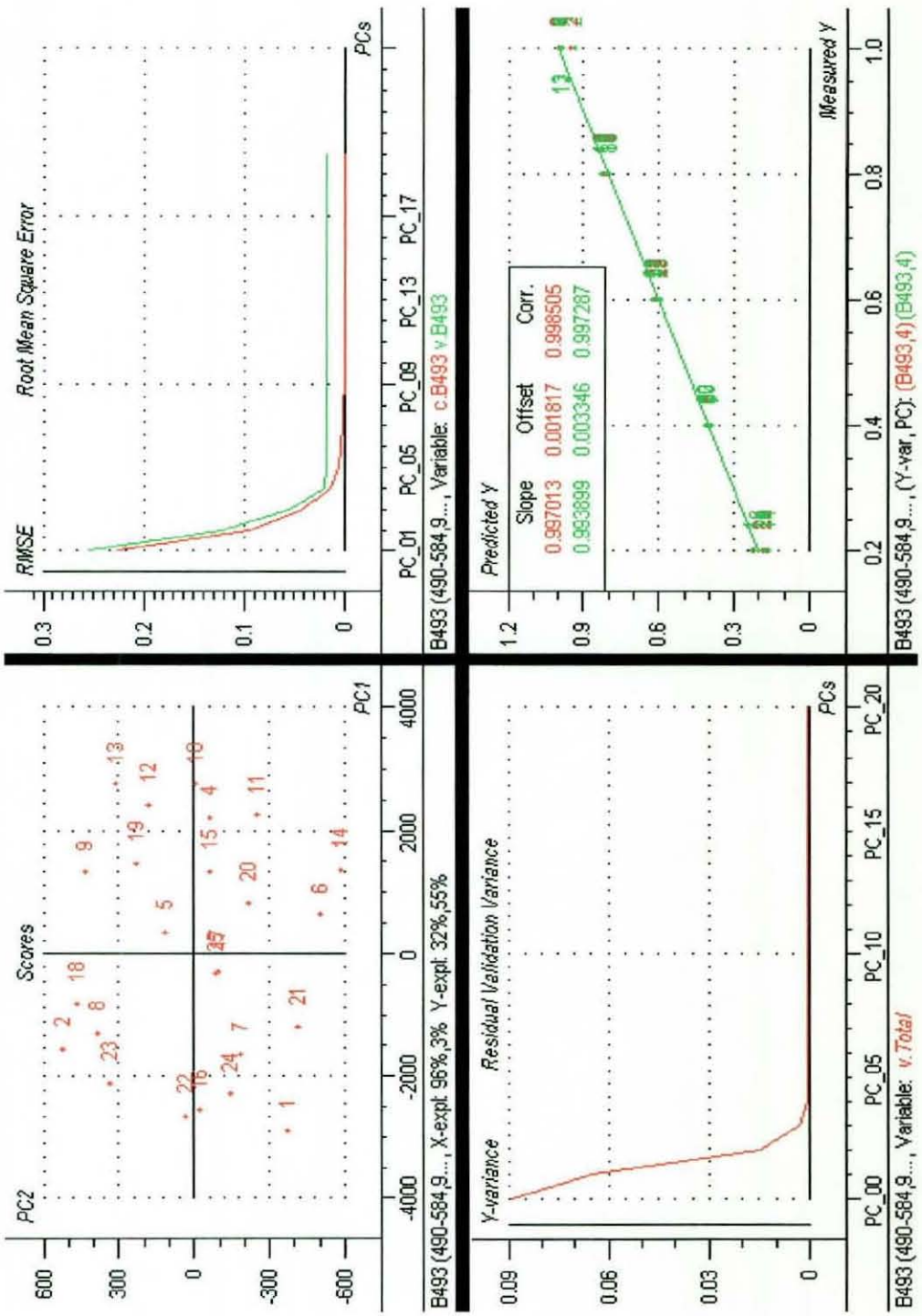

Figure E-6 The analysis plots of calibration set for B493 conjugate using PLS-1 and FCV without outlier